Studies on Synthesis and Chiral Amplification Phenomena of Polyacetylene Derivatives Bearing Dynamically Chiral Pendants

Kohei Shimomura

Studies on Synthesis and Chiral Amplification Phenomena of Polyacetylene Derivatives Bearing Dynamically Chiral Pendants

動的キラルな側鎖を有するポリアセチレン誘導体の合成と
不斉増幅挙動に関する研究

Kohei Shimomura

下村 昂平

2014

Studies on Synthesis and Chiral Amplification Phenomena of Polyacetylene Derivatives Bearing Dynamically Chiral Pendants

Table of Contents

General Introduction

The helix is an essential structural motif for many biopolymers, as represented by DNA and proteins adopting the right-handed double helix[1] and the right-handed α-helix,[2] respectively. Their helical structures are considered to play an important role in exerting their excellent functions involving molecular recognition, self-replication, information transfer, and catalytic activity.[3] Therefore, the synthesis of helical polymers or oligomers (foldamers) and supramolecules with a controlled helix-sense have been attracting significant attention with the aim of developing novel chiral materials as well as mimicking biopolymers.[4,5,6] A large number of helical polymers have been synthesized so far, which can be categorized into three types based on the nature of their helical conformations: (I) static helical polymers; (II) dynamic helical polymers; (III) foldamers (Figure 1).

Static helical polymers are represented by poly(triphenylmethyl methacrylate) (**1**),[4a, 4d, 7] polyisocyanides (**2**),[8, 9] polychloral (**3**),[10] and poly(2,3-quinoxaline)s (**4**)[11] (Figure 1A). These polymers possess bulky side groups and their helical conformations formed during polymerization process can be stably maintained in solution due to a high helix inversion barrier caused by the large steric repulsion between the pendants. Therefore, optically active helical polymers with a preferred screw-sense can be synthesized by the helix-sense-selective polymerization of the corresponding achiral monomers with optically active catalysts or initiators.

Polyisocyanates (**5**),[12, 4e, 13] polysilanes (**6**),[4f, 14, 15] and polyacetylenes (**7**)[4g, 4i, 16] are categorized as dynamic helical polymers. In dynamic helical polymers, the right- and left-handed helical conformations are interconvertible through few helix reversals that readily move along the polymer backbone (Figure 1B). An excess one-handed helical conformation can be biased in the presence of a small amount of chiral residues at the pendants or terminal

ends because of a very low helix inversion barrier. Some helical polymers can exhibit both features of the static and dynamic helical polymers depending on the structures of the constituting units because the helix inversion barrier mainly governs the boundary between the two categories.

Recently, foldamer motifs (**8** and **9)** possessing a strong tendency to adopt a preferred-handed helical conformation[6d, 6g, 17] have been utilized to the design and synthesis of novel helical polymers with a controlled helix-sense. These foldamer-based helical polymers can be regarded as a kind of dynamic helical polymer because they exhibit cooperativity during a helix formation with a controlled helix-sense through intra- and/or intermolecular noncovalent bonding interactions. However, they are different from typical dynamic helical polymers (Figure 1B) in the way that they prefer a random conformation under certain experimental conditions (Figure 1C).

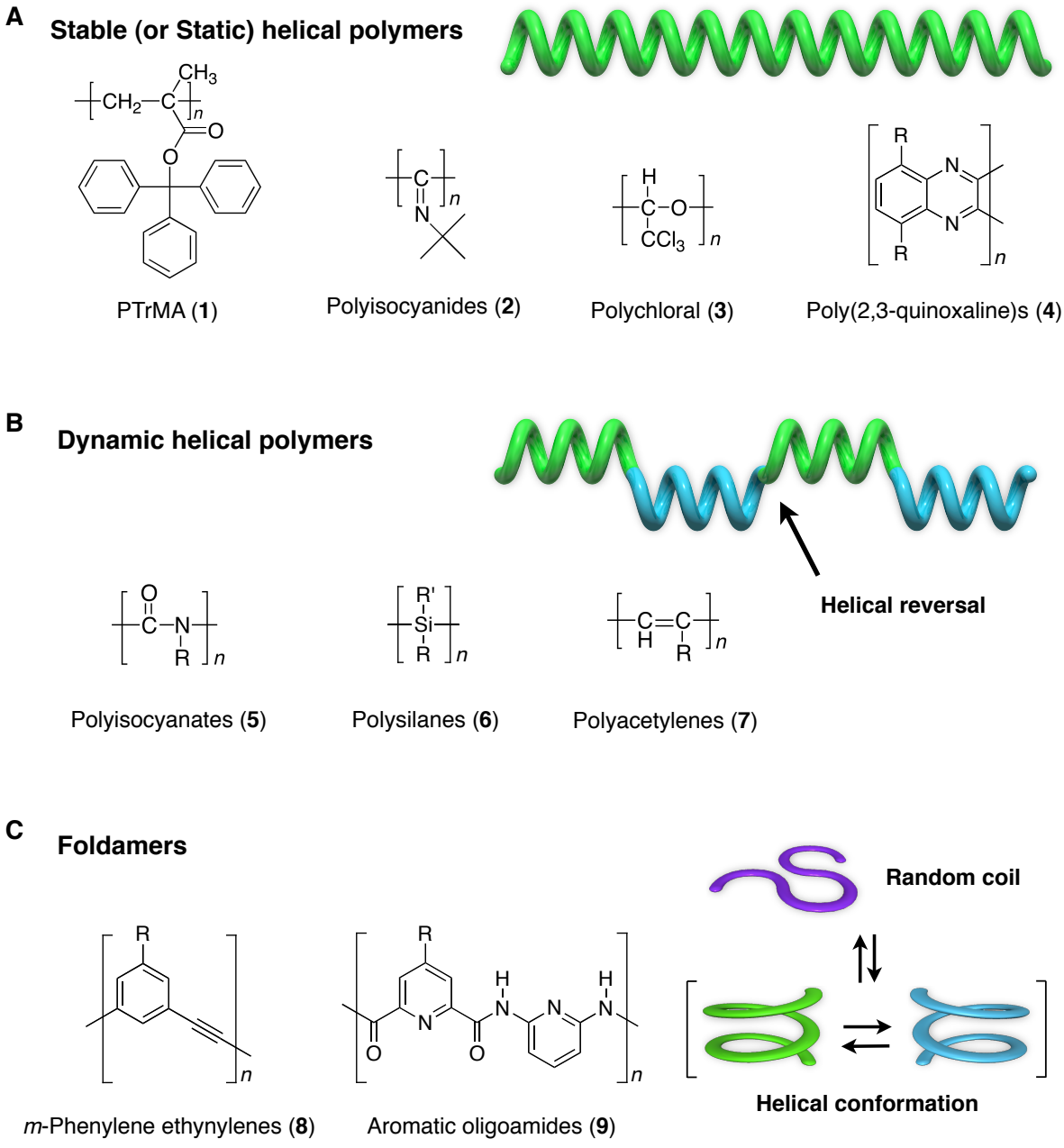

Figure 1. Three types of helical polymers and their representative structures.

Among them, dynamic helical polymers are particularly interesting because they have a characteristic feature of showing significant chiral amplification phenomena. Chiral amplification has gathered much attention in connection with the origin of homochirality in nature,[12a, 18] and is also expected to become an ideal method to produce optically active materials.[19] Green and co-workers discovered chiral amplification in polyisocyanates and

revealed the substantial nature of their dynamic macromolecular helicity from the theoretical and experimental point of view.[20] Polyisocyanates having no optically active substituents are absolutely optically inactive, but they are composed of right- and left-handed helical conformations separated by helical reversals, whose helix-sense readily inverts in solution due to the relatively small barrier energy for helical reversals in these polymers. Therefore, helical polyisocyanates are inherently chiral (or dynamically racemic) macromolecules. However, helical polyisocyanates with a preferred-handedness can be produced through the copolymerization of an achiral isocyanate with a tiny amount of an optically active isocyanate (< 1 mol %) because of the extremely low helix inversion barrier (Figure 2A).[20-21] This is a typical and excellent example of the chiral amplification in synthetic polymers. Green and coworkers named this highly cooperative amplification phenomenon the “sergeants and soldiers” effect;[20] the chiral units are sergeants and the achiral units soldiers. They further discovered that the copolymers consisting of a nonracemic isocyanate with a small enantiomeric excess (ee) also form an excess single-handed helical conformation (Figure 2B). The minority units take the same helical sense as that of the majority units in order to avoid introducing energetic helical reversals. They called this phenomenon (positive nonlinear effect in asymmetric synthesis) the "majority rule".[22] As a result, chiral information of a small amount of the chiral unit is significantly amplified through a significant cooperative manner, resulting in a higher optical activity than that expected from the constituting unit components.[12a] Since these pioneer works, similar chiral amplification phenomena have been reported for other dynamic helical polymers and supramolecules.

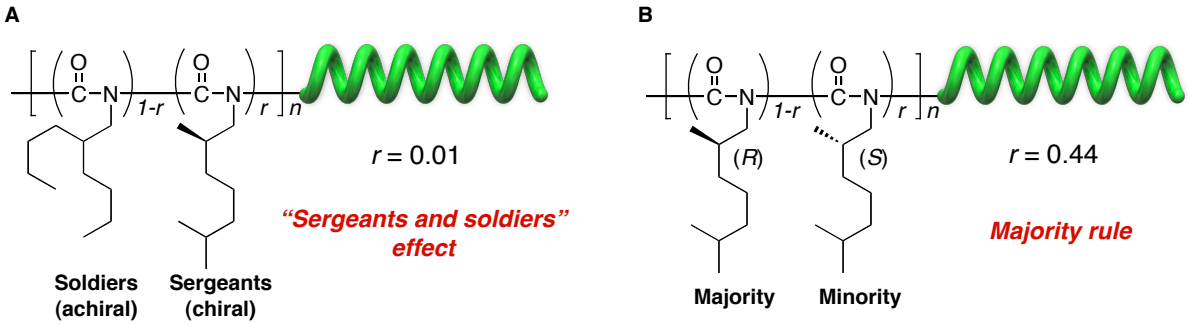

Figure 2. Schematic illustration of "sergeants and soldiers" effect (A) and majority rule (B).

On the other hand, macromolecular helicity with an excess single-handed helical sense can also be induced in optically inactive, dynamically racemic helical polymers through noncovalent bonding interactions. In 1995, Yashima and co-workers reported the first example of such a preferred-handed helical polymer induced by noncovalent chiral acid-base interactions for a cis-transoidal, stereoregular poly((4-carboxyphenyl)acetylene) (**10**).[23] A dynamic preferred-handed macromolecular helicity is induced in the polymer backbone by the complexation with optically active amines in DMSO and the polymer exhibit a characteristic induced circular dichroism (ICD) in the absorption region due to the π-conjugated polymer backbone (300-500 nm) (Figure 3). The induced Cotton effect signs corresponding to the helical sense of **10** can be used as a probe for the detection and chirality assignments of chiral amines.[23-24] Taking advantage of this helicity induction concept, a variety of poly(phenylacetylene)s with various functional groups as the pendant groups, such as boronate (**11**),[25] phosphonate (**12**)[26] and sulfonate (**13**)[26c, d, 27] residues, amino (**14**),[28] and bulky crown ether (**15**)[29] groups have been designed and synthesized. These functional poly(phenylacetylene)s also respond to the chirality of sugars, chiral amines, acid, and ammoniums, and their complexes exhibit characteristic ICDs due to the predominantly one-handed helix formation.

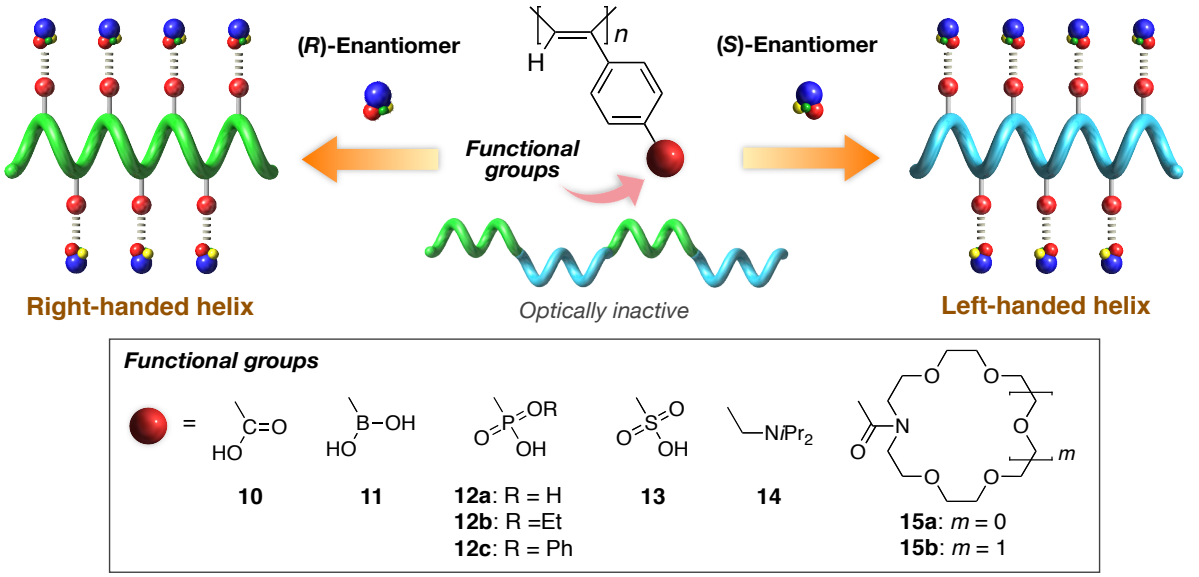

Figure 3. Schematic illustration of helicity induction in poly(phenylacetylene)s bearing various functional groups (**10**—**15**) upon complexation with chiral compounds.

This preferred-handed helicity induction concept has been applied to other dynamic helical, chromophoric polymers or oligomers as templates for macromolecular helicity induction systems. For instance, similar helicity induction in the presence of chiral molecules capable of noncovalently interacting with the polymer's functional groups has been achieved for aliphatic polyacetylenes (**16**, **17**),[30] polyphosphazene (**18**),[31] polyisocyanate (**19**),[32] polyguanidine (**20**),[33] and polyisocyanide (**21**) (Figure 4).[34]

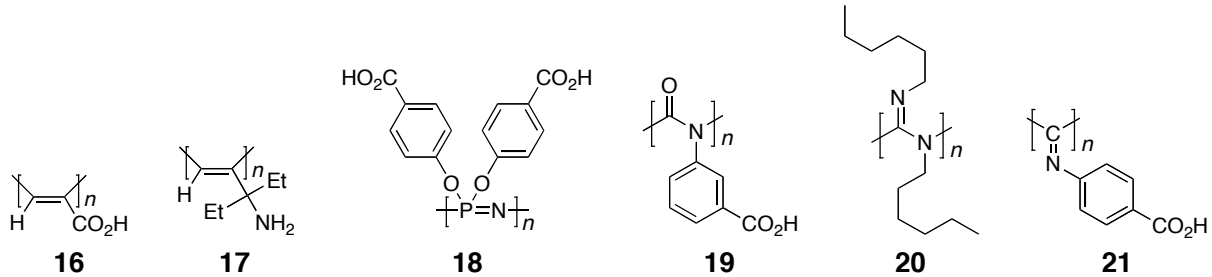

Figure 4. Structures of induced helical polymers exhibiting ICDs in the presence of optically active compounds.

Preferred-handed helicity induction in helical polymers and oligomers is also possible by incorporating chiral residues at the chain ends through covalent or noncovalent bond. Covalent terminus-triggered preferred-handed helicity induction ("covalent domino effect") has been discovered in polyisocyanates by Okamoto and coworkers[13c, d, 35] and other dynamic helical polymers and oligomers (Figure 5A).[36] These polymers and oligomers were prepared by the anionic polymerization of achiral monomers with optically active initiators, by helix-sense-selective block copolymerization, or by incorporation of chiral residues at the ends of the polymer chains. Later, Inai and co-workers reported that an optically inactive oligopeptide (**22**)[37] bearing the *N*-terminal amino group could form an induced one-handed helix upon complexation with chiral carboxylic acids to the *N*-terminal amino group of the peptide, showing an ICD derived from the one-handed helical conformation of the entire peptide chain (Figure 5B). The phenomenon is called the "noncovalent domino effect".[37-38] The chiral information of the carboxylic acids is transferred to the whole peptide chain via noncovalent interaction at the *N*-terminal amino group with a significantly large amplification.

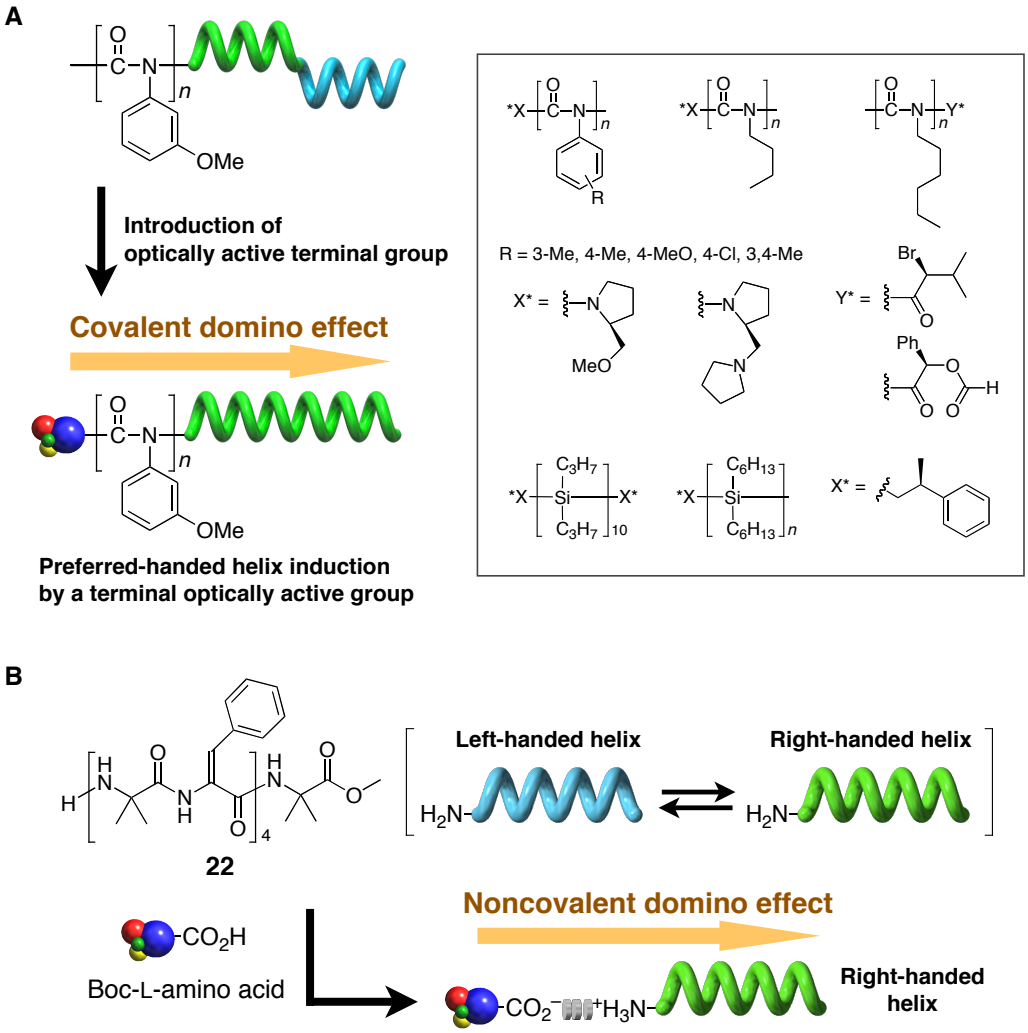

Figure 5. Schematic illustration of a preferred-handed helix induction in polyisocyanates by a terminal optically active group (A) and optically inactive oligopeptides through acid-base interaction with chiral carboxylic acids at the *N*-terminal (domino effect) (B).

The preferred-handed helical structure of **10** induced upon complexation with nonracemic amines is dynamic in nature, so that the ICD due to the macromolecular helicity disappears after the nonracemic amines are removed. However, Yashima and co-workers discovered an interesting phenomenon of macromolecular helicity memory in this dynamic helical polymer system. For example, the macromolecular helicity of **10** induced by (*R*)-1-(1-naphthyl)ethylamine (**23**) was found to be maintained, namely "memorized", after the chiral amine was completely removed by replacing with achiral amines, such as 2-aminoethanol and

n-butylamine (Figure 6) and the macromolecular helicity memory was preserved for a very long time (more than two years).[39] These results mean that the thermodynamically-controlled, dynamic helical conformations can transform into kinetically-controlled, static ones after the helicity memory chaperoned by the achiral amines. From the mechanistic study of the helicity induction and subsequent memory by various spectroscopies, it is suggested that a preferred-handed helical conformation can be cooperatively induced on **10** by the ion-pair formation of the carboxy pendants with chiral amines and the free ion formation plays an important role for the helicity memory of **10** assisted by achiral amines, because the helix inversion in the polymer backbone can be hampered by the intramolecular electrostatic repulsion between the neighboring negatively charged carboxylate ions in the pendants.[40] Therefore, the use of achiral amine as the chaperoning molecules is essential for the memory of macromolecular helicity.[26b, 26g, 27, 41] A similar chiral memory effect has also been reported for other dynamic supramolecular systems,[42] where the use of achiral guests is essential for the memory effect. In most cases, the chiral memory is instantly lost without the use of chaperoning achiral guests.

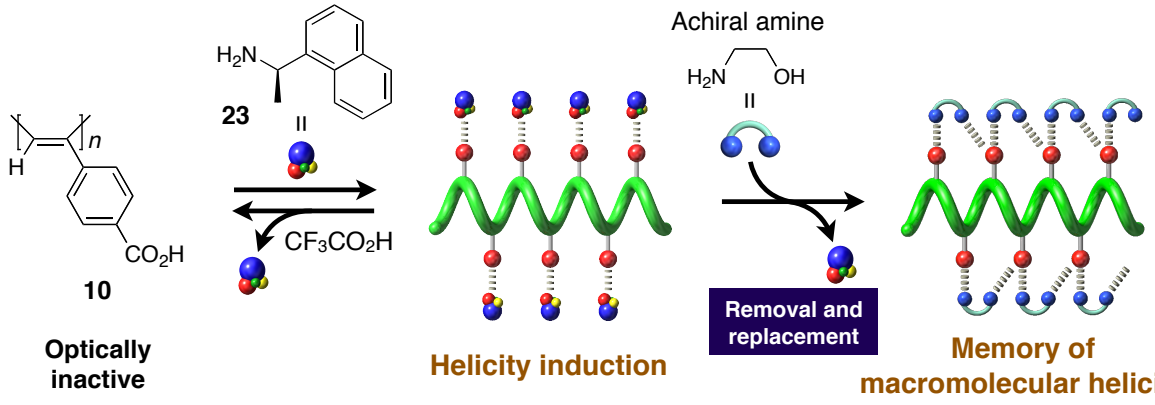

Figure 6. Schematic illustration of a preferred-handed helicity induction in **10** upon complexation with (*R*)-**23** and memory of the induced macromolecular helicity after replacement by achiral amines.

On the other hand, macromolecular helicity memory without the use of achiral guests as the chaperoning compounds has been reported for an optically inactive poly(4-carboxyphenyl isocyanide) (**21**). Upon complexation with optically active amines in water, **21** can change its structure into the prevailing one-handed helical structure and the macromolecular helicity can be "memorized" after complete removal of the chiral amines. In sharp contrast to the case in water, the macromolecular helicity induced in DMSO cannot be maintained after removing the chiral amines (Figure 7).[34, 43] Fully detailed studies on the mechanism of the helix-sense bias induction and subsequent memory by means of various spectroscopies revealed that selective configurational isomerization around the C=N double bonds into single configuration (*syn-anti* isomerism) simultaneously can occur during the preferred-handed macromolecular helicity induction in water upon complexation with optically active amines. This selective configurational isomerization is considered to assist the polymer backbone to maintain the macromolecular helicity. This memory effect discovered in the polyisocyanide has the greater advantage than that of the above described poly(phenylacetylene)s in that the chaperoning achiral amines are no longer necessary for the maintenance of the macromolecular helicity. In fact, the side groups could be further modified with keeping the macromolecular helicity memory to produce diverse helical arrays of functional pendants, such as alcohols (**24**, **25),** ether (**26**), crown ethers (**27**—**29**), oligoglycines (**30**), and pyridyl groups (**31**, **32),** along the helical polymer backbone (Figure 8).[44]

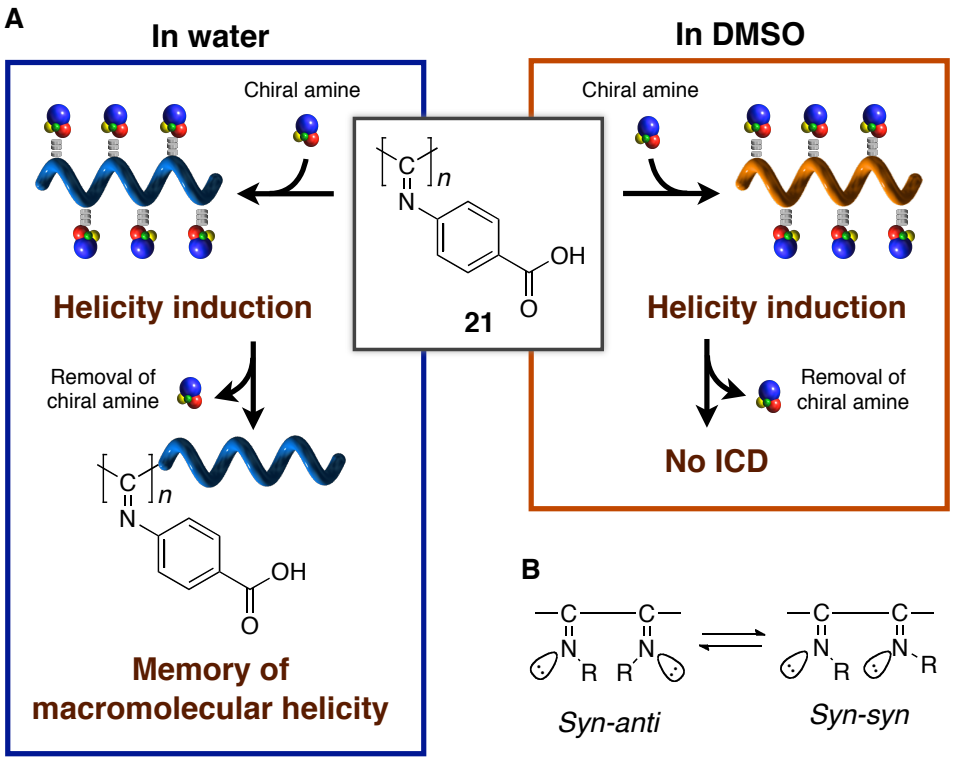

Figure 7. (A) Schematic illustration of helicity induction on **21** in DMSO and water with chiral amines. The macromolecular helicity induced in water is memorized after complete removal of chiral amines, whereas that induced in DMSO cannot be memorized. (B) Configurational *syn-anti* isomerization of polyisocyanide dyad.

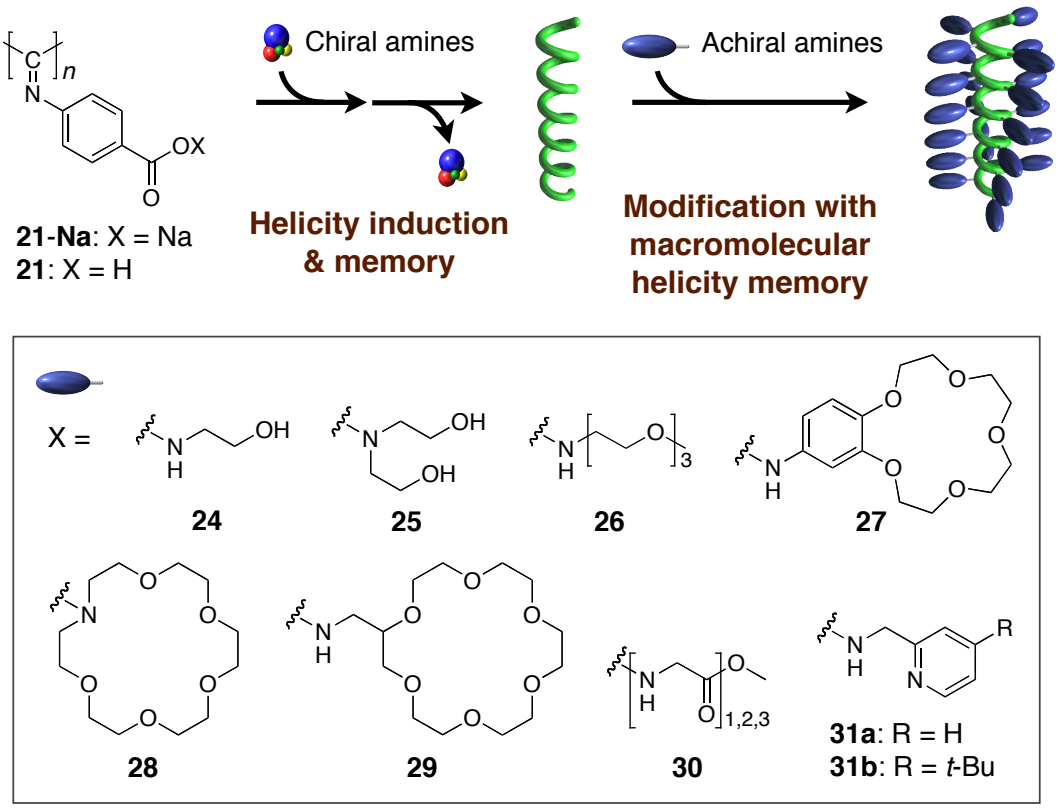

Figure 8. Schematic illustration of preferred-handed helicity induction and memory in **21-Na** or **21** and the modification of the polymer's side groups with macromolecular helicity memory.

The synthesis and structural analyses of artificial helical polymers have been significantly developed, however, their applications still remain a challenge. One attractive application of the one-handed helical polymers involves the separation of enantiomers by high-performance liquid chromatography (HPLC) where optically active helical polymers have been employed as chiral stationary phases (CSPs).[45] Chromatographic enantioseparations (resolution), particularly direct separation of enantiomers by HPLC, have become the most powerful available methods not only for determining enantiomer composition but also for obtaining both pure enantiomers on analytical and industrial scales.[46] The enantioseparation of racemic compounds, in particular, those of chiral drugs, agrochemicals, and fragrances has attracted significant attention over the past few decades because a pair of enantiomers often exhibit quite different pharmacological and physiological

activities. Nowadays, there are many commercially available CSPs for HPLC, for example, polysaccharide-, protein-, and synthetic helical polymer-based CSPs and chiral small molecule-based CSPs. Among them, the derivatives of polysaccharides, such as cellulose and amylose, are the most widely used CSPs because of excellent chiral recognition for many racemates (Figure 9A).[45a, 47] Highly ordered helical structures of their derivatives play a critical role in their remarkable resolving abilities.

Figure 9B shows the examples of synthetic helical polymer-based CSPs, such as polymethacrylates (**1** and **32**), polyacetylenes (**33**), and polyisocyanides (**34**). Okamoto et al. reported that the one-handed helical PTrMA (**1**) and analogous poly (*o*-pyridyldiphenylmethyl methacrylate) (**32**) obtained by the helix-sense selective anionic polymerization with a chiral anionic complex exhibited a high chiral recognition ability for diverse racemic compounds when used as a CSP for HPLC, thus the CSPs of **1** and **32** coated on a macroporous silica gel have been commercialized.[45a-d] Optically active PPAs (**33**) with a preferred-handed helical sense can be used as a CSP for HPLC when coated on a macroporous silica gel, which resolved several racemates.[48] Recently, Yashima and co-workers reported that optically active poly(phenyl isocyanide) bearing achiral benzanilide pendant groups (**34**) prepared from the noncovalent "helicity induction and chiral memory effect" followed by further modifications of the pendant groups showed a remarkable chiral recognition ability for various racemates when used as a CSP for HPCL.[44c] This is the first demonstration of CSPs composed of helical polymers with a macromolecular helicity memory.

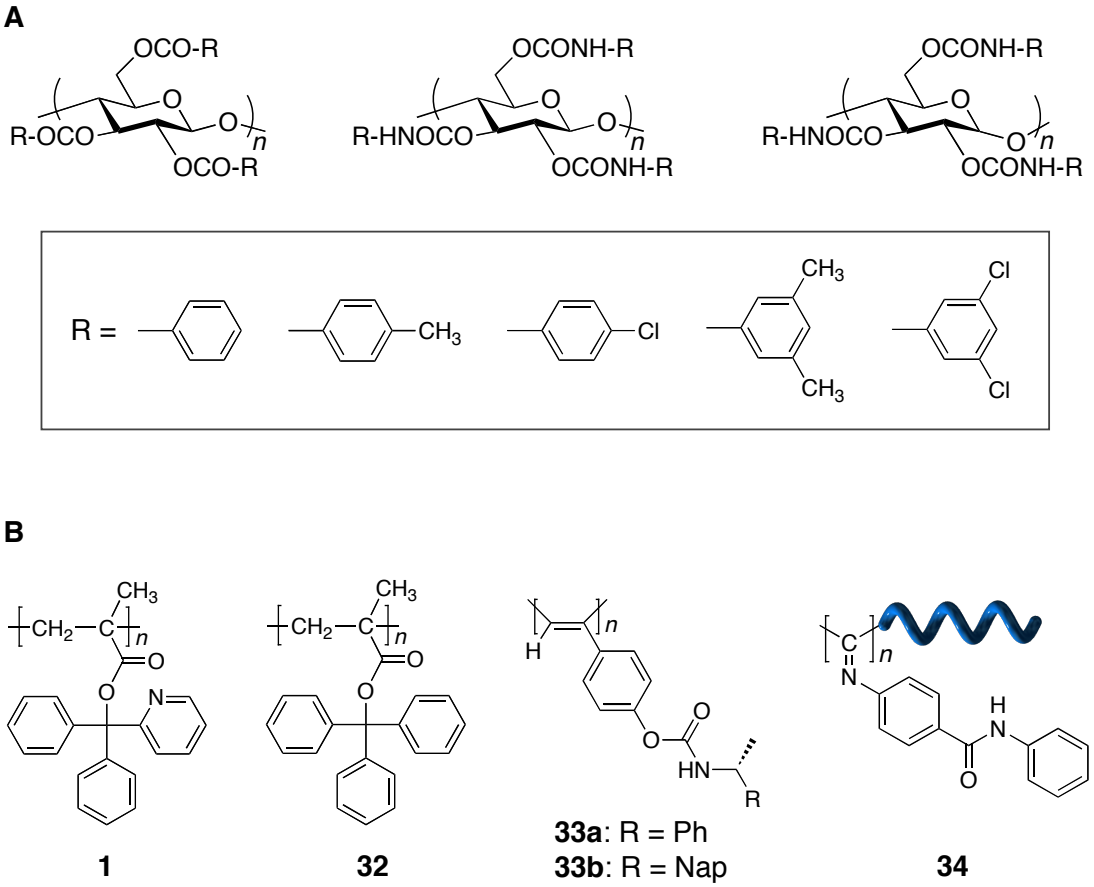

Figure 9. Examples of polysaccharide- (A) and synthetic helical polymer-based CSPs (B).

On the basis of this information, the author studied the following five areas concerning the synthesis and chiral amplification phenomena of polyacetylene derivatives bearing dynamically chiral pendants.

(1) Helical Polymer Brushes with a Preferred-Handed Helix-Sense Triggered by a Terminal Optically Active Group in the Pendant
(2) Chiral Amplification in Polymer Brushes Consisting of Dynamic Helical Polymer Chains through Long-Range Communication of Stereochemical Information
(3) Switchable Enantioseparation Based an Reversible Switching and Memory of Macromolecular Helicity and Axial Chirality of a Poly(biphenylylacetylene) in the Solid State
(4) Memory of the Enantiomeric Macromolecular Helicity Induced in a Polyacetylene with a Single Enantiomer Assisted by Temperature- and Solvent-Driven Helix Inversion
(5) Chirality Sensing of Various Chiral Compounds by Helical Polyacetylenes Bearing Biphenyl Pendants with Dynamic Axial Chirality

These studies will be described in the following five chapters.

In chapter 1, the author describes the synthesis of helical polymer brushes with a preferred-handed helix-sense composed of a poly(phenylacetylene) backbone and poly(phenyl isocyanate) pendants bearing an optically active group only at the chain end and investigated their chiroptical properties by CD spectroscopy (Chart 1). The target polymer brushes were successfully synthesized by the polymerization of poly(phenyl isocyanate) compounds bearing an optically active group at the initial chain end and a polymerizable phenylacetylene residue at the other with various degrees of polymerization (DP: 29, 48, and 70) as the macromonomers. The obtained polymer brushes formed a preferred-handed helical

structure due to the helical chirality of the pendant polyisocyanate chains triggered by the terminal optically active group based on covalent-bonding "chiral domino effect" regardless of the DP of the polyisocyanates. Therefore, it has been demonstrated that a preferred-handed helical conformation can be efficiently induced by long-range chirality transfer through dynamic helical polymer chains in the polymer brushes. The helix-sense excess of the pendant polyisocyanate chains was found to be significantly amplified after conversion to the polymer brush.

Chart 1

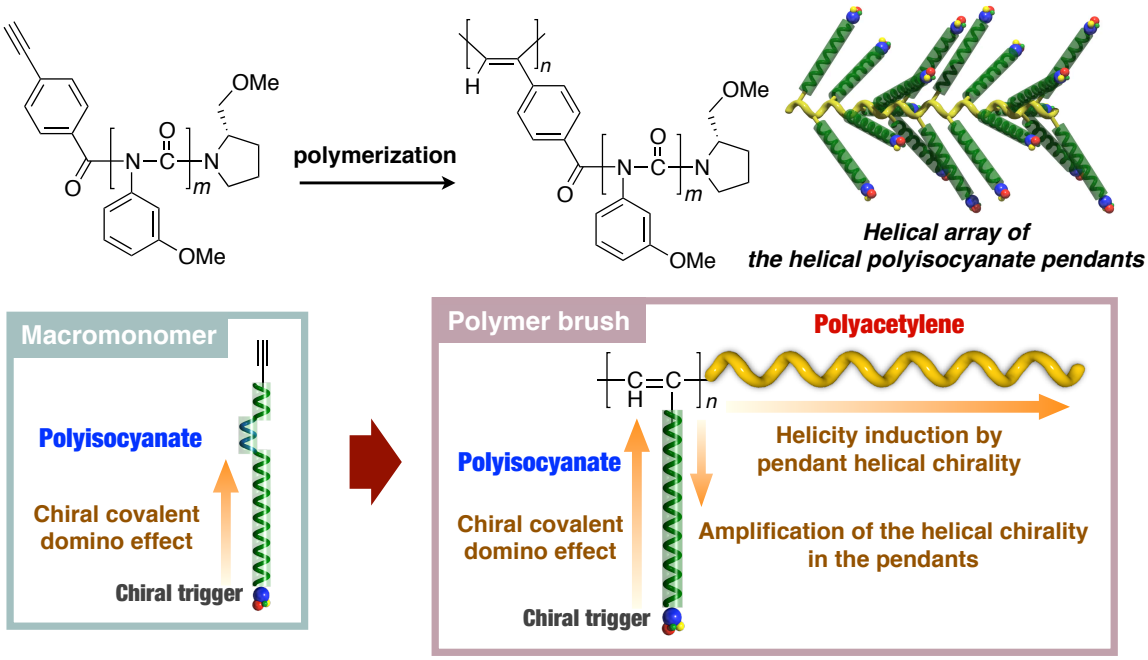

In Chapter 2, the author synthesized a series of poly(phenylacetylene)-based copolymer brushes bearing poly(phenyl isocyanate) pendants with an optically active group and an achiral group at the pendant termini ((poly-(**C**$_r$-*co*-**A**$_{1-r}$)) and investigated their chiroptical properties by using CD and vibrational circular dichroism (VCD) spectroscopies (Chart 2). When an optically active group was only partially introduced at the pendant termini far away from the backbone by the distance corresponding to more than about 27 bond lengths (*ca.* > 4 nm), the stereochemical information was effectively transmitted to the polyacetylene

backbone through the helical chirality of the pendant polyisocyanate by covalent-bonding chiral domino effect and both helical handedness of the polyacetylene backbone and the polyisocyanate pendants without an optically active terminal group were simultaneously controlled.

Chart 2

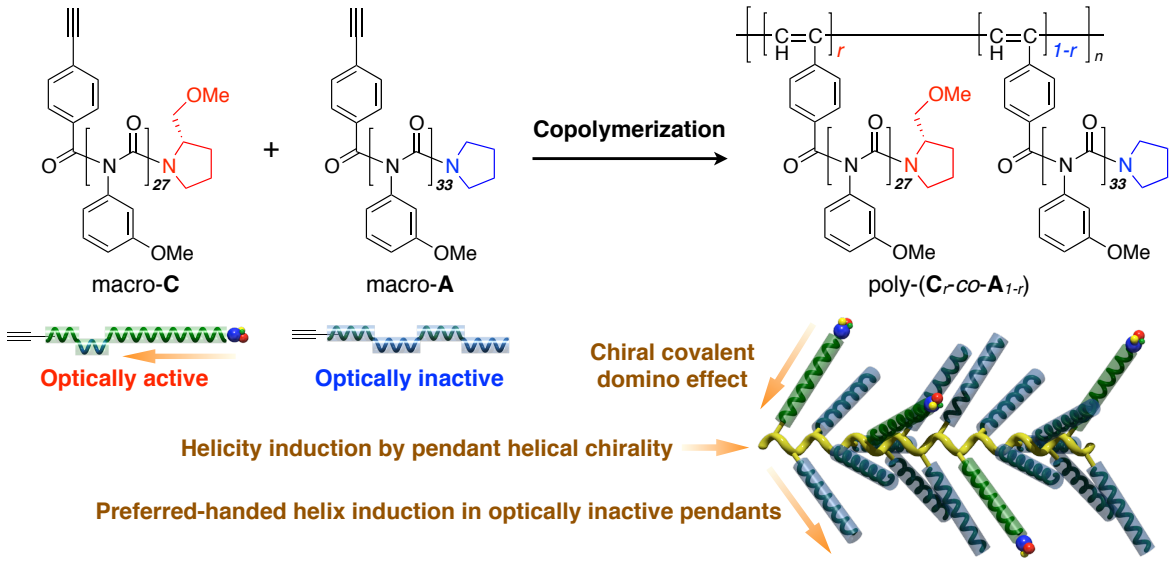

In Chapter 3, the author describes the dual chiral memory of both the conformationally labile macromolecular helicity and axial chirality of a polyacetylene bearing 2,2'-biphenol-derived pendants (poly-**35**) induced in the solid state as well as in solution by noncovalent interactions with a nonracemic alcohol, 1-phenylethylalcohol ((*S*)- or (*R*)-**36**), through significant amplification of the chirality, followed by complete removal of the alcohol (Chart 3). In sharp contrast to the previously observed chiral memory in polyacetylenes, the chaperoning achiral compounds is no longer necessary for this unique switchable dual memory that is fully attained in the solid state. The helical handedness and axial twist-sense of the polymer could be further reversibly switched in the solid state upon interaction with the opposite enantiomeric alcohol and its subsequent removal. The author demonstrated that poly-**35** with a macromolecular helicity and axially twisting memory can separate a racemic compound into the enantiomers and its elution order of the enantiomers can be switched by

inverting and subsequent memory of the macromolecular helicity and axial twist-sense of the polymer in the column using the opposite enantiomeric alcohol as an eluent. To the best of the author's knowledge, this is the first CSP capable of inverting the enantioselectivity or the elution order of the enantiomers under identical chromatographic conditions.

Chart 3

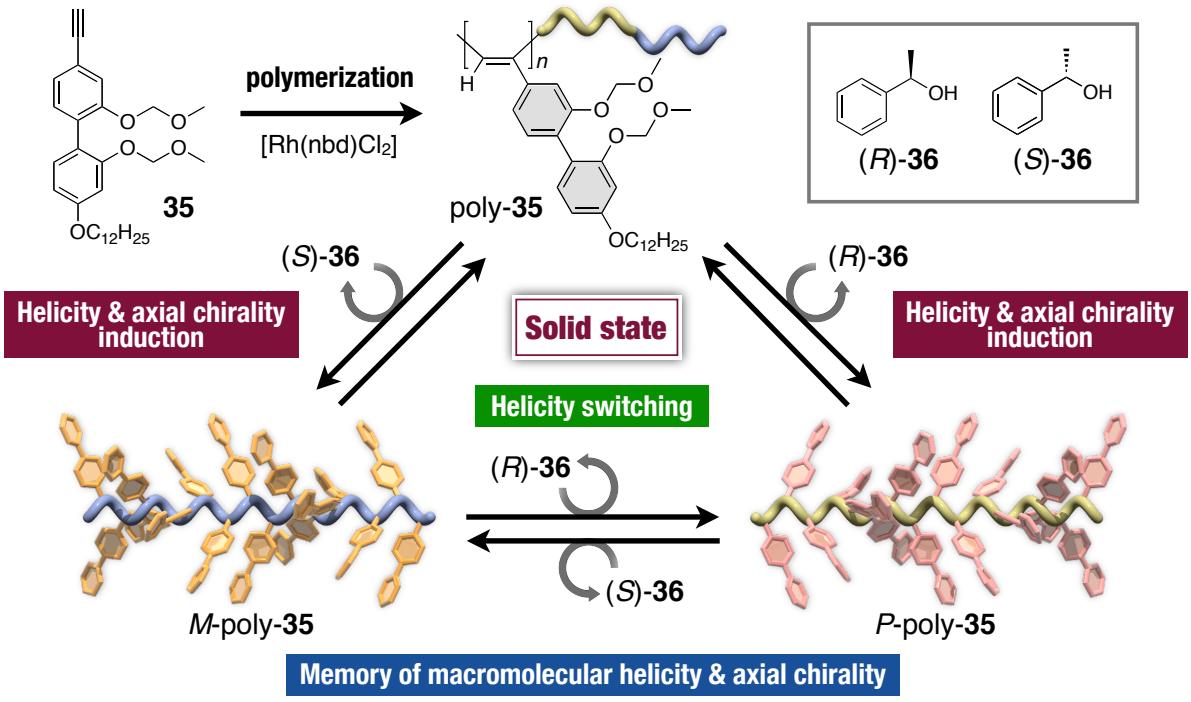

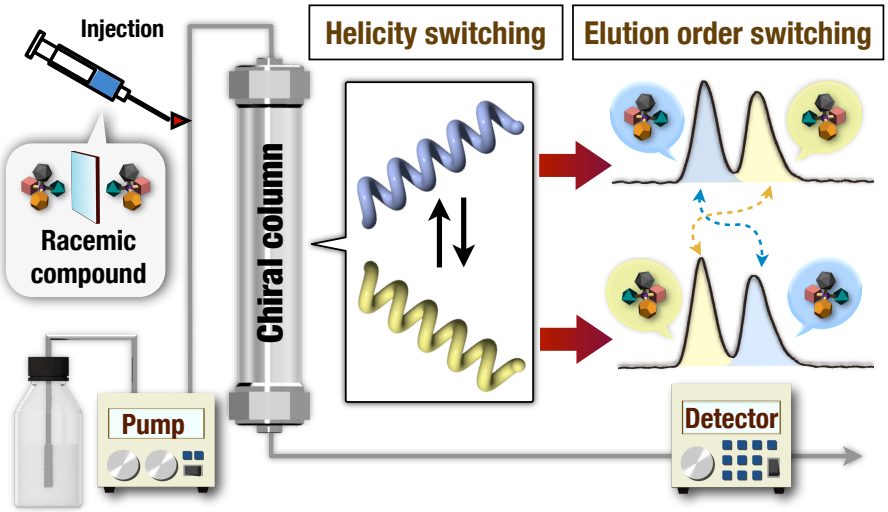

In Chapter 4, the author describes memory of the enantiomeric right- and left-handed macromolecular helicity induced in an optically inactive polyacetylene bearing 2,2'-biphenol-derived pendants, poly((2,2'-bis(ethoxymethoxy)-4'-dodecyloxy-4-biphenylyl)acetylene) (poly-**37**), with a single enantiomer assisted by the helix-sense inversion (Chart 4). Poly-**37** exhibited a split-type ICD in the polymer backbone region in the presence of (*S*)-**36**, due to a predominantly one-handed helical conformation. The author found that the helix-sense of poly-**37** induced by (*S*)-**36** inverted in response to a change in temperature as well as solvent. In addition, the right- and left-handed macromolecular helicity formed by the temperature- and solvent-driven helix-sense inversion were successfully memorized even after the complete removal of the chiral alcohol. Consequently, both the mirror-image enantiomeric helices could be obtained from the optically inactive poly-**37** by using a single enantiomer without the use of chaperoning compounds.

Chart 4

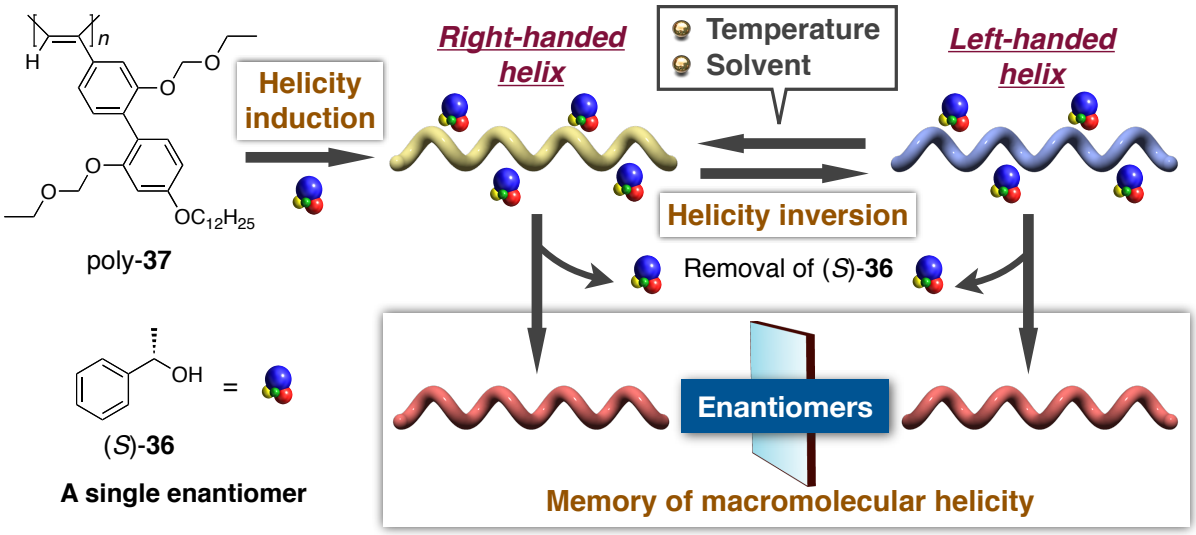

In Chapter 5, the author investigated the chirality sensing ability of an optically inactive, stereoregular polyacetylene bearing 2,2'-biphenol-derived pendants with dynamic axial chirality, poly((2,2'-bis(methoxymethoxy)-4'-dodecyloxy-4-biphenylyl)acetylene) (poly-**35**). Poly-**35** exhibited apparent ICDs in the presence of various optically active compounds

including alcohols, amines, esters, ethers, amino acid derivatives (Chart 5). Interestingly, poly-**35** could detect the chirality of chiral hydrocarbons. On the other hand, model polymer without a biphenyl unit did not show a clear ICD under the same condition as that for poly-**35**. Therefore, it seems that axial chirality of the biphenyl pendants plays an important role for the transfer of the chiral information of the guest molecules to the main chain helicity. The chiral memory effect characteristic of poly-**35** enabled the chirality sensing of a small amount of chiral hydrocarbons. Moreover, the author found that poly-**35** formed a preferred-handed helical conformation in the film state after exposure to the vapor of volatile chiral compounds.

Chart 5

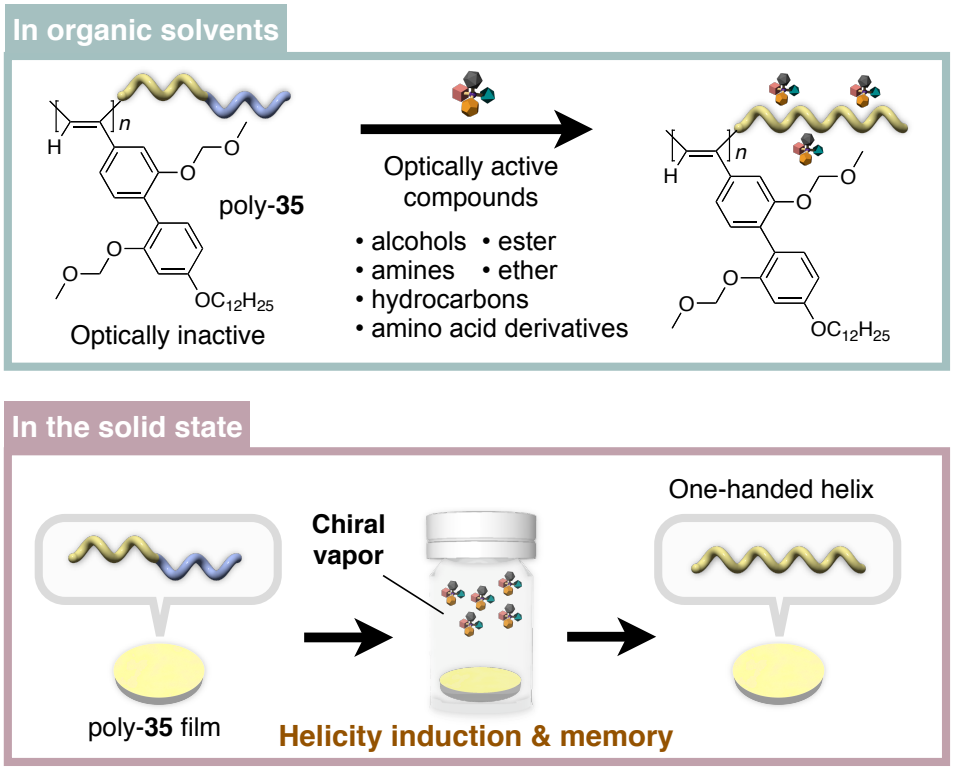

References

1. Watson, J. D.; Crick, F. H. C., *Nature* **1953**, *171*, 737-738.

2. Pauling, L.; Corey, R. B., *Proc. Natl. Acad. Sci., U. S. A.* **1951**, *37*, 241-250.

3. (a) Saenger, W., *Principles of Nucleic Acid Structure*. Springer-Verlag: New York, 1984; (b) Schulz, G. E.; Schirmer, R. H., *Principles of Protein Structure*. Springer-Verlag: New York, 1979.

4. (a) Okamoto, Y.; Nakano, T., *Chem. Rev.* **1994**, *94*, 349-372; (b) Pu, L., *Acta Polym.* **1997**, *48*, 116-141; (c) Cornelissen, J. J. L. M.; Rowan, A. E.; Nolte, R. J. M.; Sommerdijk, N. A. J. M., *Chem. Rev.* **2001**, *101*, 4039-4070; (d) Nakano, T.; Okamoto, Y., *Chem. Rev.* **2001**, *101*, 4013-4038; (e) Green, M. M.; Peterson, N. C.; Sato, T.; Teramoto, A.; Cook, R.; Lifson, S., *Science* **1995**, *268*, 1860-1866; (f) Fujiki, M., *Macromol. Rapid Commun.* **2001**, *22*, 539-563; (g) Nomura, R.; Nakako, H.; Masuda, T., *J. Mol. Catal. A: Chem.* **2002**, *190*, 197-205; (h) Maeda, K.; Yashima, E., *Top. Curr. Chem.* **2006**, *265*, 47-88; (i) Rudick, J. G.; Percec, V., *Acc. Chem. Res.* **2008**, *41*, 1641-1652; (j) Yashima, E.; Maeda, K., *Macromolecules* **2008**, *41*, 3-12; (k) Yashima, E.; Maeda, K.; Furusho, Y., *Acc. Chem. Res.* **2008**, *41*, 1166-1180; (l) Liu, J.; Lam, J. W. Y.; Tang, B. Z., *Chem. Rev.* **2009**, *109*, 5799-5867; (m) Yashima, E.; Maeda, K.; Iida, H.; Furusho, Y.; Nagai, K., *Chem. Rev.* **2009**, *109*, 6102-6211; (n) Furusho, Y.; Yashima, E., *J. Polym. Sci., Part A: Polym. Chem.* **2009**, *47*, 5195-5207; (o) Yashima, E., *Polym. J.* **2010**, *42*, 3-16.

5. (a) Pijper, D.; Feringa, B. L., *Soft Matter* **2008**, *4*, 1349-1372; (b) Brunsveld, L.; Folmer, B. J. B.; Meijer, E. W.; Sijbesma, R. P., *Chem. Rev.* **2001**, *101*, 4071-4097; (c) Elemans, J. A. A. W.; Rowan, A. E.; Nolte, R. J. M., *J. Mater. Chem.* **2003**, *13*, 2661-2670; (d) Hoeben, F. J. M.; Jonkheijm, P.; Meijer, E. W.; Schenning, A. P. H. J., *Chem. Rev.* **2005**, *105*, 1491-1546; (e) Keizer, H. M.; Sijbesma, R. P., *Chem. Soc. Rev.* **2005**, *34*, 226-234; (f) Palmans, A. R. A.; Meijer, E. W., *Angew. Chem., Int. Ed.* **2007**, *46*, 8948-8968; (g) Kim, H.-J.; Lim, Y.-B.; Lee, M., *J. Polym. Sci., Part A: Polym. Chem.* **2008**, *46*, 1925-1935.

6. (a) Li, Z.-T.; Hou, J.-L.; Li, C., *Acc. Chem. Res.* **2008**, *41*, 1343-1353; (b) Gellman, S. H., *Acc. Chem. Res.* **1998**, *31*, 173-180; (c) Cheng, R. P.; Gellman, S. H.; DeGrado, W. F., *Chem. Rev.* **2001**, *101*, 3219-3232; (d) Hill, D. J.; Mio, M. J.; Prince, R. B.; Hughes, T. S.; Moore, J. S., *Chem. Rev.* **2001**, *101*, 3893-4011; (e) Seebach, D.; Beck, A. K.; Bierbaum, D. J., *Chemistry & Biodiversity* **2004**, *1*, 1111-1239; (f) Huc, I., *Eur. J. Org. Chem.* **2004**, 17-29; (g) Hecht, S.; Huc, I., *Foldamers: Structure, Properties, and Applications*. WILEY-VCH: Weinheim, 2007; (h) Saraogi, I.; Hamilton, A. D., *Chem. Soc. Rev.* **2009**, *38*, 1726-1743; (i) Roy, A.; Prabhakaran, P.; Baruah, P. K.; Sanjayan, G. J., *Chem. Commun.* **2011**, *47*, 11593-11611; (j) Guichard, G.; Huc, I., *Chem. Commun.* **2011**, *47*, 5933-5941.

7. (a) Nakano, T.; Okamoto, Y.; Hatada, K., *J. Am. Chem. Soc.* **1992**, *114*, 1318-1329; (b) Okamoto, Y.; Suzuki, K.; Ohta, K.; Hatada, K.; Yuki, H., *J. Am. Chem. Soc.* **1979**, *101*, 4763-4765; (c) Okamoto, Y.; Yashima, E., *Prog. Polym. Sci.* **1990**, *15*, 263-298.

8. (a) Millich, F., *Adv. Polym. Sci.* **1975**, *19*, 117; (b) Nolte, R. J. M., *Chem. Soc. Rev.* **1994**, *23*, 11-19; (c) Suginome, M.; Ito, Y., *Adv. Polym. Sci.* **2004**, *17*, 77-136; (d) Amabilino, D. B.; Serrano, J.-L.; Sierra, T.; Veciana, J., *J. Polym. Sci., Part A: Polym. Chem.* **2006**, *44*, 3161-3174; (e) Schwartz, E.; Koepf, M.; Kitto, H. J.; Nolte, R. J. M.; Rowan, A. E., *Polym. Chem.* **2011**, *2*, 33-47.

9. (a) Kamer, P. C. J.; Nolte, R. J. M.; Drenth, W., *J. Am. Chem. Soc.* **1988**, *110*, 6818-6825; (b) Cornelissen, J.; Fischer, M.; Sommerdijk, N.; Nolte, R. J. M., *Science* **1998**, *280*, 1427-1430; (c) Amabilino, D. B.; Ramos, E.; Serrano, J.-L.; Sierra, T.; Veciana, J., *J. Am. Chem. Soc.* **1998**, *120*, 9126-9134; (d) Hasegawa, T.; Kondoh, S.; Matsuura, K.; Kobayashi, K., *Macromolecules* **1999**, *32*, 6595-6603; (e) Takei, F.; Yanai, K.; Onitsuka, K.; Takahashi, S., *Chem. Eur. J.* **2000**, *6*, 983-993; (f) Cornelissen, J.; Donners, J.; de Gelder, R.; Graswinckel, W. S.; Metselaar, G. A.; Rowan, A. E.; Sommerdijk, N.; Nolte, R. J. M., *Science* **2001**, *293*, 676-680; (g) Takei, F.; Hayashi, H.; Onitsuka, K.; Kobayashi, N.; Takahashi, S., *Angew. Chem., Int. Ed.* **2001**, *40*, 4092-4094; (h) Yamada, Y.; Kawai, T.; Abe, J.; Iyoda, T., *J. Polym. Sci., Part A: Polym. Chem.* **2002**, *40*, 399-408; (i) Cornelissen, J.; Graswinckel, W. S.; Rowan, A. E.; Sommerdijk, N.; Nolte, R. J. M., *J. Polym. Sci., Part A:*

Polym. Chem. **2003**, *41*, 1725-1736; (j) Hida, N.; Takei, F.; Onitsuka, K.; Shiga, K.; Asaoka, S.; Iyoda, T.; Takahashi, S., *Angew. Chem., Int. Ed.* **2003**, *42*, 4349-4352; (k) Amabilino, D. B.; Ramos, E.; Serrano, J.-L.; Sierra, T.; Veciana, J., *Polymer* **2005**, *46*, 1507-1521; (l) Onitsuka, K.; Mori, T.; Yamamoto, M.; Takei, F.; Takahashi, S., *Macromolecules* **2006**, *39*, 7224-7231.

10. (a) Ute, K.; Hirose, K.; Kashimoto, H.; Nakayama, H.; Hatada, K.; Vogl, O., *Polym. J.* **1993**, *25*, 1175-1186; (b) Vogl, O.; Jaycox, G. D.; Kratky, C.; Simonsick, W. J.; Hatada, K., *Acc. Chem. Res.* **1992**, *25*, 408-413.

11. (a) Ito, Y.; Ohara, T.; Shima, R.; Suginome, M., *J. Am. Chem. Soc.* **1996**, *118*, 9188-9189; (b) Ito, Y.; Ihara, E.; Murakami, M., *Angew.Chem. Int. Ed. Engl.* **1992**, *31*, 1509-1510; (c) Ito, Y.; Miyake, T.; Hatano, S.; Shima, R.; Ohara, T.; Suginome, M., *J. Am. Chem. Soc.* **1998**, *120*, 11880-11893; (d) Ito, Y.; Miyake, T.; Suginome, M., *Macromolecules* **2000**, *33*, 4034-4038; (e) Suginome, M.; Collet, S.; Ito, Y., *Org. Lett.* **2002**, *4*, 351-354.

12. (a) Green, M. M.; Park, J. W.; Sato, T.; Teramoto, A.; Lifson, S.; Selinger, R. L. B.; Selinger, J. V., *Angew. Chem., Int. Ed.* **1999**, *38*, 3138-3154; (b) Mayer, S.; Zentel, R., *Prog. Polym. Sci.* **2001**, *26*, 1973-2013.

13. (a) Green, M. M.; Andreola, C.; Munoz, B.; Reidy, M. P.; Zero, K., *J. Am. Chem. Soc.* **1988**, *110*, 4063-4065; (b) Lifson, S.; Andreola, C.; Peterson, N. C.; Green, M. M., *J. Am. Chem. Soc.* **1989**, *111*, 8850-8858; (c) Okamoto, Y.; Matsuda, M.; Nakano, T.; Yashima, E., *J. Polym. Sci., Part A: Polym. Chem.* **1994**, *32*, 309-315; (d) Maeda, K.; Matsuda, M.; Nakano, T.; Okamoto, Y., *Polym. J.* **1995**, *27*, 141-146; (e) Maeda, K.; Okamoto, Y., *Macromolecules* **1998**, *31*, 1046-1052; (f) Li, J.; Schuster, G. B.; Cheon, K. S.; Green, M. M.; Selinger, J. V., *J. Am. Chem. Soc.* **2000**, *122*, 2603-2612; (g) Yoshiba, K.; Hama, R.; Teramoto, A.; Nakamura, N.; Maeda, K.; Okamoto, Y.; Sato, T., *Macromolecules* **2006**, *39*, 3435-3440; (h) Nath, G. Y.; Samal, S.; Park, S. Y.; Murthy, C. N.; Lee, J. S., *Macromolecules* **2006**, *39*, 5965-5966; (i) Pijper, D.; Feringa, B. L., *Angew. Chem., Int. Ed.* **2007**, *46*, 3693-3696.

14. (a) Fujiki, M.; Koe, J. R.; Terao, K.; Sato, T.; Teramoto, A.; Watanabe, J., *Polym. J.* **2003**, *35*, 297-344; (b) Naito, M.; Fujiki, M., *Soft Matter* **2008**, *4*, 211-223.

15. (a) Fujiki, M., *J. Am. Chem. Soc.* **1994**, *116*, 11976-11981; (b) Toyoda, S.; Fujiki, M., *Macromolecules* **2001**, *34*, 640-644; (c) Koe, J. R.; Fujiki, M.; Motonaga, M.; Nakashima, H., *Macromolecules* **2001**, *34*, 1082-1089; (d) Terao, K.; Terao, Y.; Teramoto, A.; Nakamura, N.; Fujiki, M.; Sato, T., *Macromolecules* **2001**, *34*, 6519-6525; (e) Sato, T.; Terao, K.; Teramoto, A.; Fujiki, M., *Macromolecules* **2002**, *35*, 2141-2148; (f) Sato, T.; Terao, K.; Teramoto, A.; Fujiki, M., *Macromolecules* **2002**, *35*, 5355-5357; (g) Ohira, A.; Kunitake, M.; Fujiki, M.; Naito, M.; Saxena, A., *Chem. Mater.* **2004**, *16*, 3919-3923; (h) Saxena, A.; Guo, G.; Fujiki, M.; Yang, Y.; Ohira, A.; Okoshi, K.; Naito, M., *Macromolecules* **2004**, *37*, 3081-3083; (i) Kim, S. Y.; Fujiki, M.; Ohira, A.; Kwak, G.; Kawakami, Y., *Macromolecules* **2004**, *37*, 4321-4324.

16. (a) Lam, J. W. Y.; Tang, B. Z., *Acc. Chem. Res.* **2005**, *38*, 745-754; (b) Aoki, T.; Kaneko, T.; Teraguchi, M., *Polymer* **2006**, *47*, 4867-4892; (c) Rudick, J. G.; Percec, V., *New J. Chem.* **2007**, *31*, 1083-1096; (d) Masuda, T., *J. Polym. Sci., Part A: Polym. Chem.* **2007**, *45*, 165-180.

17. Berl, V.; Huc, I.; Khoury, R. G.; Krische, M. J.; Lehn, J. M., *Nature* **2000**, *407*, 720-723.

18. Feringa, B. L.; van Delden, R. A., *Angew. Chem., Int. Ed.* **1999**, *38*, 3419-3438.

19. (a) Soai, K.; Shibata, T.; Sato, I., *Acc. Chem. Res.* **2000**, *33*, 382-390; (b) Noyori, R., *Angew. Chem., Int. Ed.* **2002**, *41*, 2008-2022.

20. Green, M. M.; Reidy, M. P.; Johnson, R. J.; Darling, G.; Oleary, D. J.; Willson, G., *J. Am. Chem. Soc.* **1989**, *111*, 6452-6454.

21. Jha, S. K.; Cheon, K.-S.; Green, M. M.; Selinger, J. V., *J. Am. Chem. Soc.* **1999**, *121*, 1665-1673.

22. Green, M. M.; Garetz, B. A.; Munoz, B.; Chang, H. P.; Hoke, S.; Cooks, R. G., *J. Am. Chem. Soc.* **1995**, *117*, 4181-4182.

23. Yashima, E.; Matsushima, T.; Okamoto, Y., *J. Am. Chem. Soc.* **1995**, *117*, 11596-11597.

24. Yashima, E.; Matsushima, T.; Okamoto, Y., *J. Am. Chem. Soc.* **1997**, *119*, 6345-6359.

25. (a) Yashima, E.; Nimura, T.; Matsushima, T.; Okamoto, Y., *J. Am. Chem. Soc.* **1996**, *118*, 9800-9801; (b) Kawamura, H.; Maeda, K.; Okamoto, Y.; Yashima, E., *Chem. Lett.* **2001**, 58-59.

26. (a) Onouchi, H.; Maeda, K.; Yashima, E., *J. Am. Chem. Soc.* **2001**, *123*, 7441-7442; (b) Onouchi, H.; Kashiwagi, D.; Hayashi, K.; Maeda, K.; Yashima, E., *Macromolecules* **2004**, *37*, 5495-5503; (c) Onouchi, H.; Hasegawa, T.; Kashiwagi, D.; Ishiguro, H.; Maeda, K.; Yashima, E., *Macromolecules* **2005**, *38*, 8625-8633; (d) Onouchi, H.; Hasegawa, T.; Kashiwagi, D.; Ishiguro, H.; Maeda, K.; Yashima, E., *J. Polym. Sci., Part A: Polym. Chem.* **2006**, *44*, 5039-5048; (e) Morimoto, M.; Tamura, K.; Nagai, K.; Yashima, E., *J. Polym. Sci., Part A: Polym. Chem.* **2010**, *48*, 1383-1390; (f) Kamikawa, Y.; Kato, T.; Onouchi, H.; Kashiwagi, D.; Maeda, K.; Yashima, E., *J. Polym. Sci., Part A: Polym. Chem.* **2004**, *42*, 4580-4586; (g) Miyagawa, T.; Furuko, A.; Maeda, K.; Katagiri, H.; Furusho, Y.; Yashima, E., *J. Am. Chem. Soc.* **2005**, *127*, 5018-5019.

27. Hasegawa, T.; Maeda, K.; Ishiguro, H.; Yashima, E., *Polym. J.* **2006**, *38*, 912-919.

28. (a) Yashima, E.; Maeda, Y.; Okamoto, Y., *Chem. Lett.* **1996**, 955-956; (b) Yashima, E.; Maeda, Y.; Matsushima, T.; Okamato, Y., *Chirality* **1997**, *9*, 593-600; (c) Maeda, K.; Okada, S.; Yashima, E.; Okamoto, Y., *J. Polym. Sci., Part A: Polym. Chem.* **2001**, *39*, 3180-3189; (d) Nagai, K.; Maeda, K.; Takeyama, Y.; Sakajiri, K.; Yashima, E., *Macromolecules* **2005**, *38*, 5444-5451.

29. (a) Nonokawa, R.; Yashima, E., *J. Am. Chem. Soc.* **2003**, *125*, 1278-1283; (b) Nonokawa, R.; Yashima, E., *J. Polym. Sci., Part A: Polym. Chem.* **2003**, *41*, 1004-1013; (c) Nonokawa, R.; Oobo, M.; Yashima, E., *Macromolecules* **2003**, *36*, 6599-6606.

30. (a) Yashima, E.; Goto, H.; Okamoto, Y., *Polym. J.* **1998**, *30*, 69-71; (b) Maeda, K.; Goto, H.; Yashima, E., *Macromolecules* **2001**, *34*, 1160-1164; (c) Tabei, J.; Nomura, R.; Sanda, F.; Masuda, T., *Macromolecules* **2003**, *36*, 8603-8608.

31. (a) Yashima, E.; Maeda, K.; Yamanaka, T., *J. Am. Chem. Soc.* **2000**, *122*, 7813-7814; (b) Maeda, K.; Kuroyanagi, K.; Sakurai, S.-i.; Yamanaka, T.; Yashima, E., *Macromolecules* **2011**, *44*, 2457-2464.

32. (a) Maeda, K.; Yamamoto, N.; Okamoto, Y., *Macromolecules* **1998**, *31*, 5924-5926; (b) Sakai, R.; Satoh, T.; Kakuchi, R.; Kaga, H.; Kakuchi, T., *Macromolecules* **2003**, *36*, 3709-3713; (c) Sakai, R.; Satoh, T.; Kakuchi, R.; Kaga, H.; Kakuchi, T., *Macromolecules* **2004**, *37*, 3996-4003.

33. Schlitzer, D. S.; Novak, B. M., *J. Am. Chem. Soc.* **1998**, *120*, 2196-2197.

34. Ishikawa, M.; Maeda, K.; Yashima, E., *J. Am. Chem. Soc.* **2002**, *124*, 7448-7458.

35. Okamoto, Y.; Matsuda, M.; Nakano, T.; Yashima, E., *Polym. J.* **1993**, *25*, 391-396.

36. (a) Obata, K.; Kabuto, C.; Kira, M., *J. Am. Chem. Soc.* **1997**, *119*, 11345-11346; (b) Obata, K.; Kira, M., *Macromolecules* **1998**, *31*, 4666-4668; (c) Sanji, T.; Takase, K.; Sakurai, H., *J. Am. Chem. Soc.* **2001**, *123*, 12690-12691; (d) Sanji, T.; Takase, K.; Sakurai, H., *Bull. Chem. Soc. Jpn.* **2004**, *77*, 1607-1611; (e) Sanji, T.; Takase, K.; Sakurai, H., *Polym. Bull.* **2007**, *59*, 169-175.

37. Inai, Y.; Tagawa, K.; Takasu, A.; Hirabayashi, T.; Oshikawa, T.; Yamashita, M., *J. Am. Chem. Soc.* **2000**, *122*, 11731-11732.

38. (a) Inai, Y.; Komori, H.; Ousaka, N., *Chem. Rec.* **2007**, *7*, 191-202; (b) Ousaka, N.; Inai, Y., *J. Org. Chem.* **2009**, *74*, 1429-1439.

39. Yashima, E.; Maeda, K.; Okamoto, Y., *Nature* **1999**, *399*, 449-451.

40. Maeda, K.; Morino, K.; Okamoto, Y.; Sato, T.; Yashima, E., *J. Am. Chem. Soc.* **2004**, *126*, 4329-4342.

41. Maeda, K.; Tamaki, S.; Tamura, K.; Yashima, E., *Chem. Asian J.* **2008**, *3*, 614-624.

42. (a) Mateos-Timoneda, M. A.; Crego-Calama, M.; Reinhoudt, D. N., *Chem. Soc. Rev.* **2004**, *33*, 363-372; (b) Furusho, Y.; Kimura, T.; Mizuno, Y.; Aida, T., *J. Am. Chem. Soc.* **1997**, *119*, 5267-5268; (c) Sugasaki, A.; Ikeda, M.; Takeuchi, M.; Robertson, A.; Shinkai, S., *J. Chem. Soc. Perkin Trans. 1* **1999**, 3259-3264; (d) Prins, L. J.; De Jong, F.; Timmerman, P.; Reinhoudt, D. N., *Nature* **2000**, *408*, 181-184; (e) Kubo, Y.; Ohno, T.; Yamanaka, J.; Tokita, S.; Iida, T.; Ishimaru, Y., *J. Am. Chem. Soc.* **2001**, *123*, 12700-12701; (f) Rosaria, L.; D'Urso, A.; Mammana, A.; Purrello, R., *Chirality* **2008**, *20*, 411-419.

43. (a) Ishikawa, M.; Maeda, K.; Mitsutsuji, Y.; Yashima, E., *J. Am. Chem. Soc.* **2004**, *126*, 732-733; (b) Maeda, K.; Ishikawa, M.; Yashima, E., *J. Am. Chem. Soc.* **2004**, *126*, 15161-15166; (c) Hase, Y.; Ishikawa, M.; Muraki, R.; Maeda, K.; Yashima, E., *Macromolecules* **2006**, *39*, 6003-6008; (d) Hase, Y.; Nagai, K.; Iida, H.; Maeda, K.; Ochi, N.; Sawabe, K.; Sakajiri, K.; Okoshi, K.; Yashima, E., *J. Am. Chem. Soc.* **2009**, *131*, 10719-10732.

44. (a) Hase, Y.; Mitsutsuji, Y.; Ishikawa, M.; Maeda, K.; Okoshi, K.; Yashima, E., *Chem. Asian J.* **2007**, *2*, 755-763; (b) Miyabe, T.; Hase, Y.; Iida, H.; Maeda, K.; Yashima, E., *Chirality* **2009**, *21*, 44-50; (c) Miyabe, T.; Iida, H.; Ohnishi, A.; Yashima, E., *Chem. Sci.* **2012**, *3*, 863-867.

45. (a) Okamoto, Y.; Yashima, E., *Angew. Chem., Int. Ed.* **1998**, *37*, 1020-1043; (b) Nakano, T., *J. Chromatogr. A* **2001**, *906*, 205-225; (c) Yamamoto, C.; Okamoto, Y., *Bull. Chem. Soc. Jpn.* **2004**, *77*, 227-257; (d) Okamoto, Y.; Ikai, T., *Chem. Soc. Rev.* **2008**, *37*, 2593-2608; (e) Okamoto, Y., *J. Polym. Sci., Part A: Polym. Chem.* **2009**, *47*, 1731-1739.

46. (a) Subramanian, G., *Chiral Separation Techniques: A Practical Approach*. 3rd ed.; Wiley-VCH: Weinheim, Germany, 2007; (b) Aboul-Enein, H. Y.; Ali, I., *Chiral Separations by Liquid Chroma- tography and Related Technologies; Chromatographic Science Series,* . Marcel Dekker: New York, 2003; Vol. 90; (c) Ahuja, S., *Chiral Separations by Chromatography*. American Chemical Society: Washington, DC, 2000.

47. (a) Yashima, E., *J. Chromatogr. A* **2001**, *906*, 105-125; (b) Yashima, E.; Okamoto, Y., *Bull. Chem. Soc. Jpn.* **1995**, *68*, 3289-3307; (c) Yashima, E.; Yamamoto, C.; Okamoto, Y., *Synlett* **1998**, 344-360.

48. Yashima, E.; Huang, S.; Okamoto, Y., *J. Chem. Soc., Chem. Commun.* **1994**, 1811 - 1812.

Chapter 1

Helical Polymer Brushes with a Preferred-Handed Helix-Sense Triggered by a Terminal Optically Active Group in the Pendant

Abstract: A series of poly(phenylacetylene)-based polymer brushes bearing poly(3-methoxy phenyl isocyanate) pendants with an optically active group only at the chain end were synthesized and their chiroptical properties were investigated by circular dichroism spectral measurement. The polymer brushes formed a preferred-handed helical structure due to the helical chirality of the pendant polyisocyanate chains triggered by the terminal optically active group based on covalent-bonding "chiral domino effect". Moreover, the helix-sense excess of the pendant polyisocyanate chains was significantly amplified after conversion to the polymer brush. This helicity induction triggered by the remote optically active group simultaneously resulted in a helical array of the pendant helical polyisocyanate chains along the polyacetylene backbone with a preferred-handed helix-sense.

Introduction

Biological macromolecules, such as DNA and proteins, adopt one-handed helical structures predetermined by the chirality of their constituent units, which further self-assemble into supramolecular structures responsible for their elaborate biological functions.[1] A large number of artificial helical polymers and oligomers with controlled helicity have been synthesized, not only to mimic biological helices, but also to develop chiral materials with functionality.[2] Among them, dynamic helical polymers, represented by polyisocyanates and polyacetylenes, consist of interconvertible right- and left-handed helical conformations separated by occasional helix reversals. A preferred-handed helical conformation can be induced by introducing a small amount of optically active groups by copolymerization with a small number of optically active monomers, initiating polymerization with an optically active initiator, or interaction with chiral compounds.[2b, 2d, 2f, 2h, 2j, 2m] However, optically active groups need to be introduced close to the polymer backbone to effectively control helicity. It has been demonstrated that introduction of stereocenters into pendants at positions removed from the polymer backbone results in an almost racemic helical conformation.[3]

Very recently, Yashima and co-workers reported unique remote control of the dynamic chirality of metal complexes containing *tris*-bidentate ligands by the helical chirality of the oligopeptides attached to the ligands, which was induced by a terminal optically active unit.[4] In this study, we have designed and synthesized a series of poly(phenylacetylene)-based polymer brushes bearing poly(phenyl isocyanate) pendants with an optically active group only at the chain end (poly-$\mathbf{1}_m$), as shown in Scheme 1-1. The author anticipated that the helix-sense bias of the polyacetylene backbone in the polymer brushes would be hierarchically induced by the helical chirality of the pendant polyisocyanate chains triggered by the terminal optically active group based on the covalent-bonding "chiral domino effect",[5,6] which further results in a helical array of the helical polyisocyanate pendants with a preferred-handed helix-sense (Figure 1-1).

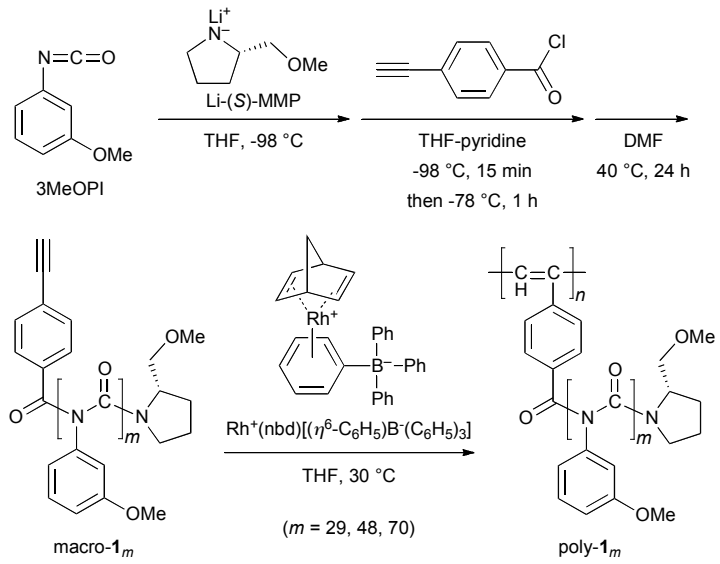

Scheme 1-1. Synthesis of Polymer Brushes Poly-**1**$_m$

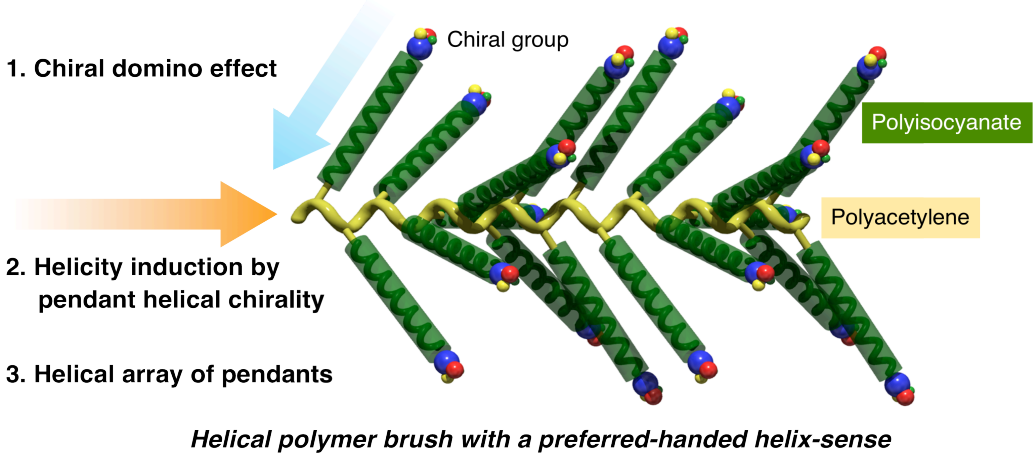

Figure 1-1. Schematic illustration of hierarchical chiral amplification in helical polymer brushes composed of dynamic helical polymer chains triggered by a terminal optically active group in the pendant.

Results and Discussion

Poly(phenyl isocyanate) compounds bearing an optically active group at the initial chain end (α-end) and a polymerizable phenylacetylene residue at the other (ω-end) with various degrees of polymerization (DP) were first synthesized as macromonomers (macro-$\mathbf{1}_m$: m represents DP) by anionic polymerization of 3-methoxyphenyl isocyanate (3MeOPI) with the lithium amide of (*S*)-2-(methoxymethyl)pyrrolidine (Li-(*S*)-MMP) as the initiator in THF at -98 °C with different molar ratios of [3MeOPI] to [Li-(*S*)-MMP], followed by termination with 4-ethynylbenzoyl chloride (Scheme 1-1 and Table 1-1).[5b, 7] The -NH terminated polymers that had not been end-capped with a 4-ethynylbenzoyl group were completely removed by selective depolymerization in DMF.[7b] The DP of the obtained macro-$\mathbf{1}_m$ were determined by ^{1}H NMR analysis to be 29 (macro-$\mathbf{1}_{29}$), 48 (macro-$\mathbf{1}_{48}$), and 70 (macro-$\mathbf{1}_{70}$) (Figure 1-5 in the Experimental Section). As expected from previous reports,[7] the circular dichroism (CD) spectra of macro-$\mathbf{1}_m$ in DMSO at 25 °C showed a positive Cotton effect in the absorption region of the polyisocyanate backbone (*ca*. 265 nm) because of the formation of a predominantly right-handed helical conformation[8] induced by the chiral group covalently attached to the α-end (Figure 1-2a–c). In agreement with previous results,[7] the CD intensities decreased in the order macro-$\mathbf{1}_{29}$ > macro-$\mathbf{1}_{48}$ > macro-$\mathbf{1}_{70}$, *i.e*., with an increase in the DP of macro-$\mathbf{1}_m$, suggesting that the helical sense bias of macro-$\mathbf{1}_m$ can persist only in a rather short range from the α-end because of helix reversal.

Table 1-1. Results of Anionic Polymerization of 3MeOPI with Li-(*S*)-MMP in THF at -98 °C[a]

Run	[3MeOPI] /[Li-(*S*)-MMP]	Polymer[b]				
		Sample code	Yield (%)	m[c]	$M_n \times 10^{-3}$ [d]	M_w/M_n[d]
1	10	macro-**1**$_{29}$	43	29	3.8	1.2
2	20	macro-**1**$_{48}$	23	48	6.0	1.3
3	30	macro-**1**$_{70}$	23	70	9.4	1.2

[a][3MeOPI] = 0.67 M. [b]Hexane-EtOH (3/1, v/v) insoluble component after standing at 40 °C for 24 h in DMF. [c]DP determined by ^{1}H NMR in $CDCl_3$. [d]Determined by SEC (polystyrene standard, eluent: $CHCl_3$).

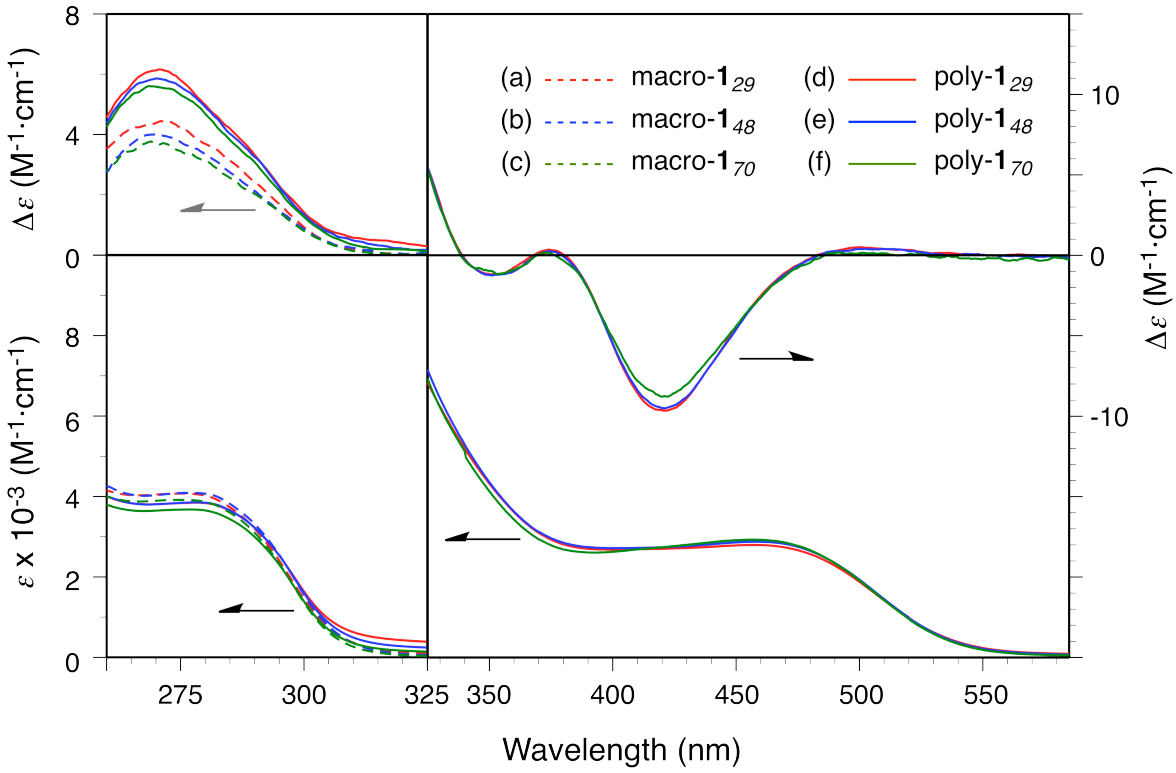

Figure 1-2. CD and absorption spectra of macro-**1**$_m$ (a–c, dotted lines) and poly-**1**$_m$ (d–f, solid lines) in DMSO at 25 °C. The molar ellipticity ($\Delta\varepsilon$) and molar absorption coefficient (ε) were calculated using the molar concentrations of 3MeOPI (250–325 nm: polyisocyanate-backbone chromophore region) and macro-**1**$_m$ (>325 nm: polyacetylene-backbone chromophore region).

The macromonomers were then polymerized with a zwitterionic rhodium complex,[9] $Rh^+(nbd)[(h^6\text{-}C_6H_5)B^-(C_6H_5)_3]$ (nbd = 2,5-norbornadiene), in THF at 30 °C to convert them into polymer brushes consisting of a poly(phenylacetylene) backbone and polyisocyanate pendants (Scheme 1-1). The author notes that the polymerization of macro-$\mathbf{1}_m$ did not proceed when $[Rh(nbd)Cl]_2$, which is often employed for stereospecific polymerization of phenylacetylene derivatives, was used as a catalyst. The results of the polymerization of macro-$\mathbf{1}_m$ are summarized in Table 1-2. All of the polymerization reactions proceeded homogeneously and afforded stereoregular (*cis-transoid*) poly(phenylacetylene)-based polymer brushes (poly-$\mathbf{1}_m$) in high yield except for poly-$\mathbf{1}_{70}$. It was difficult to evaluate the stereoregularity of poly-$\mathbf{1}_m$ using ^1H NMR spectroscopy because the peak caused by the main chain protons, which are highly useful for assigning the conformation and configuration of the polyacetylene backbone, could hardly be observed because of their very weak intensities relative to those of the protons of the pendant polyisocyanates (Figure 1-6 in the Experimental Section). Therefore, the stereoregularity of poly-$\mathbf{1}_m$ was evaluated using laser Raman spectroscopy (Figure 1-7 in the Experimental Section). The low yield of poly-$\mathbf{1}_{70}$ is probably caused by the decrease in the concentration of macro-$\mathbf{1}_{70}$ in the feed because of its limited solubility. The obtained polymer brushes were soluble in THF, DMSO, and $CHCl_3$.

Table 1-2. Polymerization of Macromonomers (macro-$\mathbf{1}_m$) with $Rh^+(nbd)[(h^6\text{-}C_6H_5)B^-(C_6H_5)_3]$ in THF at 30 °C for 5 h[a]

			Polymer			
Run	Macromonomer	[macro-$\mathbf{1}_m$] (mM)	Sample code	Yield[b] (%)	$M_n \times 10^{-4}$ [c]	M_w/M_n[c]
1	macro-$\mathbf{1}_{29}$	105	poly-$\mathbf{1}_{29}$	93	5.9	2.0
2	macro-$\mathbf{1}_{48}$	42	poly-$\mathbf{1}_{48}$	85[d]	12.0	1.7
3	macro-$\mathbf{1}_{70}$	26	poly-$\mathbf{1}_{70}$	25[e]	15.0	1.3

[a][macro-$\mathbf{1}_m$]/[Rh] = 70 (run 1) or 85 (runs 2 and 3). [b]MeOH insoluble component. [c]Determined by SEC (polystyrene standard, eluent: $CHCl_3$). [d]MeOH-THF (3:2, v/v) insoluble component. [e]MeOH-THF (1:1, v/v) insoluble component.

The chiroptical properties of the polymer brush with the shortest polyisocyanate pendants (poly-$\mathbf{1}_{29}$) were first investigated by CD and absorption spectral measurements. Poly-$\mathbf{1}_{29}$ exhibited a similar CD pattern to that of the corresponding macromonomer macro-$\mathbf{1}_{29}$ in the absorption region of the pendant polyisocyanate (<325 nm) in DMSO at 25 °C (Figure 1-2d). Interestingly, its intensity significantly increased compared with that of macro-$\mathbf{1}_{29}$. In addition, the differential CD spectral pattern between poly-$\mathbf{1}_{29}$ and macro-$\mathbf{1}_{29}$ was consistent with the CD pattern of macro-$\mathbf{1}_{29}$. Therefore, this enhancement in the CD intensity means that the helix-sense excess of the pendant polyisocyanate chains was amplified after conversion to the polymer brush. Under these conditions, only very small absorption and CD signals were observed in the absorption region of the polyacetylene backbone above 325 nm because of the very low concentration of the polyacetylene chromophore in poly-$\mathbf{1}_{29}$. However, absorption and CD signals from the polyacetylene backbone were observed above 325 nm for poly-$\mathbf{1}_{29}$ when measurements were performed using a cell that was 5 times longer at a concentration that was 2.5 times higher (Figure 1-2d). This observation indicates that a preferred-handed helical conformation was induced in the polyacetylene backbone of poly-$\mathbf{1}_{29}$ despite the fact that the optically active group attached to the pendant terminals is separated from the backbone by twenty-nine achiral isocyanate units. As illustrated in Figure 1-1, this helicity induction triggered by a remote optically active group simultaneously results in a helical array of pendant helical polyisocyanate chains along the polyacetylene backbone with a preferred-handed helix-sense. It should be noted that the CD intensity of poly-$\mathbf{1}_{29}$ in the polyacetylene chromophore region (>325 nm) as well as the polyisocyanate chromophore region (260–325 nm) increased reversibly with decreasing temperature. This suggests that both the polyacetylene backbone and polyisocyanate pendants of the polymer brush have a dynamic nature (Figure 1-3). The vibrational CD (VCD) spectra of poly-$\mathbf{1}_{29}$ in THF at 25 and -10 °C were measured in order to clearly demonstrate that the change of the CD intensity of poly-$\mathbf{1}_{29}$ in the polyisocyanate chromophore region with temperature is due to the change of the helical screw sense preference of the polyisocyanate backbone, not due to the change of

conformation adoption for the 3-methoxyphenyl side group against the polyisocyanate backbone. The VCD spectra of poly-$\mathbf{1}_{29}$ showed a bisignate couplet in the C=O stretching band region of the polyisocyanate backbone, whose intensity increased reversibly with decreasing temperature (Figure 1-4). These VCD results also support that the polyisocyanate pendants have a dynamic nature.

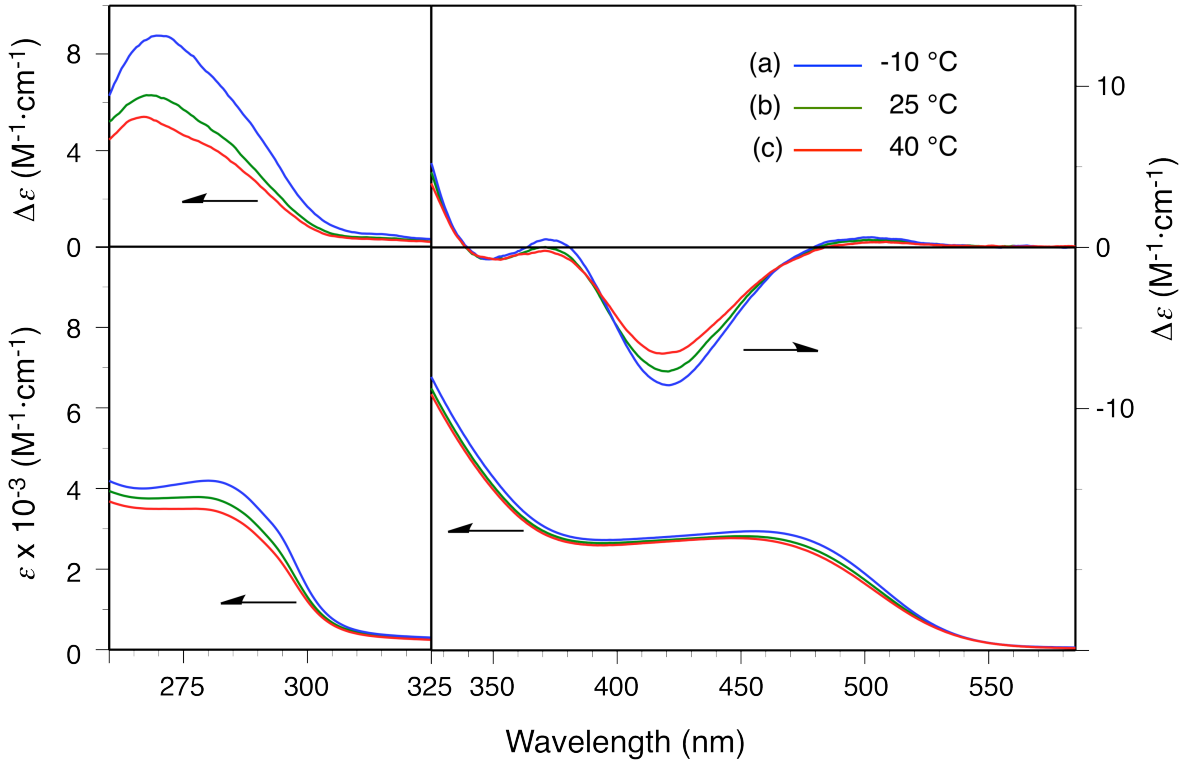

Figure 1-3. CD and absorption spectra of poly-$\mathbf{1}_{29}$ in THF at -10 (a, blue), 25 (b, green), and 40 °C (c, red). The molar ellipticity ($\Delta\varepsilon$) and molar absorption coefficient (ε) were calculated using the molar concentration of 3MeOPI (260–325 nm) and macro-$\mathbf{1}_{29}$ (> 325 nm).

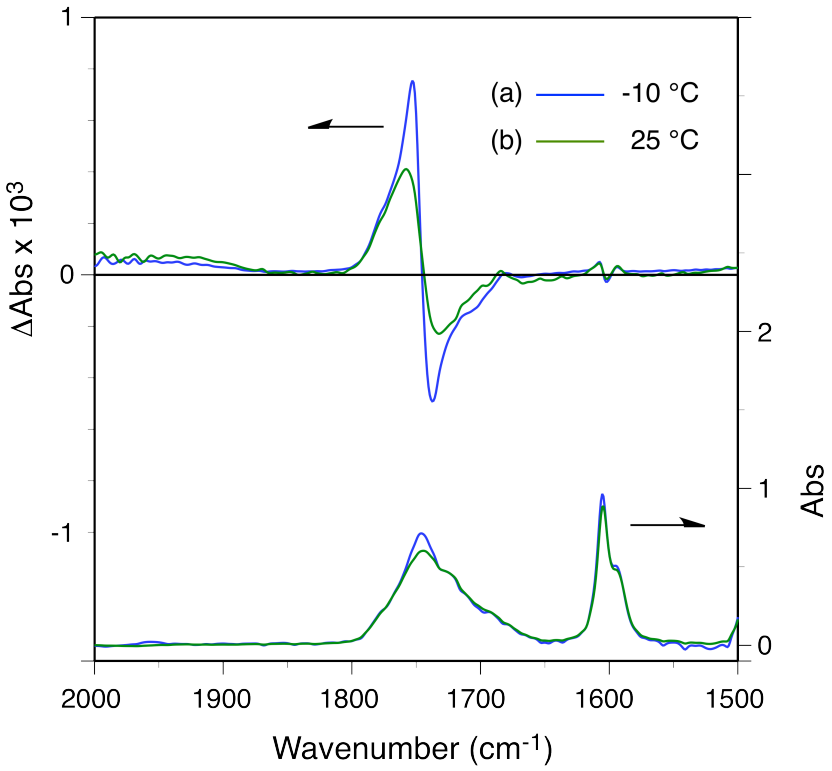

Figure 1-4. VCD and IR spectra of poly-$\mathbf{1}_{29}$ in THF at -10 (a, blue) and 25 °C (b, green). The concentration of poly-$\mathbf{1}_{29}$ was 25 mg/mL in THF. All spectra were collected for *ca*. 3 h at a resolution of 4 cm^{-1}.

To investigate the effect of the chain length of the pendant polyisocyanates bearing a terminal chiral group on the induction of helicity in the polyacetylene backbone of the polymer brushes, CD spectra were obtained for poly-$\mathbf{1}_{48}$ and poly-$\mathbf{1}_{70}$ with longer pendant chains under the same conditions. The CD intensity in the polyacetylene chromophore region (above 325 nm) of poly-$\mathbf{1}_{29}$ was apparently changed by solvents, whereas that in the polyisocyanate chromophore region (260-325 nm) of poly-$\mathbf{1}_{29}$ as well as macro-$\mathbf{1}_{29}$ was almost same independent of solvent (Figure 1-8 in the Experimental Section). Poly-$\mathbf{1}_{29}$ exhibited the most intense CD in the absorption region of the polyacetylene backbone in DMSO. Therefore, the CD and absorption spectra of poly-$\mathbf{1}_{48}$ and poly-$\mathbf{1}_{70}$ with longer pendant chains were measured in DMSO. Despite the remote location of the chiral group, the CD intensity in the polyacetylene chromophore region of poly-$\mathbf{1}_{48}$ was almost identical to that of poly-$\mathbf{1}_{29}$ (Figure

1-2e). Although poly-$\mathbf{1}_{70}$ showed a slight decrease in CD intensity, it can be presumed that the helix-sense excess of the polyacetylene backbone in poly-$\mathbf{1}_{70}$ is still rather high judging from its relatively large $\Delta\varepsilon$ compared with those of previously reported helical poly(phenylacetylene) derivatives (Figure 1-2f).[2m, 10] On the basis of these results, the author can conclude that the preferred-handed helical chirality of the pendant polyisocyanate chains induced by the chiral group at the α-end would play an essential role in the remote control of the helicity of the polyacetylene backbone in the polymer brush. As with poly-$\mathbf{1}_{29}$, the amplification of the helix-sense excess of the pendant polyisocyanate chains after conversion to the polymer brush was also observed for poly-$\mathbf{1}_{48}$ and poly-$\mathbf{1}_{70}$, showing a more intense CD signal in the absorption region of the polyisocyanate (<325 nm) than that of the corresponding macromonomers macro-$\mathbf{1}_{48}$ and macro-$\mathbf{1}_{70}$, respectively (Figures 1-2b, c, e, f). This amplification may be caused by the chiral interaction between the pendants and/or a reduction in the number of helix reversals in the polyisocyanate chains caused by the interaction between adjacent pendants as observed for polyisocyanates and polyacetylenes in a liquid crystal state.[11]

Conclusions

The author has demonstrated that poly(phenylacetylene)-based polymer brushes bearing poly(phenyl isocyanate) pendants form a preferred-handed helical structure when a chiral group is introduced only at the pendant terminal. In these polymers, the pendant helical polyisocyanate chains are arranged in a helical array with a preferred-handed helix-sense along the helical polyacetylene backbone, which is accompanied by amplification of the helix-sense excess of the pendants. This method will be applicable to the combination of other dynamic helical polymers to arrange pendant helical polymer chains in preferred-handed helical arrays using chiral amplification. The author believes that such helical polymer brushes may be useful as novel chiral materials for possible application as asymmetric catalysts and enantioselective selectors.

Experimental Section

Materials. Pyridine (Aldrich), pyrrolidine (Wako), and (*S*)-2-(methoxymethyl)pyrrolidine ((*S*)-MMP) (TCI) were dried over calcium hydride and distilled under high vacuum. TEA (Kanto Kagaku) was dried over KOH pellets under nitrogen and distilled onto 4 Å molecular sieves. These amines were stored under nitrogen. Anhydrous THF, DMSO, and CH_2Cl_2 were purchased from Kanto Kagaku. As the polymerization solvent, the as-purchased anhydrous THF was further dried over $LiAlH_4$ under nitrogen and vacuum-transferred to a dry glass ampoule just before polymerization. 3-Methoxyphenyl isocyanate (3MeOPI) (TCI) was dried over calcium hydride and distilled under high vacuum just before polymerization. Oxalyl chloride, *tert*-butyllithium (1.7 M in pentane), and anhydrous $CHCl_3$ were purchased from Aldrich. 4-Ethynylbenzoic acid[12] and $Rh^+(nbd)[(\eta^6\text{-}C_6H_5)B^-(C_6H_5)_3]$[9, 13] were synthesized according to previously reported methods.

Instruments. NMR spectra were recorded on JEOL ECA500 (500 MHz for ^1H, 125 MHz for ^{13}C) or LA400 (400 MHz for ^1H) spectrometers (Tokyo, Japan) in $CDCl_3$ using TMS as an internal standard. Number- (M_n) and weight-average (M_w) molecular weights of polymers were determined by size-exclusion chromatography (SEC) on a Tosoh TSKgel MultiporeH_{XL}-M column (Tokyo, Japan) using $CHCl_3$ as the eluent at a flow rate of 1.0 mL/min. The molecular weight calibration curve was obtained using polystyrene standards (Tosoh). IR spectra were recorded with a JASCO Fourier Transform IR-460 spectrophotometer (Hachioji, Japan). Absorption and circular dichroism (CD) spectra were measured in a quartz cell with a path length of 0.1 or 0.5 cm on a JASCO V-570 spectrophotometer and a JASCO J-725 spectropolarimeter, respectively. The temperature (-10–40 °C) was controlled with a JASCO ETC 505T (for absorption spectral measurements) and a JASCO 348WI apparatus (for CD spectral measurements). VCD spectra were measured in a 0.15-mm BaF_2 cell with a Jasco JV-2001YS spectrometer equipped with a temperature controller (EYELA NCB-1200). Elemental analyses were performed by the Research Institute

for Instrumental Analysis of Advanced Science Research Center, Kanazawa University, Kanazawa, Japan.

Synthetic Procedures

4-Ethynylbenzoyl chloride.[14] To a solution of 4-ethynylbenzoic acid (7.42 g, 49.7 mmol) in CH_2Cl_2 (150 mL) were added oxalyl chloride (8.4 mL, 100 mmol) and a catalytic amount of DMF. The reaction mixture was then stirred under nitrogen at room temperature overnight. After removal of the solvent, the residue was purified by distillation under reduced pressure to give 3.20 g of 4-ethynylbenzoyl chloride in 39% yield (bp 97 °C/10 mmHg).

Synthesis of macromonomers. Macromonomers macro-$\mathbf{1}_m$ (*m* represents the degree of polymerization (DP)) were synthesized by the polymerization of 3MeOPI with the lithium amide of (*S*)-MMP as an initiator (Scheme 1-1) in a similar manner to that reported previously.[7b] Polymerization was carried out in a dry glass ampule under a dry nitrogen atmosphere in THF at -98 °C. A typical polymerization procedure is described below.

3MeOPI (0.92 mL, 7.2 mmol) and THF (8.4 mL) were placed in a glass ampoule with a three-way stopcock using a syringe and then the solution was cooled to -98 °C. Polymerization was initiated by adding the lithium amide of (*S*)-MMP (Li-(*S*)-MMP) in THF (0.55 M), which was prepared by adding an equimolar amount of *tert*-butyllithium in pentane to a solution of (*S*)-MMP in THF at 0 °C, with a syringe. The reaction mixture was rapidly stirred for 50 min at -98 °C, and then polymerization was terminated by adding an excess amount of 4-ethynylbenzoyl chloride (4.2 mmol) in THF and pyridine (3.0 mmol). The reaction mixture was held at -98 °C for 15 min and then at -78 °C for 1 h to ensure complete termination. The mixture was poured into a large amount of MeOH, and then the precipitated polymeric product was collected by centrifugation and dried *in vacuo* at room temperature. The obtained product was dissolved in DMF and stirred for 24 h at 40 °C to remove any -NH terminated polymers that had not been capped with a 4-ethynylbenzoyl group. The solution was poured into a large amount of hexane-ethanol (3/1, v/v) to remove depolymerization products. The precipitated macromonomer (macro-$\mathbf{1}_m$) was collected by centrifugation and

dried *in vacuo* at room temperature overnight (0.46 g, 43% yield). The complete removal of -NH terminated products was confirmed by the disappearance of the signal from the -NH group (at *ca*. 10.5 ppm) in the ^{1}H NMR spectrum of the macromonomer (Figure 1-5).[7b] The DP of the obtained macromonomer was calculated to be 29 by ^{1}H NMR analysis using the peak intensity of the pendant phenyl proton resonances (4H, o + p + q + r, 5.6–7.2 ppm) relative to that of the aromatic proton resonances of the terminal phenylacetylene residue (4H, b + c, 7.7 and 7.4 ppm) (Figure 1-5).

Spectroscopic data of macro-$\mathbf{1}_{29}$: IR (KBr): ν 1721 (C=O of polyisocyanate) cm^{-1}. Anal. Calcd for $C_6H_{12}NO(C_8H_7NO_2)_{29}C_9H_5O{\cdot}2H_2O$: C, 64.43; H, 4.90; N, 9.13. Found: C, 64.46; H, 4.97; N, 8.89. For ^{1}H NMR, see Figure 1-5A.

Other macromonomers with different DPs (macro-$\mathbf{1}_{48}$ and macro-$\mathbf{1}_{70}$) were synthesized in the same manner as macro-$\mathbf{1}_{29}$; the results of polymerization are summarized in Table 1-1. ^{1}H NMR spectra of macro-$\mathbf{1}_{48}$ and macro-$\mathbf{1}_{70}$ are shown in Figure 1-5B and Figure 1-5C, respectively.

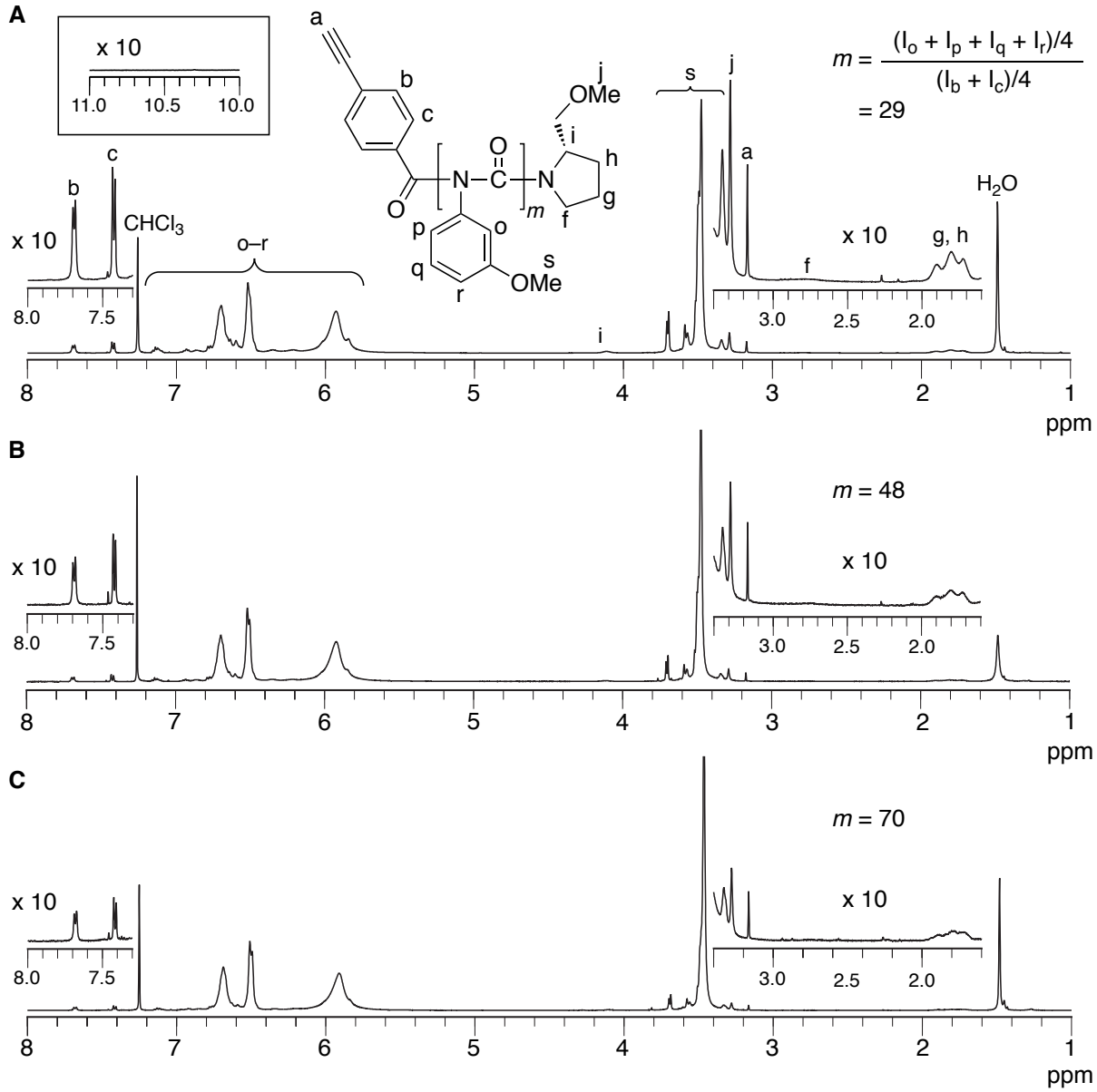

Figure 1-5. ^{1}H NMR (500 MHz) spectra of macro-$\mathbf{1}_{29}$ (A), macro-$\mathbf{1}_{48}$ (B), and macro-$\mathbf{1}_{70}$ (C) in $CDCl_3$ at 50 °C.

Synthesis of polymer brushes. Polymer brushes (poly-$\mathbf{1}_m$) were synthesized by polymerization of the corresponding macromonomers macro-$\mathbf{1}_m$ using $Rh^+(nbd)[(\eta^6\text{-}C_6H_5)B^-(C_6H_5)_3]$ as a catalyst (Scheme 1-1). A typical experimental procedure is described below.

Macro-$\mathbf{1}_{29}$ (63 mg, 0.014 mmol) was placed in a dry ampoule, which was then evacuated on a vacuum line and flushed with dry nitrogen. After this evacuation-flush procedure was repeated three times, anhydrous THF (0.08 mL) was added to the ampoule with a syringe to dissolve macro-$\mathbf{1}_{29}$. A solution of $Rh^+(nbd)[(\eta^6\text{-}C_6H_5)B^-(C_6H_5)_3]$ (3.95 mM) in THF at 30 °C was added, giving a concentration of macro-$\mathbf{1}_{29}$ and rhodium catalyst of 0.105 and 0.0015 M, respectively. After 5 h at 30 °C, the resulting polymer brush was precipitated by addition of a large amount of MeOH, collected by centrifugation, and dried *in vacuo* at room temperature overnight (59 mg, 93% yield). Poly-$\mathbf{1}_{29}$ was soluble in DMSO, THF, and $CHCl_3$. The molecular weight (M_n) and distribution (M_w/M_n) of the poly-$\mathbf{1}_{29}$ were estimated to be 5.9×10^5 and 2.02, respectively, as determined by SEC using a polystyrene standard and $CHCl_3$ as the eluent. The stereoregularity of poly-$\mathbf{1}_{29}$ was investigated by NMR and Raman spectroscopies. However, it was difficult to evaluate the stereoregularity of poly-$\mathbf{1}_{29}$ from its ^1H NMR spectrum (Figure 1-6) because the signals from the main chain protons, which are highly useful for assigning the conformation and configuration of the polyacetylene backbone,[11b, 15] could hardly be observed because of their very weak intensities relative to those of the protons of the pendant polyisocyanates. The Raman spectrum of poly-$\mathbf{1}_{29}$ gave useful information and exhibited intense peaks at 1576, 1338, and 972 cm^{-1}, which are characteristic of *cis* polyacetylenes and can be assigned to the C=C, C-C and C-H bond vibrations, respectively, while those consistent with *trans* polyacetylenes were not observed (Figure 1-7).[16] This indicates that the obtained poly-$\mathbf{1}_{29}$ possesses a highly *cis-transoidal* structure.

Spectroscopic data of poly-$\mathbf{1}_{29}$: IR (KBr): ν 1726 (C=O of polyisocyanate) cm^{-1}. Anal. Calcd for $C_6H_{12}NO(C_8H_7NO_2)_{29}C_9H_5O{\cdot}4H_2O$: C, 63.93; H, 4.95; N, 9.05. Found: C, 64.00; H, 4.86; N, 8.75. For ^1H NMR, see Figure 1-6A.

Poly-$\mathbf{1}_{48}$ and poly-$\mathbf{1}_{70}$ were synthesized by the polymerization of macro-$\mathbf{1}_{48}$ and macro-$\mathbf{1}_{70}$, respectively, using the same procedure described for poly-$\mathbf{1}_{29}$; polymerization results are summarized in Table 1-2. In the case of polymerization of macro-$\mathbf{1}_{48}$ and macro-$\mathbf{1}_{70}$, SEC measurements of the components that were insoluble in MeOH showed a bimodal SEC trace, suggesting that these polymers contain the unreacted macromonomers. To remove these unreacted macromonomers, this component was dissolved in THF and then the solution was poured into a large amount of MeOH-THF (3:2 (v/v) for poly-$\mathbf{1}_{48}$ or 1:1 (v/v) for poly-$\mathbf{1}_{70}$). The resulting precipitate was collected by centrifugation and dried *in vacuo* at room temperature overnight to give poly-$\mathbf{1}_{48}$ and poly-$\mathbf{1}_{70}$ with unimodal SEC traces. ^{1}H NMR spectra of poly-$\mathbf{1}_{48}$ and poly-$\mathbf{1}_{70}$ are shown in Figure 1-6B and Figure 1-6C, respectively.

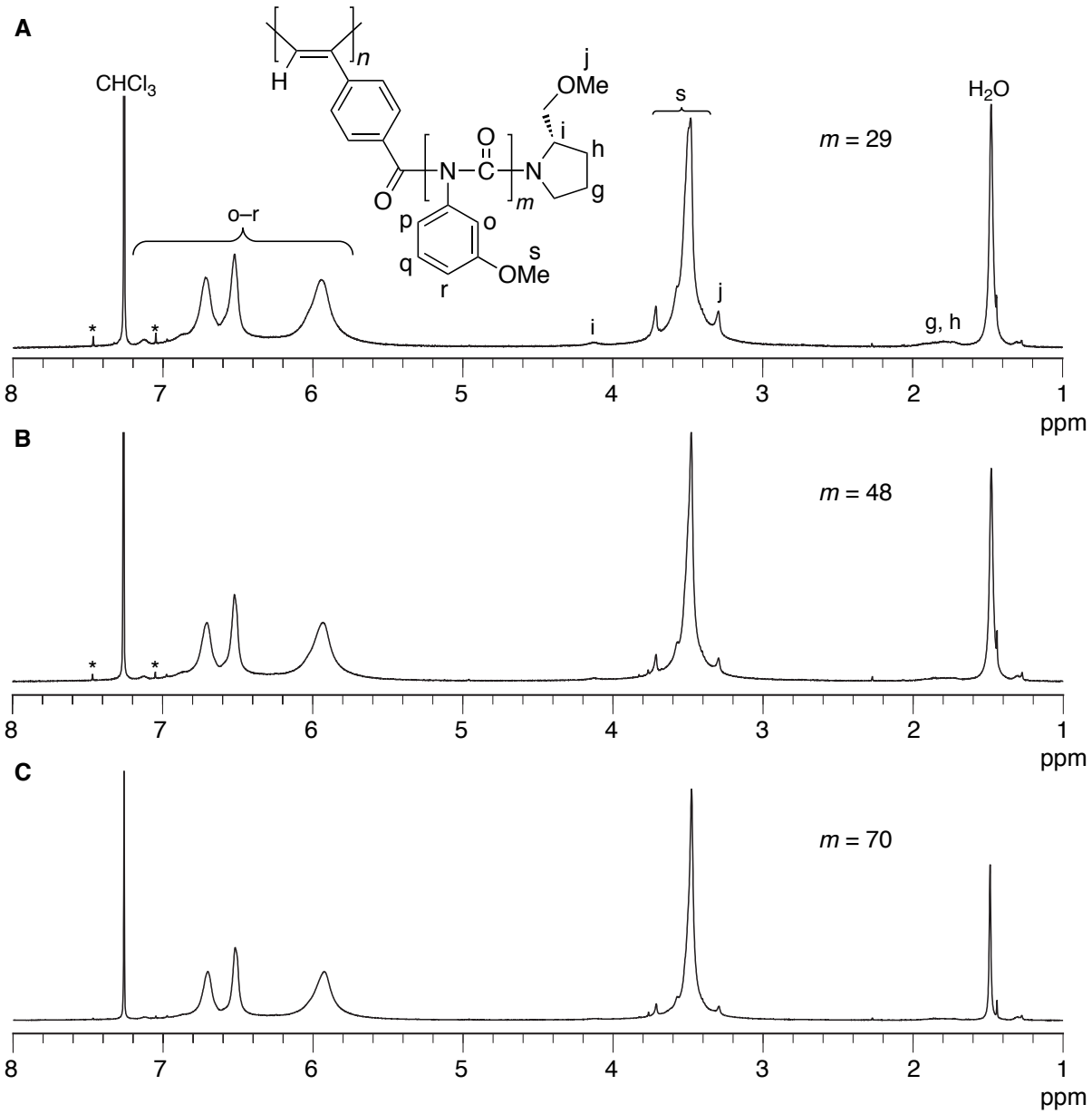

Figure 1-6. ^{1}H NMR (500 MHz) spectra of poly-$\mathbf{1}_{29}$ (A), poly-$\mathbf{1}_{48}$ (B), and poly-$\mathbf{1}_{70}$ (C) in $CDCl_3$ at 50 °C. "*" denotes the spinning side band.

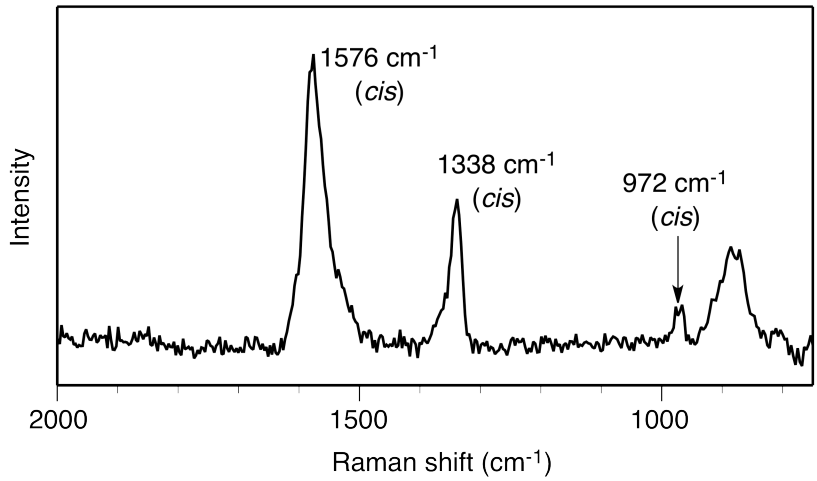

Figure 1-7. Raman spectrum of poly-$\mathbf{1}_{29}$ in the film state.

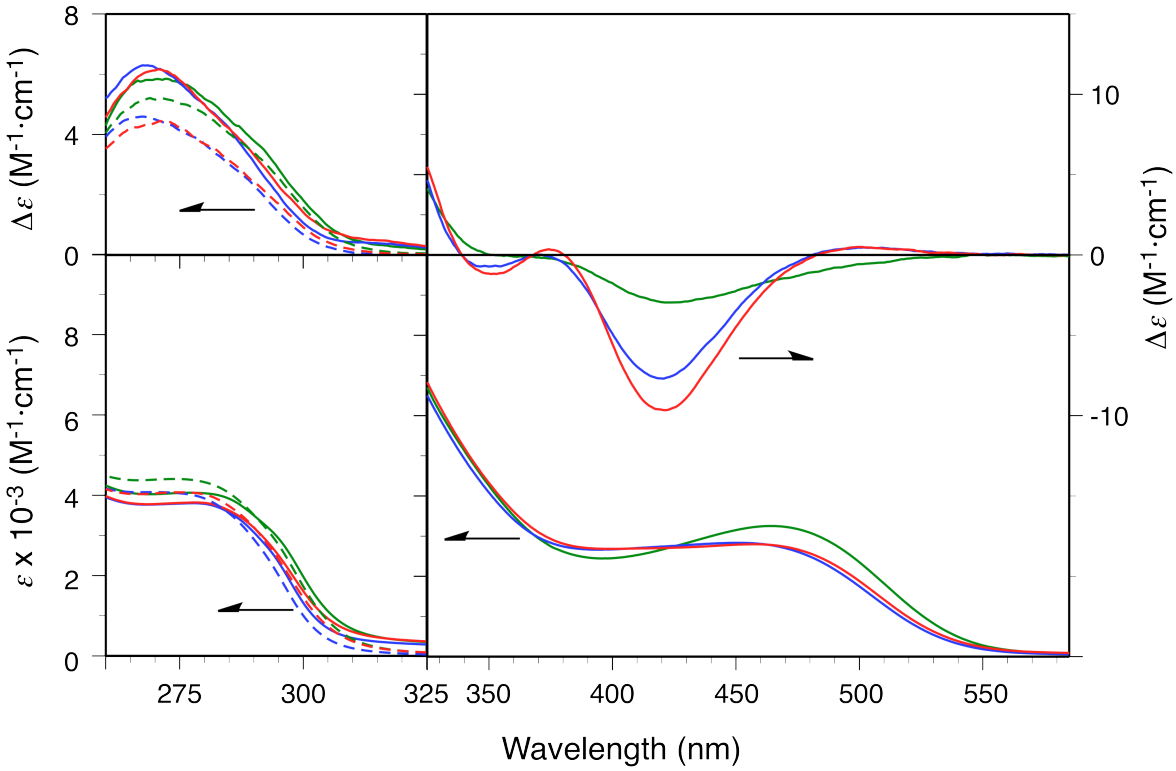

Figure 1-8. CD and absorption spectra of macro-$\mathbf{1}_{29}$ (dotted line) and poly-$\mathbf{1}_{29}$ (solid line) in DMSO (red), THF (blue), and $CHCl_3$ (green) at 25 °C. The molar ellipticity ($\Delta\varepsilon$) and molar absorption coefficient (ε) were calculated using the molar concentration of 3MeOPI (260–325 nm) and macro-$\mathbf{1}_{29}$ (> 325 nm).

References

1. (a) Saenger, W., *Principles of Nucleic Acid Structure*. Springer-Verlag: New York, 1984; (b) Branden, C.; J., T., *Introduction to Protein Structure*. 2nd ed.; Garland Publishing: New York, 1999.
2. For reviews on artificial helical polymers and oligomers, see: (a) Gellman, S. H., *Acc. Chem. Res.* **1998**, *31*, 173-180; (b) Green, M. M.; Park, J. W.; Sato, T.; Teramoto, A.; Lifson, S.; Selinger, R. L. B.; Selinger, J. V., *Angew. Chem., Int. Ed.* **1999**, *38*, 3138-3154; (c) Hill, D. J.; Mio, M. J.; Prince, R. B.; Hughes, T. S.; Moore, J. S., *Chem. Rev.* **2001**, *101*, 3893-4011; (d) Nakano, T.; Okamoto, Y., *Chem. Rev.* **2001**, *101*, 4013-4038; (e) Cornelissen, J. J. L. M.; Rowan, A. E.; Nolte, R. J. M.; Sommerdijk, N. A. J. M., *Chem. Rev.* **2001**, *101*, 4039-4070; (f) Fujiki, M., *Macromol. Rapid Commun.* **2001**, *22*, 539-563; (g) Lam, J. W. Y.; Tang, B. Z., *Acc. Chem. Res.* **2005**, *38*, 745-754; (h) Maeda, K.; Yashima, E., *Top. Curr. Chem.* **2006**, *265*, 47-88; (i) Hecht, S.; Huc, I., *Foldamers: Structure, Properties, and Applications*. WILEY-VCH: Weinheim, 2007; (j) Yashima, E.; Maeda, K.; Furusho, Y., *Acc. Chem. Res.* **2008**, *41*, 1166-1180; (k) Li, Z.-T.; Hou, J.-L.; Li, C., *Acc. Chem. Res.* **2008**, *41*, 1343-1353; (l) Rudick, J. G.; Percec, V., *Acc. Chem. Res.* **2008**, *41*, 1641-1652; (m) Yashima, E.; Maeda, K.; Iida, H.; Furusho, Y.; Nagai, K., *Chem. Rev.* **2009**, *109*, 6102-6211.
3. (a) Pieroni, O.; Matera, F.; Ciardelli, F., *Tetrahedron Lett.* **1972**, *13*, 597-600; (b) Nakako, H.; Mayahara, Y.; Nomura, R.; Tabata, M.; Masuda, T., *Macromolecules* **2000**, *33*, 3978-3982; (c) Tabei, J.; Shiotsuki, M.; Sanda, F.; Masuda, T., *Macromolecules* **2005**, *38*, 5860-5867; (d) Ishiwari, F.; Nakazono, K.; Koyama, Y.; Takata, T., *Chem. Commun.* **2011**, *47*, 11739-11741.
4. Ousaka, N.; Takeyama, Y.; Iida, H.; Yashima, E., *Nat Chem* **2011**, *3*, 856-861.
5. (a) Okamoto, Y.; Matsuda, M.; Nakano, T.; Yashima, E., *Polym. J.* **1993**, *25*, 391-396; (b) Okamoto, Y.; Matsuda, M.; Nakano, T.; Yashima, E., *J. Polym. Sci., Part A: Polym. Chem.* **1994**, *32*, 309-315.

6. (a) Inai, Y.; Tagawa, K.; Takasu, A.; Hirabayashi, T.; Oshikawa, T.; Yamashita, M., *J. Am. Chem. Soc.* **2000**, *122*, 11731-11732; (b) Inai, Y.; Ishida, Y.; Tagawa, K.; Takasu, A.; Hirabayashi, T., *J. Am. Chem. Soc.* **2002**, *124*, 2466-2473.
7. (a) Maeda, K.; Matsuda, M.; Nakano, T.; Okamoto, Y., *Polym. J.* **1995**, *27*, 141-146; (b) Maeda, K.; Okamoto, Y., *Polym. J.* **1998**, *30*, 100-105.
8. Lifson, S.; Felder, C. E.; Green, M. M., *Macromolecules* **1992**, *25*, 4142-4148.
9. Kishimoto, Y.; Itou, M.; Miyatake, T.; Ikariya, T.; Noyori, R., *Macromolecules* **1995**, *28*, 6662-6666.
10. (a) Aoki, T.; Kokai, M.; Shinohara, K.-i.; Oikawa, E., *Chem. Lett.* **1993**, *22*, 2009-2012; (b) Yashima, E.; Huang, S. L.; Matsushima, T.; Okamoto, Y., *Macromolecules* **1995**, *28*, 4184-4193; (c) Yashima, E.; Maeda, K.; Okamoto, Y., *Nature* **1999**, *399*, 449-451; (d) Morino, K.; Maeda, K.; Yashima, E., *Macromolecules* **2003**, *36*, 1480-1486; (e) Aoki, T.; Kaneko, T.; Maruyama, N.; Sumi, A.; Takahashi, M.; Sato, T.; Teraguchi, M., *J. Am. Chem. Soc.* **2003**, *125*, 6346-6347; (f) Cheuk, K. K. L.; Lam, J. W. Y.; Chen, J. W.; Lai, L. M.; Tang, B. Z., *Macromolecules* **2003**, *36*, 5947-5959; (g) Maeda, K.; Kamiya, N.; Yashima, E., *Chem. Eur. J.* **2004**, *10*, 4000-4010; (h) Maeda, K.; Mochizuki, H.; Osato, K.; Yashima, E., *Macromolecules* **2011**, *44*, 3217-3226.
11. (a) Green, M. M.; Zanella, S.; Gu, H.; Sato, T.; Gottarelli, G.; Jha, S. K.; Spada, G. P.; Schoevaars, A. M.; Feringa, B.; Teramoto, A., *J. Am. Chem. Soc.* **1998**, *120*, 9810-9817; (b) Nagai, K.; Sakajiri, K.; Maeda, K.; Okoshi, K.; Sato, T.; Yashima, E., *Macromolecules* **2006**, *39*, 5371-5380; (c) Ohsawa, S.; Sakurai, S.-i.; Nagai, K.; Banno, M.; Maeda, K.; Kumaki, J.; Yashima, E., *J. Am. Chem. Soc.* **2011**, *133*, 108-114.
12. Yashima, E.; Matsushima, T.; Okamoto, Y., *J. Am. Chem. Soc.* **1997**, *119*, 6345-6359.
13. Schrock, R. R.; Osborn, J. A., *Inorg. Chem.* **1970**, *9*, 2339-2343.
14. Yashima, E.; Maeda, K.; Sato, O., *J. Am. Chem. Soc.* **2001**, *123*, 8159-8160.
15. (a) Simionescu, C. I.; Percec, V.; Dumitrescu, S., *J. Polym. Sci., Part A: Polym. Chem.* **1977**, *15*, 2497-2509; (b) Simionescu, C. I.; Percec, V., *Prog. Polym. Sci.* **1982**, *8*, 133-214; (c) Furlani, A.; Napoletano, C.; Russo, M. V.; Feast, W. J., *Polym. Bull.* **1986**, *16*,

311-317; (d) Matsunami, S.; Kakuchi, T.; Ishii, F., *Macromolecules* **1997**, *30*, 1074-1078; (e) Kishimoto, Y.; Eckerle, P.; Miyatake, T.; Kainosho, M.; Ono, A.; Ikariya, T.; Noyori, R., *J. Am. Chem. Soc.* **1999**, *121*, 12035-12044; (f) Percec, V.; Rudick, J. G.; Peterca, M.; Wagner, M.; Obata, M.; Mitchell, C. M.; Cho, W. D.; Balagurusamy, V. S. K.; Heiney, P. A., *J. Am. Chem. Soc.* **2005**, *127*, 15257-15264; (g) Sakurai, S. I.; Okoshi, K.; Kumaki, J.; Yashima, E., *Angew. Chem., Int. Ed.* **2006**, *45*, 1245-1248; (h) Sakurai, S. I.; Okoshi, K.; Kumaki, J.; Yashima, E., *J. Am. Chem. Soc.* **2006**, *128*, 5650-5651.

16. (a) Shirakawa, H.; Ito, T.; Ikeda, S., *Polym. J.* **1973**, *4*, 460-462; (b) Tabata, M.; Tanaka, Y.; Sadahiro, Y.; Sone, T.; Yokota, K.; Miura, I., *Macromolecules* **1997**, *30*, 5200-5204.

Chapter 2

Chiral Amplification in Polymer Brushes Consisting of Dynamic Helical Polymer Chains through Long-Range Communication of Stereochemical Information

Abstract: Efficient hierarchical amplification of macromolecular helicity through long-range chiral information transfer was achieved in poly(phenylacetylene)-based copolymer brushes bearing poly(phenyl isocyanate) pendants with and without an optically active group at the pendant termini. When an optically active group was only partially introduced at the pendant termini far away from the backbone by the distance corresponding to more than about 27 bond lengths (*ca.* > 4 nm), the stereochemical information was effectively transmitted to the polyacetylene backbone through the helical chirality of the pendant polyisocyanate by covalent-bonding chiral domino effect and both helical handedness of the polyacetylene backbone and the polyisocyanate pendants without an optically active terminal group were simultaneously controlled.

Introduction

Chiral amplification has gathered great interest because it is considered to be in connection with the origin of biomolecular homochirality in nature.[1] Moreover, chiral amplification is also useful in terms of methodology for efficiently synthesizing optically active chiral materials by using a tiny amount of optically active compounds.[2] In synthetic helical polymers, Green et al. discovered that the copolymerization of achiral isocyanates with a small amount of optically active ones produced optically active polyisocyanates with a greater excess of single- handed helical conformation and termed these chiral amplification phenomena the "sergeants and soldiers effect".[1a, b, 3] Since the pioneering work, similar chiral amplification phenomena have been reported for other various helical polymers[4] and supramolecular systems.[1e, 1g, 5] However, it has been demonstrated that introduction of stereocenters into pendants at positions removed from the polymer backbone results in an almost racemic helical conformation and optically active groups need to be introduced close to the polymer backbone to effectively control helicity.[6]

In Chapter 1, the author synthesized helical polymer brushes composed of poly(phenylacetylene) backbone and poly(phenyl isocyanate) pendants and found that the helical handedness of the polyacetylene backbone can be controlled through a covalent-bonding "chiral domino effect" by introducing an optically active group, such as (*S*)-2-(methoxymethyl)pyrrolidinyl ((*S*)-MMP) group, only at the pendant termini.[7] In these polymer brushes, the polyacetylene backbone formed a predominantly one-handed helical conformation even if the chiral groups are separated from the backbone by seventy achiral isocyanate units. Here the author reports the first efficient and clear example of amplification of macromolecular helicity based on "the sergeants and soldiers effect" through long-range stereochemical communication in a series of poly(phenylacetylene)-based copolymer brushes bearing poly(phenyl isocyanate) pendants with an optically active group and an achiral group at the pendant termini (poly-(**1**S_r-*co*-**2**$_{1-r}$) and poly-(**1**R_r-*co*-**2**$_{1-r}$)) (Figure 2-1). Moreover, the author also found that the helical handedness of the polyisocyanate pendants without an

optically active terminal group is simultaneously controlled (Figure 2-2). Recently, long-range stereochemical communication over the nanomer scale has been gathered much interest from the view point of the mimic of biological system.[8, 9] However, the amplification of macromolecular helicity based on "the sergeants and soldiers effect" through long-range stereochemical communication has not been reported in dynamic helical polymers, except for dynamically chiral metal complexes.[8a, 8c]

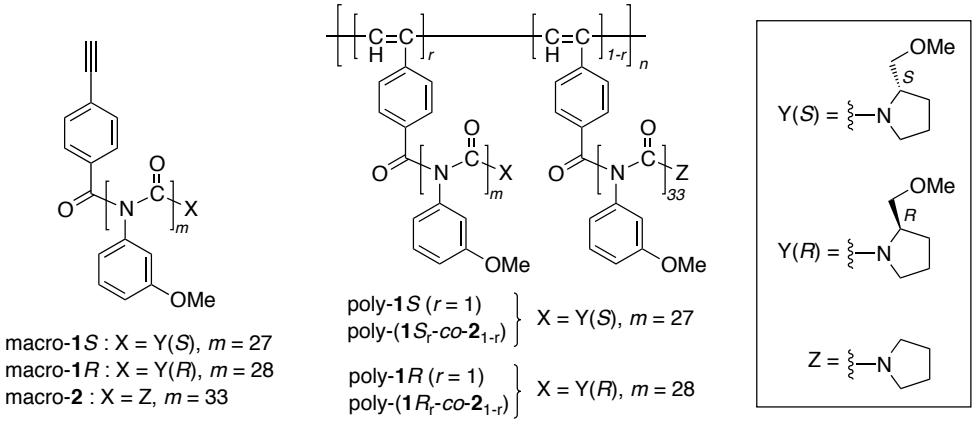

Figure 2-1. Structures of macromonomers (macro-**1***S*, macro-**1***R*, macro-**2**) and copolymer brushes (poly-**1***S*, poly-(**1***S*$_r$-*co*-**2**$_{1\text{-}r}$), poly-**1***R*, and poly-(**1***R*$_r$-*co*-**2**$_{1\text{-}r}$)).

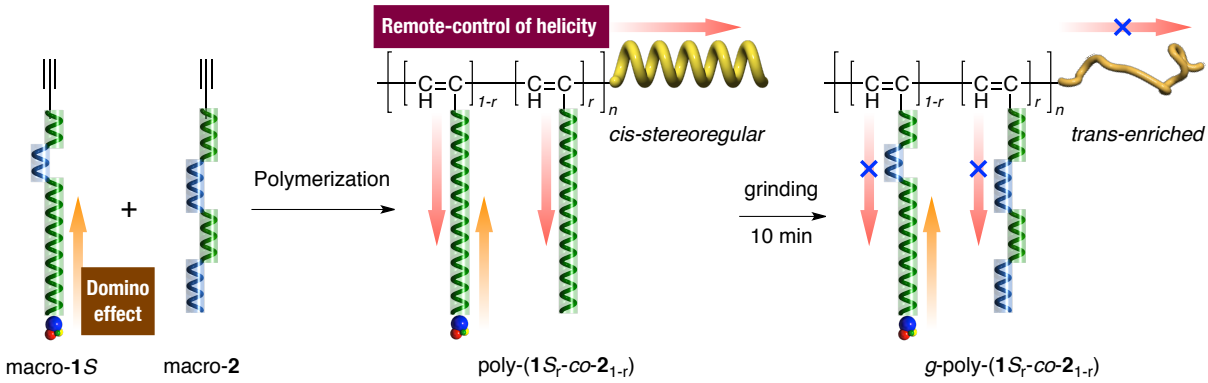

Figure 2-2. Schematic illustration of amplification of macromolecular helicity based on "sergeants and soldiers effect" through long-range communication of stereochemical information in copolymer brushes consisting of dynamic helical polymer chains (poly-(**1***S*$_r$-*co*-**2**$_{1\text{-}r}$)).

Results and Discussion

Optically active (macro-**1***S* and macro-**1***R*) and inactive (macro-**2**) macromonomers composed of poly(3-methoxyphenyl isocyanate) chain bearing an enantiopure (*S*)- or (*R*)-MMP and an achiral pyrrolidinyl group, respectively, at the initial chain end (α-end) and a polymerizable phenylacetylene moiety at the other (ω-end) were synthesized according to the reported method (Figure 2-1).[7, 10] The degree of polymerizations (*m*) of macro-**1***S*, macro-**1***R*, and macro-**2** were determined to be 27, 28, and 33, respectively, by ^{1}H NMR analysis (Figure 2-8 in the Experimental Section). Macro-**1***S* and macro-**1***R* in THF showed mirror images of intense induced circular dichroisms (ICDs) in the absorption region of polyisocyanate backbone (*ca*. 265 nm), indicating that these macromonomers form a predominantly one-handed helical conformation biased by the terminal optically active group through covalent bonding domino effect, while macro-**2** devoid of the terminal optically active group showed no ICD.[7, 10] The copolymerizations of macro-**1***S* or macro-**1***R* with macro-**2** at different feed ratios using a rhodium complex Rh(nbd)BPh_4 (nbd = 2,5-norbornadiene) in tetrahydrofuran (THF) afforded poly-(**1***S*$_r$-*co*-**2**$_{1-r}$) and poly-(**1***R*$_r$-*co*-**2**$_{1-r}$) with high molecular weight in high yields (> 90%) as shown in Table 2-1. Poly-**1***S* and poly-**1***R* were also synthesized by the homopolymerization of macro-**1***S* and macro-**1***R*, respectively, in the same way (Table 2-1). The *cis*-stereoregular structures of the obtained polymer brushes were confirmed by laser Raman spectroscopy (Figure 2-10(A) in the Experimental Section).[11]

Table 2-1. Copolymerization Results of Optically Active (macro-**1***S* or macro-**1***R*) and Optically Inactive (macro-**2**) Macromonomers with $Rh(nbd)BPh_4$ in THF at 30 °C for 5 h[a]

run	macro-**1***S* (mol %)	macro-**1***R* (mol %)	macro-**2** (mol %)	*r*	polymer			
					sample code	yield (%)[b]	M_n x 10^{-5} [c]	M_w/M_n [c]
1	100	—	0	1	poly-**1***S*	98	1.2	3.5
2	75	—	25	0.75	poly-(**1***S*$_{0.75}$-*co*-**2**$_{0.25}$)	96	1.4	3.1
3	50	—	50	0.50	poly-(**1***S*$_{0.5}$-*co*-**2**$_{0.5}$)	94	1.5	3.3
4	25	—	75	0.25	poly-(**1***S*$_{0.25}$-*co*-**2**$_{0.75}$)	93	1.5	3.2
5	10	—	90	0.10	poly-(**1***S*$_{0.1}$-*co*-**2**$_{0.9}$)	97	1.1	3.2
6	—	100	0	1	poly-**1***R*	92	1.1	3.2
7	—	75	25	0.75	poly-(**1***R*$_{0.75}$-*co*-**2**$_{0.25}$)	91	1.2	3.3
8	—	50	50	0.50	poly-(**1***R*$_{0.5}$-*co*-**2**$_{0.5}$)	94	1.4	3.7
9	—	25	75	0.25	poly-(**1***R*$_{0.25}$-*co*-**2**$_{0.75}$)	93	1.5	3.4

[a] [Macromonomer]/[Rh] = 100, [macromonomer] = 0.1 M. [b] MeOH-THF (2/1, v/v) insoluble fraction. [c] Determined by SEC (polystyrene standards) with $CHCl_3$ as the eluent.

To accurately investigate the preferred-handed helix induction in the polyacetylene backbone of the polymer brushes, the CD and absorption spectral measurements of the polymer brushes in the absorption region of polyacetylene backbone above 325 nm were performed by using a cell that was 10 times longer at a concentration that was 2 times higher (0.6 mg/mL) compared with those in the absorption region of pendant polyisocyanates below 325 nm because the concentration of the polyacetylene chromophore in the polymer brushes was much lower (*ca*. 1/30) than that of the polyisocyanate chromophore. The CD and absorption spectra of poly-(**1***S*$_r$-*co*-**2**$_{1-r}$) together with poly-**1***S* in THF at -10 °C are shown in Figure 2-3A. As previously reported for the homopolymer poly-**1***S*,[7] poly-(**1***S*$_r$-*co*-**2**$_{1-r}$) also exhibited intense ICDs in the absorption region of the polyacetylene backbone (> 325 nm) as well as in the absorption region of the polyisocyanate backbone (< 325 nm), indicating that a preferred-handed helical conformation was induced on the polyacetylene backbone of these polymer brushes. Figure 2-3B shows the plots of the ICD intensities of poly-(**1***S*$_r$-*co*-**2**$_{1-r}$) at 420 and 270 nm reflecting the helix-sense excess of the polyacetylene backbone and

polyisocyanate pendants, respectively, versus the content of the optically active macro-**1***S* units in the polymer brushes. The ICD intensities at 420 nm were out of proportion to the contents of macro-**1***S* units, showing a convex deviation from the linearity (see the red line in Figure 2-3B). Poly-(**1***S*$_r$-*co*-**2**$_{1-r}$) with even as small as 25 mol% of macro-**1***S* unit (r = 0.25) exhibited as an intense ICD as that of poly-**1***S*. This strong positive nonlinear effect clearly demonstrates that "sergeants and soldiers effect" appears in these polymer brushes despite the fact that the covalently bonded optically active groups are separated from the polyacetylene backbone by about twenty-seven achiral isocyanate units. To the best of the author's knowledge, this is the first clear example of the chiral amplification belonging to "sergeants and soldiers effect" through long-range chirality transmittance in dynamic helical polymers.

To our surprise, the ICD intensity of poly-(**1***S*$_r$-*co*-**2**$_{1-r}$) at 270 nm also nonlinearly increased with increasing macro-**1***S* unit content, showing a positive nonlinear effect. As previously reported, the ICD intensity of poly-**1***S* at 270 nm increased compared with that of the corresponding macromonomer macro-**1***S* (▲ in Figure 2-3B), suggesting that the helix-sense excess of the pendant polyisocyanate chains was amplified after conversion to the polymer brush. However, poly-(**1***S*$_r$-*co*-**2**$_{1-r}$) showed a more intense ICD intensity at 270 nm than that expected from poly-**1***S*. In the case of poly-(**1***R*$_r$-*co*-**2**$_{1-r}$) and poly-**1***R*, mirror-image results were obtained (Figure 2-4). These results indicate that a predominantly one-handed helical conformation was also induced on the polyisocyanate pendants corresponding to macro-**2** units without the terminal optically active group in the copolymer brushes. In order to confirm that the ICD at 270 nm is due to the helical screw sense preference of the polyisocyanate backbone, not due to the conformation adoption for the phenyl group against the polyisocyanate backbone,[12] the vibrational CD (VCD) spectra of the polymer brushes in THF at -10 °C were also measured. The VCD spectra of poly-(**1***S*$_r$-*co*-**2**$_{1-r}$) and poly-**1***S* exhibited characteristic Cotton effects in the C=O stretching band region of the polyisocyanate reflecting the preferred-handed helical structure of the polyisocyanate backbone, whose intensities (Δ_{abs} at 1753 cm^{-1}) also showed a positive nonlinear relationship

relative to the content of optically active units (Figure 2-5). These VCD results also support that a predominantly one-handed helical conformation was also induced on the polyisocyanate pendants without a terminal optically active group corresponding to macro-**2** units.

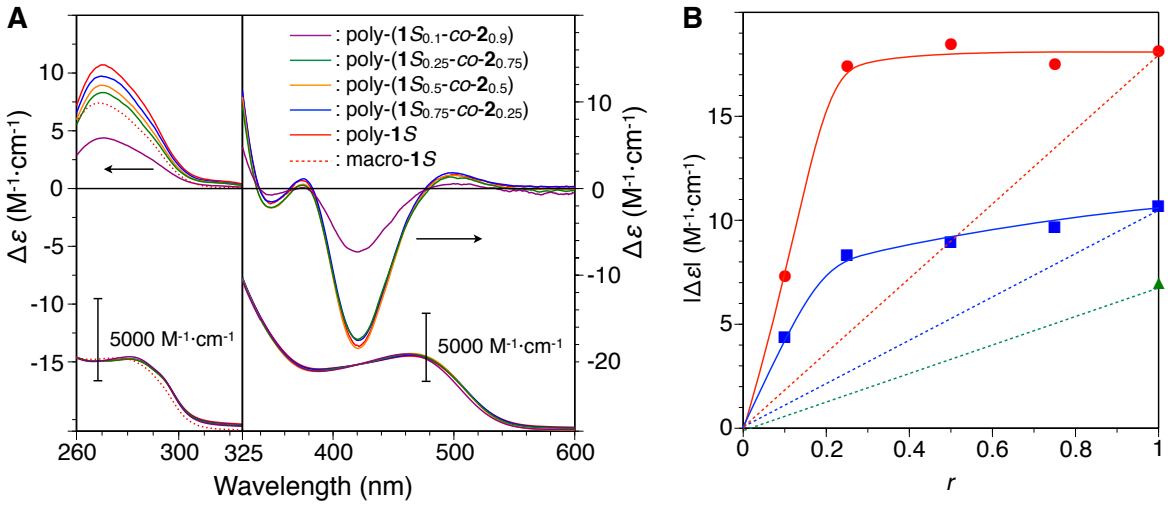

Figure 2-3. (A) CD and absorption spectra of macro-**1***S* (dotted red line), poly-**1***S* (red line), poly-(**1***S*$_{0.75}$-*co*-**2**$_{0.25}$) (blue line), poly-(**1***S*$_{0.5}$-*co*-**2**$_{0.5}$) (orange line), poly-(**1***S*$_{0.25}$-*co*-**2**$_{0.75}$) (green line), and poly-(**1***S*$_{0.1}$-*co*-**2**$_{0.9}$) (purple line) in THF at -10 °C. The molar ellipticity ($\Delta\varepsilon$) and molar absorption coefficient (ε) were calculated using the molar concentration of 3MeOPI (255–325 nm) and the corresponding macromonomers (> 325 nm). (B) Changes in the CD intensity at 420 nm (●, polyacetylene) and 270 nm (■, polyisocyanate) of poly-(**1***S*$_r$-*co*-**2**$_{1-r}$) versus the content of the optically active units (*r*) in THF at -10 °C. The CD intensity at 270 nm (▲, polyisocyanate) of macro-**1***S* is also plotted.

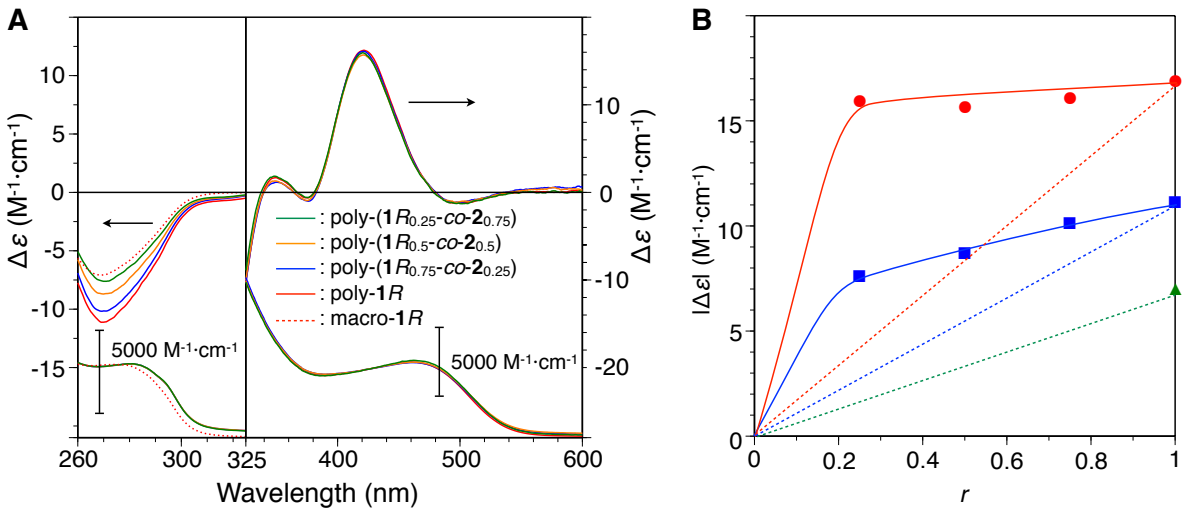

Figure 2-4. (A) CD and absorption spectra of macro-**1***R* (dotted red line), poly-**1***R* (red line), poly-(**1***R*$_{0.75}$-*co*-**2**$_{0.25}$) (blue line), poly-(**1***R*$_{0.5}$-*co*-**2**$_{0.5}$) (orange line), and poly-(**1***R*$_{0.25}$-*co*-**2**$_{0.75}$) (green line) in THF at -10 °C. The molar ellipticity (Δε) and molar absorption coefficient (ε) were calculated using the molar concentration of 3MeOPI (255–325 nm) and the corresponding macromonomers (> 325 nm). (B) Changes in the CD intensity at 420 nm (●, polyacetylene) and 270 nm (■, polyisocyanate) of poly-(**1***R*$_r$-*co*-**2**$_{1-r}$) versus the content of the optically active units (*r*) in THF at -10 °C. The CD intensity at 270 nm (▲, polyisocyanate) of macro-**1***R* is also plotted.

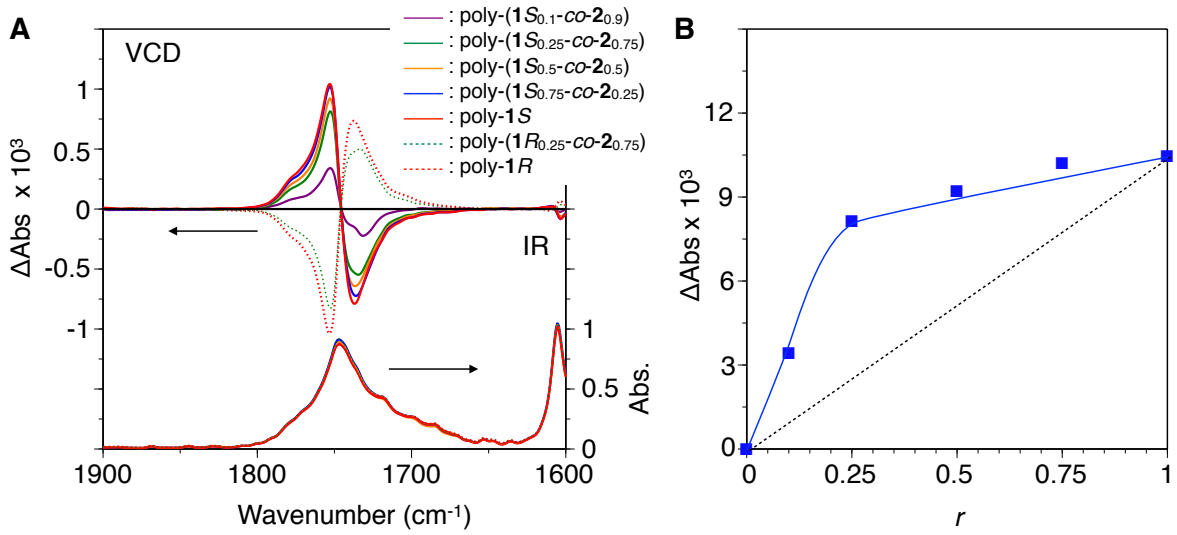

Figure 2-5. (A) VCD and IR spectra of poly-**1***S* (red line), poly-(**1***S*$_{0.75}$-*co*-**2**$_{0.25}$) (blue line), poly-(**1***S*$_{0.5}$-*co*-**2**$_{0.5}$) (orange line), poly-(**1***S*$_{0.25}$-*co*-**2**$_{0.75}$) (green line), poly-(**1***S*$_{0.1}$-*co*-**2**$_{0.9}$) (purple line), poly-**1***R* (dotted red line), and poly-(**1***R*$_{0.25}$-*co*-**2**$_{0.75}$) (dotted green line) in THF at -10 °C. (B) Changes in the VCD intensity (ΔAbs) at 1753 cm^{-1} of poly-(**1***S*$_r$-*co*-**2**$_{1-r}$) versus the content of the optically active units (*r*) in THF at -10 °C. The concentrations of poly-**1***S*, poly-(**1***S*$_r$-*co*-**2**$_{1-r}$), poly-**1***R*, and poly-(**1***R*$_{0.25}$-*co*-**2**$_{0.75}$) were 25 mg/mL in THF. All spectra were collected for *ca*. 1 h at a resolution of 4 cm^{-1}.

The author assumed that the preferred-handed macromolecular helicity induced in the polyacetylene backbone would largely contribute to the further helicity induction in the polyisocyanate pendants without the terminal optically active group in poly-(**1***S*$_r$-*co*-**2**$_{1-r}$) and poly-(**1***R*$_r$-*co*-**2**$_{1-r}$). To prove this, the *cis*-stereoregular poly-(**1***S*$_{0.25}$-*co*-**2**$_{0.75}$) was converted to the *trans*-enriched poly-(**1***S*$_{0.25}$-*co*-**2**$_{0.75}$) (*g*-poly-(**1***S*$_{0.25}$-*co*-**2**$_{0.75}$)) by grinding as confirmed by laser Raman spectroscopy because it is known that the *cis*-stereoregular main-chain structure is essential for the formation of a preferred-handed helical conformation in poly(phenylacetylene)s (Figure 2-10(B) in the Experimental Section).[11b, 13] The obtained *g*-poly-(**1***S*$_{0.25}$-*co*-**2**$_{0.75}$) almost lost its helical conformation, thus showing complete disappearance of the ICD in the polyacetylene backbone regions (Figure 2-6). As expected, *g*-poly-(**1***S*$_{0.25}$-*co*-**2**$_{0.75}$) showed a significantly decreased ICD at 270nm, whose intensity was

almost comparable to that of the mixture of macro-**1***S* with macro-**2** ([macro-**1***S*]/[macro-**2**] = 0.25/0.75, mol/mol) under the same condition. Moreover, the VCD intensity in the C=O stretching band region due to the polyisocyanate backbone of poly-(**1***S*$_{0.25}$-*co*-**2**$_{0.75}$) also remarkably decreased after conversion to *g*-poly-(**1***S*$_{0.25}$-*co*-**2**$_{0.75}$) to become almost identical to that of the mixture of macro-**1***S* with macro-**2** ([macro-**1***S*]/[macro-**2**] = 0.25/0.75, mol/mol)) (Figure 2-7). These results support that the preferred-handed helicity induction in dynamically racemic polyisocyanate pendants without the optically active terminal group can be mainly caused not by the chiral interaction with the neighboring preferred-handed polyisocyanate pendants with an optically active terminal but by the macromolecular helicity induced in the polyacetylene backbone.

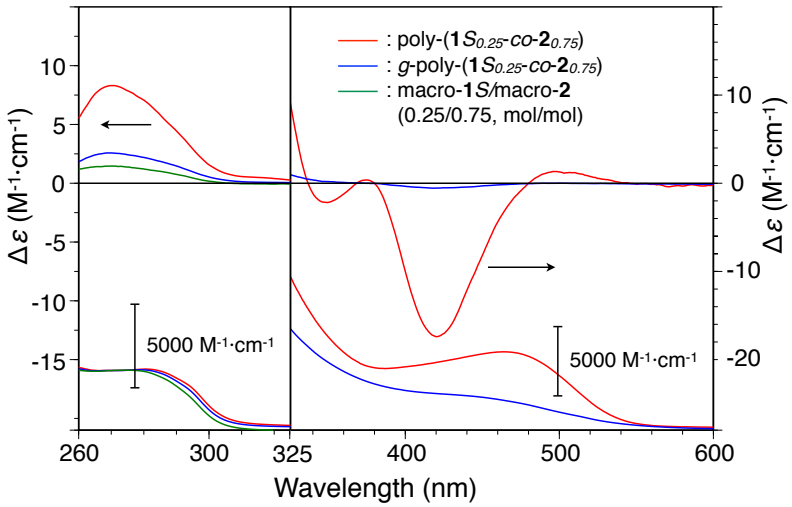

Figure 2-6. CD and absorption spectra of poly-(**1***S*$_{0.25}$-*co*-**2**$_{0.75}$) (red line) and *g*-poly-(**1***S*$_{0.25}$-*co*-**2**$_{0.75}$) (blue line) grinding and the mixture of macro-**1***S* and macro-**2** ([macro-**1***S*]/[macro-**2**] = 25/75, mol/mol) (green line) in THF at -10 °C. The molar ellipticity ($\Delta\varepsilon$) and molar absorption coefficient (ε) were calculated using the molar concentration of 3MeOPI (255–325 nm) and the corresponding macromonomers (> 325 nm).

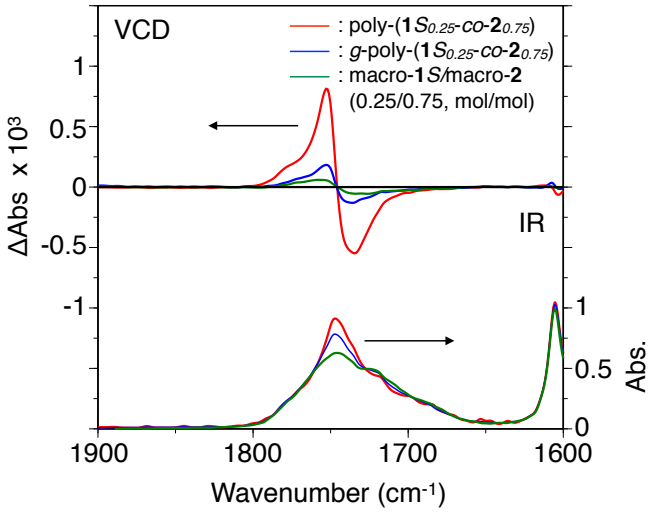

Figure 2-7. VCD and IR spectra of poly-(**1***S*$_{0.25}$-*co*-**2**$_{0.75}$) (red line) and *g*-poly-(**1***S*$_{0.25}$-*co*-**2**$_{0.75}$) (blue line) grinding and the mixture of macro-**1***S* and macro-**2** ([macro-**1***S*]/[macro-**2**] = 25/75, mol/mol) (green line) in THF at -10 °C. The concentrations of polymer brush and the mixture of macro-**1***S* and macro-**2** were 25 mg/mL in THF. All spectra were collected for *ca*. 1 h at a resolution of 4 cm^{-1}.

Conclusions

The present results clearly demonstrate that hierarchical long-range chirality transfer through helical chirality could occur in the copolymer brushes; the chirality of the optically active groups partially introduced at the pendant terminal was transmitted to the polyacetylene backbone through the helical chirality of the polyisocyanate pendants, which effectively induces the macromolecular helicity in the polyacetylene backbone with significant chiral amplification followed by the simultaneous helicity induction in the dynamically racemic polyisocyanate pendants without the optically active terminal group. In these copolymer brushes, the pendant helical polyisocyanate chains are arranged in a helical array with a preferred-handed helix-sense along the helical polyacetylene backbone accompanied by amplification of the helix-sense excess of the pendants. The author believes that the present methodology will be applicable to the combination of other dynamic helical polymers to arrange pendant helical polymer chains in preferred-handed helical arrays. Moreover, such helical polymer brushes may be useful as novel chiral materials for asymmetric catalysts and enantioselective selectors and work along this line is now in progress in our laboratory.

Experimental Section

Materials. Pyridine (Aldrich), pyrrolidine (Wako), and (*R*)- and (*S*)-2-(methoxymethyl)pyrrolidine ((*R*)- and (*S*)-MMP) (TCI) were dried over calcium hydride and distilled under high vacuum. TEA (Kanto Kagaku) was dried over KOH pellets under nitrogen and distilled onto 4 Å molecular sieves. These amines were stored under nitrogen. Anhydrous THF, DMSO, and CH_2Cl_2 were purchased from Kanto Kagaku. As the polymerization solvent, the as-purchased anhydrous THF was further dried over $LiAlH_4$ under nitrogen and vacuum-transferred to a dry glass ampoule just before polymerization. 3-Methoxyphenyl isocyanate (3MeOPI) (TCI) was dried over calcium hydride and distilled under high vacuum just before polymerization. Oxalyl chloride, *tert*-butyllithium (1.7 M in pentane), and anhydrous $CHCl_3$ were purchased from Aldrich. 4-Ethynylbenzoic acid[14] and $Rh^+(nbd)[(h^6\text{-}C_6H_5)B^-(C_6H_5)_3]$[15] were synthesized according to previously reported methods.

Instruments. NMR spectra were recorded on JEOL ECA500 (500 MHz for ^1H, 125 MHz for ^{13}C) or LA400 (400 MHz for ^1H) spectrometers (Tokyo, Japan) in CDCl3 using TMS as an internal standard. Number- (M_n) and weight-average (M_w) molecular weights of polymers were determined by size-exclusion chromatography (SEC) on a Tosoh TSKgel MultiporeH_{XL}-M column (Tokyo, Japan) using $CHCl_3$ as the eluent at a flow rate of 1.0 mL/min. The molecular weight calibration curve was obtained using polystyrene standards (Tosoh). IR spectra were recorded with a JASCO Fourier Transform IR-460 spectrophotometer (Hachioji, Japan). Absorption and circular dichroism (CD) spectra were measured in a quartz cell with a path length of 0.1 or 0.5 cm on a JASCO V-570 spectrophotometer and a JASCO J-725 spectropolarimeter, respectively. The temperature (-10–40 °C) was controlled with a JASCO ETC 505T (for absorption spectral measurements) and a JASCO 348WI apparatus (for CD spectral measurements). VCD spectra were measured in a 0.15-mm BaF_2 cell with a Jasco JV-2001YS spectrometer equipped with a temperature controller (EYELA NCB-1200). Elemental analyses were performed by the Research Institute

for Instrumental Analysis of Advanced Science Research Center, Kanazawa University, Kanazawa, Japan.

Synthesis of macromonomers. Macromonomers macro-**1***S*, macro-**1***R*, and macro-**2** were synthesized by the polymerization of 3MeOPI with the lithium amide of (*S*)-MMP (Li-(*S*)-MMP), (*R*)-MMP (Li-(*R*)-MMP), and pyrrolidine (Li-pyrrolidine), respectively as an initiator in a same manner to previously methods (Chapter 1).[7, 10] The results of polymerization are summarized in Table 2-2. ^{1}H NMR spectra of macro-**1***S*, macro-**1***R*, and macro-**2** are shown in Figure 2-8.

Table 2-2. Results of Anionic Polymerization of 3MeOPI in THF at -98 °C[a]

Run	Initiator	Polymer[b]				
		Sample code	Yield (%)	m[c]	$M_n \times 10^{-3}$ [d]	M_w/M_n[d]
1	Li-(*S*)-MMP	macro-**1***S*	40	27	3.0	1.2
2	Li-(*R*)-MMP	macro-**1***R*	39	28	3.1	1.2
3	Li-pyrrolidine	macro-**2**	51	33	3.5	1.2

[a][3MeOPI] = 0.67 M, [3MeOPI]/[initiator] = 10. [b]Hexane-EtOH (3/1, v/v) insoluble component after standing at 40 °C for 24 h in DMF. [c]DP determined by ^{1}H NMR in $CDCl_3$. [d]Determined by SEC (polystyrene standard, eluent: $CHCl_3$).

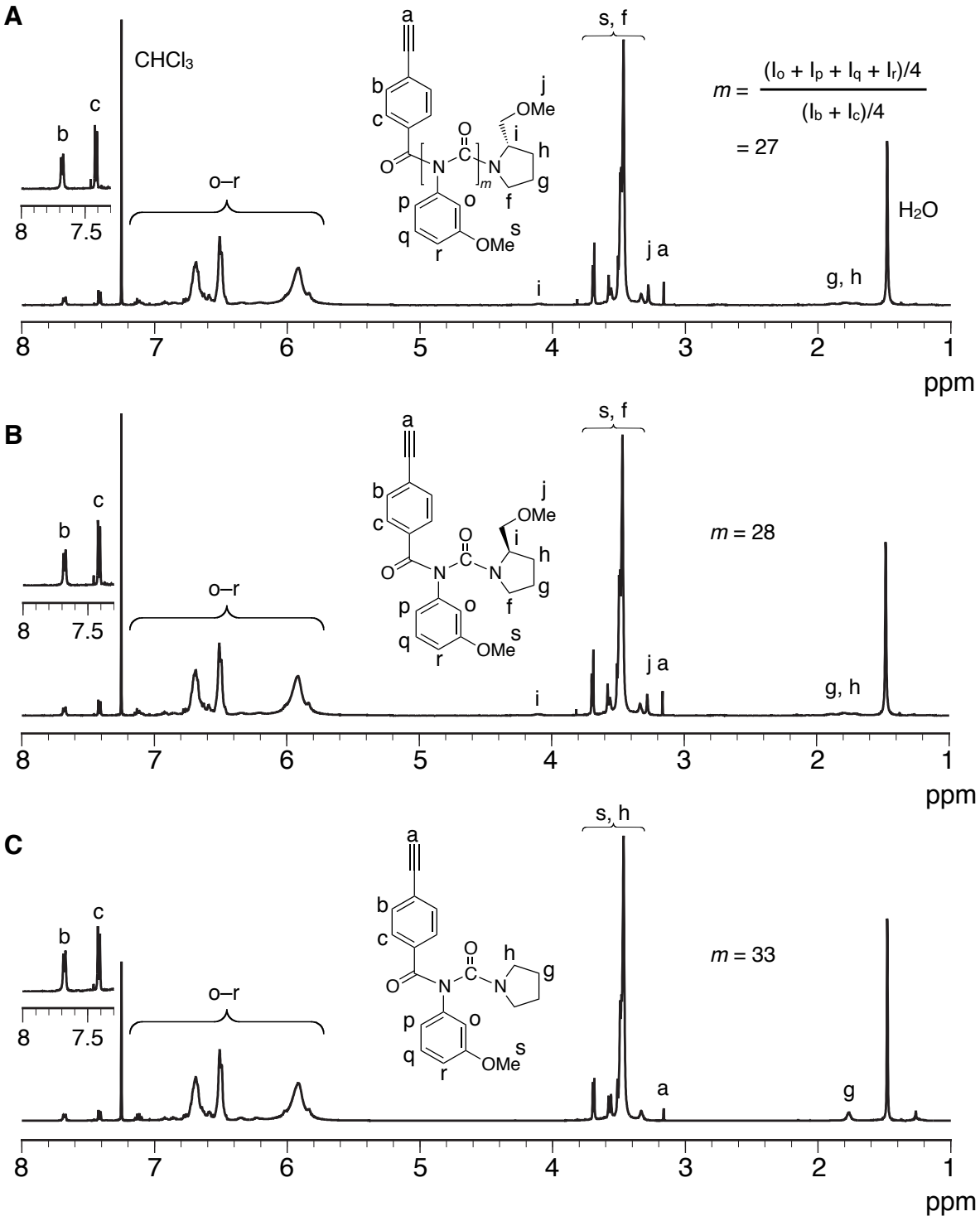

Figure 2-8. ^{1}H NMR (500 MHz) spectra of macro-**1***S* (A), macro-**1***R* (B), and macro-**2** (C) in $CDCl_3$ at 50 °C.

Synthesis of polymer brushes. Copolymerizations of macro-**1***S* and macro-**2** or macro-**1***R* and macro-**2** with different molar ratios and homopolymerizations of macro-**1***S* and macro-**1***R* were performed in a same manner to previously methods (Chapter 1).[7] The polymerization results are summarized in Table 2-1. The stereoregularity of poly-(**1***S*$_{0.25}$-*co*-**2**$_{0.75}$) was investigated by laser Raman spectroscopy and was highly *cis-transoidal* because ^{1}H NMR spectra was broad to determine the stereoregularity (see Figure 2-9 and Figure 2-10A).[11]

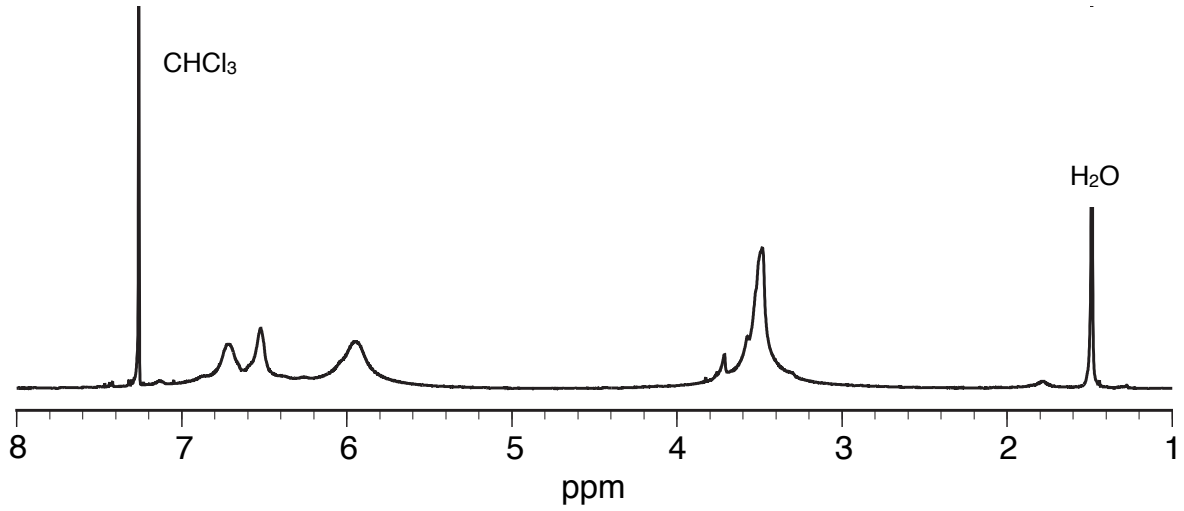

Figure 2-9. ^{1}H NMR (500 MHz) spectrum of poly-(**1***S*$_{0.25}$-*co*-**2**$_{0.75}$) in $CDCl_3$ at 50 °C.

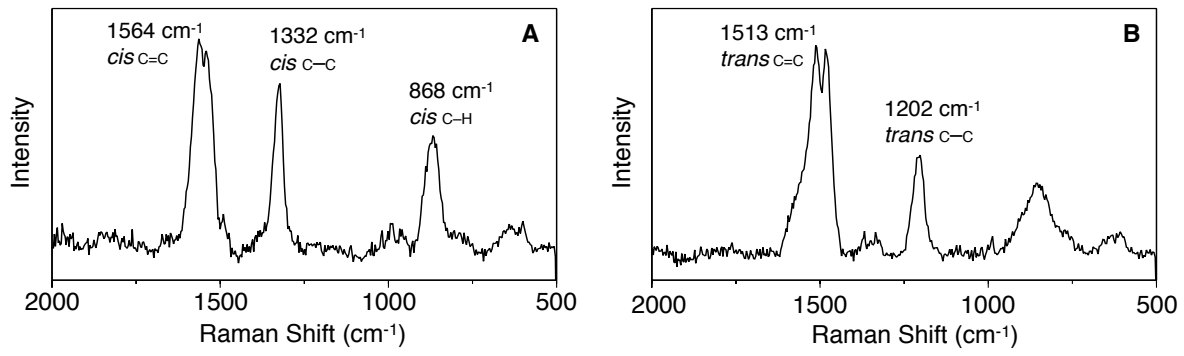

Figure 2-10. Laser Raman spectra of poly-(**1***S*$_{0.25}$-*co*-**2**$_{0.75}$) before (A) and after grinding (B) in the film state at room temperature (*ca*. 23 °C).

References

1. (a) Green, M. M.; Peterson, N. C.; Sato, T.; Teramoto, A.; Cook, R.; Lifson, S., *Science* **1995**, *268*, 1860-1866; (b) Green, M. M.; Park, J. W.; Sato, T.; Teramoto, A.; Lifson, S.; Selinger, R. L. B.; Selinger, J. V., *Angew. Chem., Int. Ed.* **1999**, *38*, 3138-3154; (c) Feringa, B. L.; van Delden, R. A., *Angew. Chem., Int. Ed.* **1999**, *38*, 3419-3438; (d) Eelkema, R.; Feringa, B. L., *Org. Biomol. Chem.* **2006**, *4*, 3729-3745; (e) Palmans, A. R. A.; Meijer, E. W., *Angew. Chem., Int. Ed.* **2007**, *46*, 8948-8968; (f) Kim, H.-J.; Lim, Y.-B.; Lee, M., *J. Polym. Sci., Part A: Polym. Chem.* **2008**, *46*, 1925-1935; (g) Pijper, D.; Feringa, B. L., *Soft Matter* **2008**, *4*, 1349-1372.
2. Noyori, R., *Angew. Chem., Int. Ed.* **2002**, *41*, 2008-2022.
3. Green, M. M.; Reidy, M. P.; Johnson, R. J.; Darling, G.; Oleary, D. J.; Willson, G., *J. Am. Chem. Soc.* **1989**, *111*, 6452-6454.
4. (a) Maeda, K.; Yashima, E., *Top. Curr. Chem.* **2006**, *265*, 47-88; (b) Yashima, E.; Maeda, K.; Nishimura, T., *Chem. Eur. J.* **2004**, *10*, 42-51; (c) Yashima, E.; Maeda, K.; Iida, H.; Furusho, Y.; Nagai, K., *Chem. Rev.* **2009**, *109*, 6102-6211; (d) Fujiki, M., *Macromol. Rapid Commun.* **2001**, *22*, 539-563.
5. (a) Mateos-Timoneda, M. A.; Crego-Calama, M.; Reinhoudt, D. N., *Chem. Soc. Rev.* **2004**, *33*, 363-372; (b) Praveen, V. K.; Babu, S. S.; Vijayakumar, C.; Varghese, R.; Ajayaghosh, A., *Bull. Chem. Soc. Jpn.* **2008**, *81*, 1196-1211; (c) Yamamoto, T.; Fukushima, T.; Aida, T., *Adv. Polym. Sci.* **2008**, *220*, 1-27.
6. (a) Pieroni, O.; Matera, F.; Ciardelli, F., *Tetrahedron Lett.* **1972**, *13*, 597-600; (b) Nakako, H.; Mayahara, Y.; Nomura, R.; Tabata, M.; Masuda, T., *Macromolecules* **2000**, *33*, 3978-3982; (c) Tabei, J.; Shiotsuki, M.; Sanda, F.; Masuda, T., *Macromolecules* **2005**, *38*, 5860-5867; (d) Ishiwari, F.; Nakazono, K.; Koyama, Y.; Takata, T., *Chem. Commun.* **2011**, *47*, 11739-11741.
7. Maeda, K.; Wakasone, S.; Shimomura, K.; Ikai, T.; Kanoh, S., *Chem. Commun.* **2012**, *48*, 3342-3344.

8. (a) Ousaka, N.; Takeyama, Y.; Iida, H.; Yashima, E., *Nat Chem* **2011**, *3*, 856-861; (b) Ousaka, N.; Grunder, S.; Castilla, A. M.; Whalley, A. C.; Stoddart, J. F.; Nitschke, J. R., *J. Am. Chem. Soc.* **2012**, *134*, 15528-15537; (c) Ousaka, N.; Takeyama, Y.; Yashima, E., *Chem. Eur. J.* **2013**, *19*, 4680-4685.
9. (a) Clayden, J.; Lund, A.; Vallverdu, L.; Helliwell, M., *Nature* **2004**, *431*, 966-971; (b) Clayden, J.; Lemiégre, L.; Morris, G. A.; Pickworth, M.; Snape, T. J.; Jones, L. H., *J. Am. Chem. Soc.* **2008**, *130*, 15193-15202; (c) Solà, J.; Fletcher, S. P.; Castellanos, A.; Clayden, J., *Angew. Chem., Int. Ed.* **2010**, *49*, 6836-6839.
10. (a) Okamoto, Y.; Matsuda, M.; Nakano, T.; Yashima, E., *J. Polym. Sci., Part A: Polym. Chem.* **1994**, *32*, 309-315; (b) Maeda, K.; Matsuda, M.; Nakano, T.; Okamoto, Y., *Polym. J.* **1995**, *27*, 141-146; (c) Maeda, K.; Okamoto, Y., *Polym. J.* **1998**, *30*, 100-105.
11. (a) Shirakawa, H.; Ito, T.; Ikeda, S., *Polym. J.* **1973**, *4*, 469-472; (b) Tabata, M.; Tanaka, Y.; Sadahiro, Y.; Sone, T.; Yokota, K.; Miura, I., *Macromolecules* **1997**, *30*, 5200-5204.
12. Tang, H.-Z.; Novak, B. M.; He, J.; Polavarapu, P. L., *Angew. Chem., Int. Ed.* **2005**, *44*, 7298-7301.
13. (a) Tang, Z.; Iida, H.; Hu, H.-Y.; Yashima, E., *ACS Macro Lett.* **2012**, *1*, 261-265; (b) Naito, Y.; Tang, Z.; Iida, H.; Miyabe, T.; Yashima, E., *Chem. Lett.* **2012**, *41*, 809-811.
14. Yashima, E.; Matsushima, T.; Okamoto, Y., *J. Am. Chem. Soc.* **1997**, *119*, 6345-6359.
15. (a) Schrock, R. R.; Osborn, J. A., *Inorg. Chem.* **1970**, *9*, 2339-2343; (b) Kishimoto, Y.; Itou, M.; Miyatake, T.; Ikariya, T.; Noyori, R., *Macromolecules* **1995**, *28*, 6662-6666.

Chapter 3

Switchable Enantioseparation Based on Reversible Switching and Memory of Macromolecular Helicity of a Polyacetylene in the Solid State

Abstract: The author reports here the dual chiral memory of both the conformationally labile macromolecular helicity and axial chirality of a polyacetylene bearing 2,2'-biphenol-derived pendants induced in the solid state as well as in solution by noncovalent interactions with a nonracemic alcohol through significant amplification of the chirality, followed by complete removal of the alcohol. The helical handedness and axial twist-sense of the polymer could be further reversibly switched in the solid state upon interaction with the opposite enantiomeric alcohol and its subsequent removal, which enables this polymer the first switchable chiral stationary phase in column liquid chromatography. The helical polyacetylene with a macromolecular helicity and axially twisting memory separates a racemic compound into the enantiomers and its elution order of the enantiomers can be switched by inverting and subsequent memory of the macromolecular helicity and axial twist-sense of the polymer in the column using the opposite enantiomeric alcohol as an eluent.

Introduction

The helix is a ubiquitous structural motif found in nature at the macromolecular and supramolecular levels as exemplified by the DNA double helix and the α-helix proteins. Due to the homochirality of their components (D-sugars and L-amino acids) endowed by Mother Nature, they have a one-handed helical structure that largely directs their sophisticated diverse functions in living systems. In polymer and supramolecular chemistry, control of helicity with a preferred handedness is an attractive challenge with implications for biological helicity and functions as well as to develop novel chiral materials for separating enantiomers and asymmetric catalysis.[1,2]

In earlier studies, Yashima and co-workers reported that an optically inactive polyacetylene, for example, poly((4-carboxyphenyl)acetylene), folds into a preferred handed helix induced by noncovalent acid-base interactions with a nonracemic amine. The helix is maintained, namely, *memorized* after the amine is replaced by achiral amines in solution under complete kinetic control.[2,3] Unlike previous approaches for helical polymer synthesis with optical activity, this strategy requires neither specific chiral monomers nor chiral catalysts for polymerization. However, the use of achiral amines is essential for the memory effect on the polyacetylenes.[2,3] Otherwise, the chiral memory is lost instantly as is in most cases observed in other chiral memory phenomena in supramolecular systems.[4]

The author herein reports the unprecedented reversible switching and memory of both the conformationally labile macromolecular helicity and axial chirality of an optically inactive polyacetylene bearing 2,2'-biphenol-derived pendants (poly-**1**) through noncovalent weak interactions with a nonracemic alcohol in the solid state as well as in solution. In sharp contrast to the previously observed chiral memory in polyacetylenes, the replacement with achiral compounds is no longer necessary for this unique switchable dual memory (Figure 3-1A) that is fully attained in the solid state. Although a number of studies on the noncovalent helicity induction in optically inactive polymers has been reported,[2] most of them are performed in solution and those in the solid state are quite rare.[5] Moreover, such switchable

helicity induction and memory in the solid state are unknown in polymer and supramolecular helical systems.[6] This has significant advantages from a practical point of view, over that in solution, and enables the present system an ideal chiral material for the separation of enantiomers as a chiral stationary phase (CSP) in column liquid chromatography whose enantioselectivity or elution order can be reversibly switched for the first time.

Separation of enantiomers, in particular by high-performance liquid chromatography (HPLC) is now an essential technique for the research and development of chiral drugs in the pharmaceutical industry and a number of CSPs has been commercialized. However, none of them can switch the elution order of enantiomers, which is one of the most important issues to resolve.[7] It is generally desirable that the minor enantiomer elutes first followed by the major one in terms of both the detection limit and the accuracy of the quantification in microanalysis of the chiral compounds.[8] For preparative separation of the enantiomers, the target enantiomer is required to elute first in order to obtain it with high optical purity because the first-eluting enantiomer often overlaps with the second one. The most convenient method for inverting the elution order is utilizing the CSPs prepared by each enantiomeric antipode. However, to the best of our knowledge, CSPs capable of inverting the enantioselectivity or the elution order of the enantiomers under identical chromatographic conditions are hitherto unknown.

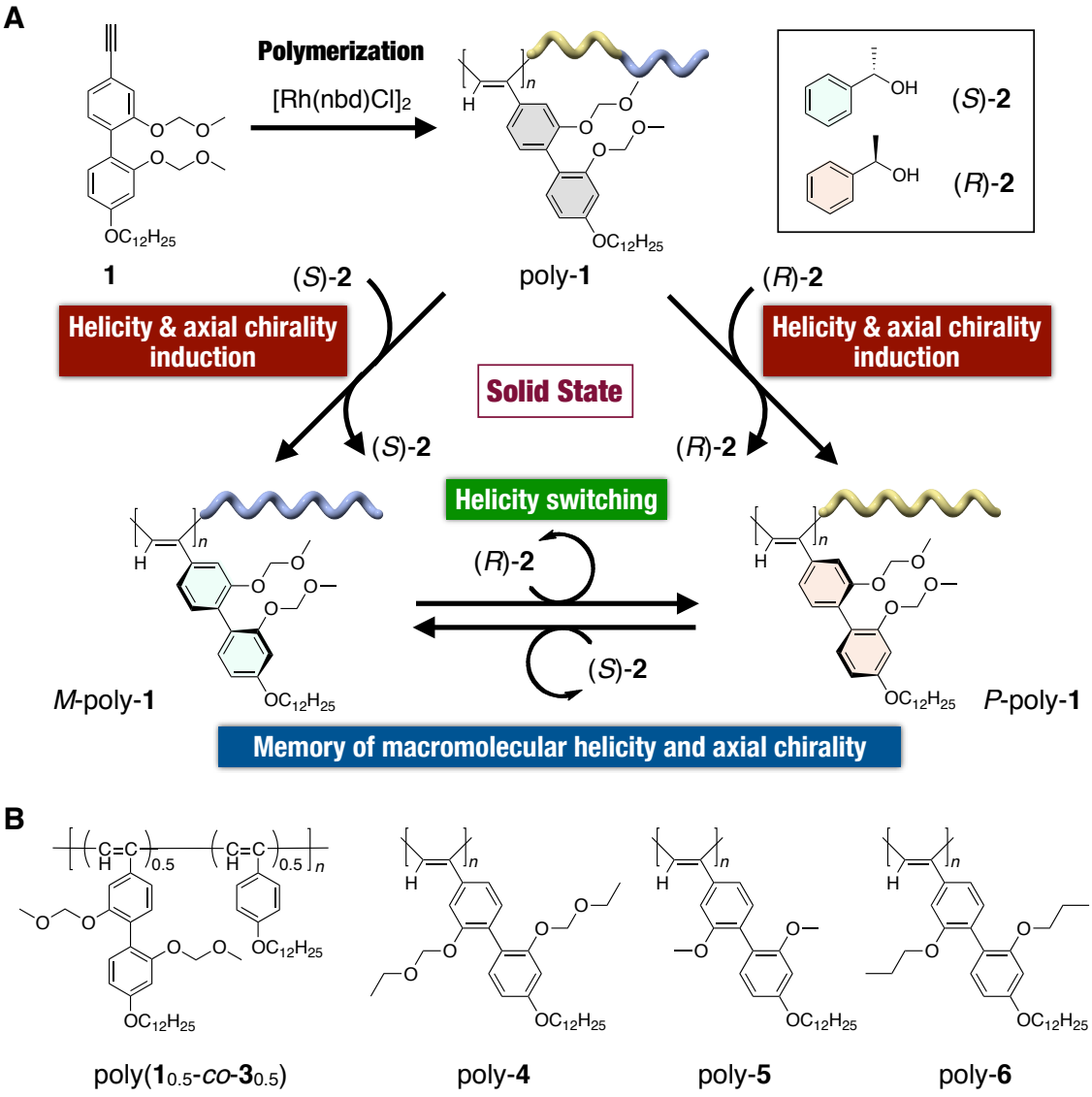

Figure 3-1. (A) Schematic illustration of reversible switching and memory of macromolecular helicity of poly-**1** and its axial chirality at the pendants in the solid state. Preferred-handed macromolecular helicity of poly-**1** and its axial chirality are induced and subsequently memorized in the optically inactive poly-**1** upon noncovalent interactions with a nonracemic alcohol (**2**) followed by complete removal of **2** in the solid state, and its helical handedness and axial twist-sense are reversibly switched in the solid state in the presence of the opposite enantiomeric alcohol. (B) Structures of the polymers.

Results and Discussion

A *cis-transoidal* stereoregular poly-**1** was synthesized by the polymerization of (2,2'-bis(methoxymethoxy)-4'-dodecyloxy-4-biphenylyl)acetylene (**1**) with a rhodium catalyst ($[Rh(nbd)Cl]_2$, nbd = norbornadiene) (Figure 3-1A) and was soluble in common organic solvents including *n*-hexane, but totally insoluble in alcohols, such as methanol and 1-phenylethanol (**2**). Poly-**1** formed a preferred-handed helix in the presence of (*S*)-1-phenylethanol ((*S*)-**2**) in *n*-hexane at 25 °C through noncovalent weak hydrogen-bonding interactions, thereby exhibiting a split-type induced circular dichroism (ICD) in the polymer backbone region (Figure 3-2A,i). The ICD intensity slightly increased with time and also at lower temperatures, reaching a near plateau value after 1 h (Figure 3-2B) and at -10 °C (Figure 3-2A,ii), respectively. The CD titration experiments of poly-**1** using (*S*)-**2** showed that the CD intensity increased with an increase in the concentration of (*S*)-**2** and reached an almost constant value in the presence of *ca*. 50 equivalent of (*S*)-**2** in *n*-hexane at 25 and -10 °C (Figure 3-3). Poly-**1** belongs to a class of dynamic helical polyacetylenes with a low helix inversion barrier,[2] therefore, nonracemic **2** with 40% enantiomeric excess (ee) efficiently biased the helical handedness via significant amplification of the helical chirality along the polymer chain, thus showing a full ICD as intense as that induced by the 100% ee of **2** in *n*-hexane (Figure 3-4).

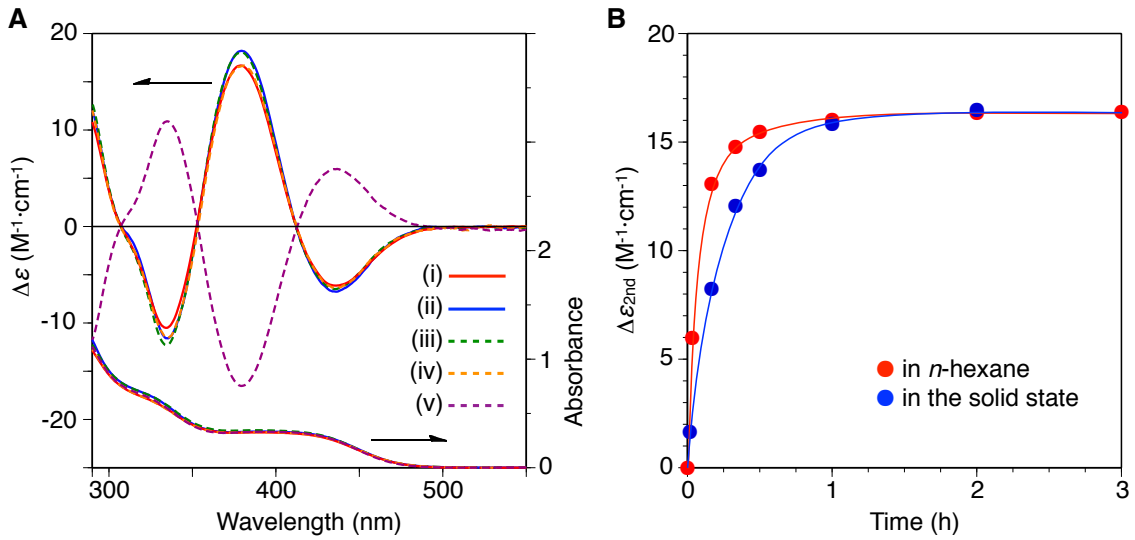

Figure 3-2. (A) CD and absorption spectra of poly-**1** with (*S*)-**2** ([(*S*)-**2**]/[poly-**1**] = 800) measured in *n*-hexane at 25 (i, red) and -10 °C (ii, blue) after standing at 25 °C for 6 h, and the isolated poly-**1** in *n*-hexane at -10 °C recovered from ii (iii, dotted green) and those of poly-**1** measured in *n*-hexane at -10 °C after immersing poly-**1** in (*S*)-**2** at 25 °C for 6 h in the solid state followed by isolation (iv, dotted orange) and subsequently immersing in (*R*)-**2** at 25 °C for 6 h (v, dotted purple). (B) Time-dependent CD intensity ($\Delta\varepsilon_{2nd}$) changes of poly-**1** with (*S*)-**2** in *n*-hexane at 25 °C (red) and those of poly-**1** measured in *n*-hexane at -10 °C after immersing poly-**1** in (*S*)-**2** in the solid state at 25 °C followed by isolation (blue). [Poly-**1**] = 1.0 mM.

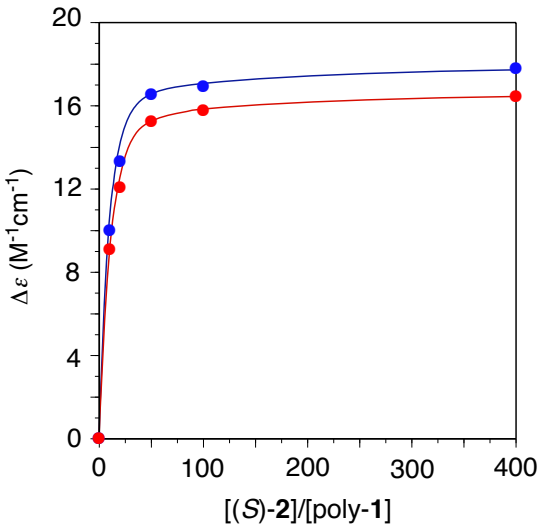

Figure 3-3. Titration curves ($\Delta\varepsilon_{2nd}$) of poly-**1** (1.0 mM) with (*S*)-**2** in *n*-hexane at 25 (●) and -10 °C (●) after standing at 25 °C for 6 h.

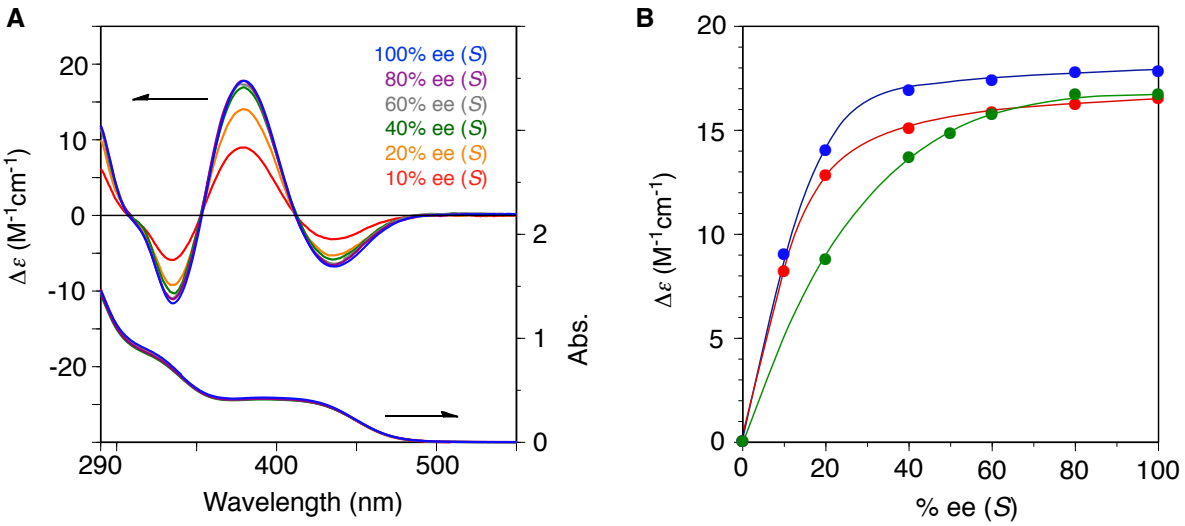

Figure 3-4. (A) CD and absorption spectra of poly-**1** (1.0 mM) with nonracemic **2** (*S*-rich, [**2**]/[poly-**1**] = 400) in *n*-hexane at -10 °C after standing at 25 °C for 6 h. (B) CD intensity ($\Delta\varepsilon_{2nd}$) changes of poly-**1** (1.0 mM) in *n*-hexane at 25 (●) and -10 °C (●) versus the % ee of **2** (*S*-rich, [**2**]/[poly-**1**] = 400) after standing in *n*-hexane at 25 °C for 6 h. The CD intensity changes ($\Delta\varepsilon_{2nd}$) of poly-**1** (1.0 mM) measured in *n*-hexane at -10 °C after immersing poly-**1** in nonracemic **2** (*S*-rich) in the solid state at 25 °C for 6 h followed by washing with methanol versus the % ee of **2** are also shown (●).

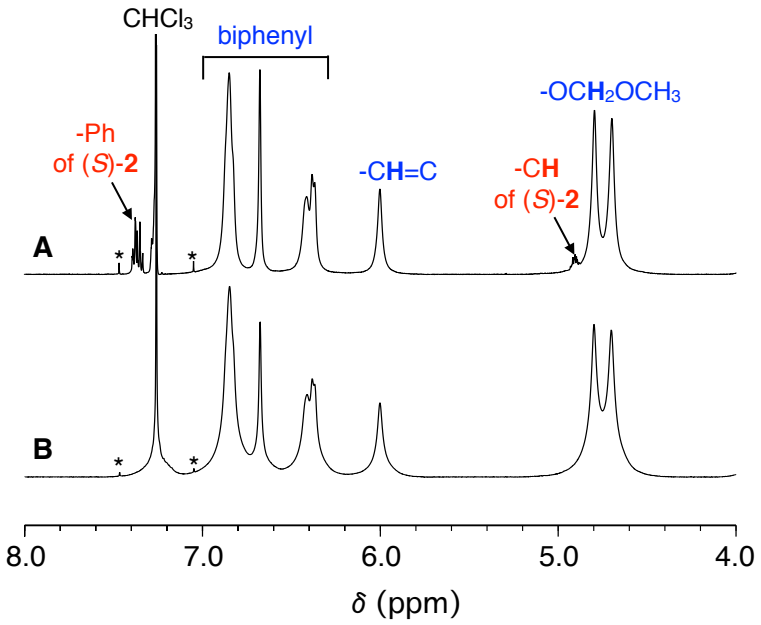

Figure 3-5. ^{1}H NMR spectra of poly-**1** with (*S*)-**2** ([(*S*)-**2**]/[poly-**1**] = 0.1) (A) and the isolated poly-**1** with helicity memory (B) in $CDCl_3$ at 50 °C. The asterisk denotes side bands of $CHCl_3$.

In strong contrast to the chiral memory observed in analogous polyacetylenes,[2,3] the induced helicity in poly-**1** retained after complete removal of (*S*)-**2** and nonracemic **2** by precipitation into methanol in the absence of achiral additives. ^{1}H NMR analysis of the isolated poly-**1** revealed that (*S*)-**2** was completely removed during precipitation of the optically active poly-**1** into methanol (Figure 3-5). The CD spectrum of the isolated poly-**1** dissolved in *n*-hexane at -10 °C (Figure 3-2A,iii) was in perfect agreement before isolation (Figure 3-2A,ii). The memory lasted for a rather long time with a half-life ($t_{1/2}$) of approximately 55 h in *n*-hexane at -10 °C (Figure 3-6). At higher temperatures (10 – 50 °C), the memory was lost rapidly and nonlinearly (Figure 3-7A). The author tried to estimate the activation energy for the racemization of the isolated poly-**1** with macromolecular helicity and axially twisting memory by Arrhenius plots of the kinetic data obtained from the time-dependent ICD intensity changes measured at several temperatures (10, 20, 30, 40, and 50 °C). However, the time-dependent ICD intensity changes due to the polymer backbone did not

obey a pseudo-first order kinetics (Figure 3-7B). The stability of the helicity memory of poly-**1** was highly dependent upon the solvents; once dissolved in tetrahydrofuran (THF) at 25 °C, the CD immediately disappeared within a few minutes. However, the helicity memory is not due to the formation of aggregates in *n*-hexane because the ICD intensity of the isolated poly-**1** hardly changed in the concentration range of 0.02–2 mM in *n*-hexane at -10 °C. Dynamic light scattering (DLS) measurements also support this conclusion; the hydrodynamic diameter (d_H) of the isolated poly-**1** in *n*-hexane (42 nm) was almost identical to that in THF (38 nm).

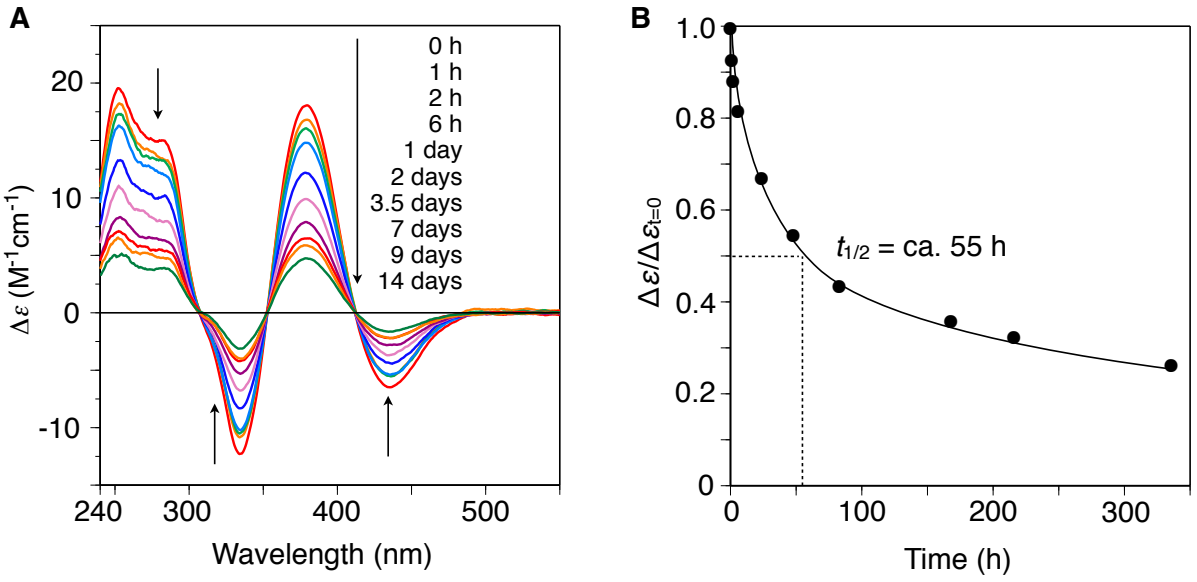

Figure 3-6. Time-dependent CD spectral changes of the isolated poly-**1** (1.0 mM) in *n*-hexane at -10 °C after helicity induction with (*S*)-**2** in *n*-hexane at 25 °C for 6 h (A) and the normalized CD intensity ($\Delta\varepsilon/\Delta\varepsilon_{t=0}$) changes against time (B). $\Delta\varepsilon_{t=0}$ represents the CD intensity of the isolated poly-**1** at 380 nm just after dissolution in *n*-hexane at -10 °C.

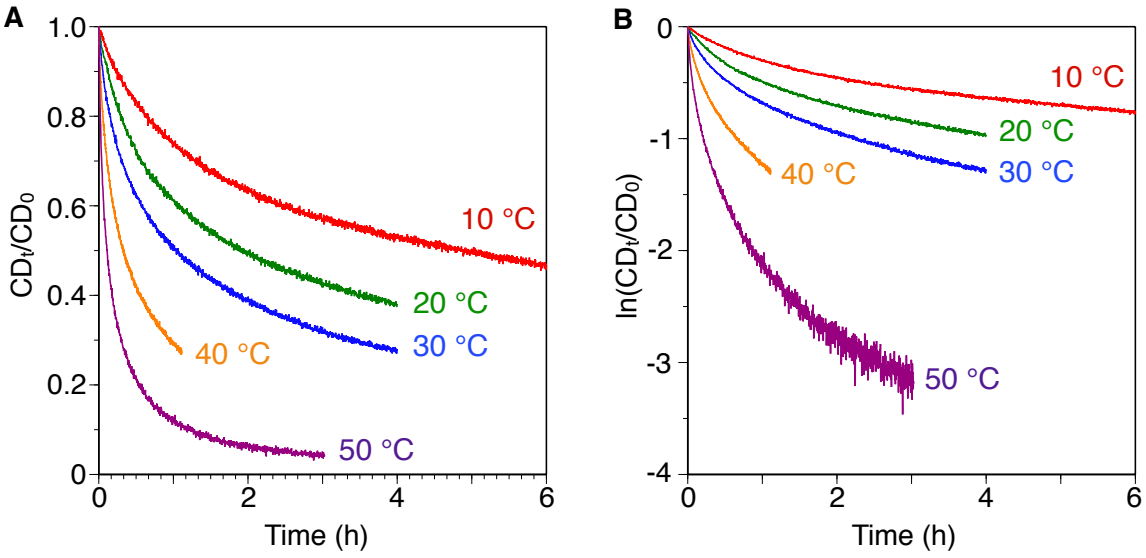

Figure 3-7. Stability of the macromolecular helicity memory of the isolated poly-**1** in *n*-hexane. Plots of the ICD intensity changes (CD_t/CD_0) (A) and $\ln(CD_t/CD_0)$ (B) at 10, 20, 30, 40, and 50 °C in *n*-hexane with time. The ICD intensity changes at 380 nm were directly followed at each temperature. CD_0 represents the initial ICD intensity of the isolated poly-**1** at 380 nm in *n*-hexane at each temperature.

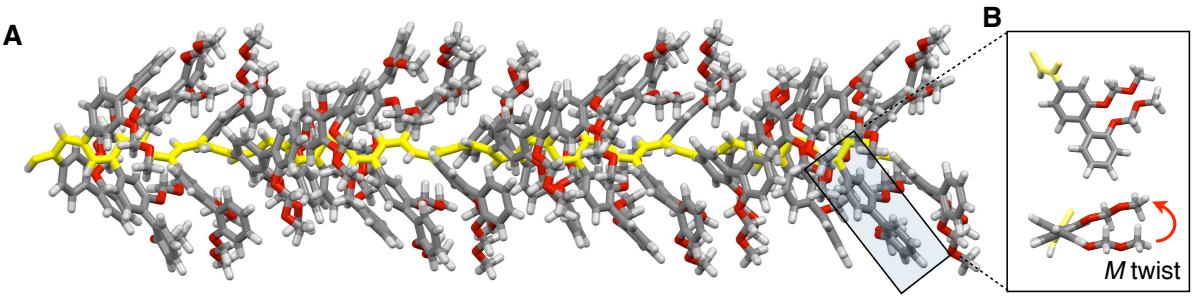

Figure 3-8. Structure of right-handed helical poly-**1**. (A) A possible structure of the right-handed helical poly-**1** induced by (*R*)-**2** (side view). The structure is represented by capped-stick models and the main-chain atoms are shown in a different color (yellow) for clarity. (B) The detailed conformation of the biphenyl pendant units of poly-**1** taken from A. The biphenyl units have a left-handed axially twisted conformation.

On the basis of the Cotton effect signs of the ICDs of analogous helical polyacetylenes and their helical senses determined by high-resolution atomic force microscopy (AFM) observations,[9] the absolute helical sense of the poly-**1** induced by (*R*)-**2**, showing a negative second Cotton effect at *ca*. 370 nm, can be assigned to be a right-handed helix with a left-handed helical array of the pendants. Molecular mechanics (MM) calculations for the model polymer (50-mer) suggest that the right-handed helical poly-**1** may force the biphenyl pendants into a left-handed axially twisted conformation (Figure 3-8). The vibrational circular dichroism (VCD) spectra of the poly-**1** with helicity memory measured in *n*-hexane at -10 °C support such a twist-sense bias in the biphenyl residues as evidenced by the appearance of an intense couplet VCD in the C-O-C stretching band region of the methoxymethoxy (OMOM) groups (around 1050 cm^{-1}) (Figure 3-9). These results provide insight into the mechanism of the present dual memory of poly-**1** that may involve a sequential or synchronized induction of the preferred-handed macromolecular helicity and the axial chirality of the pendants upon interaction with (*S*)- or (*R*)-**2**. The author speculates that cooperative close interactions between the neighboring biphenyl pendants with OMOM groups along the helical polymer backbone might be necessary for the dual memory, because the copolymer poly($\mathbf{1}_{0.5}$-*co*-$\mathbf{3}_{0.5}$) composed of an equal molar **1** and (4-dodecyloxyphenyl)acetylene (**3**) (Figure 3-1B) that lacks functional biphenyl-bound OMOM groups almost lost the memory effect under identical conditions. The ICD intensity of poly($\mathbf{1}_{r}$-*co*-$\mathbf{3}_{1-r}$) in the presence of (*S*)-**2** in *n*-hexane at -10 °C remarkably decreased with an increase in the content of **3** (Figure 3-10). Moreover, the macromolecular helicity induced in poly($\mathbf{1}_{0.5}$-*co*-$\mathbf{3}_{0.5}$) incorporating 50 mol% of **3** by (*S*)-**2** was not efficiently memorized; the ICD intensity of the isolated poly($\mathbf{1}_{0.5}$-*co*-$\mathbf{3}_{0.5}$) became less than 10% of that before removal of (*S*)-**2**. These results indicate that the cooperative interaction between the axially chiral biphenyl pendants may play an important role for both the effective helicity induction and memory effect in poly-**1**. This speculation was further supported by the fact that among analogous homopolymers (poly-**4**-poly-**6**) possessing alkoxy groups different from the OMOM groups at the biphenyl pendants (Figure 3-1B), only poly-**4**

bearing ethoxymethoxy groups showed a similar helicity induction and memory behavior as observed in poly-**1**, while poly-**5** with the methoxy groups completely lost its helicity memory once dissolved in solution and poly-**6** with the propoxy groups exhibited no helicity induction at all in (*S*)-**2**/toluene (2/3, v/v) (Figure 3-11). These results clearly indicate that not only the biphenyl pendants but also the alkoxymethoxy groups play the central role for the present unique helicity induction and memory effects. The author presumes that the biphenyl pendants with alkoxymethoxy groups may act like a molecular motor or gear along the polymer backbone, which provides an extra energy gain to dramatically increase the energy barrier between their right- and left-handed axially twisted conformations, thereby efficiently stabilizing the preferred-handed helical conformation of the main-chain as a result of the collective interactions between them.

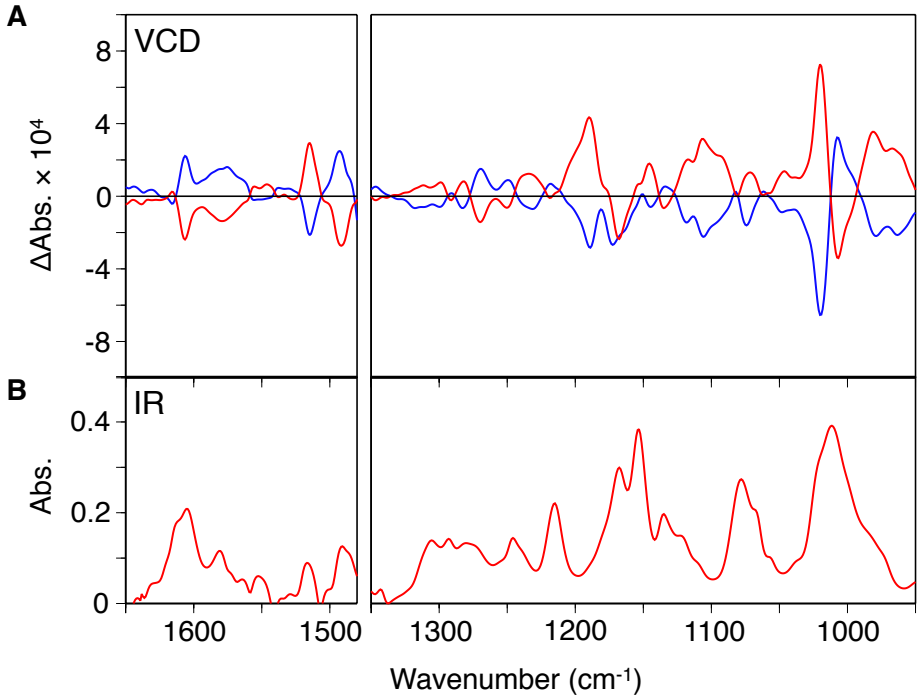

Figure 3-9. (A) VCD spectra of the isolated poly-**1** in *n*-hexane at *ca*. -10 °C after helicity induction with (*S*)-**2** (red line) and (*R*)-**2** (blue line). (B) IR spectrum of the isolated poly-**1** in *n*-hexane at *ca*. -10 °C measured after helicity induction with (*S*)-**2** is also shown.

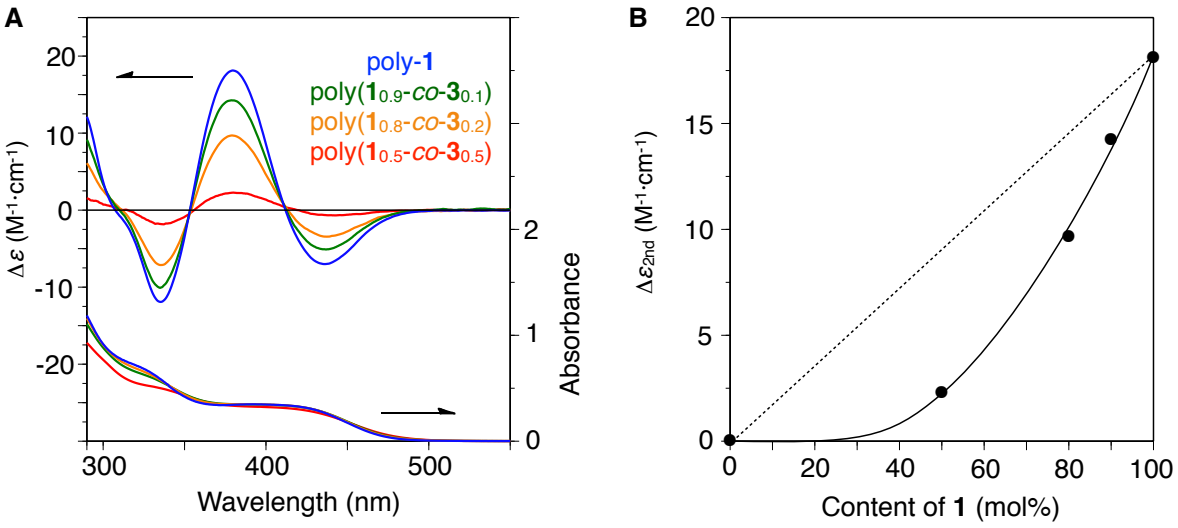

Figure 3-10. (A) CD and absorption spectra of poly-**1** (1.0 mM) and poly(**1**$_r$-*co*-**3**$_{1-r}$) (1.0 mM) with (*S*)-**2** ([(*S*)-**2**]/[poly-**1**] = 400) measured in *n*-hexane at -10 °C after standing in *n*-hexane at 25 °C for 24 h. (B) CD intensity ($\Delta\varepsilon_{2nd}$) changes of poly(**1**$_r$-*co*-**3**$_{1-r}$) (1.0 mM) with (*S*)-**2** ([(*S*)-**2**]/[polymer] = 400) in *n*-hexane at -10 °C versus the content of **1** units after standing in *n*-hexane at 25 °C for 24 h.

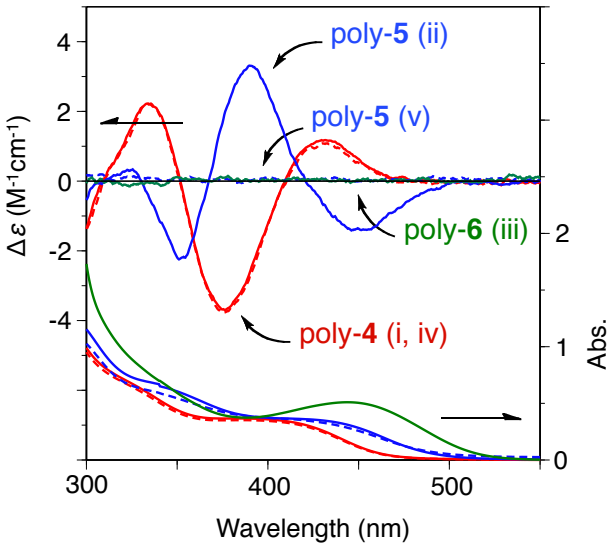

Figure 3-11. CD and absorption spectra of poly-**4** (i, red) and poly-**5** (ii, blue) with (*S*)-**2** ([(*S*)-**2**]/[polymer] = 400) measured in *n*-hexane and methylcyclohexane at -10 °C, respectively, and poly-**6** (iii, green) measured in (*S*)-**2**/toluene (2/3, v/v) at -10 °C after standing the polymers in *n*-hexane (poly-**4**), methylcyclohexane (poly-**5**), or (*S*)-**2**/toluene (poly-**6**) at 25 °C for 24 h, and the isolated poly-**4** (iv, dotted red) in *n*-hexane at -10 °C recovered from i and the isolated poly-**5** (v, dotted blue) in methylcyclohexane at -10 °C recovered from ii. [Polymer] = 1.0 mM.

During the course of this study, we discovered an unprecedented helicity induction and subsequent memory of poly-**1** in the solid state. First poly-**1** was immersed in liquid (*S*)-**2** at 25 °C for an appropriate time, and the poly-**1** was recovered by filtration followed by washing with methanol to remove (*S*)-**2** completely. The author notes that poly-**1** is totally insoluble in **2**. The isolated poly-**1** dissolved in *n*-hexane at -10 °C exhibited an apparent ICD and its ICD intensity increased with time, reaching a near plateau value after 1 h (Figure 3-2B) which is comparable to that induced in *n*-hexane in the presence of (*S*)-**2** at 25 °C (Figure 3-2A,iv). The helicity induction and its memory were accelerated at 50 °C, resulting in a full ICD only after 10 min. In addition, chiral amplification by nonracemic **2** also took place in the solid state, affording a helical poly-**1** with more excess handedness, although it was slightly weaker than that in *n*-hexane (Figure 3-4B). Therefore, it is unambiguously demonstrated that a preferred-handed helix is readily induced in poly-**1** in the solid state by just immersing poly-**1** in nonracemic liquid **2** via weak noncovalent bonding interactions, and this helicity is automatically memorized.

The macromolecular helicity memory was much more stable in the solid state than in solution and the ICD intensity remained for at least 11 months at 25 °C. When the poly-**1** with macromolecular helicity memory by (*S*)-**2** was subsequently immersed in (*R*)-**2** at 25 °C in the solid state, the helicity of poly-**1** was completely inverted and memorized as shown in the perfect mirror image ICDs in *n*-hexane (Figure 3-2A,v, Figure 3-20 in the Experimental Section). These results show that the enantiomeric right- and left-handed helices of poly-**1** can be readily obtained and its helical sense is reversibly switched in the solid state by simply immersing the polymer in nonracemic liquid **2** followed by washing with methanol. The glass transition temperature (T_g) of poly-**1** determined by differential scanning calorimetry (DSC) was -18 °C (Figure 3-12). This temperature was sufficiently lower than the temperature at which the helicity induction and memory experiments were performed. This low T_g enables the main-chain and pendant conformational changes of poly-**1** at the bulk polymer-liquid interface.[10]

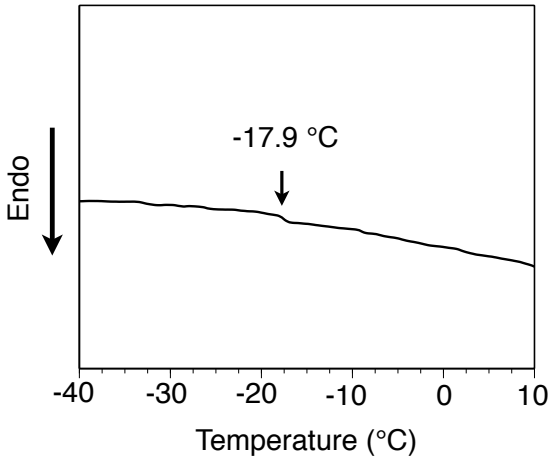

Figure 3-12. DSC thermogram of poly-**1** obtained upon second heating under a heating rate of 10 °C/min.

With these results in mind, the author applied this polymer as a CSP toward controlling the elution order of enantiomers using HPLC. As-prepared, optically inactive poly-**1** was coated on porous spherical silica gel according to the previously reported method,[11] and the obtained packing material was packed into a stainless-steel column (25 cm x 0.20 cm (i.d.)).[12] A solution of (*R*)-**2** in acetone ((*R*)-**2**/acetone = 1/1, v/v) was first filled in the column to induce the preferred-handed helicity (right-handed) in poly-**1** (Figure 3-13A). After heating at 50 °C for 10 min, the column was rinsed with methanol to remove (*R*)-**2** completely, resulting in the CSP consisting of the poly-**1** with right-handed helicity memory (*P*-poly-**1**). Figure 3-13B shows a chromatogram for the resolution of the 50% ee ((–)-isomer rich) of *trans*-stilbene oxide (**7**) on *P*-poly-**1**. The peaks were detected by a UV detector (230 nm). The minor (+)- and major (–)-enantiomers eluted at the retention times of t_1 and t_2, respectively, showing almost complete separation with the separation factor α of 1.11 (for the racemic **7**, see Figure 3-14A). On the other hand, the racemic **2** could not be separated on this CSP (α = 1.0). We note that *P*-poly-**1** prepared using 50% ee of **2** (*R*-rich) could resolve **7** with almost the same enantioselectivity (α = 1.07) as that prepared using optically pure (*R*)-**2** (> 97% ee) (Figure 3-15). The elution times of the enantiomers of **7** in Figure 3-13B, Figure 3-14A and Figure 3-15 were different from each other, probably because the CSPs used were different

and the flow rate was set to be very slow (0.025 mL/min) in order to avoid damage of the columns due to high pressure resulting from a viscous eluent (methanol–H_2O (75 : 25, v/v)) at 0 °C.

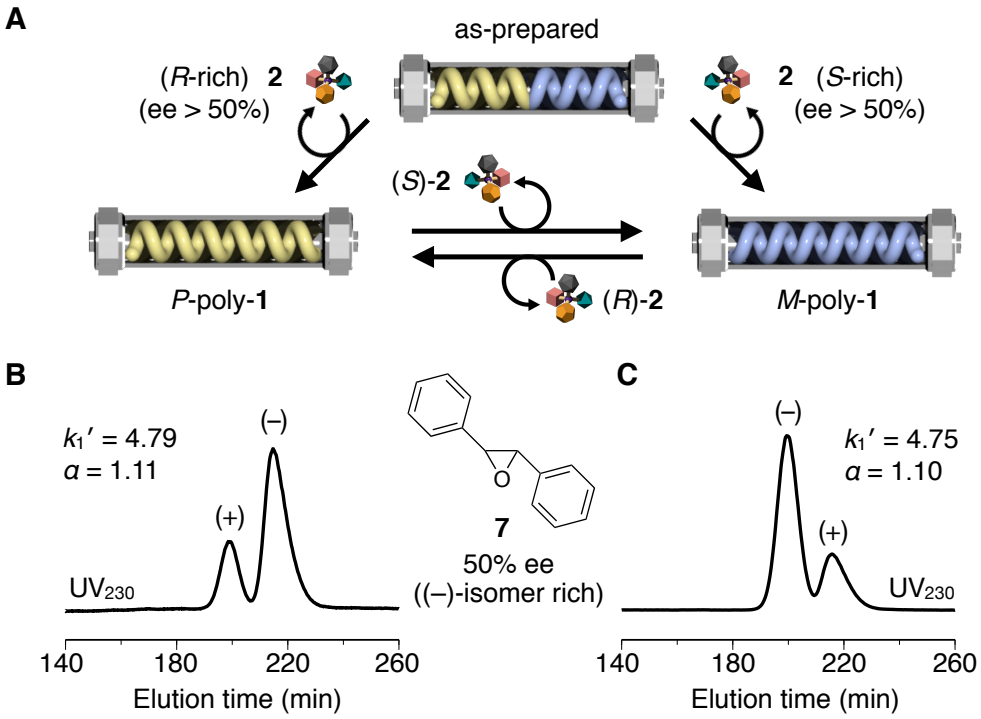

Figure 3-13. Switchable enantioseparation as a chiral stationary phase for HPLC. (A) Schematic illustration of switchable chiral stationary phase for HPLC separation of enantiomers based on reversible helicity induction and subsequent memory in poly-**1** by sequential treatment with (*R*)- and (*S*)-**2** (ee > 50%) in an alternating manner, thus producing *P*-poly-**1** and *M*-poly-**1** with opposite helical handedness from each other. (B),(C) Chromatograms for the resolution of 50% ee of **7** ((–)-isomer rich) on *P*-poly-**1** (B) and *M*-poly-**1** (C) prepared by treatment with (*R*)-**2** and (*S*)-**2** at *ca*. 0 °C, respectively. Column: 25 × 0.20 cm (i.d.). Flow rate: 0.025 mL/min. Eluent: methanol–H_2O (75 : 25, v/v). The capacity factor k_1' [= $(t_1 - t_0)/t_0$] and the separation factor α [= $(t_2 - t_0)/(t_1 - t_0)$] for B and C were 4.79 and 1.11, and 4.75 and 1.10, respectively. The separation factor (α) represents the enantioselectivity and is always more than one.

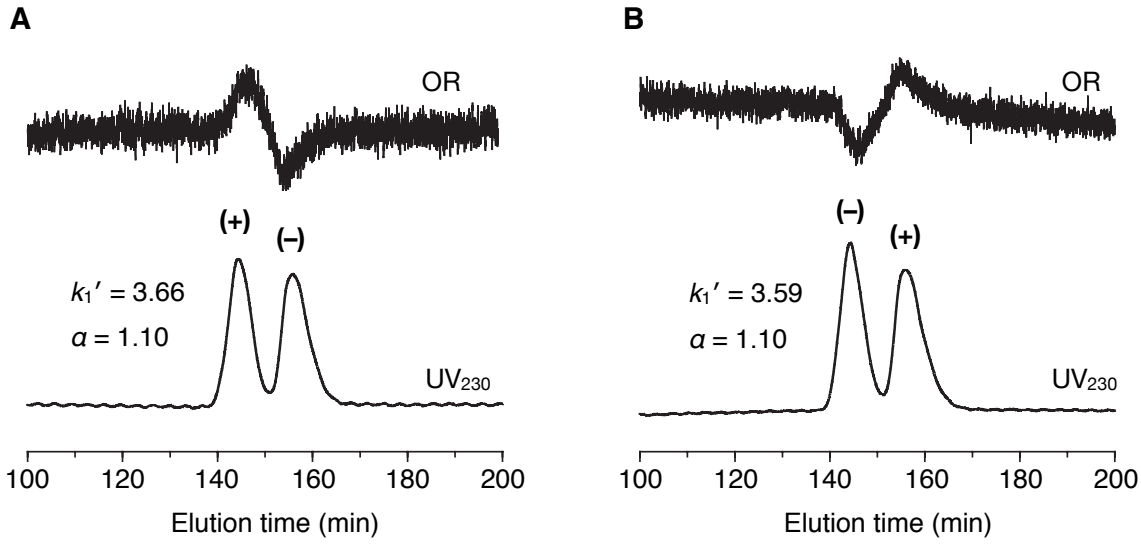

Figure 3-14. Chromatograms for the resolution of racemic **7** on *P*-poly-**1** (A) and *M*-poly-**1** (B) prepared by treatment with (*R*)-**2** and (*S*)-**2** at *ca*. 0 °C, respectively. Column: 25 × 0.20 cm (i.d.). Flow rate: 0.025 mL/min. Eluent: methanol–H_2O (75 : 25, v/v). The capacity factor k_1' [= $(t_1 - t_0)/t_0$] and the separation factor α [= $(t_2 - t_0)/(t_1 - t_0)$] for A and B were 3.66 and 1.10, and 3.59 and 1.10, respectively. The separation factor (α) represents the enantioselectivity and is always more than one.

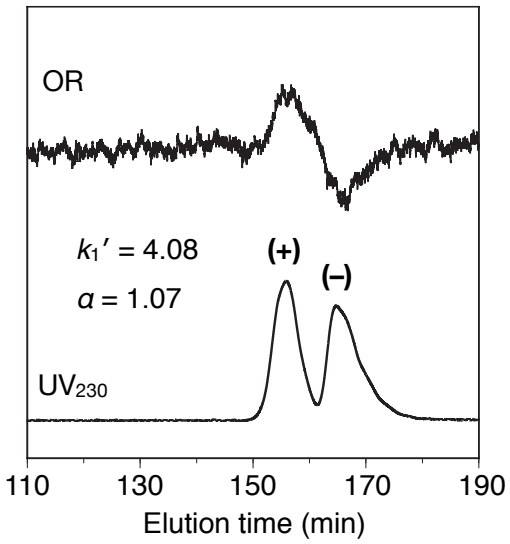

Figure 3-15. Chromatograms for the resolution of **7** on poly-**1** after treating with 50% ee of **2** (*R*-rich). Column: 25 × 0.20 cm (i.d.). Flow rate: 0.025 mL/min. Eluent: methanol–H_2O (75 : 25, v/v). The capacity factor k_1' and the separation factor α were 4.08 and 1.07, respectively.

Further treatment of the *P*-poly-**1** with (*S*)-**2** in acetone ((*S*)-**2**/acetone = 1/1, v/v) (Figure 3-13A) in the column brought about an inversion of the helicity from the right- to left-handed helix, thereby producing a CSP composed of *M*-poly-**1** with an opposite helicity memory, which also separated the enantiomers of **7**, but with a completely reversed elution order; the major (–)-enantiomer eluted first followed by the minor (+)-enantiomer with almost the same k_1' and α values (Figure 3-13C) (for the racemic **7**, see Figure 3-14B). Thus, the switchable separation of enantiomers was for the first time achieved using the CSP composed of a helical sense-switchable polymer resulting from macromolecular helicity memory.

Conclusions

In summary, the author has demonstrated a quite unique helical polyacetylene whose main-chain helicity and axial chirality of the pendants are induced accompanied by chiral amplification in a sequential or synchronized fashion upon interaction with a nonracemic alcohol. The induced macromolecular helicity and axial chirality are automatically memorized and further switched in the solid state. This remarkable feature allows us to develop an unprecedented chiral packing material for separating enantiomers whose elution order or enantioselectivity can be reversibly switched. The author believes that such a helical polymer with switchable memories of both the macromolecular helicity and axial chirality in the solid state will provide a novel and promising class of intelligent chiral materials as enantioselective permeable membranes and asymmetric catalysis whose enantioselectivities can be switched by further modification of the pendant units, and work along this line is now in progress in our laboratory.

Experimental Section

Materials. Anhydrous THF, dichloromethane, *N*,*N*-dimethylformamide (DMF), and acetone were obtained from Kanto Kagaku (Tokyo, Japan). Anhydrous *n*-hexane was purchased from Wako (Osaka, Japan). Triethylamine (NEt_3) was dried over KOH pellets and distilled onto KOH under nitrogen. These solvents were stored under nitrogen. 4-Bromoresorcinol, *p*-toluenesulfonyl chloride (TsCl), chloromethyl methyl ether (MOMCl), benzylbromide (BnBr), potassium carbonate, *n*-butyllithium (1.6 M in *n*-hexane), trimethoxyborane, dimethoxyethane (DME), 2,6-lutidine, and *p*-iodophenol were purchased from Wako. 1-Bromododecane, tetrakis(triphenylphosphine)palladium(0), trifluoromethanesulfonic anhydride (Tf_2O), bis(triphenylphosphine)palladium(II) dichloride, chloromethyl ethyl ether, 1-bromopropane, iodomethane, and *trans*-stilbene oxide (**7**) were from Tokyo Kasei (TCI, Tokyo, Japan). Triphenylphosphine and copper(I) iodide were obtained from Kanto Kagaku. Palladium (5 wt% on activated carbon), $[(norbornadiene)rhodium(I)\ chloride]_2$ $[Rh(nbd)Cl_2]$, tetra-*n*-butylammonium fluoride (1.0 M in THF), anhydrous acetonitrile, and (*R*)- and (*S*)-**2** were available from Aldrich (Milwaukee, WI、USA). The porous spherical silica gel with a mean particle size of 5 μm and a mean pore diameter of 30 nm (Daiso gel SP-300-5P) and (trimethylsilyl)acetylene (TMSA) were kindly supplied from Daiso Chemicals (Osaka, Japan) and Shinetsu Chemical (Tokyo, Japan), respectively. (4-Dodecyloxyphenyl)acetylene (**3**) was synthesized according to the literature.[13] The 50% ee of **7** ((–)-isomer rich) was prepared by mixing the commercially available racemic **7** with an appropriate amount of enantiomerically pure (–)-**7**, which had been obtained by separation of the racemic **7** using a preparative chiral HPLC column, Chiralcel OD (25 × 2.0 cm (i.d.), Daicel).

Instruments. Melting points were measured on a Yanako melting point apparatus and were uncorrected. NMR spectra were taken on a Varian Mercury 300 (300 MHz for ^1H, 75 MHz for ^{13}C) or a JNA-LA 400 (JEOL) (400 MHz for ^1H) or a JNM-ECA 500 (JEOL) (500 MHz for ^1H, 125 MHz for ^{13}C) spectrometer in $CDCl_3$ using TMS (for $CDCl_3$, ^1H and ^{13}C) as

the internal standard. Recycling preparative HPLC was performed with an LC-9201 liquid chromatograph (JAI, Tokyo, Japan) equipped with UV–visible (JASCO UV-2075 (JASCO, Hachioji, japan)) and RI detectors (JAI RI-50s) at room temperature. HPLC columns, JAIGEL-1H and JAIGEL-2H were connected in series, and $CHCl_3$ was used as the eluent. IR spectra were recorded with a JASCO Fourier Transform IR-460 spectrophotometer. Size exclusion chromatography (SEC) measurements were performed with a JASCO PU-2080 liquid chromatograph equipped with a UV-vis (JASCO UV-970) detector at 40 °C. The temperature was controlled with a JASCO CO-1560 column oven. A Shodex (Tokyo, Japan) KF-805L (30 cm) column was used for SEC measurements and THF was used as the eluent at flow rate of 1.0 mL/min. The molecular weight calibration curves were obtained with polystyrene standards (Tosoh). Absorption and CD spectra were measured in a 1.0- or 0.1-mm quartz cell on a JASCO V-570 spectrophotometer and a JASCO J-725 spectropolarimeter, respectively. The temperature was controlled with a JASCO ETC-505T (absorption spectroscopy) and a JASCO PTC-348WI apparatus (CD spectroscopy). The concentration of poly-**1** was calculated based on the monomer units and was 1.0 mM unless otherwise stated, which was corrected using the ε (molar absorptivity) value of poly-**1** (ε_{380} = 3240 $M^{-1}\cdot cm^{-1}$) in *n*-hexane. VCD spectra were measured in a 0.15 mm BaF_2 cell with a JASCO JV-2001YS spectrometer equipped with a temperature controller (EYELA NCB-1200). The concentration was 20 mg/mL in *n*-hexane, and temperature was *ca*. -10 °C. All spectra were collected for *ca*. 4 h at a resolution of 4 cm^{-1}. Dynamic light scattering (DLS) measurements were performed on a Photal DLS-7070YN (Otsuka Electronics Co., Ltd., Osaka, Japan) equipped with a 10 mW He-Ne laser (632.8 nm) at 25 °C. Differential scanning calorimetric (DSC) analysis was performed on a Jade DSC (Perkin Elmer, Massachusetts, USA) under a heating rate of 10.0 °C/min. The chromatographic separations of enantiomers were performed using a JASCO PU-2080 Plus liquid chromatograph equipped with Multi UV-Vis (JASCO MD-910) and polarimetric (JASCO OR-990, Hg–Xe without filter) detectors at *ca*. 0 °C. Thermogravimetric (TG) analysis was conducted on a SEIKO EXSTAR6000 TG/DTA 6200

(Seiko Instruments Inc., Chiba, Japan) under a heating rate of 20 °C/min. Elemental analyses were performed by the Research Institute for Instrumental Analysis of Advanced Science Research Center, Kanazawa University, Kanazawa, Japan.

Monomers **1**, **4**, **5**, and **6** were prepared according to Scheme 3-1.

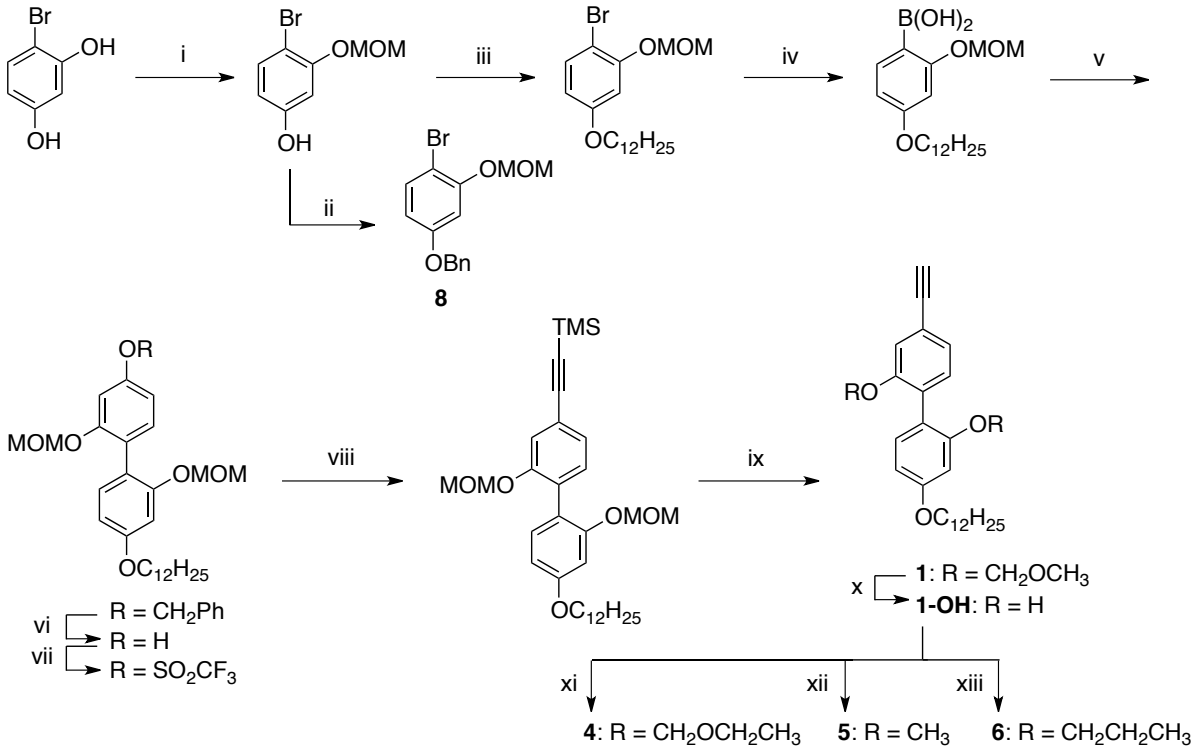

i) TsCl, K_2CO_3, acetone, reflux; then MOMCl, reflux; then KOH, ethanol/H_2O, 60 °C, ii) BnBr, K_2CO_3, acetone, reflux, iii) $C_{12}H_{25}Br$, K_2CO_3, DMF, 140 °C, iv) *n*-BuLi, $B(OMe)_3$, THF, -78 °C then rt, v) **8**, $Pd(PPh_3)_4$, K_2CO_3, DME/H_2O, 80 °C, vi) H_2, Pd/C, ethyl acetate, rt, vii) Tf_2O, 2,6-lutidine, dichloromethane, -78 °C then rt, viii) TMSA, $Pd(PPh_3)_2Cl_2$, Et_3N/DMF, 90 °C, ix) K_2CO_3, THF/methanol, rt, x) conc. HCl, THF/methanol, rt, xi) chloromethyl ethyl ether, K_2CO_3, acetonitrile, reflux, xii) iodomethane, K_2CO_3, acetone, 75 °C, xiii) 1-bromopropane, K_2CO_3, acetonitrile, 70 °C.

Scheme 3-1. Synthesis of **1**, **4**, **5**, and **6**

4-Bromo-3-methoxymethoxyphenol.[14] To a solution of 4-bromoresorcinol (15.0 g, 0.0794 mol) in anhydrous acetone (300 mL) was added K_2CO_3 (32.9 g, 0.238 mol) and *p*-toluenesulfonyl chloride (16.6 g, 0.0873 mol). The mixture was refluxed for 21 h and then chloromethyl methyl ether (7.16 mL, 0.0952 mol) was added to the reaction mixture. After 3 h under reflux, the reaction mixture was filtered and the solvent was removed under reduced pressure. The residue was diluted with diethyl ether and the solution was washed with water and then dried over $MgSO_4$. After filtration, the solvent was removed by evaporation, the crude product was purified by silica gel chromatography using ethyl acetate—*n*-hexane (1/10, v/v) as the eluent to give 4-bromo-3-methoxymethoxyphenyl *p*-toluenesulfonate as a white solid (25.9 g, 84% yield). The obtained product (7.15 g) was dissolved in ethanol (290 mL) and then 3.2 N KOH aqueous solution (29 mL, 0.092 mmol) was slowly added to the solution. The mixture was stirred at 60 °C for 2 h. After cooling to room temperature, the reaction mixture was neutralized with 3 N HCl aqueous solution and the solvent was removed under reduced pressure. The residue was diluted with diethyl ether, and the solution was washed with water, and dried over Na_2SO_4. After filtration, the solvent was removed by evaporation to give the desired product as a white solid (4.20 g, 98% yield). This was used for the next reaction without further purification. ^{1}H NMR (300 MHz, $CDCl_3$, rt): δ 7.36 (d, J = 8.7 Hz, 1H, Ar–H), 6.71 (d, J = 2.7 Hz, 1H, Ar–H), 6.41 (dd, J = 2.7, 8.7 Hz, 1H, Ar–H), 5.22 (s, 2H, OCH_2O), 4.94 (brs, 1H, OH), 3.52 (s, 3H, OCH_3).

1-Benzyloxy-4-bromo-3-methoxymethoxybenzene (8). To a solution of 4-bromo-3-methoxymethoxyphenol (4.10 g, 17.6 mmol) in anhydrous acetone (165 mL) was added K_2CO_3 (7.29 g, 52.8 mmol) and benzylbromide (2.51 mL, 21.1 mmol). After 2 h under reflux, the reaction mixture was filtered and the solvent was removed under reduced pressure. The residue was diluted with diethyl ether and the solution was washed with water and brine, and then dried over Na_2SO_4. After filtration, the solvent was removed by evaporation and the crude product was purified by silica gel chromatography using ethyl acetate—*n*-hexane (1/15, v/v) as the eluent to give **8** as a colorless oil (5.07 g, 89% yield). ^{1}H NMR (300 MHz, $CDCl_3$,

rt): δ 7.30-7.47 (m, 6H, Ar–H), 6.84 (d, J = 2.7 Hz, 1H, Ar–H), 6.53 (dd, J = 8.7, 2.7 Hz, 1H, Ar–H), 5.21 (s, 2H, OCH_2O), 5.02 (s, 2H, OCH_2Bn), 3.50 (s, 3H, OCH_3).

4-Bromo-1-dodecyloxy-3-methoxymethoxybenzene. To a solution of 4-bromo-3-methoxymethoxyphenol (2.00 g, 8.58 mmol) in DMF (5 mL) was added K_2CO_3 (2.50 g, 18.1 mmol) and 1-bromododecane (4.0 mL, 16.8 mmol). The mixture was stirred at 140 °C for 2 h. After evaporating the solvent, the residue was diluted with diethyl ether, and the solution was washed with water and brine, and dried over $MgSO_4$. After filtration, the solvent was removed by evaporation and the crude product was purified by silica gel chromatography using ethyl acetate—*n*-hexane (1/50, v/v) as the eluent to give the desired product as a white solid quantitatively (3.56 g). ^{1}H NMR (300 MHz, $CDCl_3$, rt): δ 7.39 (d, J = 8.7 Hz, 1H, Ar–H), 6.74 (d, J = 2.7 Hz, 1H, Ar–H), 6.45 (dd, J = 2.7, 8.7 Hz, 1H, Ar–H), 5.23 (s, 2H, OCH_2O), 3.91 (t, J = 6.6 Hz, 2H, OCH_2CH_2), 3.52 (s, 3H, OCH_3), 1.76 (quint, J = 6.6 Hz, 2H, OCH_2CH_2), 1.22-1.50 (m, 18H, $9CH_2$), 0.88 (t, J = 6.3 Hz, 3H, CH_3).

4-Dodecyloxy-2-methoxymethoxyphenylboronic acid. To a solution of 4-bromo-1-dodecyloxy-3-methoxymethoxybenzene (7.02 g, 17.5 mmol) in THF (175 mL) was added *n*-butyllithium (1.6 M in *n*-hexane) (13.1 mL, 21.0 mmol) at -78 °C. After stirring at -78 °C for 20 min, trimethoxyborane (4.13 mL, 35.0 mmol) was added to the solution. The reaction mixture was stirred at -78 °C for 0.5 h, and subsequently at room temperature for 2 h. After adding 1 N HCl aqueous solution (18.5 mL), the mixture was stirred for 0.5 h and then extracted with diethyl ether. The aqueous phase was extracted with diethyl ether and the combined organic layer was washed with water and brine, and then dried over $MgSO_4$. After filtration, the solvents were removed by evaporation and the crude product was purified by silica gel chromatography using ethyl acetate—*n*-hexane (1/2, v/v) as the eluent to give the desired product as a white solid (4.28 g, 67% yield). ^{1}H NMR (300 MHz, $CDCl_3$, rt): δ 7.75 (d, J = 8.4 Hz, 1H, Ar–H), 6.68 (d, J = 2.4 Hz, 1H, Ar–H), 6.61 (dd, J = 2.4, 8.4 Hz, 1H, Ar–H), 5.49 (s, 2H, OH), 5.27 (s, 2H, OCH_2O), 3.97 (t, J = 6.6 Hz, 2H, OCH_2CH_2), 3.51 (s, 3H,

OCH_3), 1.78 (quint, J = 6.6 Hz, 2H, OCH_2CH_2), 1.21-1.50 (m, 18H, $9CH_2$), 0.88 (t, J = 6.3 Hz, 3H, CH_3).

4-Benzyloxy-4'-dodecyloxy-2,2'-bis(methoxymethoxy)biphenyl. To a solution of 4-dodecyloxy-2-methoxymethoxyphenylboronic acid (5.20 g, 16.1 mmol) in DME/H_2O (3/1, v/v) (800 mL) was added **8** (6.41 g, 17.5 mmol) and $Pd(PPh_3)_4$ (1.84 g, 1.60 mmol). The mixture was stirred at 80 °C for 17 h. After evaporating the solvent, the residue was diluted with diethyl ether and the solution was washed with water and brine, and then dried over $MgSO_4$. After filtration, the solvent was removed under reduced pressure and the crude product was then purified by silica gel chromatography using ethyl acetate—*n*-hexane (1/10, v/v) as the eluent to give the desired product as a white solid (8.44 g, 93% yield). ^{1}H NMR (300 MHz, $CDCl_3$, rt): δ 7.32-7.48 (m, 5H, Ar–H), 7.14 (d, J = 5.1 Hz, 1H, Ar–H), 7.11 (d, J = 5.1 Hz, 1H, Ar–H), 6.90 (d, J = 2.7 Hz, 1H, Ar–H), 6.79 (d, J = 2.1 Hz, 1H, Ar–H), 6.67 (dd, J = 2.7, 8.6 Hz, 1H, Ar–H), 6.60 (dd, J = 2.7, 8.6 Hz, 1H, Ar–H), 5.07 (s, 2H, CH_2Bn), 5.05 (s, 2H, OCH_2O), 5.04 (s, 2H, OCH_2O), 3.96 (t, J = 6.6 Hz, 2H, OCH_2CH_2), 3.35 (s, 6H, OCH_3), 1.79 (quint, J = 6.6 Hz, 2H, OCH_2CH_2), 1.40-1.51 (m, 2H, CH_2), 1.19-1.39 (m, 16H, $8CH_2$), 0.88 (t, J = 6.9 Hz, 3H, CH_3).

4-(4-Dodecyloxy-2-methoxymethoxyphenyl)-3-methoxymethoxyphenol. Palladium-activated carbon (5% Pd–C, 500 mg) was added to a solution of 4-benzyloxy-4'-dodecyloxy-2,2'-bis(methoxymethoxy)biphenyl (3.48 g, 6.16 mmol) in ethyl acetate (50 mL) under nitrogen. The mixture was stirred at room temperature for 16 h under an atmosphere of hydrogen. After filtration using Celite, the solvent was removed by evaporation. The crude product was then purified by silica gel chromatography using ethyl acetate—*n*-hexane (1/3, v/v) as the eluent to give the desired product as a white solid (2.62 g, 90% yield). ^{1}H NMR (300 MHz, $CDCl_3$, rt): δ 7.11 (d, J = 8.4 Hz, 1H, Ar–H), 7.07 (d, J = 8.4 Hz, 1H, Ar–H), 6.78 (d, J = 2.4 Hz, 1H, Ar–H), 6.73 (d, J = 2.4 Hz, 1H, Ar–H), 6.60 (dd, J = 2.4, 8.4 Hz, 1H, Ar–H), 6.52 (dd, J = 2.4, 8.4 Hz, 1H, Ar–H), 5.53 (brs, 1H, OH), 5.05 (s, 2H, OCH_2O), 5.04 (s, 2H, OCH_2O), 3.96 (t, J = 6.6 Hz, 2H, OCH_2CH_2), 3.36 (s, 3H, OCH_3), 3.35 (s, 3H, OCH_3),

1.79 (quint, J = 6.6 Hz, 2H, OCH_2CH_2), 1.40-1.51 (m, 2H, CH_2), 1.22-1.39 (m, 16H, $8CH_2$), 0.88 (t, J = 6.6 Hz, 3H, CH_3).

4-(4-Dodecyloxy-2-methoxymethoxyphenyl)-3-methoxymethoxyphenyl trifuluoro-methanesulfonate. 2,6-Lutidine (3.22 mL, 27.6 mmol) and 4-(4-dodecyloxy-2-methoxymethoxyphenyl)-3-methoxymethoxyphenol (2.62 g, 5.52 mmol) were dissolved in dichloromethane (500 mL) and the solution was cooled to -78 °C. To this solution was slowly added trifluoromethanesulfonic anhydride (0.994 mL, 6.07 mmol) and the mixture was stirred at -78 °C for 1 h and then at room temperature for 1 h. The solution was washed with saturated $NaHCO_3$ aqueous solution and brine, and then dried over $MgSO_4$. After filtration, the solvent was removed by evaporation and the crude product was purified by silica gel chromatography using ethyl acetate—*n*-hexane (1/4, v/v) as the eluent to give the desired product as a colorless oil (3.36 g, quantitatively). ^{1}H NMR (300 MHz, $CDCl_3$, rt): δ 7.28 (d, J = 8.7 Hz, 1H, Ar–H), 7.15 (d, J = 2.4 Hz, 1H, Ar–H), 7.10 (d, J = 8.7 Hz, 1H, Ar–H), 6.96 (dd, J = 2.4, 8.4 Hz, 1H, Ar–H), 6.80 (d, J = 2.4 Hz, 1H, Ar–H), 6.61 (dd, J = 2.4, 8.4 Hz, 1H, Ar–H), 5.08 (s, 2H, OCH_2O), 5.06 (s, 2H, OCH_2O), 3.97 (t, J = 6.6 Hz, 2H, OCH_2CH_2), 3.38 (s, 3H, OCH_3), 3.33 (s, 3H, OCH_3), 1.79 (quint, J = 6.6 Hz, 2H, OCH_2CH_2), 1.40-1.52 (m, 2H, CH_2), 1.22-1.34 (m, 16H, $8CH_2$), 0.88 (t, J = 6.6 Hz, 3H, CH_3).

4-Dodecyloxy-2,2'-bis(methoxymethoxy)-4'-(trimethylsilylethynyl)biphenyl. To a solution of 4-(4-dodecyloxy-2-methoxymethoxyphenyl)-3-methoxymethoxyphenyl trifuluoromethanesulfonate (3.36 g, 5.54 mmol) in DMF/Et_3N (5/1, v/v) (84 mL) were added (trimethylsilyl)acetylene (1.61 mL, 11.6 mmol) and $Pd(PPh_3)_2Cl_2$ (389 mg, 0.554 mmol). The solution was stirred at 90 °C for 39 h. After cooling to room temperature, the mixture was diluted with diethyl ether and the ethereal solution was washed with 1 N HCl aqueous solution and water, and then dried over $MgSO_4$. After filtration, the solvent was removed by evaporation and the crude product was purified by silica gel chromatography using ethyl acetate—*n*-hexane (1/20, v/v) as the eluent to give the desired product as a colorless oil (2.85 g, 93% yield). ^{1}H NMR (300 MHz, $CDCl_3$, rt): δ 7.30 (s, 1H, Ar–H), 7.09-7.17 (m, 3H, Ar–

H), 6.77 (d, J = 2.1 Hz, 1H, Ar–H), 6.60 (dd, J = 2.7, 8.4 Hz, 1H, Ar–H), 5.06 (s, 2H, OCH_2O), 5.03 (s, 2H, OCH_2O), 3.96 (t, J = 6.6 Hz, 2H, OCH_2CH_2), 3.36 (s, 3H, OCH_3), 3.32 (s, 3H, OCH_3), 1.79 (quint, J = 6.6 Hz, 2H, OCH_2CH_2), 1.24-1.52 (m, 18H, $9CH_2$), 0.88 (t, J = 6.9 Hz, 3H, CH_3), 0.25 (s, 9H, TMS).

(2,2'-Bis(methoxymethoxy)-4'-dodecyloxy-4-biphenylyl)acetylene (1). To a solution of 4-dodecyloxy-2,2'-bis(methoxymethoxy)-4'-(trimethylsilylethynyl)biphenyl (162 mg, 0.292 mmol) in THF/methanol (3/1, v/v) (10 mL) was added K_2CO_3 (240 mg, 1.74 mmol). After stirring at room temperature for 15 h, the mixture was filtered and the filtrate was condensed under reduced pressure. The residue was diluted with dichloromethane and the solution was washed with water and brine, and then dried over Na_2SO_4. After filtration, the solvent was removed by evaporation and the residue was purified by silica gel chromatography using ethyl acetate—*n*-hexane (1/7, v/v) as the eluent and then further purified by recycling preparative HPLC to give **1** as a white solid (130 mg, 93% yield). Mp: 37.8–38.6 °C. IR (KBr, cm^{-1}): 3241 (≡CH), 2106 (C≡C). ^1H NMR (400 MHz, $CDCl_3$, rt): δ 7.34 (s, 1H, Ar–H), 7.19 (s, 2H, Ar–H), 7.12 (d, J = 8.5 Hz, 1H, Ar–H), 6.80 (d, J = 2.2 Hz, 1H, Ar–H), 6.61 (dd, J = 8.5, 2.4 Hz, 1H, Ar–H), 5.06 (s, 2H, OCH_2O), 5.05 (s, 2H, OCH_2O), 3.97 (t, J = 6.5 Hz, 2H, OCH_2CH_2), 3.36 (s, 3H, OCH_3), 3.34 (s, 3H, OCH_3), 3.08 (s, 1H, CH), 1.79 (quint, J = 6.8 Hz, 2H, OCH_2CH_2), 1.43-1.50 (m, 2H, CH_2), 1.24-1.39 (m, 16H, $8CH_2$), 0.88 (t, J = 6.8 Hz, 3H, CH_3). ^{13}C NMR (125 MHz, $CDCl_3$, rt): δ 160.12, 155.83, 154.96, 131.89, 131.72, 130.29, 125.82, 121.99, 120.65, 119.23, 107.28, 102.94, 95.37 (2C), 83.81, 77.12, 68.23, 56.10 (2C), 32.07, 29.82, 29.79, 29.76, 29.75, 29.58, 29.51, 29.47, 26.24, 22.85, 14.27. Calcd for $C_{30}H_{42}O_5$: C, 74.65; H, 8.77. Found: C, 74.46; H, 8.94.

(2,2'-Dihydroxy-4'-dodecyloxy-4-biphenylyl)acetylene (1-OH). To a solution of compound **1** (430 mg, 0.892 mmol) in THF/methanol (1/1, v/v) (120 mL) was slowly added conc. HCl (1.0 mL). After stirring at room temperature for 12 h, the solvent was removed under reduced pressure. The residue was diluted with dichloromethane and the solution was washed with water and brine, and then dried over Na_2SO_4. After filtration, the solvent was

removed by evaporation and the crude product was purified by silica gel chromatography using ethyl acetate—*n*-hexane (1/7, v/v) as the eluent to give **1-OH** as a white solid (315 mg, 90% yield). Mp: 71.9–72.6 °C. IR (KBr, cm^{-1}): 3310 (≡CH), 2111 (C≡C). ^{1}H NMR (300 MHz, $CDCl_3$, rt): δ 7.08-7.21 (m, 4H, Ar–H), 6.62 (dd, J = 9.3, 2.7 Hz, 1H, Ar–H), 6.56 (d, J = 2.1 Hz, 1H, Ar–H), 3.96 (t, J = 6.6 Hz, 2H, OCH_2CH$_2$), 3.10 (s, 1H, CH), 1.78 (quint, J = 7.8 Hz, 2H, OCH$_2$CH_2), 1.18-1.51 (m, 18H, 9CH$_2$), 0.88 (t, J = 6.6 Hz, 3H, CH$_3$). ^{13}C NMR (75 MHz, $CDCl_3$, rt): δ 160.21, 154.01, 152.98, 132.03, 131.60, 125.59, 125.03, 123.34, 120.30, 115.24, 108.83, 102.93, 83.26, 77.98, 68.50, 32.16, 29.90, 29.87, 29.84, 29.82, 29.61, 29.59, 29.40, 26.26, 22.93, 14.36. Calcd for $C_{26}H_{34}O_3 \cdot 0.05H_2O$: C, 78.97; H, 8.69. Found: C, 78.92; H, 8.82.

(2,2'-Bis(ethoxymethoxy)-4'-dodecyloxy-4-biphenylyl)acetylene (4). To a solution of **1-OH** (127 mg, 0.321 mmol) in anhydrous acetonitrile (2.0 mL) was added K_2CO_3 (267 mg, 1.93 mmol) and chloromethyl ethyl ether (120 μL, 1.29 mmol). After refluxing for 23 h, the reaction mixture was filtered and the solvents were removed under reduced pressure. The residue was diluted with diethyl ether and the solution was washed with water and then dried over Na_2SO_4. After filtration, the solvent was removed by evaporation and the crude product was purified by silica gel chromatography using ethyl acetate—*n*-hexane (1/20, v/v) as the eluent to give **4** as a colorless oil (122 mg, 74% yield). IR (KBr, cm^{-1}): 3289 (≡CH), 2108 (C≡C). ^{1}H NMR (500 MHz, $CDCl_3$, rt): δ 7.36 (s, 1H, Ar–H), 7.17 (s, 2H, Ar–H), 7.10 (d, J = 8.0 Hz, 1H, Ar–H), 6.82 (d, J = 2.3 Hz, 1H, Ar–H), 6.59 (dd, J = 8.0, 2.3 Hz, 1H, Ar–H), 5.10 (s, 2H, OCH$_2$O), 5.09 (s, 2H, OCH$_2$O), 3.97 (t, J = 6.6 Hz, 2H, OCH_2CH$_2$), 3.59 (q, J = 7.1 Hz, 2H, OCH_2CH$_3$), 3.57 (q, J = 7.1 Hz, 2H, OCH_2CH$_3$), 3.07 (s, 1H, CH), 1.79 (quint, J = 6.3 Hz, 2H, OCH$_2$CH_2), 1.43-1.49 (m, 2H, CH$_2$), 1.21-1.39 (m, 16H, 8CH$_2$), 1.17 (t, J = 6.9 Hz, 3H, OCH$_2$CH_3), 1.16 (t, J = 6.9 Hz, 3H, OCH$_2$CH_3), 0.88 (t, J = 6.9 Hz, 3H, CH$_3$). ^{13}C NMR (125 MHz, $CDCl_3$, rt): δ 160.06, 155.99, 155.10, 131.84, 131.67, 130.23, 125.64, 121.90, 120.59, 119.16, 119.13, 107.18, 102.89, 94.04, 83.89, 77.05, 77.02, 68.21, 64.28, 64.23, 32.06, 29.81, 29.78, 29.76, 29.75, 29.57, 29.50, 29.45, 26.24, 22.84, 15.20, 14.27. Calcd for $C_{32}H_{46}O_5$: C, 75.26; H, 9.08. Found: C, 75.44; H, 9.17.

(2,2'-Dimethoxy-4'-dodecyloxy-4-biphenylyl)acetylene (5). To a solution of **1-OH** (85.0 mg, 0.215 mmol) in anhydrous acetone (2.0 mL) was added K_2CO_3 (149 mg, 1.08 mmol) and iodomethane (54 μL, 0.86 mmol). The reaction mixture was stirred at 75 °C for 19 h. After adding methanol and water, the solvents were removed under reduced pressure. The residue was diluted with diethyl ether and the solution was washed with water and then dried over Na_2SO_4. After filtration, the solvent was removed by evaporation and the crude product was purified by silica gel chromatography using ethyl acetate—*n*-hexane (1/19, v/v) as the eluent to give **5** as a white solid (84.2 mg, 93% yield). Mp: 56.3–56.6 °C. IR (KBr, cm^{-1}): 3251 (≡CH), 2107 (C≡C). ^{1}H NMR (500 MHz, $CDCl_3$, rt): δ 7.18 (d, J = 7.4 Hz, 1H, Ar–H), 7.14 (d, J = 1.7 Hz,1H, Ar–H), 7.12 (d, J = 8.0 Hz, 1H, Ar–H), 7.06 (d, J = 1.1Hz, 1H, Ar–H), 6.52-6.54 (m, 2H, Ar–H), 3.98 (t, J = 6.6 Hz, 2H, OCH_2CH$_2$), 3.77 (s, 3H, OCH_3), 3.75 (s, 3H, OCH_3), 3.08 (s, 1H, CH), 1.80 (quint, J = 6.3 Hz, 2H, OCH_2CH_2), 1.41-1.48 (m, 2H, CH_2), 1.21-1.40 (m, 16H, 8CH_2), 0.88 (t, J = 6.9 Hz, 3H, CH_3). ^{13}C NMR (125 MHz, $CDCl_3$, rt): δ 160.25, 158.02, 156.98, 131.82, 131.76, 128.97, 124.49, 121.81, 119.41, 114.66, 114.62, 104.93, 99.49, 84.13, 68.20, 55.85, 55.77, 32.07, 29.82, 29.79, 29.76, 29.75, 29.57, 29.51, 29.49, 26.25, 22.85, 14.28. Calcd for $C_{28}H_{38}O_3 \cdot 0.25H_2O$: C, 78.74; H, 9.09. Found: C, 78.82; H, 9.08.

(2,2'-Dipropoxy-4'-dodecyloxy-4-biphenylyl)acetylene (6). To a solution of **1-OH** (78.0 mg, 0.198 mmol) in anhydrous acetonitrile (2.0 mL) was added K_2CO_3 (137 mg, 0.989 mmol) and 1-bromopropane (72 μL, 0.79 mmol). After stirring at 70 °C for 22 h, the mixture was filtered and the filtrate was condensed under reduced pressure. The residue was diluted with diethyl ether and the solution was washed with water and then dried over Na_2SO_4. After filtration, the solvent was removed by evaporation and the crude product was purified by silica gel chromatography using ethyl acetate—*n*-hexane (1/20, v/v) as the eluent to give **6** as a white solid (87.7 mg, 93% yield). Mp: 54.0–54.3 °C. IR (KBr, cm^{-1}): 3291 (≡CH), 2107 (C≡C). ^{1}H NMR (500 MHz, $CDCl_3$, rt): δ 7.20 (d, J = 8.0 Hz, 1H, Ar–H), 7.14 (d, J = 8.6 Hz, 1H, Ar–H), 7.10 (dd, J = 7.7, 1.4 Hz, 1H, Ar–H), 7.03 (d, J = 1.1 Hz, 1H, Ar–H), 6.50-6.34

(m, 2H, Ar–H), 3.98 (t, J = 6.6 Hz, 2H, OCH_2CH$_2$), 3.86 (t, J = 6.6 Hz, 2H, OCH_2CH$_2$CH$_3$), 3.84 (t, J = 6.6 Hz, 2H, OCH_2CH$_2$CH$_3$), 3.07 (s, 1H, CH), 1.79 (quint, J = 6.3 Hz, 2H, OCH$_2$CH_2), 1.60-1.69 (m, 4H, OCH$_2$CH_2CH$_3$), 1.43-1.49 (m, 2H, CH$_2$), 1.14-1.39 (m, 16H, 8CH$_2$), 0.81-0.92 (m, 9H, CH$_3$). ^{13}C NMR (125 MHz, CDCl$_3$, rt): δ 159.76, 157.37, 156.33, 131.75, 131.64, 129.30, 123.95, 121.12, 119.73, 115.33, 1004.48, 99.91, 84.17, 76.42, 69.79, 69.68, 68.02, 31.91, 29.66, 29.63, 29.60, 29.59, 29.43, 29.35 (2C), 26.09, 22.69, 22.49 (2C), 14.12, 10.53, 10.50. Calcd for $C_{32}H_{46}O_3 \cdot 0.25H_2O$: C, 79.54; H, 9.70. Found: C, 79.49; H, 9.63.

Polymerization. Homopolymerization of **1**, **4**, **5**, and **6** and copolymerization of **1** with **3** were carried out according to Scheme 3-2 in a dry glass ampule under a dry nitrogen atmosphere using $[Rh(nbd)Cl]_2$ as a catalyst in a similar way as reported previously.[3e, 15] Typical polymerization procedures are described below. Monomer **1** (300 mg, 0.626 mmol) was placed in a dry ampule, which was then evacuated on a vacuum line and flushed with dry nitrogen. After this evacuation-flush procedure was repeated three times, a three-way stopcock was attached to the ampule, and dry THF (883 μL) and Et_3N (260 μL) ($[Et_3N]/[\mathbf{1}] = 3$) were added with a syringe. To this was added a solution of $[Rh(nbd)Cl]_2$ (0.0311 M) in THF (100 μL) at 30 °C. The concentrations of **1** and the rhodium catalyst were 0.5 M and 0.005 M, respectively. The color of the mixture changed instantly to reddish brown. After 3 h, the resulting polymer (poly-**1**) was precipitated into a large amount of methanol, collected by centrifugation, and dried *in vacuo* at room temperature overnight (298 mg, 98%). The number-averaged molecular weight (M_n) of poly-**1** and its distribution (M_w/M_n) were estimated to be 4.9×10^5 and 1.8, respectively, by size exclusion chromatography (SEC) with polystyrene standards and THF as the eluent at a flow rate of 1.0 mL/min. Poly-**4**–poly-**6** were also prepared by polymerization of the corresponding monomers, in the same way. The results of the homopolymerization and copolymerization are summarized in Table 3-1 and Table 3-2, respectively. The copolymer compositions were estimated by their ^{1}H NMR spectra (Figure 3-16).

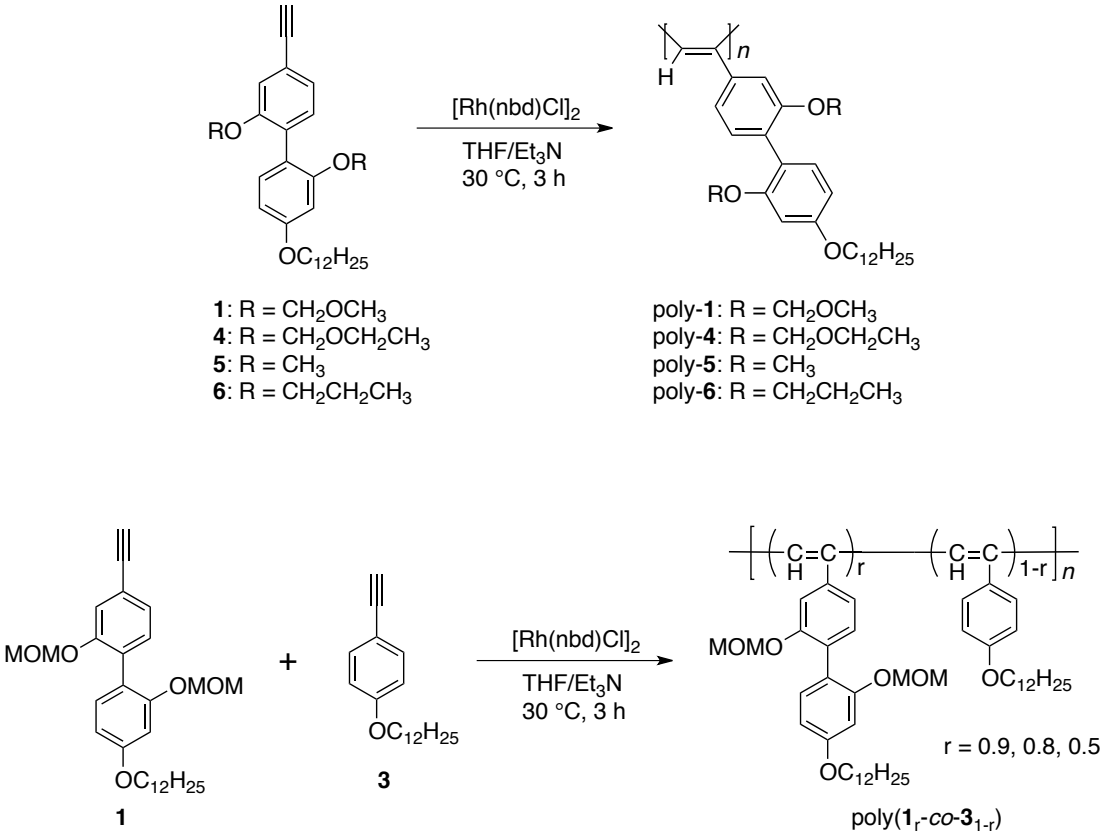

Scheme 3-2. Synthesis of Poly-**1**, Poly-**4**, Poly-**5**, Poly-**6**, and Poly($\mathbf{1}_r$-*co*-$\mathbf{3}_{1-r}$)

Table 3-1. Polymerization Results of **1**, **4**, **5**, and **6** with $[Rh(nbd)Cl]_2$ in THF/Et_3N at 30 °C for 3 h[a]

monomer	sample code	yield (%)[b]	$M_n \times 10^{-5}$[c]	M_w/M_n[c]
1	poly-**1**	98	4.9	1.8
4	poly-**4**	92	5.8	1.6
5	poly-**5**	99	6.5	1.4
6	poly-**6**	99	5.6	1.5

[a] [Monomer] = 0.5 M, $[Rh(nbd)Cl]_2$ = 0.005 M. [b] Methanol insoluble part. [c] Determined by SEC (polystyrene standards) with THF as the eluent.

Table 3-2. Copolymerization Results of **1** and **3** with $[Rh(nbd)Cl]_2$ in THF/Et_3N at 30 °C for 3 h[a]

in feed	copolymer				
1 (mol%)	sample code	yield (%)[b]	$M_n \times 10^{-5}$[c]	M_w/M_n[c]	**1** (mol%)[d]
90	poly($\mathbf{1}_{0.9}$-*co*-$\mathbf{3}_{0.1}$)	99	4.9	1.9	88
80	poly($\mathbf{1}_{0.8}$-*co*-$\mathbf{3}_{0.2}$)	98	4.9	2.0	77
50	poly($\mathbf{1}_{0.5}$-*co*-$\mathbf{3}_{0.5}$)	97	7.2	1.8	48

[a] [Monomer] = 0.5 M, $[Rh(nbd)Cl]_2$ = 0.005 M. [b] Methanol insoluble part. [c] Determined by SEC (polystyrene standards) with THF as the eluent. [d] Estimated by ^1H NMR.

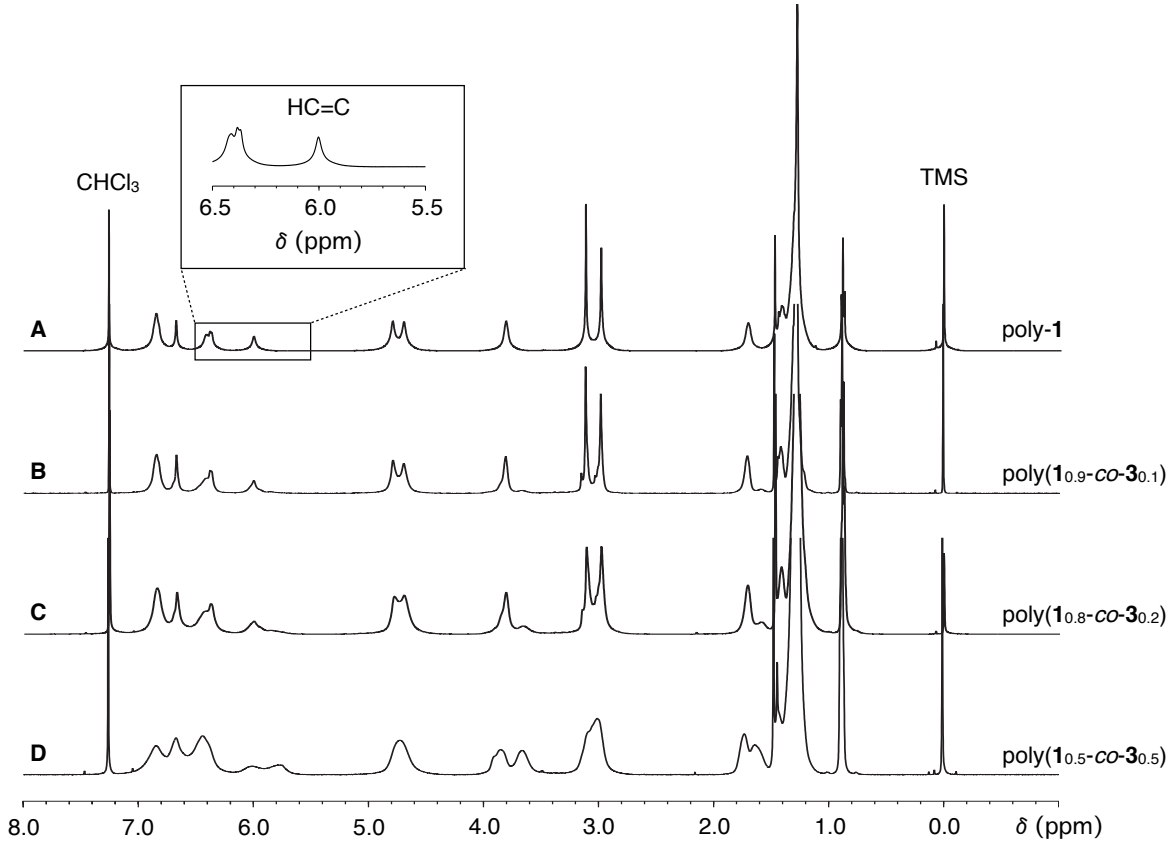

Figure 3-16. ^{1}H NMR spectra of poly-**1** (A), poly($\mathbf{1}_{0.9}$-*co*-$\mathbf{3}_{0.1}$) (B), poly($\mathbf{1}_{0.8}$-*co*-$\mathbf{3}_{0.2}$) (C), and poly($\mathbf{1}_{0.5}$-*co*-$\mathbf{3}_{0.5}$) (D) in $CDCl_3$ at 50 °C.

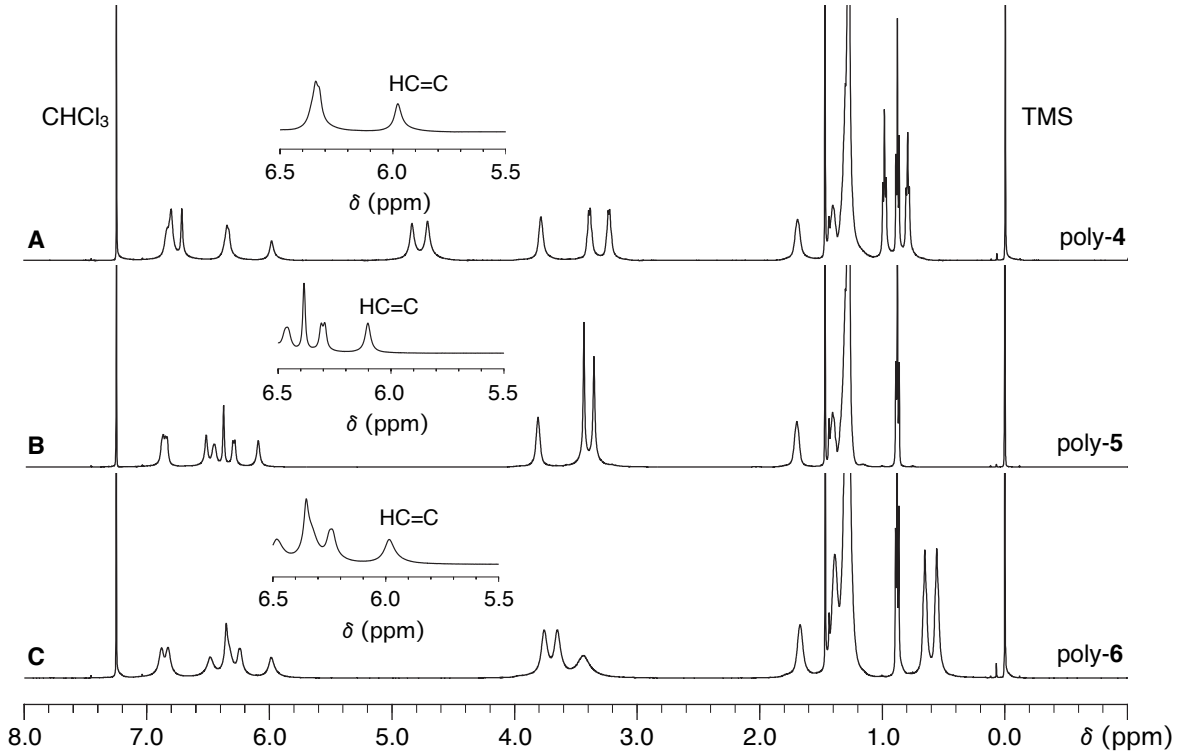

Figure 3-17. ^{1}H NMR spectra of poly-**4** (A), poly-**5** (B), and poly-**6** (C) in $CDCl_3$ at 50 °C.

The stereoregularities of the polymers were investigated by ^{1}H NMR and laser Raman spectroscopies. The ^{1}H NMR spectra of poly-**1**, poly-**4**, poly-**5**, and poly-**6** at 50 °C showed a sharp singlet centered around 6 ppm due to the main chain protons, indicating that the polymers possess a highly *cis-transoidal* stereoregular structure (Figure 3-16A and Figure 3-17).[16] However, the author could not estimate the stereoregularities of the copolymers by their ^{1}H NMR spectra because of the broadening of the main chain protons even at 50 °C (Figure 3-16B–D). The Raman spectra of the copolymers gave useful information. As shown in Figure 3-18, poly($\mathbf{1}_{0.5}$-*co*-$\mathbf{3}_{0.5}$) gave almost the same Raman spectrum to that of poly-**1**, in which intense peaks at 1572 and 1345 cm^{-1} were observed, which can be assigned to the C=C and C-C bond vibrations in the *cis* polyacetylenes, while those in the *trans* polyacetylene were not observed.[17] Therefore, these copolymers also likely possess highly *cis-transoidal* structures.

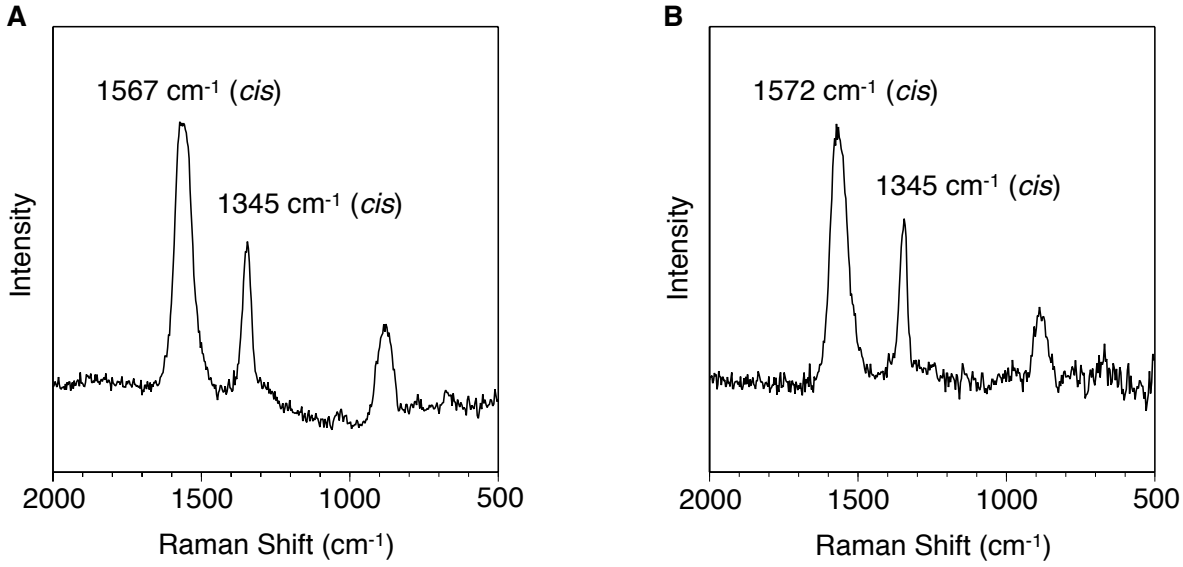

Figure 3-18. Laser Raman spectra of poly-**1** (A) and poly($\mathbf{1}_{0.5}$-*co*-$\mathbf{3}_{0.5}$) (B) in the solid state at room temperature.

Spectroscopic data of poly-**1**. ^{1}H NMR (500 MHz, $CDCl_3$, 50 °C): δ 6.76-7.06 (br, 3H, Ar–H), 6.68 (s, 1H, Ar–H), 6.29-6.54 (br, 2H, Ar–H), 6.00 (s, 1H, =CH), 4.80 (s, 2H, OCH_2O), 4.70 (s, 2H, OCH_2O), 3.82 (br, 2H, OCH_2CH_2), 3.12 (s, 3H, OCH_3), 2.99 (s, 3H, OCH_3), 1.72 (br, 2H, OCH_2CH_2), 1.22-1.52 (m, 18H, $9CH_2$), 0.90 (t, J = 6.3 Hz, 3H, CH_3). Calcd for $C_{30}H_{42}O_5$: C, 74.65; H, 8.77. Found: C, 74.25; H, 8.98.

Spectroscopic data of poly($\mathbf{1}_{0.9}$-*co*-$\mathbf{3}_{0.1}$). ^{1}H NMR (500 MHz, $CDCl_3$, 50 °C): δ 6.28-6.99 (m, 5.8H, Ar–H), 5.89-6.12 (br, 0.9H, =CH), 5.79-5.89 (br, 0.1H, =CH), 4.80 (s, 1.8H, OCH_2O), 4.70 (s, 1.8H, OCH_2O), 3.72-3.98 (br, 1.8H, OCH_2CH_2), 3.58-3.72 (br, 0.2H, OCH_2CH_2), 2.84-3.22 (m, 5.4H, OCH_3), 1.63-1.84 (br, 1.8H, OCH_2CH_2), 1.53-1.63 (br, 0.2H, CH_2), 1.14-1.46 (m, 18H, $9CH_2$), 0.84-0.94 (br, 3H, CH_3). Calcd for $(0.88C_{30}H_{42}O_5{\cdot}0.12C_{20}H_{30}O)_n$: C, 75.34; H, 8.90. Found: C, 76.29; H, 9.32.

Spectroscopic data of poly($\mathbf{1}_{0.8}$-*co*-$\mathbf{3}_{0.2}$). ^{1}H NMR (500 MHz, $CDCl_3$, 50 °C): δ 6.21-7.00 (m, 5.6H, Ar–H), 5.67-6.12 (br, 1H, =CH), 4.44-5.05 (br, 3.2H, OCH_2O), 3.72-3.99 (br, 1.6H, OCH_2CH_2), 3.54-3.72 (br, 0.4H, OCH_2CH_2), 2.75-3.26 (m, 4.8H, OCH_3), 1.52-1.90 (br, 2H,

OCH_2CH_2), 1.06-1.52 (m, 18H, $9CH_2$), 0.76-0.95 (br, 3H, CH_3). Calcd for $(0.77C_{30}H_{42}O_5{\cdot}0.23C_{20}H_{30}O{\cdot}0.4H_2O)_n$: C, 74.81; H, 9.07. Found: C, 74.76; H, 9.08.

Spectroscopic data of poly($\mathbf{1}_{0.5}$-*co*-$\mathbf{3}_{0.5}$). ^{1}H NMR (500 MHz, $CDCl_3$, 50 °C): δ 6.19-7.09 (m, 5H, Ar–H), 5.63-6.19 (br, 1H, =CH), 4.73 (br, 2H, OCH_2O), 3.76-4.00 (br, 1H, OCH_2CH_2), 3.54-3.76 (br, 1H, OCH_2CH_2), 2.77-3.28 (br, 3H, OCH_3), 1.52-1.90 (br, 2H, OCH_2CH_2), 1.05-1.50 (m, 18H, $9CH_2$), 0.76-0.95 (br, 3H, CH_3). Calcd for $(0.48C_{30}H_{42}O_5{\cdot}0.52C_{20}H_{30}O{\cdot}0.25H_2O)_n$: C, 77.34; H, 9.49. Found: C, 77.48; H, 9.58.

Spectroscopic data of poly-**4**. ^{1}H NMR (500 MHz, $CDCl_3$, 50 °C): δ 6.69-6.88 (br, 4H, Ar–H), 6.25-6.40 (br, 2H, Ar–H), 5.98 (s, 1H, =CH), 4.84 (s, 2H, OCH_2O), 4.71 (s, 2H, OCH_2O), 3.79 (br, 2H, OCH_2CH_2), 3.39 (br, 2H, OCH_2CH_3), 3.23 (br, 2H, OCH_2CH_3), 1.69 (br, 2H, OCH_2CH_2), 1.16-1.52 (m, 18H, $9CH_2$), 0.99 (t, J = 6.3 Hz, 3H, OCH_2CH_3), 0.88 (t, J = 6.3 Hz, 3H, CH_3) 0.80 (t, J = 6.3 Hz, 3H, OCH_2CH_3). Calcd for $C_{32}H_{46}O_5{\cdot}0.25H_2O$: C, 74.60; H, 9.10. Found: C, 74.59; H, 9.24.

Spectroscopic data of poly-**5**. ^{1}H NMR (500 MHz, $CDCl_3$, 50 °C): δ 6.82-6.92 (m, 2H, Ar–H), 6.43-6.55 (m, 2H, Ar–H), 6.39 (br, 1H, Ar–H), 6.10 (d, J = 6.9 Hz,1H, Ar–H), 6.10 (s, 1H, =CH), 3.82 (br, 2H, OCH_2CH_2), 3.45 (s, 3H, OCH_3), 3.36 (s, 3H, OCH_3), 1.72 (br, 2H, OCH_2CH_2), 1.24-1.44 (m, 18H, $9CH_2$), 0.89 (t, J = 6.6 Hz, 3H, CH_3). Calcd for $C_{28}H_{38}O_3{\cdot}0.25H_2O$: C, 78.74; H, 9.09. Found: C, 78.71; H, 9.12.

Spectroscopic data of poly-**6**. ^{1}H NMR (500 MHz, $CDCl_3$, 50 °C): δ 6.78-6.93 (br, 2H, Ar–H), 6.19-6.55 (br, 4H, Ar–H), 5.98 (s, 1H, =CH), 3.76 (s, 2H, $OCH_2CH_2CH_3$), 3.65 (s, 2H, $OCH_2CH_2CH_3$), 3.44 (br, 2H, OCH_2CH_2), 1.67 (br, 2H, OCH_2CH_2), 1.19-1.42 (m, 22H, $11CH_2$), 0.88 (t, J = 6.9 Hz, 3H, CH_3), 0.65 (br, 2H, $OCH_2CH_2CH_3$), 0.56 (br, 2H, $OCH_2CH_2CH_3$). Calcd for $C_{32}H_{46}O_3{\cdot}0.3H_2O$: C, 79.39; H, 9.70. Found: C, 79.37; H, 9.77.

Helicity Induction in Poly-1 in Solution. A stock solution of poly-**1** (2.0 mM) in *n*-hexane was prepared in a 2-mL flask equipped with a stopcock. A 500 μL aliquot of the poly-**1** solution was transferred to a vessel equipped with a screwcap using a Hamilton microsyringe. An appropriate amount of (*R*)- or (*S*)-**2** was added to the vessel and the solution was immediately mixed with a vibrator (Iuchi, Japan). After the solution was allowed to stand for an appropriate time at 25 °C, the absorption and CD spectra were recorded at 25 °C and -10 °C (Figure 3-2A,i and ii). For CD titration experiments, stock solutions of poly-**1** (2.0 mM) and (*S*)-**2** (165.4 mM) in *n*-hexane were prepared. A 500 μL aliquot of the poly-**1** solution was transferred to five 1 mL flasks equipped with stopcocks using a Hamilton microsyringe. An appropriate amount of the stock solution of (*S*)-**2** was added to the flasks. The solutions were immediately mixed with a vibrator and finally diluted with *n*-hexane to keep the poly-**1** concentration at 1.0 mM. After the solution was allowed to stand at 25 °C for 6 h, the absorption and CD spectra were taken at 25 °C and -10 °C for each flask to give the titration curve (Figure 3-3).

Chiral Amplification in Poly-1 in Solution. The nonlinear effect between the ICD intensity of poly-**1** against percent ee of **2** during the helicity induction in solution was investigated in *n*-hexane at 25 and -10 °C. The poly-**1** concentration and the molar ratio of **2** to the monomer units of poly-**1** were held constant at 1.0 mM and 400 mol/mol, respectively. Stock solutions of poly-**1** (1.0 mg/mL (2.0 mM)), (*R*)-**2** (800 mM), and (*S*)-**2** (800 mM) were prepared in *n*-hexane. Aliquots of the stock solutions of (*R*)- and (*S*)-**2** were placed into six vessels so that the percent ee of the mixtures (*S* rich) became 10, 20, 40, 60, 80, and 100, respectively. To the vessels was added a 500 μL aliquot of the stock solution of poly-**1**, and the resulting solutions were immediately mixed using a vibrator. After the solutions were allowed to stand at 25 °C for 6 h, the absorption and CD spectra were then taken for each vessel to determine the changes in the CD intensity at 381 nm (second Cotton) (Figure 3-4A and 3-4B,● and ●).

Memory of the Macromolecular Helicity in Solution. A stock solution of poly-**1** (1.0 mg/mL (2.0 mM)) with (*S*)-**2** (1.6 M) ([(*S*)-**2**]/[poly-**1**] = 800 mol/mol) was prepared in *n*-hexane. The solution was allowed to stand at 25 °C for 6 h. After the solution was cooled to -10 °C, the solution was poured into a large amount of methanol at -10 °C to remove (*S*)-**2**. The precipitated poly-**1** was collected by centrifugation, washed with methanol, and then dried in vacuo at room temperature over night. The complete removal of (*S*)-**2** was confirmed by ^{1}H NMR measurement of the isolated poly-**1** (Figure 3-5). After the isolated poly-**1** was dissolved in *n*-hexane at -10 °C, the absorption and CD spectra were then recorded (Figure 3-2A,iii).

Dynamic Light Scattering Measurements. A stock solution of poly-**1** (1.0 mM) in *n*-hexane was prepared in a 5-mL flask equipped with a stopcock. The solution was filtered with a 0.45 μm syringe filter (Toyo Roshi Co. Ltd., Japan), and then the DLS measurement of the sample was performed at a fixed scattering angle of 90° at *ca*. 25 °C. The corresponding hydrodynamic diameter (d_H) was calculated using the Stokes-Einstein equation: $d_H = k_BT/(3\pi\eta D)$, where k_B, η, and T are the Boltzmann constant, the solvent viscosity, and the absolute temperature, respectively. The d_H value of poly-**1** was estimated to be 42.0±5.2 in *n*-hexane, which is comparable to those for poly((*S*)-(+)-(4-((1-(1-naphthyl)ethyl)carbamoyl)phenyl) acetylene) (d_H = 56 nm, $M_n = 6.0 \times 10^5$)[18] as well as poly(*n*-hexyl isocyanate) (d_H = *ca*. 60 nm, $M_v = 2.8 \times 10^5$).[19] These results indicate that the formation of aggregates of polymer main chains can be excluded.

Molecular Modeling and Calculations. The molecular modeling and molecular mechanics calculations of poly-**1** were conducted with the Compass force field as implemented in the MS Modeling software (version 4.4, Accelrys, San Diego, CA) operated using a PC running under Windows XP. The polymer model (50 repeating monomer units) of a right-handed helical poly-**1** was constructed by a Polymer Builder module in the MS Modeling software. The main-chain geometrical parameters, such as the bond lengths, the bond angles, and the internal rotation angles were defined as a 23 unit/10 turn (23/10) helix

on the basis of the helical structure of a poly(phenylacetylene) bearing *N*,*N*-diisopropylaminomethyl pendants (poly-**A**) determined by X-ray analysis because poly-**1** showed almost the same CD pattern as that of poly-**A**.[16a] The dodecyloxy groups of the pendants were replaced by hydrogen atoms for clarity. The initial dihedral angle between the phenyl groups of the pendant biphenyl units was set to be ± 64.2° (right- and left-handed twists (*cisoid*)) on the basis of the structure of the corresponding monomer **1** determined by X-ray analysis as shown in Figure 3-19. For each of the right- and left-handed twists in the biphenyl pendant, the following two possible conformers were taken into consideration.

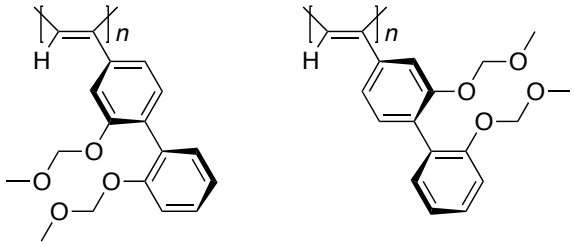

The geometry optimizations of each constructed model (50 mer) were carried out without any cutoff by the smart minimizer in three steps. First, the starting conformations were subject to the steepest decent optimization to eliminate the worse steric conflicts. Second, subsequent optimization until the convergence using a conjugate gradient algorithm was performed. The fully optimized poly-**1** models were obtained by the further energy minimization using the Newton method with the 0.1 kcal·mol^{-1}·Å^{-1} convergence criterion. The most stable structure obtained is shown in Figure 3-8A and B, where the right-handed helical poly-**1** possesses a left-handed twisted conformation in the biphenyl units.

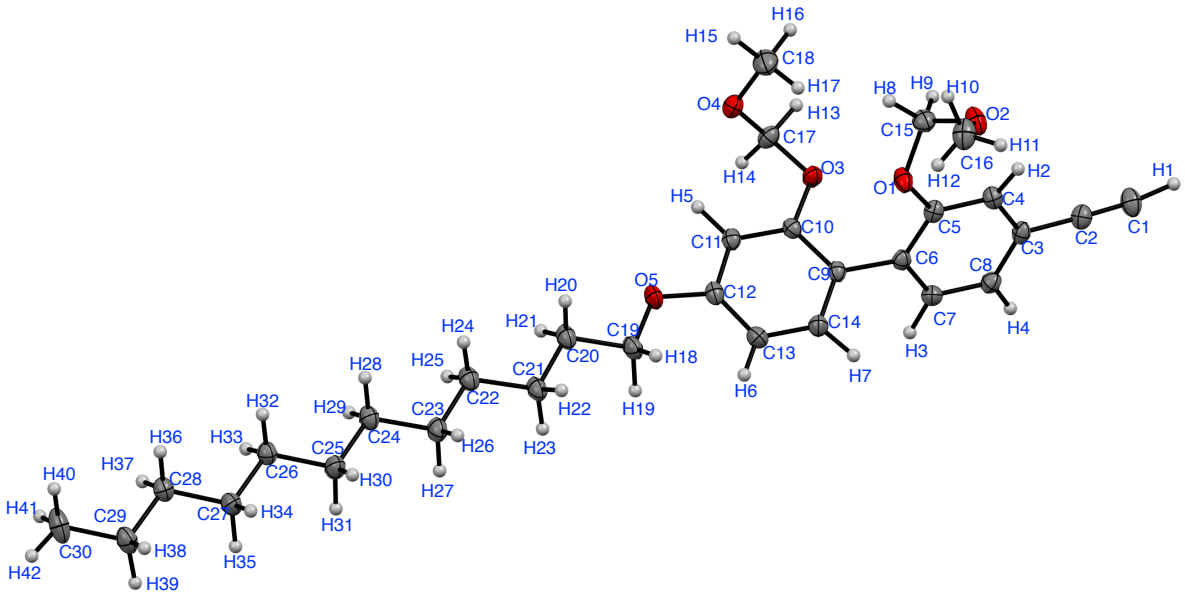

Figure 3-19. ORTEP drawing of **1** with a full atom-numbering scheme. Thermal ellipsoids are drawn at the 50% probability level.

Helicity induction and memory of poly-1 in the solid state. Poly-**1** (1 mg) was placed in a 2-mL vessel equipped with a screw cap. A 100 μL of (*S*)-**2** was then added to the vessel to give a suspended solution because poly-**1** was insoluble in (*S*)-**2**. After the suspended solution was allowed to stand for an appropriate time at 25 °C to induce the preferred-handed helicity on poly-**1** in the solid state, the poly-**1** was collected by filtration and washed with methanol several times to remove (*S*)-**2**. The isolated poly-**1** was then dried in vacuo at room temperature over night. The complete removal of (*S*)-**2** was confirmed by ^{1}H NMR measurement of the isolated poly-**1**. After the isolated poly-**1** was dissolved in *n*-hexane at -10 °C, the absorption and CD spectra were then recorded. The same procedure was done for the isolation of poly-**1** induced by nonracemic **2** with different ee values (20, 40, 50, 60, 80% ee) in the solid state at 25 °C. Solubility of poly-**1** in liquid **2** was investigated by UV-Vis spectroscopy as follows; after poly-**1** (1 mg) was suspended in **2** (1 mL) at 25 °C for 1 h, the supernatant showed no detectable absorption due to the poly-**1**.

Preparation of an HPLC column using optically inactive poly-1. As-prepared, optically inactive poly-**1** (480 mg) dissolved in *n*-hexane was coated on a silica gel (2.42 g)

according to the previously reported method,[11] and the solvent was evaporated under reduced pressure. The content of poly-**1** onto silica gel was estimated by thermogravimetric (TG) analysis and was 16 wt%. After fractionating the packing materials with sieves, the obtained column packing material was packed into a stainless-steel tube (25 cm × 0.20 cm (i.d.)) by a conventional high-pressure slurry packing technique using an ECONO-PACKER MODEL CPP-085 (Chemco, Osaka, Japan).[12] The plate number of the column was 3400 for benzene with methanol as the eluent at a flow rate of 0.025 mL/min at *ca*. 0 °C. The dead time (t_0) was estimated using acetone as the nonretained compound.

Switchable helicity Induction and memory of poly-1 in the column. The as-prepared poly-**1**-based HPLC column was filled with (*R*)-**2** in acetone ((*R*)-**2**/acetone = 1/1, v/v) and allowed to stand at 50 °C for 10 min and then at 25 °C for 10 min to induce the preferred-handed helicity on poly-**1** in the solid state. We used an acetone solution of (*R*)- and (*S*)-**2** (**2**/acetone = 1/1, v/v) for the helicity induction in the column instead of liquid (*R*)- and (*S*)-**2** in order to prevent high pressure arising from the high viscosity of **2** in the column, which may damage the column, resulting in decreasing its theoretical plate number. The acetone solution of (*R*)-**2** in the column was then completely removed and replaced with methanol by flowing an excess amount of methanol at *ca*. 10 °C for 60 min at a flow rate of 0.05 mL/min, resulting in the CSP consisting of *P*-poly-**1**. The author notes that the macromolecular helicity memory of *P*-poly-**1** is stable in methanol at 25 °C. The CD intensity ($\Delta\varepsilon_{2nd}$) changes of *M*-poly-**1** with macromolecular helicity memory prepared by (*S*)-**2** were followed after immersing it in liquid (*R*)-**2**, racemic **2**, benzyl alcohol, and methanol in the solid state at 0, 25, and 50 °C (Figure 3-20). The helix-sense of *M*-poly-**1** was completely switched within 10 min at 50 °C as described in the text and 6 h at 25 °C when the polymer was immersed in (*R*)-**2**. However, *M*-poly-**1** maintained its helical sense in (*R*)-**2** even after 6 h at 0 °C and its CD intensity slightly decreased, indicating that the helix inversion of *M*-poly-**1** took place very slowly at 0 °C even with the (*R*)-**2** enantiomer in the solid state. *M*-poly-**1** was very stable in racemic **2** and benzyl alcohol over 6 h at 0 °C, showing no CD intensity change, whereas it

was racemized to some extent at 25 °C after 6 h. Most importantly, *M*-poly-**1** is quite stable in methanol used as the solvent to wash the columns to preserve the helicity, and its CD intensity hardly changed at 25 and 0 °C even after 6 h. The chiral recognition ability of the poly-**1** with helicity memory was investigated by HPLC under the reverse-phase condition using methanol-H_2O (75:25, v/v) as the eluent because poly-**1** is soluble in most organic solvents under the normal-phase condition. The column packed with the *P*-poly-**1** was then treated with (*S*)-**2** in acetone ((*S*)-**2**/acetone = 1/1, v/v) in the same way, giving the CSP composed of *M*-poly-**1** with an opposite helical handedness and used for enantioseparation.

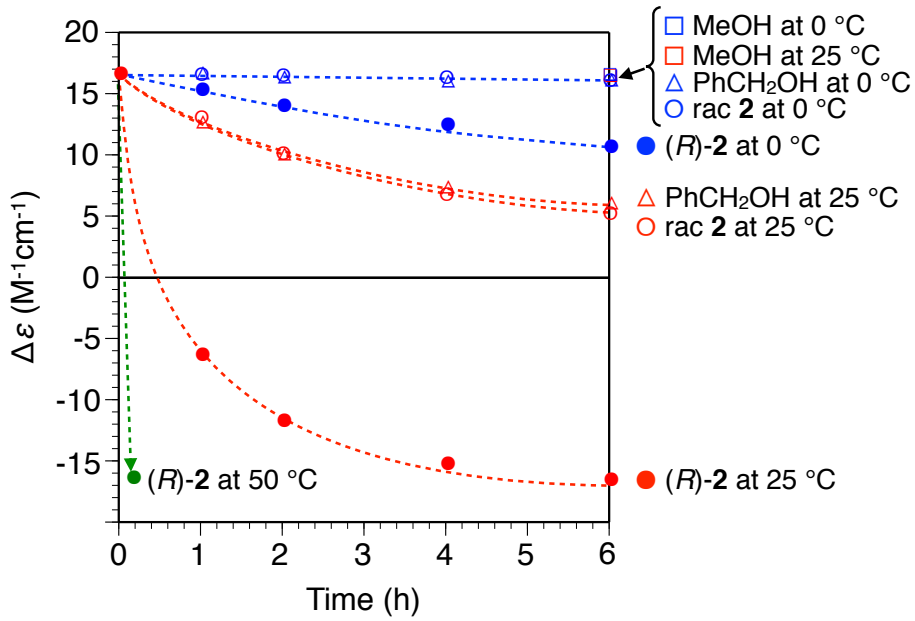

Figure 3-20. Time-dependent CD intensity ($\Delta\varepsilon_{2nd}$) changes of *M*-poly-**1** with macromolecular helicity memory prepared by (*S*)-**2** measured in *n*-hexane at -10 °C after immersing *M*-poly-**1** in liquid (*R*)-**2** (●), racemic **2** (○), benzyl alcohol (△), and methanol (□) in the solid state at 0 °C (blue), 25 °C (red), and 50 °C (green) followed by isolation. [Poly-**1**] = 1.0 mM. The polymer was insoluble in these solvents.

References

1. (a) Gellman, S. H., *Acc. Chem. Res.* **1998**, *31*, 173-180; (b) Green, M. M.; Park, J. W.; Sato, T.; Teramoto, A.; Lifson, S.; Selinger, R. L. B.; Selinger, J. V., *Angew. Chem., Int. Ed.* **1999**, *38*, 3138-3154; (c) Hill, D. J.; Mio, M. J.; Prince, R. B.; Hughes, T. S.; Moore, J. S., *Chem. Rev.* **2001**, *101*, 3893-4011; (d) Nakano, T.; Okamoto, Y., *Chem. Rev.* **2001**, *101*, 4013-4038; (e) Cornelissen, J. J. L. M.; Rowan, A. E.; Nolte, R. J. M.; Sommerdijk, N. A. J. M., *Chem. Rev.* **2001**, *101*, 4039-4070; (f) Fujiki, M., *Macromol. Rapid Commun.* **2001**, *22*, 539-563; (g) Lam, J. W. Y.; Tang, B. Z., *Acc. Chem. Res.* **2005**, *38*, 745-754; (h) Hecht, S.; Huc, I., *Foldamers: Structure, Properties, and Applications*. WILEY-VCH: Weinheim, 2007; (i) Rudick, J. G.; Percec, V., *Acc. Chem. Res.* **2008**, *41*, 1641-1652.
2. Yashima, E.; Maeda, K.; Iida, H.; Furusho, Y.; Nagai, K., *Chem. Rev.* **2009**, *109*, 6102-6211.
3. (a) Yashima, E.; Maeda, K.; Okamoto, Y., *Nature* **1999**, *399*, 449-451; (b) Maeda, K.; Morino, K.; Okamoto, Y.; Sato, T.; Yashima, E., *J. Am. Chem. Soc.* **2004**, *126*, 4329-4342; (c) Onouchi, H.; Kashiwagi, D.; Hayashi, K.; Maeda, K.; Yashima, E., *Macromolecules* **2004**, *37*, 5495-5503; (d) Miyagawa, T.; Furuko, A.; Maeda, K.; Katagiri, H.; Furusho, Y.; Yashima, E., *J. Am. Chem. Soc.* **2005**, *127*, 5018-5019; (e) Maeda, K.; Tamaki, S.; Tamura, K.; Yashima, E., *Chem. Asian J.* **2008**, *3*, 614-624.
4. (a) Furusho, Y.; Kimura, T.; Mizuno, Y.; Aida, T., *J. Am. Chem. Soc.* **1997**, *119*, 5267-5268; (b) Bellacchio, E.; Lauceri, R.; Gurrieri, S.; Scolaro, L. M.; Romeo, A.; Purrello, R., *J. Am. Chem. Soc.* **1998**, *120*, 12353-12354; (c) Prins, L. J.; De Jong, F.; Timmerman, P.; Reinhoudt, D. N., *Nature* **2000**, *408*, 181-184; (d) Kubo, Y.; Ohno, T.; Yamanaka, J.; Tokita, S.; Iida, T.; Ishimaru, Y., *J. Am. Chem. Soc.* **2001**, *123*, 12700-12701; (e) Wilson, A. J.; Masuda, M.; Sijbesma, R. P.; Meijer, E. W., *Angew. Chem., Int. Ed.* **2005**, *44*, 2275-2279; (f) Ikeda, C.; Yoon, Z. S.; Park, M.; Inoue, H.; Kim, D.; Osuka, A., *J. Am. Chem. Soc.* **2005**, *127*, 534-535; (g) Ousaka, N.; Inai, Y.; Kuroda, R., *J. Am. Chem. Soc.* **2008**, *130*, 12266-12267.

5. (a) Buono, A. M.; Immediata, I.; Rizzo, P.; Guerra, G., *J. Am. Chem. Soc.* **2007**, *129*, 10992-10993; (b) Guadagno, L.; Raimondo, M.; Silvestre, C.; Immediata, I.; Rizzo, P.; Guerra, G., *J. Mater. Chem.* **2008**, *18*, 567-572; (c) Saxena, A.; Guo, G.; Fujiki, M.; Yang, Y.; Ohira, A.; Okoshi, K.; Naito, M., *Macromolecules* **2004**, *37*, 3081-3083; (d) Maeda, K.; Hatanaka, K.; Yashima, E., *Mendeleev Commun.* **2004**, 231-233.
6. (a) Randazzo, R.; Mammana, A.; D'Urso, A.; Lauceri, R.; Purrello, R., *Angew. Chem., Int. Ed.* **2008**, *47*, 9879-9882; (b) Helmich, F.; Lee, C. C.; Schenning, A. P. H. J.; Meijer, E. W., *J. Am. Chem. Soc.* **2010**, *132*, 16753-16755; (c) Zhang, W.; Jin, W.; Fukushima, T.; Ishii, N.; Aida, T., *J. Am. Chem. Soc.* **2013**, *135*, 114-117.
7. Okamoto, M., *J. Pharm. Biomed. Anal.* **2002**, *27*, 401-407.
8. Perry, J. A.; Rateike, J. D.; Szczerba, T. J., *J. Chromatogr. A* **1987**, *389*, 57-64.
9. (a) Sakurai, S. I.; Okoshi, K.; Kumaki, J.; Yashima, E., *Angew. Chem., Int. Ed.* **2006**, *45*, 1245-1248; (b) Sakurai, S. I.; Okoshi, K.; Kumaki, J.; Yashima, E., *J. Am. Chem. Soc.* **2006**, *128*, 5650-5651.
10. Shundo, A.; Hori, K.; Ikeda, T.; Kimizuka, N.; Tanaka, K., *J. Am. Chem. Soc.* **2013**, *135*, 10282-10285.
11. Okamoto, Y.; Aburatani, R.; Hatada, K., *J. Chromatogr. A* **1987**, *389*, 95-102.
12. Okamoto, Y.; Kawashima, M.; Hatada, K., *J. Chromatogr. A* **1986**, *363*, 173-186.
13. (a) Tabata, M.; Mawatari, Y.; Sone, T.; Miyasaka, A.; Kai, H.; Orito, K.; Sadahiro, Y., *Macromolecular Symposia* **2006**, *239*, 7-12; (b) Mawatari, Y.; Tabata, M.; Sone, T.; Ito, K.; Sadahiro, Y., *Macromolecules* **2001**, *34*, 3776-3782.
14. Hiroya, K.; Suzuki, N.; Yasuhara, A.; Egawa, Y.; Kasano, A.; Sakamoto, T., *J. Chem. Soc., Perkin Trans. 1* **2000**, 4339-4346.
15. (a) Yashima, E.; Matsushima, T.; Okamoto, Y., *J. Am. Chem. Soc.* **1995**, *117*, 11596-11597; (b) Yashima, E.; Matsushima, T.; Okamoto, Y., *J. Am. Chem. Soc.* **1997**, *119*, 6345-6359.
16. (a) Nagai, K.; Sakajiri, K.; Maeda, K.; Okoshi, K.; Sato, T.; Yashima, E., *Macromolecules* **2006**, *39*, 5371-5380; (b) Simionescu, C. I.; Percec, V.; Dumitrescu, S.,

J. Polym. Sci., Part A: Polym. Chem. **1977**, *15*, 2497-2509; (c) Simionescu, C. I.; Percec, V., *Prog. Polym. Sci.* **1982**, *8*, 133-214; (d) Furlani, A.; Napoletano, C.; Russo, M. V.; Feast, W. J., *Polym. Bull.* **1986**, *16*, 311-317; (e) Kishimoto, Y.; Eckerle, P.; Miyatake, T.; Kainosho, M.; Ono, A.; Ikariya, T.; Noyori, R., *J. Am. Chem. Soc.* **1999**, *121*, 12035-12044; (f) Percec, V.; Rudick, J. G.; Peterca, M.; Wagner, M.; Obata, M.; Mitchell, C. M.; Cho, W. D.; Balagurusamy, V. S. K.; Heiney, P. A., *J. Am. Chem. Soc.* **2005**, *127*, 15257-15264.

17. (a) Tabata, M.; Tanaka, Y.; Sadahiro, Y.; Sone, T.; Yokota, K.; Miura, I., *Macromolecules* **1997**, *30*, 5200-5204; (b) Maeda, K.; Goto, H.; Yashima, E., *Macromolecules* **2001**, *34*, 1160-1164; (c) Shirakawa, H.; Ito, T.; Ikeda, S., *Polym. J.* **1973**, *4*, 469-472.
18. Morino, K.; Maeda, K.; Yashima, E., *Macromolecules* **2003**, *36*, 1480-1486.
19. Guenet, J.-M.; Jeon, H. S.; Khatri, C.; Jha, S. K.; Balsara, N. P.; Green, M. M.; Brulet, A.; Thierry, A., *Macromolecules* **1997**, *30*, 4590-4596.

Chapter 4

Memory of the Enantiomeric Macromolecular Helicity Induced in a Polyacetylene with a Single Enantiomer Assisted by Temperature- and Solvent-driven Helix Inversion

Abstract: An optically inactive polyacetylene bearing 2,2'-biphenol-derived pendants, poly((2,2'-bis(ethoxymethoxy)-4'-dodecyloxy-4-biphenylyl)acetylene) (poly-**1**-MOE), formed a preferred-handed helical conformation in the presence of a nonracemic alcohol, (*S*)-1-phenylethylalcohol ((*S*)-**2**), in solution. The helix-sense of poly-**1**-MOE induced by (*S*)-**2** through weak noncovalent interaction inverted in response to a change in temperature as well as solvent. Moreover, the right- and left-handed macromolecular helicity formed by the temperature- and solvent-driven helix-sense inversion were successfully memorized even after the complete removal of the chiral alcohol. Consequently, both enantiomeric helices could be obtained from the optically inactive poly-**1**-MOE by using a single enantiomer without the use of chaperoning compounds.

Introduction

Synthesis of helical polymers with a preferred helix-sense has been attracting much attention not only to mimic biological helices, but also for their wide variety of possible applications as novel chiral materials for separation of enantiomers and enantioselective catalysis.[1] The polymerization of optically active monomers and the helix-sense selective polymerization of achiral bulky monomers with chiral catalysts or initiators are well-known typical methods for preparing synthetic helical polymers with a controlled helix-sense.[1e, 1r] The noncovalent helicity induction in optically inactive polymers combined with the helicity memory is a unique alternative method to produce optically active polymers with a preferred-handed helical conformation.[1j, 1n, o, 1r, 2] This method has a great advantage especially in that the predominant helix-sense can be determined after polymerization. However, the opposite enantiomeric helicity memory requires the opposite enantiomeric guest, followed by replacement with achiral chaperoning molecules, because the predominant helix-sense is predetermined by the chirality of the enantiomeric guests used.

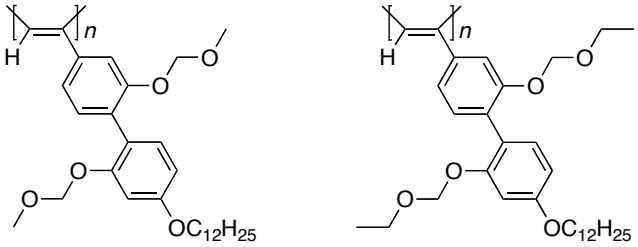

poly-**1**-MOM poly-**1**-MOE

Chart 4-1. Structures of Poly-**1**-MOM and Poly-**1**-MOE

As mentioned in Chapter 3, a preferred-handed helicity induced in optically inactive polyacetylenes bearing 2,2'-biphenol-derived pendants (poly-**1**-MOM and poly-1-MOE, Chart 4-1) by an optically active alcohol can be automatically "memorized" even after complete removal of the chiral alcohol. The author now found that the helix-sense of poly-**1**-MOE induced by (*S*)-1-phenylethanol ((*S*)-**2**) inverted by a change in temperature and solvent.

Moreover, the author also found that both the enantiomeric right- and left-handed helical conformations induced in poly-**1**-MOE by a single enantiomer (*S*)-**2** assisted by the temperature- and solvent-driven macromolecular helicity inversion were automatically memorized without the use of chaperoning compounds (Figure 4-1). Similar "dual memory" of enantiomeric helices has been reported for other poly(phenylacetylene) derivatives bearing acid functional pendants based on the noncovalent "helicity induction and chiral memory" concept assisted by inversion of the macromolecular helicity with temperature.[3] However, the present result is significantly different from the previous ones in view of the fact that the previous dual memory systems necessarily require the replacement with achiral amines as chaperoning compounds.

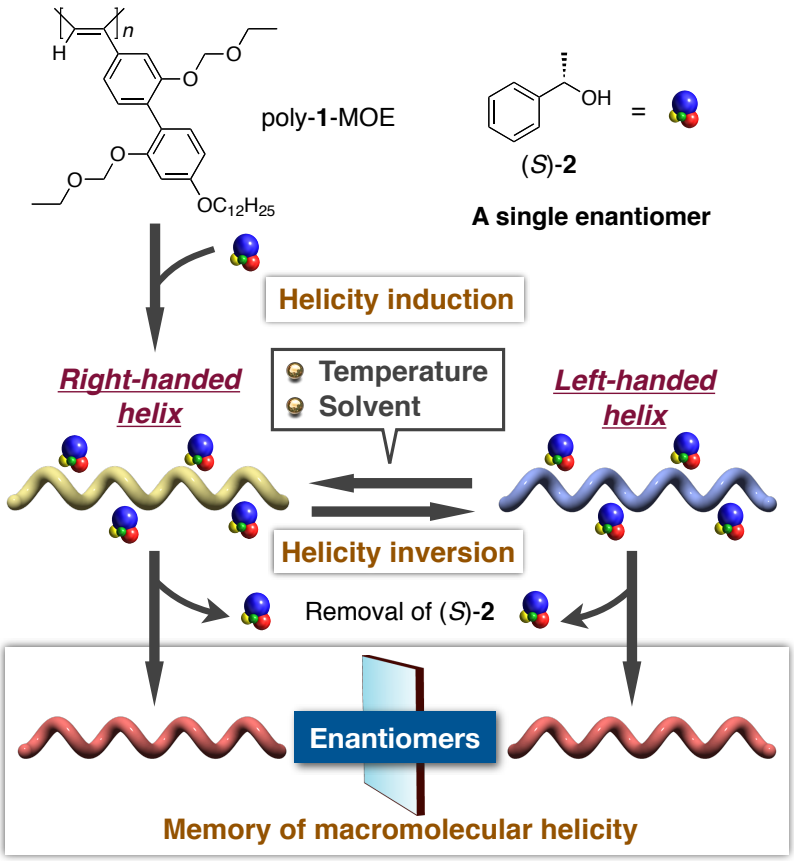

Figure 4-1. Schematic illustration of temperature- and solvent-driven helix sense inversion of the helical conformation of poly-**1**-MOE induced by (*S*)-**2** and subsequent macromolecular helicity memory after removal of (*S*)-**2**.

Results and Discussion

Helicity Induction and Inversion in Poly-1-MOE with (*S*)-2. Poly-**1**-MOE showed split-type induced CDs (ICDs) in the absorption region of the polymer backbone in the presence of (*S*)-**2** ([(*S*)-**2**]/[poly-**1**-MOE] = 400) in hexane at 25 °C (a in Figure 4-2A). Although the ICD intensity was very small just after the sample preparation, it increased with time to reach a constant value after 2 h at 25 °C (a in Figure 4-2B). These results indicate that poly-**1**-MOE formed a preferred-handed helical conformation upon complexation with (*S*)-**2** through noncovalent weak hydrogen-bonding interactions. When the sample was cooled to -10 °C, the ICD intensity further increased very slowly with time and reached an almost constant value after 5 days (b in Figure 4-2A,B). Interestingly, the CD spectral pattern immediately inverted upon heating the sample at 50 °C accompanied by a very slight change in the absorption spectrum (c in Figure 4-2A,B). When the sample was again cooled to 25 °C, the ICD intensity reverted to the plateau value at 25 °C within 2 h (d in Figure 4-2B). These spectral changes could be repeated (e–g in Figure 4-2B). Therefore, these results suggest that the preferred-handed helix-sense of poly-**1**-MOE induced by (*S*)-**2** through noncovalent interactions can be reversibly switched by changing the temperature. Although a similar macromolecular helicity inversion assisted by external stimuli, such as a change in temperature and solvent, has been reported for various helical polymers bearing optically active substituents,[1g, 1j, 1n, o, 1r] it is still quite rare for the induced helical polymers, whose helical senses can be biased through chiral noncovalent bonding interactions.[3-4] The preferred-handed helical sense of the poly-**1**-MOE induced by (*S*)-**2** in hexane at -10 °C and 50 °C showing a negative and positive second Cotton effect at *ca*. 370 nm, respectively, can be assigned to be right-handed and left-handed, respectively, on the basis of the Cotton effect signs of the ICDs of analogous helical polyacetylenes and their helical senses determined by high-resolution atomic force microscopy (AFM) observations.[5] The right- and left-handed helices of poly-**1**-MOE induced at -10 °C and 50 °C are not enantiomers, but diastereomers

because of the presence of the chiral (*S*)-**2** interacting with poly-**1**-MOE; therefore, their CD and absorption spectra slightly differ from one another.

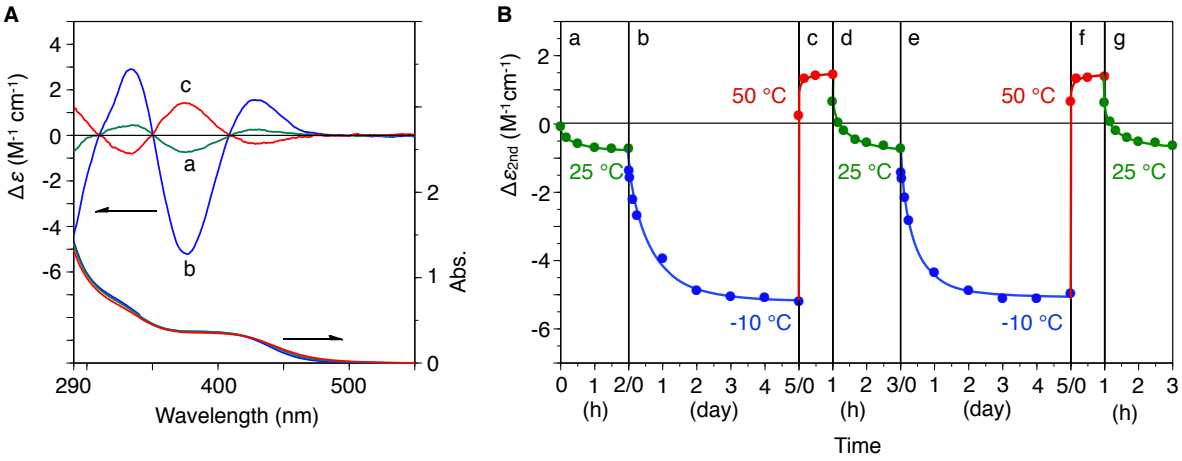

Figure 4-2. (A) CD and absorption spectra of poly-**1**-MOE (1.0 mM) with (*S*)-**2** ([(*S*)-**2**]/[poly-**1**-MOE] = 400) in hexane at 25 °C after 2 h (a, green), at -10 °C after 5 days (b, blue) and at 50 °C after 1 h (c, red). (B) The plots of ICD intensity $\Delta\varepsilon_{2nd}$ of poly-**1**-MOE with (*S*)-**2** ([(*S*)-**2**]/[poly-**1**-MOE] = 400) in hexane versus induced time. [Poly-**1**-MOE] = 1.0 mM.

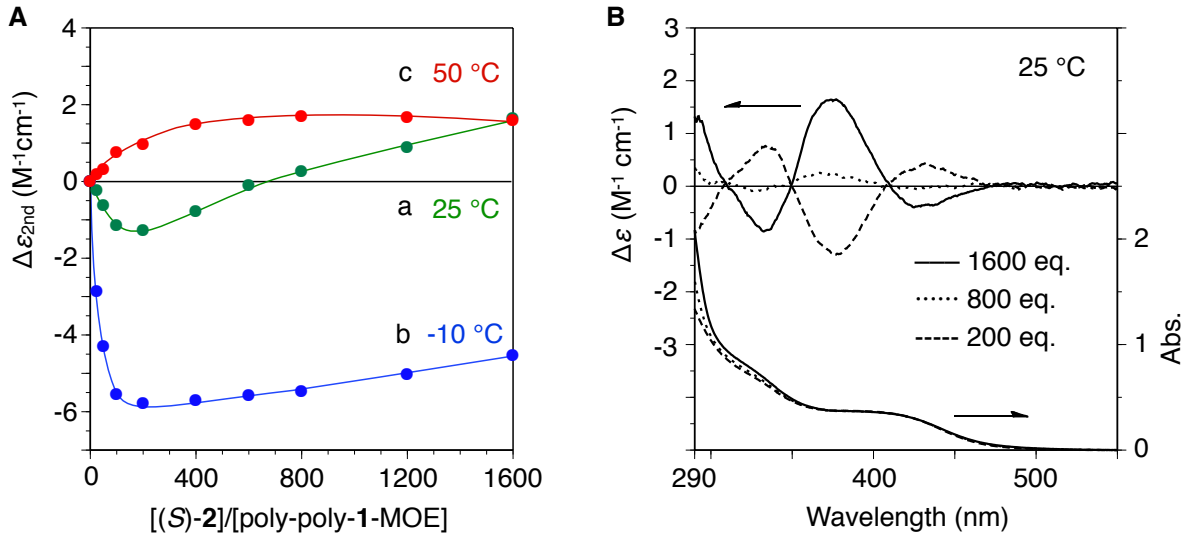

Figure 4-3. (A) Titration curves of poly-**1**-MOE ($\Delta\varepsilon_{2nd}$) with (*S*)-**2** in hexane at 25 °C after 2 h (a, green), -10 °C after 7 days (b, blue) and 50 °C after 1 h (c, red). [Poly-**1**-MOE] = 1.0 mM. (B) CD and absorption spectra of poly-**1**-MOE (1.0 mM) with (*S*)-**2** (0.2 M (dashed line), 0.8 M (dotted line), and 1.6 M (solid line)) in hexane at 25 °C after 2 h.

The similar ICD inversion was also observed in the CD titration experiments of poly-**1**-MOE with (*S*)-**2** in hexane at 25 °C (a in Figure 4-3A and Figure 4-3B). The ICD intensity of the second Cotton effect at 25 °C increased in the negative direction with an increase in the concentration of (*S*)-**2** and reached a maximum value at around [(*S*)-**2**]/[poly-**1**-MOE] = 200. Further addition of (*S*)-**2** caused the inversion of the second Cotton effect sign at around [(*S*)-**2**]/[poly-**1**-MOE] = 800 at 25 °C and the ICD intensity then continued to increase in the positive direction with increasing concentration of (*S*)-**2**. However, such an inversion of the Cotton effects was not observed at -10 °C and 50 °C; the ICD intensity reached an almost constant value at [(*S*)-**2**]/[poly-**1**-MOE] = 200 at -10 °C and at [(*S*)-**2**]/[poly-**1**-MOE] = 800 at 50 °C (b and c Figure 4-3A).

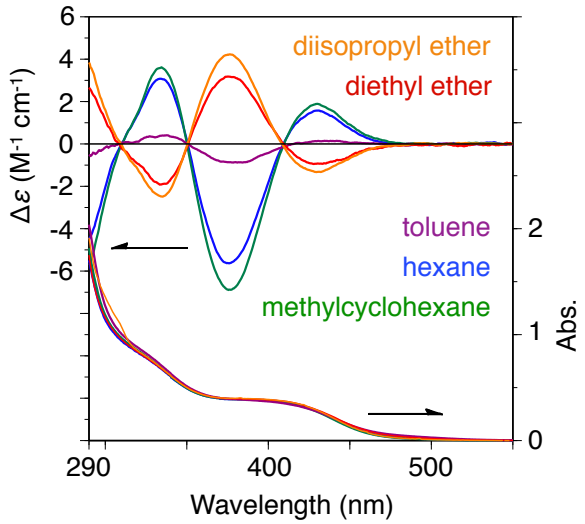

Figure 4-4. CD and absorption spectra of poly-**1**-MOE (1.0 mM) with (*S*)-**2** ([(*S*)-**2**]/[poly-**1**-MOE] = 800) in hexane (—), methylcyclohexane (—), toluene (—), diethyl ether (—), and diisopropyl ether (—) at -10 °C after 7 days.

Since poly-**1**-MOE is soluble in various solvents, we then investigated the possibility of solvent-driven helix-sense inversion for poly-**1**-MOE with (*S*)-**2**. Figure 4-4 shows the CD and absorption spectra of poly-**1**-MOE with (*S*)-**2** in various solvents after standing at -10 °C for 7 days. Poly-**1**-MOE with (*S*)-**2** showed a negative second Cotton effect in methylcyclohexane and toluene as well as hexane. However, the Cotton effect signs of the poly-**1**-MOE with (*S*)-**2** in diethyl ether and diisopropyl ether were completely opposite to that in hexane, showing a positive second Cotton effect. This indicates that the preferred-handed helical senses induced in poly-**1**-MOE with (*S*)-**2** in hexane, methylcyclohexane, and toluene, are opposite to those in diethyl ether and diisopropyl ether. It seems that poly-**1**-MOE with (*S*)-**2** tends to form a preferred right-handed helix in nonpolar solvents such as hexane, methylcyclohexane, and toluene, whereas the opposite left-handed helix is induced in polar solvents such as diethyl ether and diisopropyl ether.

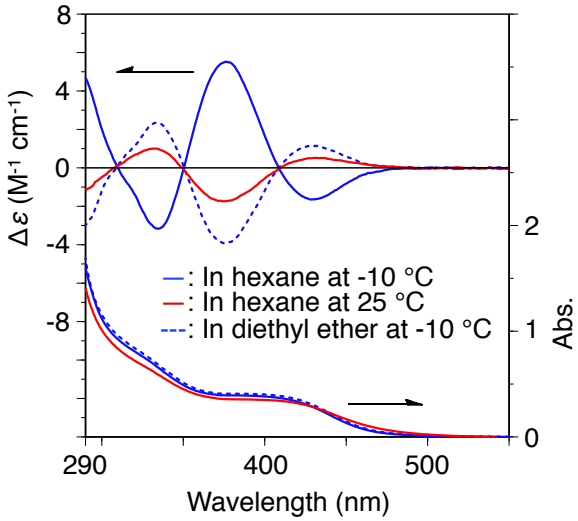

Figure 4-5. CD and absorption spectra of poly-**1**-MOE (1.0 mM) with (*R*)-**2** ([(*R*)-**2**]/[poly-**1**-MOE] = 800) in hexane (solid line) and diethyl ether (dashed line) at 50 °C after 1 h (red) and at -10 °C after 7 days (blue).

When (*R*)-**2** was used as the chiral guest instead of (*S*)-**2**, poly-**1**-MOE with the opposite helicity was induced, which underwent a reversible inversion of the helicity by a change in temperature and solvent (Figure 4-5). On the other hand, analogous polyacetylene (poly-**1**-MOM) bearing 2,2'-biphenol-derived pendants did not show such temperature- and solvent-dependent CD spectral inversions in the presence of (*S*)-**2**. The author notes that poly-**1**-MOM with (*S*)-**2** showed the positive second Cotton effect in hexane, methylcyclohexane, and diethyl ether, although the ICD intensity slightly changed with temperature (Figure 4-6). These results suggest that the ethoxymethoxy groups on the biphenyl pendant should play an important role for the helix-helix transition of the polymer backbone and the predominant helix-sense should be significantly affected by a delicate interaction between the alkoxymethoxy groups on the biphenyl pendants and the chiral guest, although the detailed mechanism is still unclear at present.

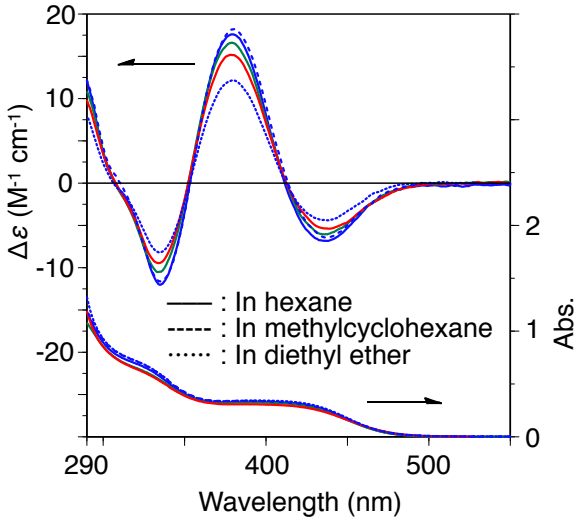

Figure 4-6. CD and absorption spectra of poly-**1**-MOM (1.0 mM) with (*S*)-**2** ([(*S*)-**2**]/[poly-**1**-MOM] = 400) in hexane (solid line), methylcyclohexane (dashed line), and diethyl ether (dotted line) at -10 °C (blue), 25 °C (green), and 50 °C (red) after 1 day.

Memory of the Enantiomeric Helices of Poly-1-MOE Induced by (*S*)-2. As described above, the author found that the macromolecular helicity induced in poly-**1**-MOM upon interaction with (*S*)- or (*R*)-**2** could be memorized after complete removal of the chiral guest in hexane. In contrast to the chiral memory observed in analogous polyacetylenes,[2-3, 6] replacement of the chiral guests with achiral chaperoning molecules is no longer needed for the chiral memory in poly-**1**-MOM. The author then investigated if the right- and left-handed helical conformations of poly-**1**-MOE induced by (*S*)-**2** under different conditions could retain after complete removal of the chiral guest. First, the poly-**1**-MOE—(*S*)-**2** complex ([(*S*)-**2**]/[poly-**1**-MOE] = 800) in hexane showing negative second Cotton effect ($\Delta\varepsilon_{2nd}$ = –5.63) after standing at -10 °C for 7 days (a in Figure 4-7) was poured into excess amount of methanol at -10 °C followed by washing with methanol in order to isolate the poly-**1**-MOE. The complete removal of (*S*)-**2** was confirmed by ^{1}H NMR measurement of the isolated poly-**1**-MOE. The ^{1}H NMR spectrum of the isolated poly-**1**-MOE in $CDCl_3$ at 50 °C showed no peak due to (*S*)-**2** (A in Figure 4-8) whereas apparent peaks due to (*S*)-**2** were observed for the poly-**1**-MOE containing (*S*)-**2** ([(*S*)-**2**]/[poly-**1**-MOE] = 0.1) under the same condition (B in Figure 4-8), indicating that (*S*)-**2** was completely removed during precipitation of the poly-**1**-MOE—(*S*)-**2** complex into methanol followed by washing with methanol. Despite the complete removal of the chiral guest (*S*)-**2**, the CD spectrum of the isolated polymer dissolved in hexane at -10 °C was almost in perfect agreement before isolation (b in Figure 4-7). These results clearly demonstrate that the macromolecular helicity of poly-**1**-MOE induced by (*S*)-**2** in hexane at -10 °C can be automatically memorized without using any chaperoning compounds. Next, in the same way, the poly-**1**-MOE was isolated from the poly-**1**-MOE—(*S*)-**2** ([(*S*)-**2**]/[poly-**1**-MOE] = 800) complex in hexane at 50 °C showing positive second Cotton effect ($\Delta\varepsilon_{2nd}$ = +1.79) (c in Figure 4-7). The isolated polymer dissolved in hexane at -10 °C also exhibited similar ICDs before isolation, suggesting that the enantiomeric opposite helical poly-**1**-MOE was also memorized (d in Figure 4-7). The ICD patterns of the poly-**1**-MOEs isolated from the complexes in hexane at -10 °C and 50 °C were complete mirror

images from each other and their absorption spectra were perfectly identical. The memory efficiencies estimated on the ICD values of poly-**1**-MOE with (*S*)-**2** at 50 °C and -10 °C as the base values were 74.3 and 99.5 %, respectively. Almost perfect memory was attained at -10 °C, while some racemization occurred for the memory of the macromolecular helicity induced at 50 °C. The memory lasted for a rather long time with a half-life ($t_{1/2}$) of approximately 25 h in *n*-hexane at -10 °C (Figure 4-9), which is shorter to that of poly-**1**-MOM.

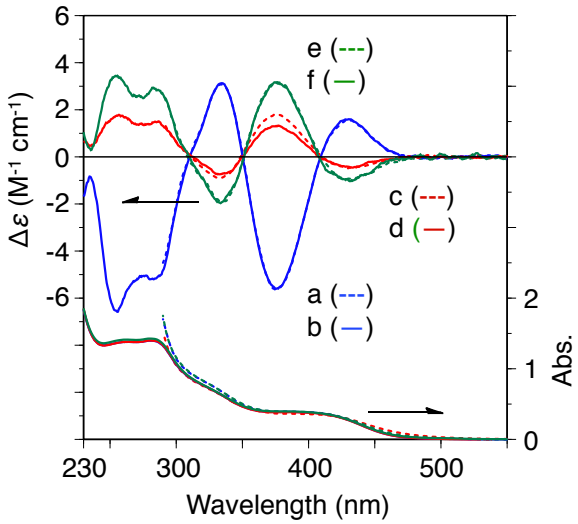

Figure 4-7. CD and absorption spectra of poly-**1**-MOE (1.0 mM) with (*S*)-**2** ([(*S*)-**2**]/[poly-**1**-MOE] = 800) in hexane at -10 °C after 7 days (a, ---) and at 50 °C after 1 h (c, ---), and in diethyl ether at -10 °C after 7 days (e, ---) and the isolated poly-**1**-MOE from a (b, —), c (d, —), and e (f, —) in hexane at -10 °C.

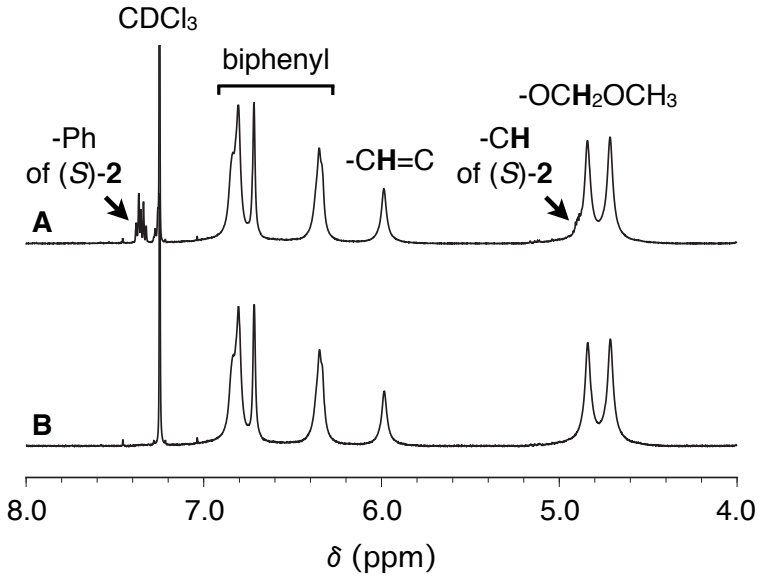

Figure 4-8. ^{1}H NMR spectra of poly-**1**-MOE with (*S*)-**2** ([(*S*)-**2**]/[poly-**1**-MOE] = 0.1) (A) and isolated poly-**1**-MOE (B) in $CDCl_3$ at 50 °C.

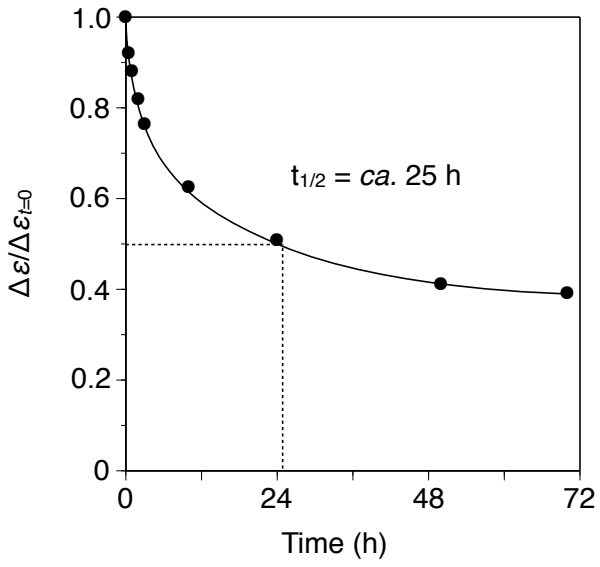

Figure 4-9. Stability of the macromolecular helicity memory of isolated poly-**1**-MOE. The normalized CD intensity ($\Delta\varepsilon/\Delta\varepsilon_{t=0}$) changes against time. $\Delta\varepsilon_{t=0}$ represents the CD intensity of the isolated poly-**1**-MOE at 376 nm just after dissolution in hexane at -10 °C.

On the other hand, when the poly-**1**-MOE was isolated from the poly-**1**-MOE—(*S*)-**2** ([(*S*)-**2**]/[poly-**1**-MOE] = 800) complex showing positive second Cotton effect ($\Delta\varepsilon_{2nd}$ = +3.18) in diethyl ether after standing at -10 °C for 7 days (e in Figure 4-7), the isolated polymer showed a almost same ICDs as the before isolation after dissolving in hexane at -10 °C (f in Figure 4-7). Therefore, the enantiomeric opposite helical poly-**1**-MOE was successfully memorized with almost perfect memory efficiency by using the solvent-driven helix inversion. This "dual memory" of enantiomeric helices is significantly different from the previous ones observed in other poly(phenylacetylene) derivatives bearing acid functional pendants in view of the fact that the previous dual memory systems necessarily requires the replacement with achiral amines.[2-3, 6]

Conclusions

In summary, the author has found that the helix-sense of poly-**1**-MOE induced by (*S*)-**2** could be switched not only by temperature but also by solvent. The resulting right- and left-handed helices of poly-**1**-MOE induced by (*S*)-**2** at different temperatures or in different solvents could be automatically memorized after complete removal of the chiral alcohol. Accordingly, both mirror-image enantiomeric helices could be produced from an optically inactive polymer by using a single enantiomer. This is the first example of the dual memory without the use of chaperoning compounds assisted by the temperature- and solvent-driven macromolecular helicity inversion. The present results will provide new approaches for the rational design of novel switchable helical architectures and the construction of new chiral materials in areas such as liquid crystals, chiral selectors, and chiral sensors.

Experimental Section

Materials. Anhydrous THF, dichloromethane, *N*,*N*-dimethylformamide (DMF), acetone, and toluene were obtained from Kanto Kagaku (Tokyo, Japan). Anhydrous *n*-hexane and diethyl ether were purchased from Wako (Osaka, Japan). Triethylamine (NEt_3) was dried over KOH pellets and distilled onto KOH under nitrogen. These solvents were stored under nitrogen. 4-Bromoresorcinol, *p*-toluenesulfonyl chloride (TsCl), benzylbromide (BnBr), potassium carbonate, *n*-butyllithium (1.6 M in *n*-hexane), trimethoxyborane, dimethoxyethane (DME), and 2,6-lutidine were purchased from Wako. 1-Bromododecane, tetrakis(triphenylphosphine)palladium(0), trifluoromethanesulfonic anhydride (Tf_2O), bis(triphenylphosphine)palladium(II) dichloride, and chloromethyl ethyl ether were from Tokyo Kasei (TCI, Tokyo, Japan). Triphenylphosphine and (*R*)- and (*S*)-**2** were obtained from Kanto Kagaku. Palladium (5 wt% on activated carbon), [(norbornadiene)rhodium(I) chloride]$_2$ [Rh(nbd)Cl_2], and anhydrous acetonitrile were available from Aldrich (Milwaukee, WI、USA). (Trimethylsilyl)acetylene (TMSA) was kindly supplied from Shinetsu Chemical (Tokyo, Japan). (2,2'-Bis(ethoxymethoxy)-4'-dodecyloxy-4-biphenylyl)acetylene (**1**-MOE) was prepared according to the previously reported methods (see Chapter 3).

Instruments. Melting points were measured on a Yanako melting point apparatus and were uncorrected. NMR spectra were taken on a JNM-ECA 500 (JEOL) (500 MHz for ^{1}H, 125 MHz for ^{13}C) spectrometer in $CDCl_3$ using TMS (for $CDCl_3$, ^{1}H and ^{13}C) as the internal standard. Size exclusion chromatography (SEC) measurements were performed with a JASCO PU-2080 liquid chromatograph equipped with a UV-vis (JASCO UV-970) detector at 40 °C. The temperature was controlled with a JASCO CO-1560 column oven. A Shodex (Tokyo, Japan) KF-805L (30 cm) column was used for SEC measurements and THF was used as the eluent at flow rate of 1.0 mL/min. The molecular weight calibration curves were obtained with polystyrene standards (Tosoh). Absorption and CD spectra were measured in a 1.0-mm quartz cell on a JASCO V-570 spectrophotometer and a JASCO J-725 spectropolarimeter, respectively. The temperature was controlled with a JASCO ETC-505T

(absorption spectroscopy) and a JASCO PTC-348WI apparatus (CD spectroscopy). Elemental analyses were performed by the Research Institute for Instrumental Analysis of Advanced Science Research Center, Kanazawa University, Kanazawa, Japan.

Polymerization. Polymerization of **1**-MOE was carried out in a dry glass ampule under a dry nitrogen atmosphere using $[Rh(nbd)Cl]_2$ as a catalyst in a similar way previously reported (Scheme 4-1).[2, 6a, 6d]

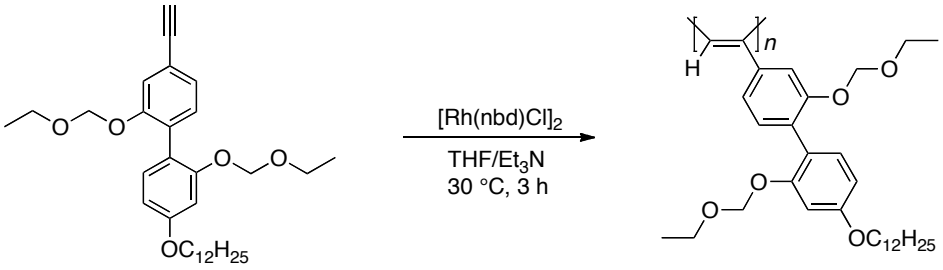

Scheme 4-1. Synthesis of Poly-**1**-MOE

Monomer **1**-MOE (75.0 mg, 0.157 mmol) was placed in a dry ampule, which was then evacuated on a vacuum line and flushed with dry nitrogen. After this evacuation-flush procedure was repeated three times, a three-way stopcock was attached to the ampule, and dry THF (200 μL) and Et_3N (65.5 μL) ($[Et_3N]/[$**1**-MOE$] = 3$) were added with a syringe. To this was added a solution of $[Rh(nbd)Cl]_2$ (0.0157 M) in THF (50.0 μL) at 30 °C. The concentrations of **1**-MOE and the rhodium catalyst were 0.5 M and 0.005 M, respectively. The color of the mixture changed instantly to reddish brown. After 3 h, the resulting polymer (poly-**1**-MOE) was precipitated into a large amount of methanol, collected by centrifugation, and dried *in vacuo* at room temperature overnight (68.5 mg, 91%). The number-averaged molecular weight (M_n) and its distribution (M_w/M_n) of poly-**1**-MOE were estimated to be 1.8×10^5 and 2.5, respectively, by SEC with polystyrene standards and THF as the eluent. The stereoregularity of poly-**1**-MOE was determined to be highly *cis-transoidal* because its ^1H NMR spectrum showed a sharp singlet centered around 6 ppm due to the main chain protons.[7]

Spectroscopic data of poly-**1**-MOE. ^{1}H NMR (500 MHz, $CDCl_3$, 50 °C): δ 6.69-6.88 (br, 4H, Ar–H), 6.25-6.40 (br, 2H, Ar–H), 5.98 (s, 1H, Ar–H), 4.84 (s, 2H, OCH_2O), 4.71 (s, 2H, OCH_2O), 3.79 (br, 2H, OCH_2CH_2), 3.39 (br, 2H, OCH_2CH_3), 3.23 (br, 2H, OCH_2CH_3), 1.69 (br, 2H, OCH_2CH_2), 1.16-1.52 (m, 18H, $9CH_2$), 0.99 (t, J = 6.3 Hz, 3H, OCH_2CH_3), 0.88 (t, J = 6.3 Hz, 3H, CH_3) 0.80 (t, J = 6.3 Hz, 3H, OCH_2CH_3). Calcd for $C_{32}H_{46}O_5 \cdot 0.25H_2O$: C, 74.60; H, 9.10. Found: C, 74.59; H, 9.24.

Helicity Induction in Poly-1-MOE in Solution. The concentration of poly-**1**-MOE was calculated based on the monomer units and was 1.0 mM unless otherwise stated. A stock solution of poly-**1**-MOE (5.0 mM) in *n*-hexane was prepared in a 2-mL flask equipped with a stopcock. A 100 μL aliquot of the poly-**1**-MOE solution was transferred to a vessel equipped with a screwcap using a Hamilton microsyringe. An appropriate amount of (*R*)- or (*S*)-**2** was added to the vessel and the solution was diluted with hexane to keep the poly-**1**-MOE concentration at 1.0 mM, then the solution was immediately mixed with a vibrator (Iuchi, Japan). After the solution was allowed to stand for 7 days at -10 °C, the absorption and CD spectra were recorded at -10 °C. For CD titration experiments, CD measurements at 50 °C were performed after standing at -10 °C for 7 days.

Memory of the Macromolecular Helicity in Solution. A stock solution of poly-**1**-MOE (1.0 mM) with (*S*)-**2** (0.8 M) ([(*S*)-**2**]/[poly-**1**-MOE] = 800 mol/mol) was prepared in *n*-hexane or diethyl ether. The solution was allowed to stand at -10 °C for 7 days. The solution was poured into a large amount of methanol at -10 °C to remove (*S*)-**2**. The precipitated poly-**1**-MOE was collected by centrifugation, washed with methanol, and then dried in vacuo at room temperature over night. After the isolated poly-**1**-MOE was dissolved in *n*-hexane at -10 °C, the absorption and CD spectra were then recorded. Memory of the macromolecular helicity at 50 °C was performed as follows. A stock solution of poly-**1**-MOE (1.0 mM) with (*S*)-**2** (0.8 M) ([(*S*)-**2**]/[poly-**1**-MOE] = 800 mol/mol) was prepared in *n*-hexane. The solution was allowed to stand at 50 °C for 1 h. The solution was poured into a large amount of ice-cold methanol to remove (*S*)-**2**. The precipitated poly-**1**-MOE was collected by centrifugation,

washed with methanol, and then dried in vacuo at room temperature over night. After the isolated poly-**1**-MOE was dissolved in *n*-hexane at -10 °C, the absorption and CD spectra were then recorded.

References

1. (a) Green, M. M.; Peterson, N. C.; Sato, T.; Teramoto, A.; Cook, R.; Lifson, S., *Science* **1995**, *268*, 1860-1866; (b) Okamoto, Y.; Yashima, E., *Angew. Chem., Int. Ed.* **1998**, *37*, 1020-1043; (c) Green, M. M.; Park, J. W.; Sato, T.; Teramoto, A.; Lifson, S.; Selinger, R. L. B.; Selinger, J. V., *Angew. Chem., Int. Ed.* **1999**, *38*, 3138-3154; (d) Fujiki, M., *Macromol. Rapid Commun.* **2001**, *22*, 539-563; (e) Nakano, T.; Okamoto, Y., *Chem. Rev.* **2001**, *101*, 4013-4038; (f) Brunsveld, L.; Folmer, B. J. B.; Meijer, E. W.; Sijbesma, R. P., *Chem. Rev.* **2001**, *101*, 4071-4097; (g) Yashima, E.; Maeda, K.; Nishimura, T., *Chem. Eur. J.* **2004**, *10*, 42-51; (h) Reggelin, M.; Doerr, S.; Klussmann, M.; Schultz, M.; Holbach, M., *Proc. Natl. Acad. Sci., U. S. A.* **2004**, *101*, 5461-5466; (i) Lam, J. W. Y.; Tang, B. Z., *Acc. Chem. Res.* **2005**, *38*, 745-754; (j) Maeda, K.; Yashima, E., *Top. Curr. Chem.* **2006**, *265*, 47-88; (k) Aoki, T.; Kaneko, T.; Teraguchi, M., *Polymer* **2006**, *47*, 4867-4892; (l) Masuda, T., *J. Polym. Sci., Part A: Polym. Chem.* **2007**, *45*, 165-180; (m) Rudick, J. G.; Percec, V., *New J. Chem.* **2007**, *31*, 1083-1096; (n) Yashima, E.; Maeda, K., *Macromolecules* **2008**, *41*, 3-12; (o) Yashima, E.; Maeda, K.; Furusho, Y., *Acc. Chem. Res.* **2008**, *41*, 1166-1180; (p) Pijper, D.; Feringa, B. L., *Soft Matter* **2008**, *4*, 1349-1372; (q) Kim, H.-J.; Lim, Y.-B.; Lee, M., *J. Polym. Sci., Part A: Polym. Chem.* **2008**, *46*, 1925-1935; (r) Yashima, E.; Maeda, K.; Iida, H.; Furusho, Y.; Nagai, K., *Chem. Rev.* **2009**, *109*, 6102-6211; (s) Schwartz, E.; Koepf, M.; Kitto, H. J.; Nolte, R. J. M.; Rowan, A. E., *Polym. Chem.* **2011**, *2*, 33-47; (t) Yamamoto, T.; Suginome, M., *Angew. Chem., Int. Ed.* **2009**, *48*, 539-542; (u) Yamamoto, T.; Yamada, T.; Nagata, Y.; Suginome, M., *J. Am. Chem. Soc.* **2010**, *132*, 7899-7901; (v) Yamamoto, T.; Akai, Y.; Nagata, Y.; Suginome, M., *Angew. Chem., Int. Ed.* **2011**, *50*, 8844-8847.
2. Yashima, E.; Maeda, K.; Okamoto, Y., *Nature* **1999**, *399*, 449-451.
3. (a) Miyagawa, T.; Furuko, A.; Maeda, K.; Katagiri, H.; Furusho, Y.; Yashima, E., *J. Am. Chem. Soc.* **2005**, *127*, 5018-5019; (b) Hasegawa, T.; Morino, K.; Tanaka, Y.; Katagiri, H.; Furusho, Y.; Yashima, E., *Macromolecules* **2006**, *39*, 482-488.

4. Maeda, K.; Morino, K.; Yashima, E., *J. Polym. Sci., Part A: Polym. Chem.* **2003**, *41*, 3625-3631.
5. (a) Sakurai, S. I.; Okoshi, K.; Kumaki, J.; Yashima, E., *Angew. Chem., Int. Ed.* **2006**, *45*, 1245-1248; (b) Sakurai, S. I.; Okoshi, K.; Kumaki, J.; Yashima, E., *J. Am. Chem. Soc.* **2006**, *128*, 5650-5651.
6. (a) Maeda, K.; Morino, K.; Okamoto, Y.; Sato, T.; Yashima, E., *J. Am. Chem. Soc.* **2004**, *126*, 4329-4342; (b) Onouchi, H.; Kashiwagi, D.; Hayashi, K.; Maeda, K.; Yashima, E., *Macromolecules* **2004**, *37*, 5495-5503; (c) Hasegawa, T.; Maeda, K.; Ishiguro, H.; Yashima, E., *Polym. J.* **2006**, *38*, 912-919; (d) Maeda, K.; Tamaki, S.; Tamura, K.; Yashima, E., *Chem. Asian J.* **2008**, *3*, 614-624.
7. (a) Nagai, K.; Sakajiri, K.; Maeda, K.; Okoshi, K.; Sato, T.; Yashima, E., *Macromolecules* **2006**, *39*, 5371-5380; (b) Simionescu, C. I.; Percec, V.; Dumitrescu, S., *J. Polym. Sci., Part A: Polym. Chem.* **1977**, *15*, 2497-2509; (c) Simionescu, C. I.; Percec, V., *Prog. Polym. Sci.* **1982**, *8*, 133-214; (d) Furlani, A.; Napoletano, C.; Russo, M. V.; Feast, W. J., *Polym. Bull.* **1986**, *16*, 311-317; (e) Kishimoto, Y.; Eckerle, P.; Miyatake, T.; Kainosho, M.; Ono, A.; Ikariya, T.; Noyori, R., *J. Am. Chem. Soc.* **1999**, *121*, 12035-12044; (f) Percec, V.; Rudick, J. G.; Peterca, M.; Wagner, M.; Obata, M.; Mitchell, C. M.; Cho, W. D.; Balagurusamy, V. S. K.; Heiney, P. A., *J. Am. Chem. Soc.* **2005**, *127*, 15257-15264.

Chapter 5

Chirality Sensing of Various Chiral Compounds by Helical Polyacetylenes Bearing Biphenyl Pendants with Dynamic Axial Chirality

Abstract: An optically inactive, stereoregular polyacetylene bearing 2,2'-biphenol-derived pendants with dynamic axial chirality, poly((2,2'-bis(methoxymethoxy)-4'-dodecyloxy-4-biphenylyl)acetylene) (poly-**1**), was found to show characteristic induced circular dichroisms in the UV–visible region of the polymer backbone due to the formation of a preferred-handed helical conformation in response to the chirality of various chiral compounds such as alcohols, amines, esters, ethers, amino acid derivatives, and hydrocarbons. Taking advantage of chiral memory effect, the author demonstrated that poly-**1** could detect the chirality of the small amount of simple chiral hydrocarbons with high sensitivity. Moreover, poly-**1** formed a preferred-handed helical conformation in the film state after exposure to the vapor of volatile chiral compounds.

Introduction

Chirality is a significant factor in living systems because living creatures are composed of various optically active small molecules and macromolecules and often show quite different biological activities toward a pair of enantiomers. Hence, the detection and assignment of the chirality of molecules at molecular and supramolecular levels have become exceedingly important in recent years. Among various spectroscopies, CD spectroscopy, which provides spectra directly reflecting the chirality and/or optical activity of the target chiral compounds, is one of the most powerful tool for chirality sensing.[1] In particular, when a receptor molecule is achiral or dynamically racemic with a chromophore, one of the enantiomeric or diastereomeric twisted or helical conformers induced by specific complexation with chiral guests may give a characteristic induced circular dichroism (ICD) in the absorption region of the receptor.[2] Such systems will provide the basis to construct a novel chirality-sensing probe to determine the absolute configuration and enantiomeric excess (ee) of the guest molecules.

In 1995, Yashima and co-workers reported the helicity induction in an optically inactive, stereoregular (*cis-transoidal*) poly((4-carboxyphenyl)acetylene) (PCPA), which can change their structures into the preferred-handed helices upon complexation with optically active amines, thus showing a characteristic ICD in the absorption region due to the polymer backbone in solution.[3] The Cotton effect signs corresponding to the helical sense of the polymer can be used as a novel probe for the chirality assignments of the chiral amines.[3-4] Since then, this methodology of a preferred-handed helicity induction with specific chiral guests has been applied to other dynamically racemic helical polymers after the introduction of specific functional groups as the pendants.[2c, 5] Moreover, the right- or left-handed macromolecular helicity of PCPA induced by optically active amines can be maintained, that is "memorized", when the optically active amines are replaced by various achiral amines.[6,7]

As described in Chapter 3, the author developed a quite unique helical polyacetylene bearing 2,2'-biphenol-derived pendants (poly-**1**) whose main-chain helicity and axial chirality

of the pendants are induced in the solid state as well as in hexane upon interaction with nonracemic alcohol 1-phenylethanol (**2**), thereby exhibiting split-type ICDs in the polymer backbone region. Moreover, the author found that the induced macromolecular helicity and axial chirality of poly-**1** are automatically memorized after removal of the chiral guest and further switched even in the solid state upon interaction with the opposite enantiomeric alcohol and its subsequent removal. Taking full advantage of this unique feature, the author succeeded in developing an unprecedented chiral packing material for separating enantiomers whose elution order or enantioselectivity can be reversibly switched.

In this chapter, the author investigated chirality sensing ability of poly-**1** toward various optically active compounds in solution as well as in the solid state by using CD spectroscopy. The author found that poly-**1** could respond to the chirality of a large variety of chiral compounds including alcohols, amines, amino alcohols, esters, ethers, amino acid derivatives, and hydrocarbons, thus showing an apparent ICDs in the polymer backbone region due to the formation of preferred-handed helical conformation. Owing to the chiral memory effect, poly-**1** could detect the chirality of the very small amount of simple chiral hydrocarbons with high sensitivity, suggesting that poly-**1** is useful for a practical chirality sensor for chiral hydrocarbons. Moreover, the author also discovered an unprecedented helicity induction of poly-**1** in the solid state in response to the vapor of volatile chiral compounds. To the best of the author's knowledge, preferred-handed helicity induction in dynamic helical polymers upon exposure to the vapor of chiral compounds is hitherto unknown.[8]

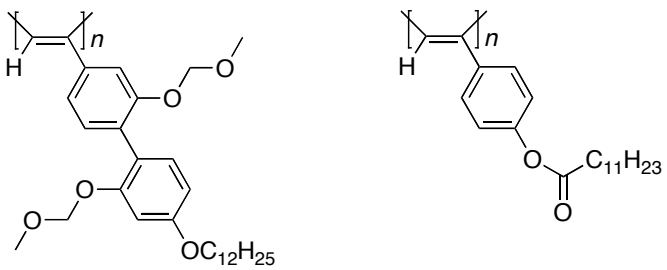

poly-**1** **PPAC12**

Chart 5-1. Structures of Poly-**1** and Model Polymer **PPAC12**

Results and Discussion

Helicity induction in poly-1 with various chiral compounds in solution. As described in Chapter 3, poly-**1** formed a preferred-handed helical conformation in response to the chirality of optically active alcohol **2** in hexane to show an intense ICD in the polymer backbone region despite the absence of specific functional pendants capable of strongly interacting with the chiral guests. First, the author investigated the effect of the solvent on the helicity induction in poly-**1**. Figure 5-1 shows the CD and absorption spectra of poly-**1** in the presence of (*S*)-**2** in various solvents at –10 °C. Poly-**1** exhibited similar ICDs in toluene and THF as well as in hexane, but the ICD intensity in THF remarkably decreased (Figure 5-1c). On the other hand, poly-**1** with (*S*)-**2** in $CHCl_3$ showed a large red-shift in the absorption spectrum and no ICD was observed (Figure 5-1d). The reason is not clear at the present stage, but poly-**1** may form a different helical conformation with a more relaxed helical pitch in $CHCl_3$ than that in other solvents such as hexane, toluene, and THF. The CD titrations using (*S*)-**2** in hexane, toluene, and THF showed that the plots of the CD intensities of the second Cotton ($\Delta\varepsilon_{2nd}$) of poly-**1** as a function of the concentration of (*S*)-**2** gave a saturated binding isotherm (Figure 5-2). The Hill plot analyses[9] of the data in hexane, toluene, and THF resulted in binding constants (*K*) of 145, 16, and 1.2, respectively. These results suggest that a preferred-handed helical conformation can be induced in poly-**1** most efficiently in hexane because both hydrogen bonding interaction between the OMOM groups in poly-**1** with the hydroxy group in (*S*)-**2** and π–π interaction between the phenyl groups in poly-**1** and (*S*)-**2** are most effectively possible in hexane.

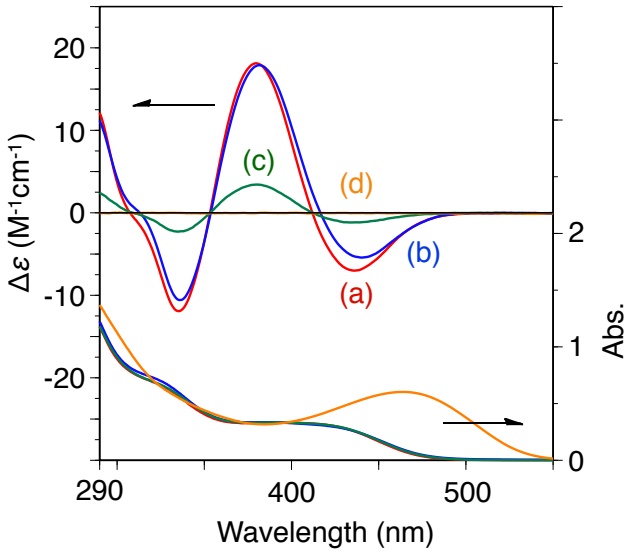

Figure 5-1. CD and absorption spectra of poly-**1** (1.0 mM) in the presence of (*S*)-**2** ([**2**]/[poly-**1**] = 400) in hexane (a), toluene (b), THF (c), and $CHCl_3$ (d) at -10 °C after standing at 25 °C for 24 h.

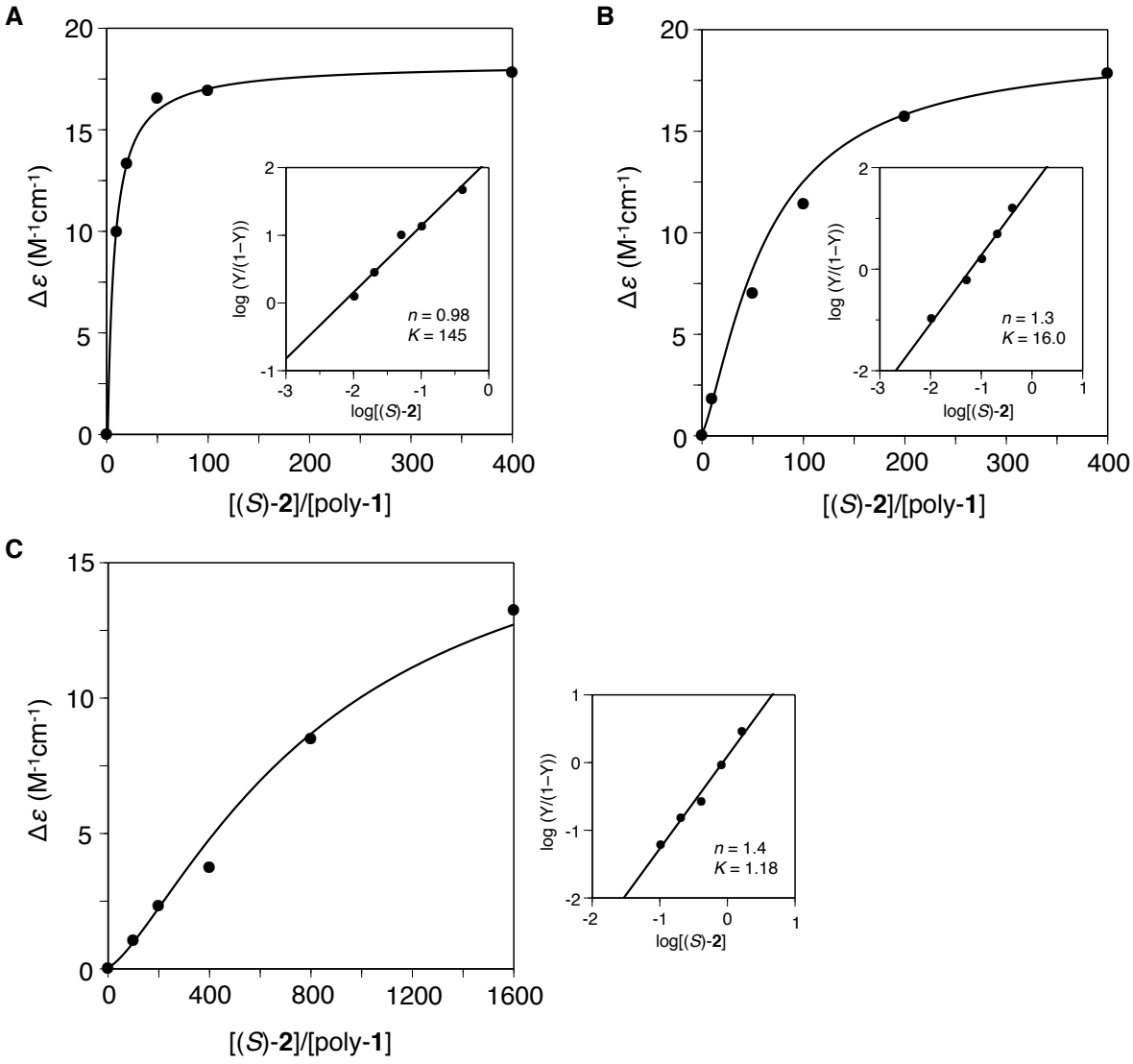

Figure 5-2. Titration curves ($\Delta\varepsilon_{2nd}$) of poly-**1** (1.0 mM) with (*S*)-**2** in hexane (A), toluene (B), and THF (C) at -10 °C. The CD spectra were measured after the samples had been allowed to stand at 25 °C for 6 h (A and B) and at -10 °C for 48 h (C). The insets show the Hill plots of log (Y/(1 – Y)) vs log [(*S*)-**2**] (Y = $\Delta\varepsilon/\Delta\varepsilon_{max}$). Curves in the plots of were calculated using parameters determined from the fits to the solid lines in the Hill plots.

The author then measured CD spectra of poly-**1** in the presence of various chiral compounds shown in Chart 5-2 in hexane or toluene at –10 °C. We note that toluene was used as the solvent for the guests that are insoluble in hexane. The results of the ICD are summarized in Table 5-1. Poly-**1** showed apparent ICDs in the presence of all the tested chiral compounds including alcohols (**2**–**9**), amines (**10**–**12**), amino alcohols (**13**–**15**), esters (**16**–**17**), ethers (**18**–**19**), and amino acid derivatives (**20**–**23**). Structurally similar chiral alcohols (**2**–**5**), amino alcohols (**13**–**15**), and esters (**16**,**17**) of the same configuration gave the same signs of the Cotton effect. On the other hand, there is no clear relation between the signs of the induced Cotton effect for poly-**1** and the absolute configurations of the diols (**7**–**9**), amines (**10**–**12**), and ethers (**18**, **19**). This is probably because the binding direction of the chiral guests to poly-**1** may be nonspecific due to their weak interaction. However, these results indicate that poly-**1** can efficiently detect the chirality of various compounds even if the interaction with the chiral guests is quite weak, which stimulated the author to investigate whether poly-**1** can respond to the chirality of chiral hydrocarbons without any functional groups because poly-**1** can be soluble in hydrocarbons. Although there are a few reports on the ICD induction in optically inactive host molecules with optically active hydrocarbons,[10] the chirality sensing of simple chiral hydrocarbons still remains challenging issue.[11,12]

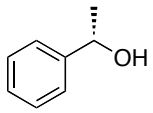

(*S*)-**2**

(*S*)-**3**

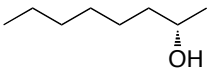

(*S*)-**4**

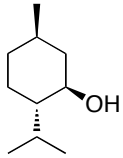

(1*R*)-**5**

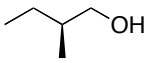

(*S*)-**6**

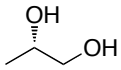

(*S*)-**7**

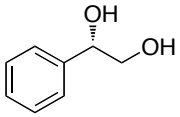

(*S*)-**8**

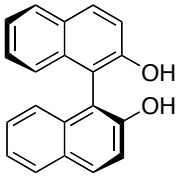

(*S*)-**9**

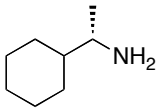

(*S*)-**10**

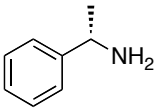

(*S*)-**11**

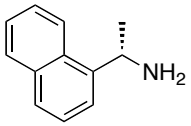

(*S*)-**12**

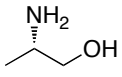

(*S*)-**13**

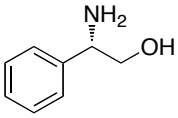

(*S*)-**14**

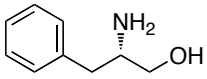

(*S*)-**15**

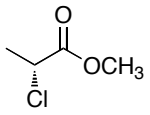

(*R*)-**16**

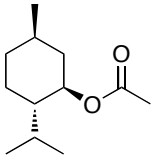

(1*R*)-**17**

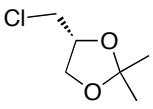

(*R*)-**18**

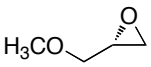

(*R*)-**19**

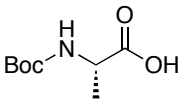

L-**20**

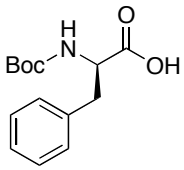

D-**21**

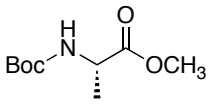

L-**22**

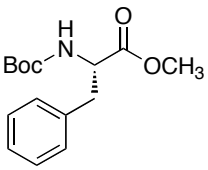

L-**23**

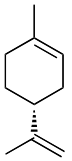

(*R*)-**24**

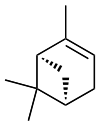

(1*R*)-**25**

Chart 5-2. Structures of Various Chiral Guest Compounds (**2**–**25**)

Table 5-1. Signs and Differences in Exciton Coefficient of the Second Cotton ($\Delta\varepsilon_{2nd}$) for Poly-**1** with Various Optically Active Compounds (**2**–**25**) in Hexane or Toluene at -10 °C

guest		second Cotton		
		sign	$\Delta\varepsilon$ [$M^{-1}cm^{-1}$]	(λ [nm])
alcohols[a]	(*S*)-**2**	+	17.79	(380)
	(*S*)-**3**	+	2.46	(381)
	(*S*)-**4**	+	9.49	(379)
	(1*R*)-**5**	–	5.82	(380)
	(*S*)-**6**	–	1.67	(379)
diols[b]	(*S*)-**7**	+	0.10	(378)
	(*S*)-**8**	–	4.76	(380)
	(*S*)-**9**	+	10.17	(381)
amines[c]	(*S*)-**10**	–	0.36	(381)
	(*S*)-**11**	+	7.45	(382)
	(*S*)-**12**	–	5.43	(380)
amino alcohols[b]	(*S*)-**13**	–	0.12	(379)
	(*S*)-**14**	–	0.71	(381)
	(*S*)-**15**	–	0.11	(380)
esters[a]	(*R*)-**16**	+	13.99	(378)
	(1*R*)-**17**	+	13.78	(379)
ethers[c]	(*R*)-**18**	+	2.10	(380)
	(*R*)-**19**	–	0.96	(380)
Boc-amino acids[d]	L-**20**	–	0.31	(378)
	D-**21**	+	10.49	(381)
Boc-amino acid methyl eters[d]	L-**22**	+	3.89	(380)
	L-**23**	+	2.64	(379)
hydrocarbons[e]	(*R*)-**24**	–	3.72	(379)
	(1*R*)-**25**	–	4.18	(378)

[a] [Guest]/[poly-**1**] = 400 in hexane. [b] [Guest]/[poly-**1**] = 20 in toluene. [c] [Guest]/[poly-**1**] = 400 in toluene. [d] [Guest]/[poly-**1**] = 50 in toluene. [e] Neat.

To assess the chirality sensing ability of poly-**1** toward chiral hydrocarbons, the CD and absorption spectra of poly-**1** were measured in (*R*)-limonene ((*R*)-**24**) and (1*R*)-α-pinene ((1*R*)-**25**). Poly-**1** exhibited a relatively strong ICD in the polymer backbone region in (*R*)-**24** and (1*R*)-**25** at -10 °C (a, b in Figure 5-3), suggesting that poly-**1** can form a preferred-handed helical conformation in response to the chirality of (*R*)-**24** and (1*R*)-**25**, although its binding affinity to poly-**1** probably through CH-π interaction is expected to be very weak.[11a] The CD titrations using (*R*)-**24** in hexane was performed in order to estimate the *K* value of (*R*)-**24** to poly-**1**. However, the Hill plot analysis of the data resulted in the failure of the linear fitting probably because its *K* value is too small to estimate. On the other hand, model polymer **PPAC12** without biphenyl pendants showed no ICD in (*R*)-**24**–toluene (9/1, v/v) (c in Figure 5-3). The CD and absorption spectra of **PPAC12** were measured in (*R*)-**24**–toluene (9/1, v/v) because **PPAC12** was insoluble in (*R*)-**24**. Under the same condition, poly-**1** showed an apparent ICD (d in Figure 5-3). These results indicate that the biphenyl chirality in the pendants may play an important role to the macromolecular helicity induction in poly-**1** through weak interactions. We assume that the central chirality of the chiral hydrocarbons such as (*R*)-**24** and (1*R*)-**25** is first transferred to the axial chirality in the biphenyl pendants of poly-**1** and the resulting slight excess of the axially twisted conformation in the pendants then may bias the helical screw-sense of the polymer backbone.

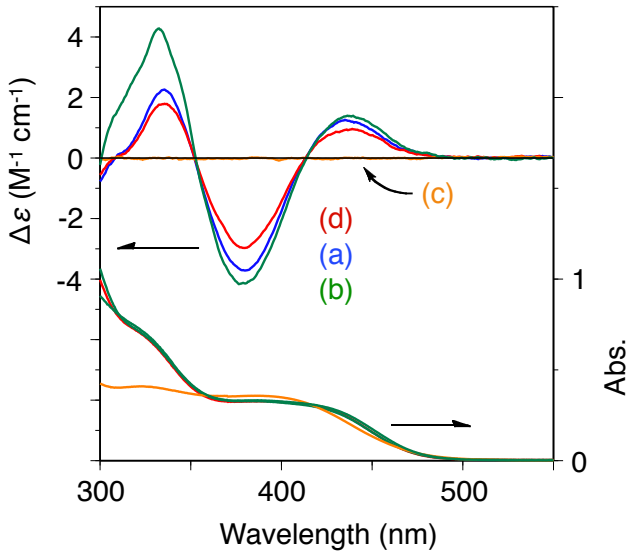

Figure 5-3. CD and absorption spectra of poly-**1** (a, b, d) and poly-**PPAC12** (c) ([polymer] = 1.0 mM) in (*R*)-**24** (a), (1*R*)-**25** (b), and (*R*)-**24**–toluene (9/1, v/v) (c, d) at -10 °C after standing at 25 °C for 24 h.

Because of the very weak interaction with the hydrocarbons, it is desirable to perform the CD measurements in a neat or a large excess amount of the chiral hydrocarbons in order to induce apparent ICDs.[10-11] For example, in the presence of small amount of (*R*)-**24** (200 mM), poly-**1** showed very weak ICDs in hexane due to the lack of a preferred-handed helical conformation (a in Figure 5-4). However, the helical chirality induced in poly-**1** can be maintained even after removal of the chiral compounds. Therefore, taking advantage of this chiral memory effect, poly-**1** can detect the chirality of chiral hydrocarbons by using a small amount of them. Figure 5-4b shows the CD spectrum of poly-**1** in the presence of small amount of (*R*)-**24** (200 mM) after helicity induction in (*R*)-**24** (16 μL) followed by dilution with large amount of hexane; the second Cotton ICD intensity was approximately six times larger than that of the ICD observed under the same condition without memory effect.

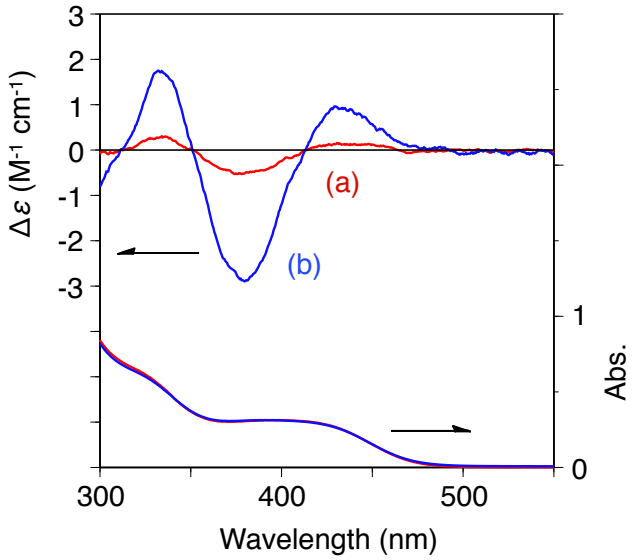

Figure 5-4. CD and absorption spectra of poly-**1** (1.0 mM) in the presence of (*R*)-**24** (200 mM) in hexane at -10 °C after standing at 25 °C for 24 h (a) and after helicity induction in (*R*)-**24** at 25 °C for 24 h (b).

The results of the chirality sensing toward various chiral hydrocarbons by using this chiral memory effect in poly-**1** are shown in Figure 5-5 and summarized in Table 5-2. Poly-**1** exhibited apparent ICDs for all the simple chiral hydrocarbons shown in Chart 5-3. There is a good correlation between the sign of the ICDs and their stereochemistry, which are represented in a similar way as shown in Figure 5-6, where the "L" and "S" are the bulkiest and the smaller alkyl substituents, respectively. The helical sense appears to be controlled by the difference in the bulkiness of the L and S groups on the stereogenic center. Interestingly, a good liner relationship between the enantiomeric excess (ee) of **24** and the ICD values of poly-**1** was observed as shown in Figure 5-7, although the CD values of poly-**1** showed a strong positive nonlinear relationship with respect to the ee of **2** as described in Chapter 3. This is probably because the interaction of poly-**1** with a chiral hydrocarbon **24** is very weak. However, these results suggest that poly-**1** can be used to detect the chirality of chiral hydrocarbons and to determine their stereochemistry and enantiomeric purity.

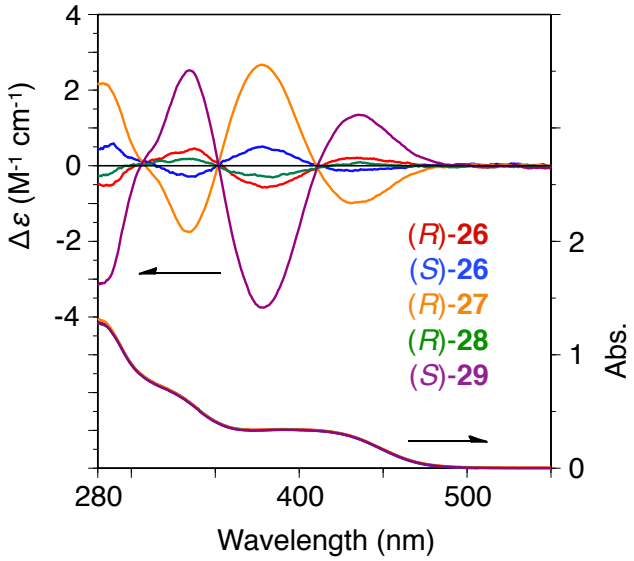

Figure 5-5. CD and absorption spectra of poly-**1** (1.0 mM) in hexane at -10 °C after helicity induction in various optically active hydrocarbons (**26**–**29**) at 25 °C for 24 h followed by dilution with hexane.

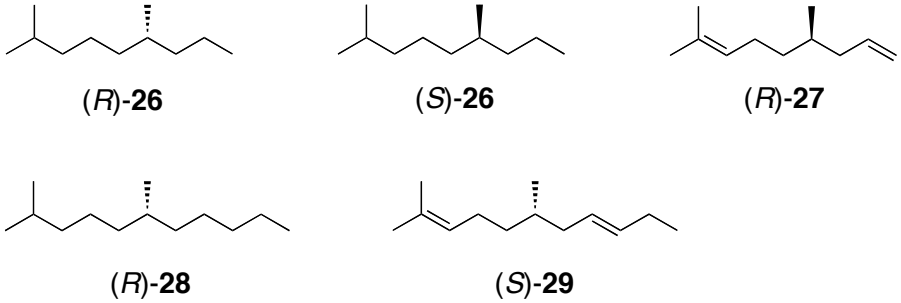

Chart 5-3. Structures of Chiral Hydrocarbons

Table 5-2. Signs and Differences in Exciton Coefficient of the Second Cotton ($\Delta\varepsilon_{2nd}$) for Poly-**1** in Hexane at -10 °C after Helicity Induction in Various Optically Active Hydrocarbons (**26**–**29**) for 10 min at 50 °C, then 10 min at -10 °C

chiral hydrocarbon	second Cotton		
	sign	$\Delta\varepsilon$ [$M^{-1}cm^{-1}$]	(λ [nm])
(*R*)-**26**	–	0.57	(381)
(*S*)-**26**	+	0.51	(378)
(*R*)-**27**	+	2.67	(378)
(*R*)-**28**	–	0.31	(384)
(*S*)-**29**	–	3.75	(379)

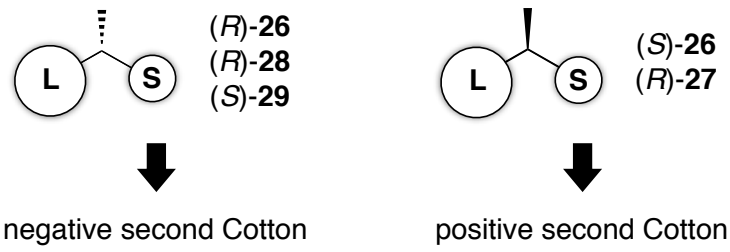

Figure 5-6. Schematic representation of the relationship between the stereochemistry of chiral hydrocarbons and the sign of the second Cotton effect. The "L" and "S" are the bulkiest and the smaller alkyl substituents, respectively.

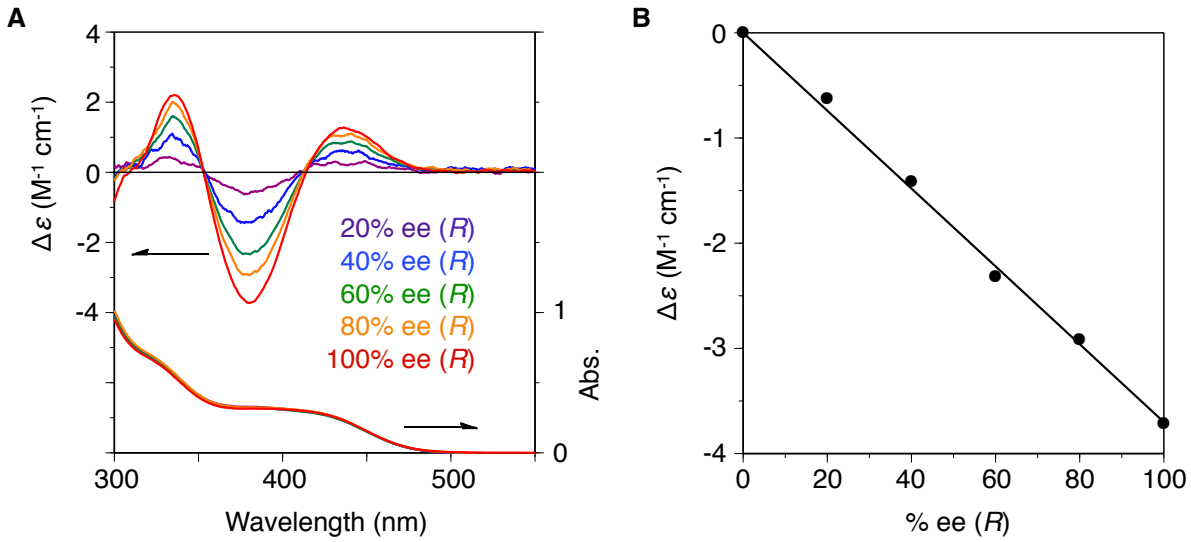

Figure 5-7. (A) CD and absorption spectra of poly-**1** (1.0 mM) in nonracemic **24** at -10 °C after standing at 25 °C for 24 h. (B) CD intensity ($\Delta\varepsilon_{2nd}$) changes of poly-**1** (1.0 mM) at -10 °C versus the % ee of **24** (*R*-rich) after standing in nonracemic **24** at 25 °C for 24 h.

Helicity induction in poly-1 film on exposure to the vapor of chiral compounds. As described in Chapter 3, poly-**1** forms a preferred-handed helical conformation in response to the chirality of a chiral alcohol in the solid state as well as in solution. We then investigated a similar helicity induction in the poly-**1** film upon exposure to the vapor of volatile chiral compounds. A poly-**1** film spin-coated on a quartz plate was placed in a vessel saturated with (*S*)-**2** and hexane vapors at 25 °C and the CD and absorption spectral measurements were then performed for an appropriate time interval. As shown in Figure 5-8A and B, the poly-**1** film showed a weak, but apparent ICD in the polymer backbone region after exposure to the vapor of (*S*)-**2** for 3 h, and the ICD intensity gradually increased with time, resulting in a maximum value after three days. When (*R*)-**2** was used instead, the poly-**1** film exhibited the mirror image of the split-type ICDs (f in Figure 5-8A). We also measured the linear dichroism (LD) spectra of the films and found that contribution from the LD was negligible in the CD spectra.[13] However, the Cotton effect pattern was different from that of the complexes with (*S*)-**2** in hexane (a in Figure 5-1). As mentioned in Chapter 3, the induced macromolecular helicity in poly-**1** could be maintained after complete removal of the nonracemic guests even in hexane, which enables us to easily confirm whether a preferred-handed helix is induced in the polymer backbone of poly-**1** in the solid state after exposure to the vapor of (*S*)-**2** by measuring CD in hexane after helicity induction in the solid state. After exposure to the vapor of (*S*)-**2** at 25 °C for three days, the poly-**1** film was dissolved in hexane at -10 °C, which exhibited an intense ICD comparable to that induced in hexane in the presence of (*S*)-**2** at 25 °C (Figure 5-8C). Therefore, it is unambiguously demonstrated that a preferred-handed helix is readily induced in poly-**1** even in the solid state by just exposure to the vapor of nonracemic **2** despite the very weak noncovalent bonding interaction and automatically memorized. A similar helicity induction in poly-**1** films was also possible for the other volatile chiral compounds ((1*R*)-**17**, (*R*)-**24**, and (1*S*)-**25**) (see Chart 5-2 and Figure 5-9). Consequently, the present results demonstrated that a preferred-handed helicity induction can be possible in the film state on exposure to the vapor of the chiral compounds by a vapor-

solid interaction. The advantage of the present system is easy preparation into a chirality-responsive film, which can respond to the chirality of the vapor of nonracemic compounds in the solid to show strong ICDs. The present method is more convenient to sense the chirality of volatile chiral compounds than the solution method.

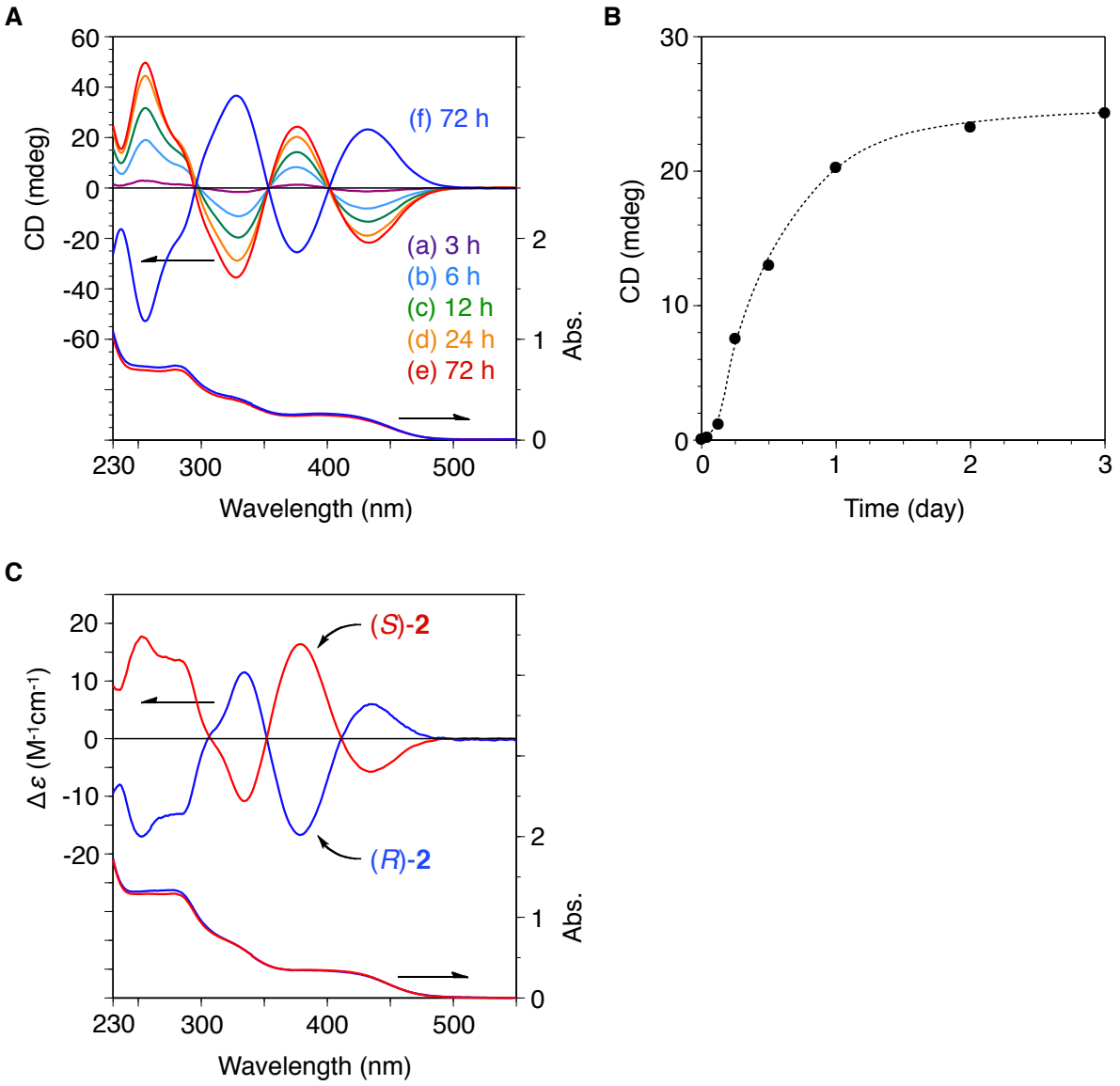

Figure 5-8. (A) CD spectral changes of poly-**1** film on exposure to the vapor of (*S*)-**2** at 25 °C with time (a–e). Absorption spectra of poly-**1** film after exposure to the vapor of (*S*)-**2** at 25 °C for 3 days are also shown in (e). CD and absorption spectra of poly-**1** film on exposure to the vapor of (*R*)-**2** at 25 °C for 3 days (f). (B) Plots of ICD intensity (2nd Cotton) of the poly-**1** film on exposure to the vapor of (*S*)-**2** at 25 °C versus time. (C) CD and absorption spectra of poly-**1** after dissolving the poly-**1** film in hexane at -10 °C after helicity induction on exposure to the vapor of (*R*)- and (*S*)-**2** at 25 °C for 3 days.

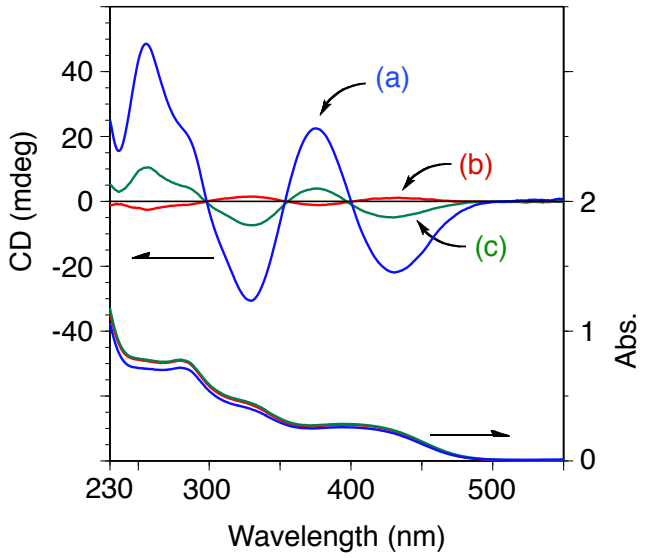

Figure 5-9. CD and absorption spectra of poly-**1** film on exposure to the vapor of (1*R*)-**17** (a), (*R*)-**24** (b), and (1*S*)-**25** (c) at 25 °C for 2 days.

Conclusions

The author has demonstrated that a polyacetylene that bears a 2,2'-biphenol-derived pendant (poly-**1**) could form a preferred-handed helical conformation in response to the chirality of a very broad range of chiral molecules including chiral hydrocarbons, thus showing characteristic ICDs in the absorption region of the polymer backbone. The biphenyl pendant with dynamic axial chirality appears to be important for its high sensitivity to chirality because a model polymer without biphenyl pendants showed no ICD signal under the same condition. The chiral memory effect characteristic of poly-**1** enabled the chirality sensing of a small amount of chiral hydrocarbons. Moreover, the author has found that poly-**1** could change its structure to a preferred-handed helical conformation by just exposing to the vapor of chiral compounds. The author believes that these findings will contribute to the development of the design of more sensitive helical polymers for the chirality sensing of various chiral molecules.

Experimental Section

Materials. Anhydrous THF were toluene obtained from Kanto Kagaku (Tokyo, Japan). Triethylamine (NEt_3) was dried over KOH pellets and distilled onto KOH under nitrogen. These solvents were stored under nitrogen. Anhydrous *n*-hexane and *p*-iodophenol were purchased from Wako (Osaka, Japan). Bis(triphenylphosphine)palladium(II) dichloride was from Tokyo Kasei (TCI, Tokyo, Japan). Copper(I) iodide, and lauroyl chloride were obtained from Kanto Kagaku. [(Norbornadiene)rhodium(I) chloride]$_2$ [Rh(nbd)Cl_2], and tetra-*n*-butylammonium fluoride (1.0 M in THF) were obtained from Aldrich. (Trimethylsilyl)acetylene (TMSA) was kindly supplied by Shinetsu Chemical (Tokyo, Japan). (*S*)-(-)-1-Phenylethylamine ((*S*)-**11**) and (*S*)-(+)-1-(1-naphthyl)ethylamine ((*S*)-**12**) were kindly supplied from Yamakawa Chemical (Tokyo, Japan). (4-Trimethylsilylethynyl)phenol[14] and **26**–**29**[12] were synthesized according to the literature. L-**22** was prepared by methyl esterification of L-**20** using diazomethane in diethyl ether solution. Other optically active compounds (**2**-**11**, **13**-**19**, **21**, and **22**-**25**) were available from Aldrich, AZmax (Ciba, Japan), Kanto Kagaku, TCI, or Wako. Poly-**1** was prepared by the polymerization of the corresponding monomer (**1**) with [Rh(nbd)Cl]$_2$ (nbd = norbornadiene) according to a previously reported method (Chapter 3). The number-average molecular weight (M_n) and its molecular weight distribution (M_w/M_n) were 4.9×10^5 and 1.8, respectively, as determined by size exclusion chromatography (SEC). The stereoregularity of poly-**1** was determined to be highly *cis-transoidal* because its ^{1}H NMR spectrum showed a sharp singlet centered around 6 ppm due to the main chain protons.[15]

Instruments. Melting points were measured on a Yanako melting point apparatus and were uncorrected. NMR spectra were taken on a Varian Mercury 300 (300 MHz for ^{1}H, 75 MHz for ^{13}C, and 121.5 MHz for ^{31}P) or a Varian VXR-500S (500 MHz for ^{1}H, 125 MHz for ^{13}C) or a JNA-LA 400 (JEOL) (400 MHz for ^{1}H, 100 MHz for ^{13}C) or a JNM-ECA 500 (JEOL) (500 MHz for ^{1}H, 125 MHz for ^{13}C) spectrometer in $CDCl_3$ or DMSO-d_6 using TMS (for $CDCl_3$, ^{1}H and ^{13}C) or a solvent residual peak (for DMSO-d_6, ^{1}H and ^{13}C) as the internal

standard. Recycling preparative HPLC was performed with LC-9201 liquid chromatograph (JAI, Tokyo, Japan) equipped with a UV–visible detector (Jasco (Hachioji, japan) UV-2075) at room temperature. HPLC columns, JAIGEL-1H and JAIGEL-2H were connected in series, and $CHCl_3$ was used as the eluent. IR spectra were recorded with a Jasco Fourier Transform IR-460 spectrophotometer. Laser Raman spectra were recorded on a Jasco NRS-1000 spectrophotometer. Optical rotation was measured in a 20 mm quartz cell on a Jasco P-1030 polarimeter. Absorption and CD spectra were measured in a 1.0-mm quartz cell on a Jasco V-570 spectrophotometer and a Jasco J-725 spectropolarimeter, respectively. The temperature was controlled with a Jasco PTC-348WI apparatus. Size exclusion chromatography (SEC) measurements were performed with a Jasco PU-2080 liquid chromatograph equipped with a UV-vis (Jasco UV-970) detector at 40 °C. The temperature was controlled with a Jasco CO-1560 column oven. A Tosoh TSKgel MultiporeH_{XL}-M (30 cm) column was used for SEC measurements of poly-**1** and poly-**2** and THF was used as the eluent at flow rate of 1.0 mL/min. The molecular weight calibration curves were obtained with polystyrene standards (Tosoh).

Synthesis of PPAC12. Model polymer **PPAC12** was prepared according to Scheme 5-5.

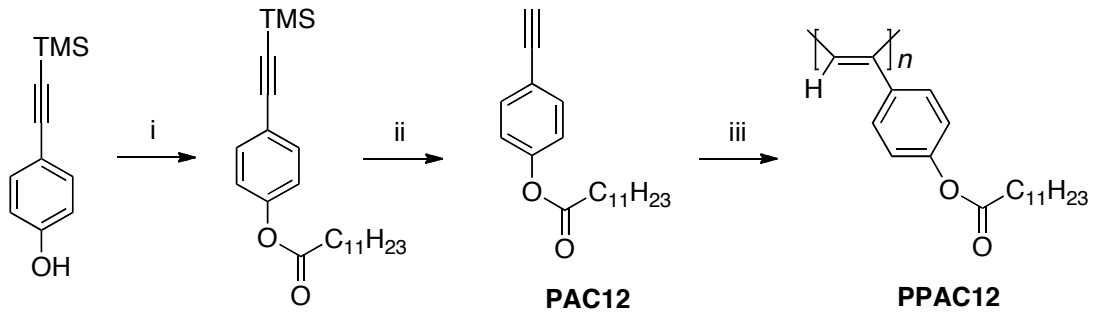

i) $C_{11}H_{23}COCl$, pyridine, rt, ii) TBAF, THF, 0 °C, iii) $[Rh(nbd)Cl]_2$, Et_3N/THF, 30 °C, 3 h.

Scheme 5-5. Synthesis of **PPAC12**

(4-Trimethylsilylethynyl)benzoyl laurate. To a solution of (4-trimethylsilylethynyl)phenol (350 mg, 1.84 mmol) in pyridine (11 mL) was added lauroyl

chloride (0.525 ml, 2.21 mmol). The solution was stirred at room temperature for 12 h. The reaction mixture was filtered and the solvent was removed under reduced pressure. The residue was diluted with diethyl ether and the solution was washed with sat. $NaHCO_3$ aq., water, and brine, and then dried over Na_2SO_4. After evaporating the solvent, the crude product was purified by silica gel chromatography using ethyl acetate—*n*-hexane (1/20, v/v) as the eluent to give (4-trimethylsilylethynyl)benzoyl laurate (606 mg, 88% yield). ^{1}H NMR (400 MHz, $CDCl_3$, rt): δ 7.46 (d, J = 8.8 Hz, 2H, Ar–H), 7.02 (d, J = 8.5 Hz, 2H, Ar–H), 2.54 (t, J = 7.4 Hz, 2H, CO$CH_2$$CH_2$), 1.74 (quint, J = 7.3 Hz, 2H, $COCH_2CH_2$), 1.23-1.44 (m, 16H, 8CH_2), 0.88 (t, J = 6.8 Hz, 3H, CH_3), 0.24 (s, 9H, TMS).

4-Ethynylphenyl dodecanoate (PAC12). To a solution of (4-trimethylsilylethynyl)benzoyl laurate (200 mg, 0.537 mmol) in THF (8.0 mL) was added TBAF (1.0 M in THF) (0.805 mL, 0.805 mmol) at 0 °C. The reaction mixture was stirred at 0 °C for 1 h. After addition of water, the mixture was extracted with ethyl acetate. The organic layer was washed with 1 N HCl, water, and brine, and then dried over $MgSO_4$. After evaporating the solvent, the crude product was purified by silica gel chromatography using ethyl acetate—*n*-hexane (1/20, v/v) as the eluent to give **PAC12** as white solid (114 mg, 71% yield). Mp: 42.1–42.5 °C. IR (KBr, cm^{-1}): 3276 (≡C–H), 2111 (C≡C), 1748 (C=O). ^{1}H NMR (400 MHz, $CDCl_3$, rt): δ 7.50 (d, J = 8.8 Hz, 2H, Ar–H), 7.05 (d, J = 8.8 Hz, 2H, Ar–H), 3.06 (s, 1H, CH), 2.55 (t, J = 7.4 Hz, 2H, CO$CH_2$$CH_2$), 1.75 (quint, J = 7.3 Hz, 2H, $COCH_2CH_2$), 1.22-1.45 (m, 16H, 8CH_2), 0.88 (t, J = 6.8 Hz, 3H, CH_3). ^{13}C NMR (100 MHz, $CDCl_3$, rt): δ 172.11, 151.11, 133.44 (2C), 121.86 (2C), 119.75, 83.01, 77.37, 34.52, 32.05, 29.74 (2C), 29.59, 29.48, 29.39, 29.23, 25.03, 22.84. Calcd for $C_{20}H_{28}O_2$: C, 79.96; H, 9.39. Found: C, 79.48; H, 9.41.

Polymerization. Polymerizations of **PAC12** was carried out according to Scheme 5-5 in a dry glass ampule under a dry nitrogen atmosphere using $[Rh(nbd)Cl]_2$ as a catalyst in a similar way as reported previously.[6, 7c] Monomer **PAC12** (70.0 mg, 0.313 mmol) was placed in a dry ampule, which was then evacuated on a vacuum line and flushed with dry nitrogen.

After this evacuation-flush procedure was repeated three times, a three-way stopcock was attached to the ampule, and THF/Et_3N (3/1, v/v) (0.366 mL) ([Et_3N]/[**PAC12**] = 3) was added with a syringe. To this was added a solution of $[Rh(nbd)Cl]_2$ (0.100 mL) (0.0117 M) in THF at 30 °C. The concentrations of **PAC12** and the rhodium catalyst were 0.5 M and 0.005 M, respectively. The color of the mixture changed instantly to reddish brown. After 3 h, the resulting polymer (**PPAC12**) was precipitated into a large amount of methanol, collected by centrifugation, and dried *in vacuo* at room temperature overnight (56 mg, 80% yield). The M_n and M_w/M_n of **PPAC12** were estimated to be 3.5×10^5 and 1.4, respectively, as determined by SEC with polystyrene standards and THF as the eluent. The stereoregularity of **PPAC12** was determined to be highly *cis-transoidal* because its ^1H NMR spectrum showed a sharp singlet centered around 6 ppm due to the main chain protons.[15]

Spectroscopic data of **PPAC12**. IR (KBr, cm^{-1}): 1759(C=O). ^1H NMR (400 MHz, $CDCl_3$, 50 °C): δ 6.66 (br, 4H, Ar–H), 5.79 (s, 1H, =CH), 2.45 (br, 2H, COCH_2CH_2), 1.69 (br, 2H, COCH_2CH_2), 1.19-1.42 (br, 16H, $8CH_2$), 0.89 (t, 3H, CH_3). Calcd for $C_{20}H_{28}O_2$: C, 79.96; H, 9.39. Found: C, 79.55; H, 9.49.

CD Measurements. Anhydrous toluene, hexane, and THF were used throughout for all measurements. A typical experimental procedure is described below. The concentration of poly-**1** was calculated based on the monomer units and was 1.0 mM (monomer units) unless otherwise stated. A stock solution of poly-**1** (5.0 mM) in *n*-hexane and toluene were prepared in a 2-mL flask equipped with a stopcock. A 100 μL aliquot of the poly-**1** solution was transferred to a vessel equipped with a screwcap using a Hamilton microsyringe. An appropriate amount of chiral guests were added to the vessel. The solution was immediately mixed with a vibrator (Iuchi, Japan) and absorption and CD spectra were measured.

CD Titrations of Poly-1 with (*S*)-2 and Hill Plots. The stock solutions of poly-**1** (2.0 mM) and (*S*)-**2** (165.4 mM) in *n*-hexane were prepared. A 500 μL aliquot of the poly-**1** solution was transferred to five 1 mL flasks equipped with stopcocks using a Hamilton microsyringe. An appropriate amount of the stock solution of (*S*)-**2** was added to the flasks.

The solutions were immediately mixed with a vibrator and finally diluted with *n*-hexane to keep the poly-**1** concentration at 1.0 mM. After the solution was allowed to stand at 25 °C for 6 h (in *n*-hexane and toluene) or at -10 °C for 48 h (in THF), the absorption and CD spectra were taken at -10 °C for each flask to give the titration curve (Figure 5-2). The Hill plot analysis of the data resulted in apparent binding constants (*K*s) according to the Hill equation, $\log(Y/(1-Y)) = n\log[G] + n\log K$, where Y, *n*, and [G] represent the fractional saturation, the Hill coefficient, and the concentration of the guest, respectively.[9a]

CD Measurements of Poly-1 in Limonene at Varying Molar Ratios of Its Enantiomers. A stock solution of poly-**1** (5.0 mM) in *n*-hexane was prepared. A 200 μL aliquot of the poly-**1** solution was transferred to a vessel equipped with a screwcap using a Hamilton microsyringe, and solvent was evaporated under reduced pressured. Aliquots of (*R*)- and (*S*)-**24** were placed into five vessels so that the percent ee of the mixtures (*R* rich) became 20, 40, 60, 80, and 100, respectively. Then, the resulting solutions were immediately mixed using a vibrator. After the solutions were allowed to stand at 25 °C for 24 h, the absorption and CD spectra were then taken for each vessel to determine the changes in the CD intensity at 379 nm (second Cotton) (Figure 5-7).

Chirality Sensing Toward Various Chiral Hydrocarbons by Using Chiral Memory Effect A stock solutions of poly-**1** (20 mM) in *n*-hexane was prepared. A 15 μL aliquot of the poly-**1** solution was transferred to a vessel equipped with a screwcap using a Hamilton microsyringe, and solvent was evaporated under reduced pressured and then, (*R*)-**26** (10 μL) was added. After standing at 50 °C for 10 min and at -10 °C for 10 min, the solution was diluted with *n*-hexane at -10°C to keep the poly-**1** concentration at 1.0 mM. Then the absorption and CD spectra were recorded.

Helicity Induction in Poly-1-MOE in The Film State. Poly-**1** films were prepared by spin casting 200 μL of a *n*-hexane solution of poly-**1** (10 mg/mL) on a cylindrical quartz plate, followed by drying under reduced pressure in a desiccator. The chiral vapor atmosphere were prepared by putting a vessel containing 0.5 mL of *n*-hexane and 0.5 mL of (*R*)- or (*S*)-**2** inside

a 50 mL flask, and the poly-**1** films were then placed in the 50 mL flask and allowed to stand at 25 °C. The CD and absorption spectral measurements were then performed for an appropriate time interval.

References

1. Nakanishi, K.; Berova, N.; Woody, R. W., *Circular Dichroisms Principles and Applications*. 2nd ed.; VCH: New York, 2000.
2. (a) Canary, J. W.; Holmes, A. E.; Liu, J., *Enantiomer* **2001**, *6*, 181-188; (b) Allenmark, S., *Chirality* **2003**, *15*, 409-422; (c) Yashima, E.; Maeda, K.; Nishimura, T., *Chem. Eur. J.* **2004**, *10*, 42-51; (d) Borovkov, V. V.; Hembury, G. A.; Inoue, Y., *Acc. Chem. Res.* **2004**, *37*, 449-459; (e) Hembury, G. A.; Borovkov, V. V.; Inoue, Y., *Chem. Rev.* **2008**, *108*, 1-73.
3. Yashima, E.; Matsushima, T.; Okamoto, Y., *J. Am. Chem. Soc.* **1995**, *117*, 11596-11597.
4. (a) Yashima, E.; Matsushima, T.; Okamoto, Y., *J. Am. Chem. Soc.* **1997**, *119*, 6345-6359; (b) Yashima, E., *Anal. Sci.* **2002**, *18*, 3-6.
5. (a) Maeda, K.; Yashima, E., *Top. Curr. Chem.* **2006**, *265*, 47-88; (b) Yashima, E.; Maeda, K., *Macromolecules* **2008**, *41*, 3-12; (c) Yashima, E.; Maeda, K.; Furusho, Y., *Acc. Chem. Res.* **2008**, *41*, 1166-1180; (d) Yashima, E.; Maeda, K.; Iida, H.; Furusho, Y.; Nagai, K., *Chem. Rev.* **2009**, *109*, 6102-6211.
6. (a) Yashima, E.; Maeda, K.; Okamoto, Y., *Nature* **1999**, *399*, 449-451; (b) Maeda, K.; Morino, K.; Okamoto, Y.; Sato, T.; Yashima, E., *J. Am. Chem. Soc.* **2004**, *126*, 4329-4342.
7. (a) Onouchi, H.; Kashiwagi, D.; Hayashi, K.; Maeda, K.; Yashima, E., *Macromolecules* **2004**, *37*, 5495-5503; (b) Hasegawa, T.; Maeda, K.; Ishiguro, H.; Yashima, E., *Polym. J.* **2006**, *38*, 912-919; (c) Maeda, K.; Tamaki, S.; Tamura, K.; Yashima, E., *Chem. Asian J.* **2008**, *3*, 614-624; (d) Miyagawa, T.; Furuko, A.; Maeda, K.; Katagiri, H.; Furusho, Y.; Yashima, E., *J. Am. Chem. Soc.* **2005**, *127*, 5018-5019.
8. (a) Buono, A. M.; Immediata, I.; Rizzo, P.; Guerra, G., *J. Am. Chem. Soc.* **2007**, *129*, 10992-10993; (b) Guadagno, L.; Raimondo, M.; Silvestre, C.; Immediata, I.; Rizzo, P.; Guerra, G., *J. Mater. Chem.* **2008**, *18*, 567-572.
9. (a) Connors, K. A., *Binding Constants*. John Wiley: New York, 1987; (b) Yashima, E.; Maeda, K.; Sato, O., *J. Am. Chem. Soc.* **2001**, *123*, 8159-8160.

10. (a) Green, M. M.; Khatri, C.; Peterson, N. C., *J. Am. Chem. Soc.* **1993**, *115*, 4941-4942; (b) Aimi, J.; Oya, K.; Tsuda, A.; Aida, T., *Angew. Chem., Int. Ed.* **2007**, *46*, 2031-2035; (c) Dellaportas, P.; Jones, R. G.; Holder, S. J., *Macromol. Rapid Commun.* **2002**, *23*, 99-103.
11. (a) Kobayashi, K.; Asakawa, Y.; Kikuchi, Y.; Toi, H.; Aoyama, Y., *J. Am. Chem. Soc.* **1993**, *115*, 2648-2654; (b) Paolesse, R.; Monti, D.; Monica, L. L.; Venanzi, M.; Froiio, A.; Nardis, S.; Natale, C. D.; Martinelli, E.; D'Amico, A., *Chem. Eur. J.* **2002**, *8*, 2476-2483; (c) Prince, R. B.; Barnes, S. A.; Moore, J. S., *J. Am. Chem. Soc.* **2000**, *122*, 2758-2762; (d) Kawagoe, Y.; Fujiki, M.; Nakano, Y., *New J. Chem.* **2010**, *34*, 637-647.
12. Kawasaki, T.; Tanaka, H.; Tsutsumi, T.; Kasahara, T.; Sato, I.; Soai, K., *J. Am. Chem. Soc.* **2006**, *128*, 6032-6033.
13. Kuroda, R.; Harada, T.; Shindo, Y., *Rev. Sci. Instrum.* **2001**, *72*, 3802-3810.
14. Yashima, E.; Huang, S. L.; Matsushima, T.; Okamoto, Y., *Macromolecules* **1995**, *28*, 4184-4193.
15. (a) Nagai, K.; Sakajiri, K.; Maeda, K.; Okoshi, K.; Sato, T.; Yashima, E., *Macromolecules* **2006**, *39*, 5371-5380; (b) Simionescu, C. I.; Percec, V.; Dumitrescu, S., *J. Polym. Sci., Part A: Polym. Chem.* **1977**, *15*, 2497-2509; (c) Simionescu, C. I.; Percec, V., *Prog. Polym. Sci.* **1982**, *8*, 133-214; (d) Furlani, A.; Napoletano, C.; Russo, M. V.; Feast, W. J., *Polym. Bull.* **1986**, *16*, 311-317; (e) Kishimoto, Y.; Eckerle, P.; Miyatake, T.; Kainosho, M.; Ono, A.; Ikariya, T.; Noyori, R., *J. Am. Chem. Soc.* **1999**, *121*, 12035-12044; (f) Percec, V.; Rudick, J. G.; Peterca, M.; Wagner, M.; Obata, M.; Mitchell, C. M.; Cho, W. D.; Balagurusamy, V. S. K.; Heiney, P. A., *J. Am. Chem. Soc.* **2005**, *127*, 15257-15264.

List of Publications

Papers

1) "Helical Polymer Brushes with a Preferred-Handed Helix-Sense Triggered by a Terminal Optically Active Group in the Pendant"
Katsuhiro Maeda, Shiho Wakasone, Kohei Shimomura, Tomoyuki Ikai, and Shigeyoshi Kanoh
Chem. Commun. **2012**, *48*, 3342-3344.

2) "Chiral Amplification in Polymer Brushes Consisting of Dynamic Helical Polymer Chains through Long-Range Communication of Stereochemical Information"
Katsuhiro Maeda, Shiho Wakasone, Kohei Shimomura, Tomoyuki Ikai, and Shigeyoshi Kanoh
in preparation.

3) "Switchable Enantioseparation Based on Macromolecular Memory of a Helical Polyacetylene in the Solid State"
Kohei Shimomura, Tomoyuki Ikai, Shigeyoshi Kanoh, Eiji Yashima, and Katsuhiro Maeda
Nature Chem, accepted.

4) "Memory of the Enantiomeric Macromolecular Helicity Induced in a Polyacetylene with a Single Enantiomer Assisted by Temperature- and Solvent-driven Helix Inversion"
Kohei Shimomura, Tomoyuki Ikai, Shigeyoshi Kanoh, Eiji Yashima, and Katsuhiro Maeda
in preparation.

5) "Chirality Sensing of Various Chiral Compounds by Helical Polyacetylenes Bearing Biphenyl Pendants with Dynamic Axial Chirality"
Kohei Shimomura, Tomoyuki Ikai, Shigeyoshi Kanoh, Eiji Yashima, and Katsuhiro Maeda
in preparation.

Acknowledgment

The present study was carried out at the Graduate School of Natural Science and Technology, Kanazawa University, during 2008—2014.

The author wishes to express his grateful acknowledgment to Professor Katsuhiro Maeda whose encouragement and helpful suggestions have been indispensable to the completion of the present thesis. He would also like to acknowledge Professor Shigeyoshi Kanoh and Dr. Tomoyuki Ikai for his constant guidance, encouragement, pertinent and tolerant advice, and helpful discussion. The author is deeply indebted to Professor Eiji Yashima of Nagoya University for fruitful discussion. It is pleasure to express his appreciation to the colleagues of Professor Kanoh Laboratory for their encouragement and friendship, and especially to Ms. Shiho Wakasone for valuable contributions.

Finally, he would like to give his special thanks to Professors Tada-aki Yamagishi, Tomoki Ogoshi, and Mitsunori Honda for serving on his dissertation committee.

March, 2014

Kohei Shimomura